SMART MATERIALS FOR THE REALIZATION OF AN ADAPTIVE BUILDING COMPONENT

CHARLOTTE LELIEVELD

Propositions

appended to the PhD thesis

Smart Materials For The Realization Of An Adaptive Building Component

Charlotte Lelieveld

1. Users are receptive to adaptive architecture, but architecture is not receptive to the adaptiveness of the user. (this thesis)

2. Adaptive architecture will lead to a whole new paradigm of the building design and use. (this thesis)

3. By controlling material properties on micro-scale, multifunctionality and technical integration will lead to an increase of smart material systems in our society.

4. Simulation is a valuable tool for predicting the performance of a construction but can never replace reality, as the unpredicted can never be predicted.

5. The moment a PhD candidate gains a clear vision of how the research should be conducted, it is time to finish the PhD research.

6. The ultimate achievement in material sustainability is attained when recycling can be achieved on a nano-scale, through molecular manufacturing.

7. A quota for women in leadership roles is urgent and important, but remains a short term solution for improving gender diversity. In the long run, a change in culture will be required and a quota is therefore not a sustainable solution.

8. Budget cuts in research lead to inventive sources of financing and research outcome. This is not necessarily positive.

9. Innovation is the capacity to translate dreams into reality.

10. Fire may create room for renewal, but when applied in a faculty, its timing and selectiveness conflicts with the research interests.

11. The line between science-fiction and reality when it comes to time travel is as fine as the measurement error. (Adam, T., et al. (2012). "Measurement of the neutrino velocity with the OPERA detector in the CNGS beam." Journal of High Energy Physics(10))

These propositions are regarded as opposable and defendable, and have been approved as such by the supervisor Prof. Dr.-Ing. P.M. Teuffel.

Stellingen

behorende bij het proefschrift

Slimme Materialen Voor Het Realiseren Van Een Adaptief Gebouwcomponent

Charlotte Lelieveld

1. Gebruikers zijn ontvankelijk voor aanpasbare architectuur, maar architectuur is niet ontvankelijk voor de verandering in de behoefte van gebruikers.

2. Adaptieve architectuur zal leiden tot een nieuw paradigma van het architectonische ontwerpen en het gebouw gebruik. (deze dissertatie)

3. Door het beheersen van materialen op microschaal zullen multifunctionaliteit en technische integratie leiden tot een toename van slimme materiaalsystemen.

4. Simulatie is een waardevolle methode om het gedrag van een constructie te voorspellen maar kan de werkelijkheid nooit vervangen, omdat het onvoorspelbare nooit voorspeld kan worden.

5. Op het moment dat een promovendus een helder beeld krijgt hoe het onderzoek uitgevoerd moet worden, is het tijd om het promotie onderzoek af te ronden.

6. De ultieme duurzaamheid wordt behaald wanneer hergebruik gerealiseerd kan worden op nanoschaal door middel van moleculaire fabricage.

7. Een quota voor vrouwen in leidinggevende functies is belangrijk en urgent, maar blijft een korte-termijn oplossing voor de verbetering van genderdiversiteit. Op de lange termijn vergt het een culture verandering en is om die reden is een quota niet duurzaam.

8. Bezuiniging in onderzoek leidt tot inventieve financieringsmiddelen en onderzoeksresultaten. Dit is niet per definitie positief.

9. Innovatie is het vermogen om dromen te vertalen in realiteit.

10. Brand schept weliswaar ruimte voor vernieuwing maar wanneer deze wordt toegepast in een faculteit conflicteert de timing en selectiviteit met de onderzoeksbelangen.

11. De lijn tussen sciencefiction en werkelijkheid met betrekking tot tijdreizen is zo scherp als de meetfout. (Adam, T., et al. (2012). "Measurement of the neutrino velocity with the OPERA detector in the CNGS beam." Journal of High Energy Physics(10))

Deze stellingen worden opponeerbaar en verdedigbaar geacht en zijn als zodanig goedgekeurd door de promotor Prof. Dr.-Ing. P.M. Teuffel.

Smart Materials For The Realization Of An Adaptive Building Component

Smart Materials For The Realization Of An Adaptive Building Component

Thesis
Delft University of Technology
Faculty of Architecture

ISBN: 978-94-6186-114-6

Illustrations and cover design: Charlotte Lelieveld, Ph.D.
Editing: Nicolette Lelieveld, MSc
paranimfen: ir. Alexander van de Kleij, ir. Janneke Dries
Printed by Wöhrmann Print Service

charlottelelieveld@yahoo.com

Financial support for the printing this thesis was kindly provided by Delft Centre for Materials.

Smart Materials For The Realization Of An Adaptive Building Component

Proefschrift

ter verkrijging van de graad van doctor
aan de Technische Universiteit Delft,
op gezag van de Rector Magnificus prof.ir. K.C.A.M. Luyben,
voorzitter van het College voor Promoties,
in het openbaar te verdedigen op vrijdag 8 februari 2013 om 12.30 uur
door
Charlotte Margaretha Johanna Laurette LELIEVELD

Bouwkundig ingenieur
geboren te Zoetermeer

Dit proefschift is goedgekeurd door de promotoren
Prof. Dr.-Ing. P.M.Teuffel

Copromotor: Dr. ir. K.M.B. Jansen

Samenstelling promotiecommisie

Rector Magnificus,	voorzitter
Prof. Dr.- Ing. P.M. Teuffel,	Technische Universiteit Delft, promotor
Dr. ir. K.M.B. Jansen,	Technische Universiteit Delft, copromotor
Prof. dr. ir. A.C.J.M. Eekhout,	Technische Universiteit Delft
Prof. dr. ir. S. van der Zwaag,	Technische Universiteit Delft
Prof. dr. ir. D.J. Broer,	Technische Univertiteit Eindhoven
Prof. dr. V. Evers,	Universiteit Twente
Prof. Dr.-Ing. M.Holzbach,	Offenbach Univerity of Art and Design

TABLE OF CONTENT

LIST OF TERMS SYMBOLS AND ABBREVIATIONS

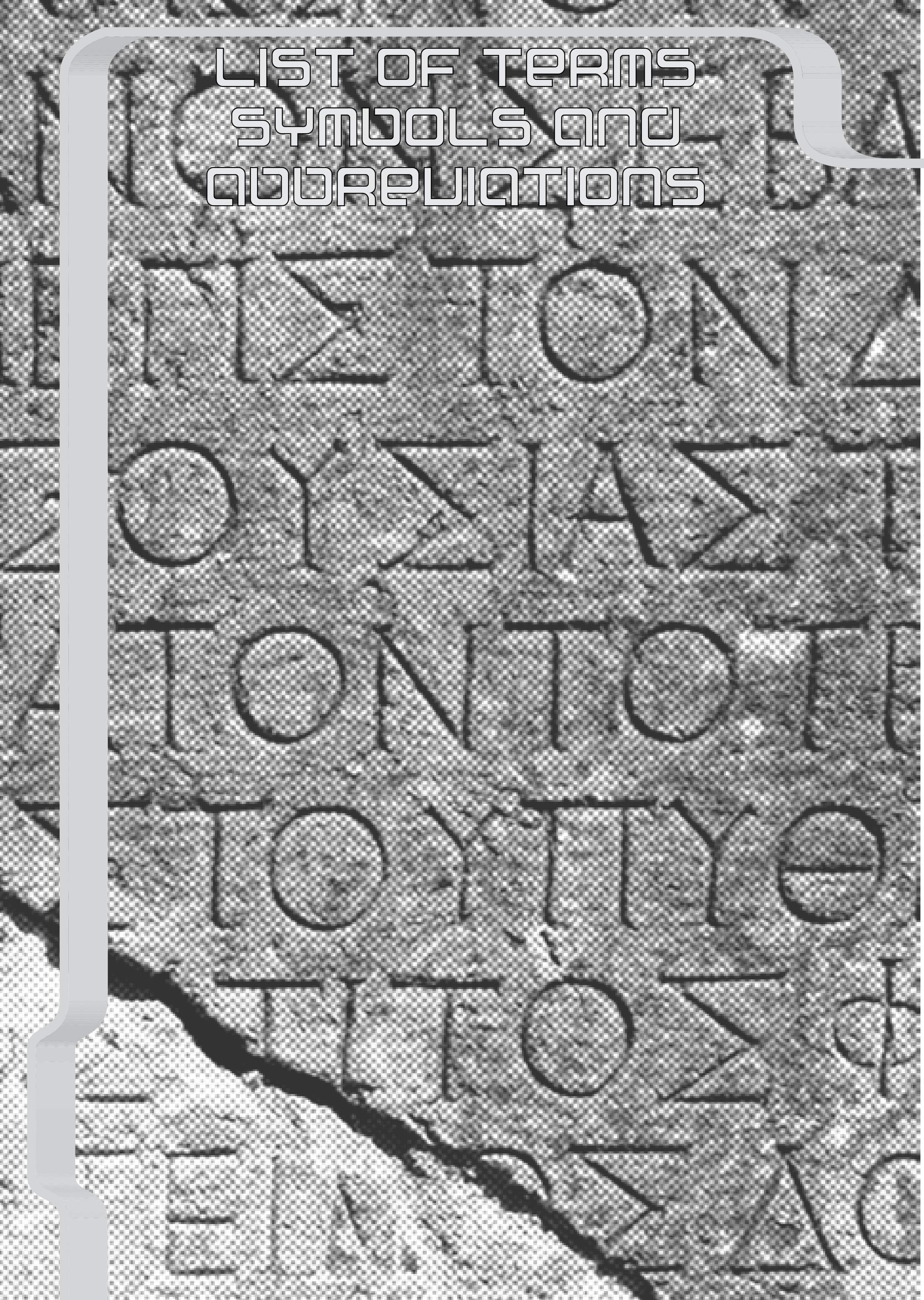

Term/ symbol/ abbreviation	Explanation
A	Cross-section area in squared meters (m^2).
ABC	Adaptive Building Component.
A_f (Austenite finishing temperature)	The phase transition of the SMA covers a temperature range. The finishing temperature indicates that the SMA is in full austenite condition.
ANSYS	Finite element method; program used for modelling of material behaviour.
A_s (Austenite start temperature)	The phase transition of the SMA covers a temperature range. The temperature at which the phase transition to austenite phase is initiated is indicated as the austenite start temperature.
Austenite phase	High temperature phase of SMA; strong material phase, strong molecule lattice, rigid.
Composite	Material which is assembled of multiple materials and thereby behaves as one material. In this research it refers to a composition of Shape Memory Polymer and Shape Memory Alloy.
Conduction	Energy transfer between bodies.
Constantan	Alloy assembled of Nickel and Copper, used for resistive heating, known for its constant material properties by variable temperatures. Has a very high resistivity.
Convection	Energy transfer by fluids or gases.
C_p	Specific heat (J/kgK).
DMA	Dynamic Mechanical Analysis; determines the viscoelastic material characteristics by the stress-strain relation. As this characteristic is temperature dependent, the test can be performed by increasing temperature values or a set temperature.
DSC	Differential Scanning Calorimeter; used for thermal analyses of material properties.
E	Energy in Joule (J).
E	Elasticity modulus/ Young modulus.
Endothermic reaction	Reaction where energy is absorbed in order to enable the reaction.
Exothermic reaction	Reaction where energy is released.
hconv	Convection coefficient

I	Current in Amperes (A).
k	Thermal conductivity
l	Length in meters (m).
Loss modulus	Defines the viscous behaviour of the material
m	Mass in kilograms (kg).
Martensite phase	Low temperature phase of SMA; low tensile strength and Young modulus, the material can be deformed easily.
MATLAB	(Matrix Laboratory) Technical Computing Software used for data analyses.
Numeric data	Data obtained by finite element calculation.
P	P the power in Watt (W)
Q_{rad}	Radiation energy.
R	Resistance in Ohms (Ω)
Radiation	Energy transfer by medium or space.
SC	Smart Composite
Simulation	Calculated problem solution by numeric model.
SMA	Shape Memory Alloy; alloy with memory characteristics; enables shape deformation.
Smart Composite	Composite of SMA actuators in SMP matrix. Enables shape morphing performance, by deformation, fixation and subsequent recovery.
SMP	Shape Memory Polymer; polymer with memory characteristics; applied as surface material.
Storage modulus	Defines the stored elastic energy during deformation
t	time in seconds (s).
Tan delta	Damping coefficient.
T_{glass}	Glass transition temperature is the temperature point where the material transforms from glassy to elastic phase. Below this temperature, the polymer is glassy state, which is considered a rigid phase. Above this temperature the polymer is rubbery and easy to deform.
Thermoelectric activation	To enable temperature increase, electric resistivity is applied.
Transformation temperature	Temperature point when transition is initiated (austenite or martensite start temperature).
U	The potential difference in Volts (V).
Young modulus	Elastic modulus, determines the elasticity stiffness of a material.
ΔT	The temperature difference in degree Celsius (^{o}C).

ε	Emissivity, ratio of heat radiation emitted by a body in relation to the heat emission of radiation by a black body.
ρ	Resistivity in ohm*meter.
σ	Stefan-Boltzmann Constant (5.67*10e^{-8} W/(m^{2}K^{4}).

CHAPTER 1

INTRODUCTION AND RESEARCH OUTLINE

1.1 Electronic Era and Personification

Over the last 150 years, more technological developments have been found compared to any time in history. The pace of the succession of developments has increased enormously. Rapid innovations in the material and computer science, have led to an increase of electronic devices and the miniaturization of these devices.

Electronic devices as well as virtual environments are subject to personalization. We can shape our digital world according to our preferences and wishes. By personalizing webpages, program interfaces and electronic attributes, among others, our individual preferences can be communicated to the world. Customization of products plays an important role in product development. Digital fabrication methods, such as rapid prototyping, enable instant manufacturing of one-of-a-kind design models.

The high pace of innovation and the fast succession of products require frequent renewal of devices and virtual environments. A cellular phone, for example, has a maximum life time of 2 years. It is generally accepted that electronic devices are renewed frequently. Additionally, virtual environments and interfaces are subject of frequent succession of new versions and hypes. Humans have hereby become more compliant to fast developments. Electronic attributes are embedded in all layers of the society and everyday activities. These changes have an enormous influence on socio-cultural developments. The way we live has changed substantially over the last century.

Seeing these changes take place on the field of electronic devices, it is remarkable that developments in architecture are lagging behind in terms of immediate personification. The built environment does not comply with these digital and electronic advances. Buildings are built to house inhabitants over various generations. Customization and personification often means renovation and refurbishment, which generally demands a certain effort. The dynamic virtual and electronic world is a clear contrast with the static world we are living in; it does not fit our way of living.

This living environment, or built environment is designed to meet the problems of earlier generations (Studer 1970). Corbusier already pointed out at the beginning of the technological era that “our external world has been enormously transformed in its outward appearance, and in the use made of it, by reason of machine. We have gained a new perspective and a new social life, but we have not adapted the house hereto” (Corbusier 1986). Instead of being constrained by behavioural assumptions, an architecture that adapts to our changing behaviour and environmental parameters will provide a better living situation (Brand 1994). This thesis will respond to these assumptions and will focus on immediate adaptive architecture. Adaptive architecture has the ability to transform its configuration and settings immediately to meet the preferences of the users and its environment. Technological advancements play a crucial role by the accomplishment of this performance.

Aspects such as mobility and adaptability have been applied in a considerable amount of visionary projects and concepts over the last century (Kronenburg 2002). However, a translation to the commercial building industry was not always found. These visionary projects were linked to the technological developments of that time. Mainly, these technological advancements were found in other knowledge fields and were transferred into the architectural field to enhance the building performance. This knowledge transfer has played an important role in the building innovation.

1.2 Context

During the Industrial era, machine and technology influenced the experimental projects of the Avant-garde. The comparison of architecture with a machine is typical for this period (Corbusier 1986). The use of new building materials, such as glass, steel and reinforced concrete, was directly influenced by industrial developments.

In the 1960s and 1970s, Futurists and Situationists developed concepts based on multimedia techniques and the free state of mind. Groups like Superstudio and Archigram created spaceship-like designs which played a crucial role in the architectural theory (Cook 1972). With mobility and mobile parts, a step further was taken regarding the realization of the house as a machine. Constant Nieuwenhuys proposed the concept of New Babylon, in which the environment is constantly changing; every place would be different when you would return to it. Most of these visionary projects were kept on paper or built for expositions and fairs not so much for living. Unfortunately, the step to realization into the habitable environment was not supported by the available technologies.

In the early eighties, Kendall and Habraken introduced the Open Building concept as the solution for a flexible use of architecture (Kendall, et al. 2002). The main idea behind this concept was to construct the house out of a rigid main frame and lightweight subsystems. These subsystems could be changed and renewed individually without any interrelation. When specific building components were outdated, or did not meet the requirements of the users, these could be renewed without demolishing the other components. The building could be adapted easier to the user's preferences. However, the relocation of indoor walls required in most cases the help of specialized firms. It did not mean that the users could change the floor plan configuration within days.

At the end of the 1990s the computer began to play an important role in the design process (Kolarevic 2003). The computer became more and more a method of representation and was eventually used as a design tool. Digital design processes were accomplished based on dynamic input parameters. By the implementation of dynamic parameters, which defined different settings over time, adaptive design models were generated. These digital models reflected the optimization of the building setting for every specific time. The design models gained a performative character.

A different design paradigm was created by the development of the parametric design method. Parametric design was based on non-Euclidean geometry, where multidimensional solutions provided an infinite number of geometrical models (Kolarevic 2003). Contemporary design changed considerable as a result of this development in Computer-Aided Architectural Design. The progress in Computer–

Aided Manufacturing technologies allowed the translation of computer generated design model into physical buildings.

1.2.1 Performative Design

The introduction of digital design increased the possibilities to design beyond realization. Digital architectural design, with the implementation of generative processes and performance based models, translated parametric input into an adaptive building model. These parametric criteria can be related to user, environmental or structural aspects, among others. Performative architecture has thus the capacity of responding to changing social, cultural, functional, environmental and technological conditions, with an important shift from building appearances to processes of formation (Kolarevic, et al. 2005). Michael Meredith describes: "architecture should perform rather than simply form; structurally, environmentally, economically, programmatically, contextually, or in multiple formal arenas" (Meredith 2007).

With performative design, the settings of the building model, such as shape, window location, floor plan or structure, can be constantly optimized, determined by a set of parameters and programs. In terms of climate design, heat load or loss can be prevented by constant optimization of the building model. Structurally, the model can react to large forces or "normal" load situations and generate an optimal building structure. In practice, these optimizations will lead to a decrease of material use and sustainable design solutions. However, practical realization has not met the performative design models yet.

Generative and performative modelling changed architectural design from "form making" to "form finding" (Kolarevic 2003). Complex structures which transform according to performative parameters strengthen the relation between building and performance. Generative digital design models represent a dynamic configuration of the building geometry.

An example of performative design can be found in the work of Ali Rahim. Animation techniques were used as a representation tool for the geometrical shape (Rahim 2006). Spatial formations were generated by the use of dynamic systems (Figure 1.1).

Figure 1.1 Contemporary Architecture Practice, Commercial Office Tower, Dubai 2007. Image courtesy CAP.

Architect Greg Lynn implemented environmental actors in the design process with his competition entry for the Yokohama International Port Terminal. A shape-morphing animation translated these actors in a constant adaptive building. The movement and flow of pedestrians, cars and busses determined the behaviour of the building. Aspects like the speed and density of the surrounding traffic became influential parameters for the design criteria (Lynn 2008).

Performative design models play an important role in shape optimization of structural systems. The work of Mutsuro Sasaki is an example of this structural design method (Sasaki 2007). In his work the geometrical shape was analysed, in order to develop an optimal structural shape with minimal strain and deformation occurrences. This has led to a minimization of material use and structural optimization. In Figure 1.2, the structural optimization process of the roof of the Kakamigahara Crematorium is shown to illustrate this principle (Toyo Ito, 2004-2006). The force distribution in the building structure was optimized until extreme vibration in the nodes was minimized.

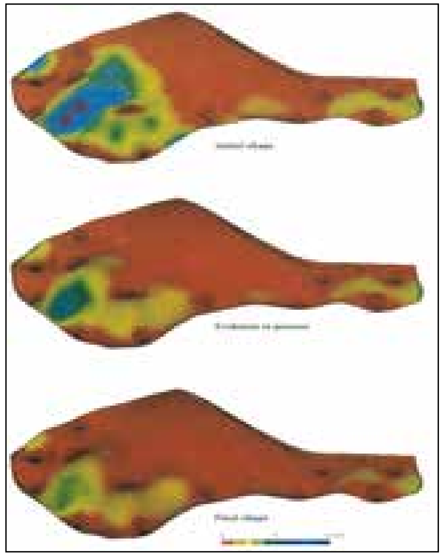

Figure 1.2 Kakamigahara Crematorium, Toyo Ito. Image courtesy (Sasaki 2007)

The parameterization of the building process has expanded on manufacturing level. Generative design processes have developed complex shapes and constructions. These shapes can now be manufactured by Computer Numerical Controlled (CNC) manufacturing or 3D printing. With the use of new manufacturing methods, such as file-to-factory[1], a direct translation can be made from the parametric design model into the building component. An example of file-to-factory is the Hessing Cockpit designed by ONL (ONL [Oosterhuis_Lénárd]). For the realization of the parametric model, numbered milling files were generated. The numbered building components were milled by automation after which the building could be assembled like a jigsaw puzzle (see Figure 1.3).

It should be noted that the adaptive aspects are hardly implemented in the realized building. In general, when the design models are realized, the performative behaviour is found to be more on the geometrical level than on an operational level. Although dynamic parameters were the basis of the adaptive design models, the realization of these models in real-time buildings remain permanent and static. Michael Speaks recognizes this issue, and stated: “there is an “apparent contradiction between the responsive dynamism of these animate models and inherently static nature of buildings” (Toy, et al. 1999).

1. File-to-factory; parametric drawings are directly translated to manufacturing files.

Figure 1.3 Hessing Cockpit, Utrecht, the Netherlands, 2005. Image courtesy (ONL [Oosterhuis_Lénárd] webpage)

Naturally, the digital models are not restricted by reality aspects, such as material technology and natural forces. This freedom enhances the immediate adaptive character of the digital design model. The aspect *time* can be very well integrated in this optimized digital environment. In real-time, this performance is restricted by technological aspects. Now the dynamic parameters are analysed and the building performance is determined by the designer, the realization of these adaptive models into tangible performative buildings is an interesting issue. The next step in generative design will be found in a direct translation of the parametric model into tangible adaptive buildings, thus creating performative environments. However, this requires a large development of material and system technology.

In conclusion, the digital design has emerged from building visualization and representation into geometrical design models. It has evolved into performative digital environments and enabled computer controlled fabrication. The next step should be found in the realization of performative buildings that can inherently adapt according to determined parameters. The immediate adaptive building performance will relate to time and movement.

Current buildings are designed to endure extreme environmental conditions. Even if the building will not meet such extreme forces during its life-time, these aspects are enclosed by rules and regulations. In terms of safety, this is fully logical. But this plays a crucial role in over-dimensioning and material usage. When the building is able to react immediately to extreme conditions by changing its settings and configurations for a short amount of time, material use can be decreased or collapse of buildings prevented. However, technological innovation is required to fulfil such performance.

1.3 Multi-Functionality

Increasing urbanization has led to conflicting situations in relation to high living standards. The incomes rise increases the demand for larger houses. Cities have become over-populated and the floor space became scarce. In some cities floor space prices have rocketed sky-high. The small floor index demands for a multi-functional use of the available space.

In contrast to the demand of larger floor spaces in cities, a majority of the buildings remain unoccupied during a considerable amount of their life-time. In general, utility buildings are in use during office hours, whereas entertainment buildings, such as theatres and clubs are mostly occupied during night-time. Outside these hours low occupancy rates can be found. Additionally, large amounts of utility buildings remain unoccupied due to functional decline.

This contradiction is hardly acceptable. Ideally, the occupancy rate must be optimized by the development of multifunctional buildings. However, practically and technically it is very complex to, for example, transfer offices into clubs during unused hours. The functional requirements are extremely different.

In order to facilitate an optimized used of the building stock, adaptive buildings which can immediately adapt to functional requirements are necessary. Buildings must become more compliant to functional use by increasing the adaptive character. Immediate adaptation of the built environment will enhance the multi-functional use and enlarge the utilization of the space.

1.4 Adaptive Architecture

In this thesis *adaptive architecture* is defined as architecture of which specific building components can adapt in response to changing parameters, such as user preferences, environmental aspects or mechanical changes (Lelieveld, et al. 2007). This performance is reversible and can be repeated. Adaptability in architecture is not a new phenomenon; many building components have adaptive characteristics. Building components can be changed according to function and usage; doors and windows can be opened and closed, walls can be demolished or constructed, etcetera. In most cases the adaption is a conscious adjustment carried out by users.

When considering the building structure, such as walls, facades or roofs, adaption is based on a certain amount of effort and requires a longer time span. To initiate change often means that renovation or redecoration is required. These examples are considered *adaptable*. Adaptive architecture is based on a system that realizes immediate, reversible and effortless transformations.

Various housing projects have been executed with adaptive wall components. Different spatial configurations are possible by moving the inner walls. The technique behind these systems is based on hinges, sliding walls or bolting systems. In the case of bolting systems, a considerable amount of effort is required for the reposition of the wall.

Follow-up studies on the use of these adaptive systems in the Netherlands showed that in practice the adaptive components were not intensively used (Motmans, et al. 1991; Verweij, et al. 2006). In most cases the adaptive wall systems were not used at all. Occupants who bought the house second or third hand were sometimes not conscious of the fact that their house had the option of an adaptive floor plan. In general, these systems were not used due to the fact that these were relatively complex. In some cases, the call of a company service was required to envision the change of the wall systems. Additionally, problems such as noise were indicated as large disadvantages of the system during practice. These arguments address that the failure of the adaptable wall systems did not directly indicate that the users did not prefer an adaptive wall system. Moreover, the technical translation of these systems requires optimization (Motmans, et al. 1991; Verweij, et al. 2006). It is clear that the importance lies in the optimization of the design and improvement of these technical solutions.

Adaptation of building components can also be realized by an automated process. Here, complex mechanical components are implicated in the building system, which lead to larger construction sizes, high maintenance, high costs and noise generation. An example can be found in the exterior application of adaptive daylight systems. These systems control the thermal load and blinding by the sun. The application of these devices leads to the addition of heavy systems, which generate noise during operation and frequent break down (Figure 1.4).

Figure 1.4 Adaptive mechanical daylight system.

The purpose of this research is to investigate the current state of adaptive architecture and search for technological advancements for the optimization of the adaptive performance. This will be illustrated by a case study on an adaptive building component. Additionally, the user receptiveness on adaptive environments is analysed, to gain insight on the functional perception.

1.4.1 Adaptive Building Component

The purpose of this research project is to translate the concept of an immediate adaptive architecture into a tangible expressive environment. The performance of this tactile environment will be facilitated the realization of an adaptive building component (ABC). The focus hereby lies on a reversible shape-morphing building component, which enables an immediate performance. The desired deformation is based on a hinge-like shape-morphing performance. Figure 1.5 illustrates the two-dimensional deformation of the adaptive building component.

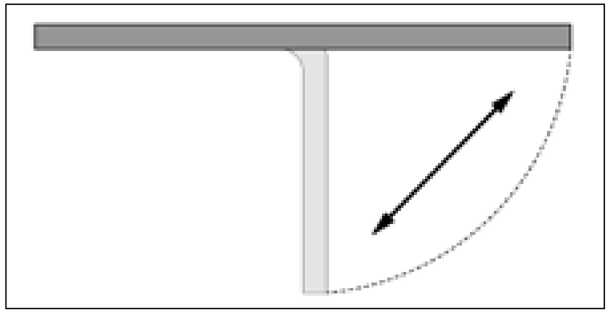

Figure 1.5 Schematic drawing of deflecting performance

The desired deformation should be realized without the addition of external actuation mechanisms. The presented slim dimensions are an important aspect, and should be leading during the material selection process. Therefore, particular attention should be paid to advanced material technologies. Smart materials have the ability to realize shape deformation based on intrinsic material characteristics. This research will indicate if these materials are suitable for the desired performance.

Current material research has shown significant advances with the development of "smart" materials. Smart materials are materials "capable of automatically and inherently sensing or detecting changes in their environment and responding to those changes with some kind of actuation or action" (Ansari, et al. 1997). These materials have the characteristic to detect an external stimulus and to initiate an appropriate action, by adapting the material properties (Srinivasan, et al. 2001). This means that the material possesses over both sensory[2] and actuation[3] characteristics.

This deformation should be fixated without a continuous energy input. After the deformation, the ABC should initiate a subsequent recovery and return to its initial flat shape. The ABC should meet the structural requirements for application in the outfit, infill or interior of the building system, such as ceilings, non-loadbearing walls, facades and furniture.

1.5 Research Objective

The objective of this thesis is:

The realization of an adaptive building component with the use of smart material technology

The following aspects will be studied in order to realize this objective:

1. Adaptive architecture

The state-of-the-art of adaptive architecture is analysed to gain insight into the current technologies and realizations. During this study, the projects are analysed according to technological attributes and categorized accordingly.

2. Smart material technology

2. When a material has sensor characteristics, it is able to detect a certain signal or stimulus.
3. An actuator is able to perform a function. The device is able to give a physical action.

The emphasis of this research project lies on the application of advanced material technologies, whereby adaptation will be established by intrinsic[4] material properties. This indicates that the materials should have performative material characteristics, to enable some sort of property change. Smart materials dispose over such behavioural properties. To gain insight into the practical application, the application of smart material systems in realized building projects is analysed.

By introducing smart materials in the building system, the building system can sense, diagnose, process, control, (re)act and be optimized on the level of performance. A new functional relationship is established between the environment and the users. By integrating different functions in the building system, the performance and usage of the building will get a different meaning. In other knowledge fields the advances of smart materials show promising application possibilities. It is time to implement this knowledge and realize that building components do not have to be necessarily static. Material behaviour can be optimized on the level of performance.

3. Design scenarios

To show the application of the shape-morphing adaptive component in the building system, different design propositions will be presented. The performance of the adaptive component will be illustrated by the application on different scales.

4. User receptiveness

A user study will be performed, to analyse user preferences and acceptability on the subject of adaptive architecture. Is instant adaptability of the building acceptable? To what extent do users want to adapt their environment? The user preferences of different adaptive building components will be analysed.

5. Study of adaptive building component

The implementation of smart material systems in the built environment is subject of this research aspect. After the theoretical analysis, the realization of the ABC based on the presented requirements is analysed. The emphasis lies hereby on the realization of the shape-morphing performance, based on smart material technology. The concept of shape-morphing building components is founded by the fabrication of a working prototype.

6. Characterization and optimization

The performance of the prototype will be characterized and optimized by material experimentation and validation. Since the activation of the smart materials requires a precise control system for optimum performance, special attention has been drawn to this subject. By the use of numerical models, the optimal control settings will be simulated.

4. Based on material characteristics.

1.6 Knowledge Diffusion and Technology Transfer

This research project makes use of the theory of product development processes. A process of product development is based on three different knowledge domains (Poelman 2005). These domains are covered by the fundamental knowledge of materials (the technology), the application of these materials in design and the fabrication. The process of product development is visualized by Eekhout (Figure 1.6) (2005). Innovation is found on the level of technology development, where fundamental developments find their way in the application design. The technology development functions as an interdisciplinary platform between fundamental research and practice (Eekhout 2005). By moving through the different stages of the knowledge domains, cross-fertilization will lead to new insights and developments and enhance innovation.

This research project borders the fundamental technical level with the characterization of the smart material systems and the practical level by the application in architecture. The smart material systems will be applied in an adaptive building component, which will be tested, justified and optimized to prove the performative principle; the technology development. Hereby, the process comprehends the fundamental research domain, the design and the practical applicability. This indicates that this project is moving constantly through the different knowledge domains.

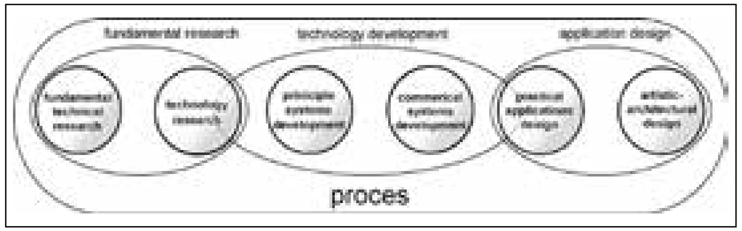

Figure 1.6 Linear model of the product development (Eekhout 2005)

The relation of engineering, processing and realization leading processes in product development is visualized in Figure 1.7. This figure is based on the material triangle of W. Poelman (2005). Innovation is initiated by analysing the work areas of the different domains and filling the void between these areas. By crossing the borders of the different knowledge domains, new insights can be obtained for practical application. The interrelation between the three knowledge domains plays a crucial role for the developments of new products. Developments on one field influence the other knowledge domains sincerely. Different fabrication techniques do influence the design and the related materials. Specific materials require a specific fabrication technique and therefore determine the design possibilities.

The technology diffusion process could be regarded as an associative process between desired functions and existing technologies. A general bottleneck in the diffusion of technological knowledge in the design process is the availability of knowledge about the existing technologies (Poelman, et al. 2007). Improving the communication between the different parties will lead to further innovation.

The process of this research project will cover the three knowledge domains; material research, design and fabrication. By stepping back and forth through the different domains, the adaptive building component will be validated and optimized. Working as an architect on the fabrication and material level, will gain new insight into the application field of the specific material technologies. Since the utilized material technologies are relatively new, it is crucial to acquire knowledge on material level and implement this knowledge in a working prototype. By translating the adaptive performance of the prototype in different design scenarios, the practical application is visualized.

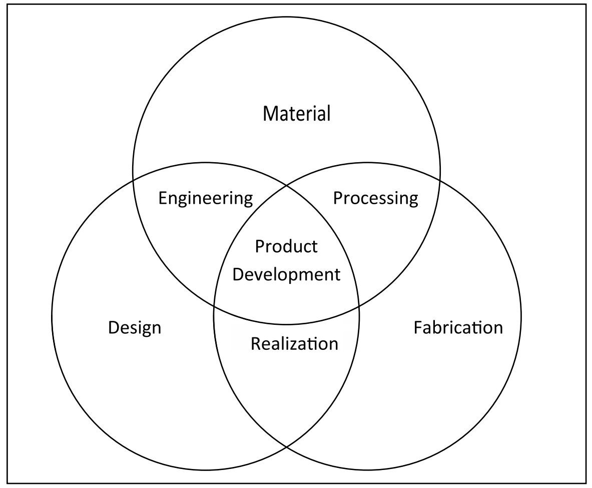

Figure 1.7 Technology transfer between the different knowedge domains based on the materials triangle of W. Poelman (2005)

In addition to knowledge diffusion on the level of knowledge domains, the diffusion between different professions is also an important aspect in the innovation process. In industries like aerospace, maritime, medical and automotive, material innovation is developing at a higher pace compared to architecture. Especially in these fields, technological achievements can be found of smart material systems. Due to technology transfer between different industries, unexpected applications of materials and techniques can be discovered. An important aspect in this research project is the implementation of knowledge and technologies from other professions into the field of architecture.

1.7 Research Method

This project will be performed on the bidirectional level of *research driven design* and *design driven research*. In the course of *research driven design*, technical research will be implemented into the design activity, to enhance technical applications and product innovations. The aim of *design driven research* is to explain implications of design interventions” (Breen 2002). In this research process the technical applications of the design content will be validated by empirical research. In Figure 1.8, a representation of this iterative process is defined.

The process is initiated with a design concept of an adaptive building component with shape-morphing properties. This performance will form the foundation of the research process. An analysis is carried out to gain an insight on the realization of the adaptive component. Different manufacturing strategies as well as materialization solutions are included in this step. The adaptive component will be evaluated and validated by experimentation. The acquired knowledge will be implemented in the design model. Finally, the adaptive component will be optimized, after which the components will be tested and validated.

Due to the iterative nature of this process, the adaptive component will become more detailed and optimized. Ideally, this process will be finalized by the application of the adaptive component in the building system.

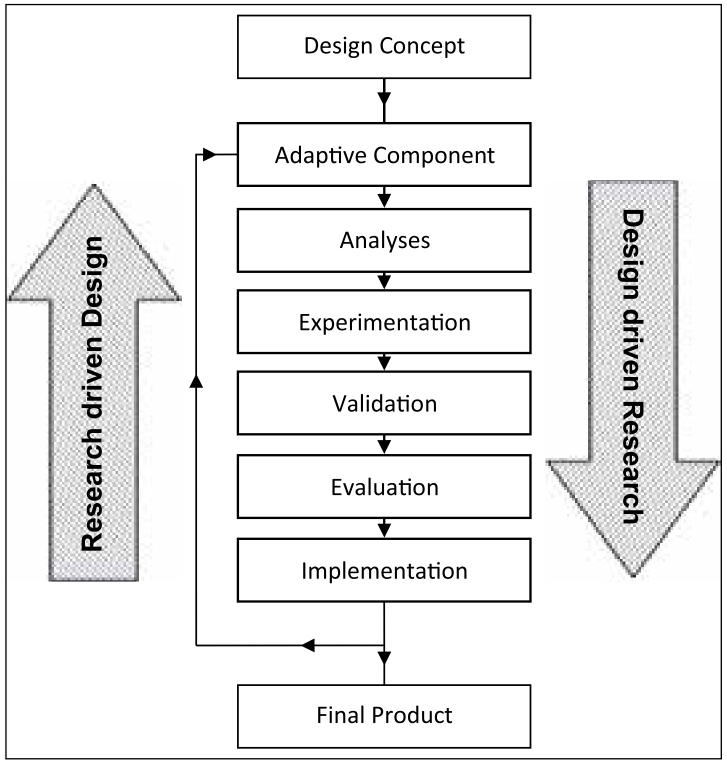

Figure 1.8 Iterative research process of adaptive building component

1.8 Dissertation Outline

The outline of this dissertation is presented in Figure 1.9. This dissertation is divided into 4 main parts. Each part focusses on a specific procedure. This partitioning will underline the function of each chapter.

Part 1 presents the introduction; this includes the research background and outline

Part 2 focusses on the theory and concept. The theory behind the two main subjects of this thesis is studied, namely adaptive architecture and smart material systems. Finally, the application of the adaptive building component into the building system is illustrated by different design scenarios.

Part 3 discusses the realization of an adaptive building component. This includes the experimentation, characterization, fabrication and optimization of a shape-morphing building component. To gain understanding of the user receptiveness on adaptive environments, a user study has been performed.

Part 4 will finalize this thesis with the conclusions and discussion.

This thesis will start with the theory of adaptive architecture and smart material systems. Chapter 2 provides insight into the subject of adaptive architecture. Different levels of adaptive architecture are determined, associated with technological innovation. An overview is given of realized adaptive projects, with a retrospective of the technological framework and level of adaptation. Chapter 3 focusses on the practical application of smart material systems in architecture. This chapter is concluded by defining the design constraints of an adaptive building component.

Chapter 4 will present application concepts of the adaptive building component (ABC) in an architectural framework. Various behaviour aspects of building elements will be presented which are proved to be feasible within the presented properties of the prototype.

Chapter 5 will present the results of a user inquiry on the receptiveness of adaptive environments. This study will gain insight regarding the ideas of the users on the subject of adaptive architecture. Different adaptive concepts are validated and will generate perception of adaptive architecture in relation to its users.

Chapter 6 describes the performative aspects of the adaptive component, after which the material selection of the component will be presented. With the implementation of shape memory materials it will be possible to fabricate a shape-morphing prototype. Not only are the material characteristics discussed in this chapter, but also the application of these smart materials in the prototype. The working principle of the ABC is presented based on the selected smart materials.

In chapter 7, the material properties will be characterized by experimentation for the intended application in the prototype. Mechanical characterization of the specific components will gain insight into the performance and fabrication. Chapter 7 will present a real-time shape-morphing prototype.

In chapter 8, the thermoelectric activation of the ABC is studied. A numeric model is developed which matches the thermal performance of the presented prototype. This numeric model is validated for consistency and correctness by thermal experimentation. In this chapter, optimized operation settings are presented.

Chapter 9 draws the conclusion from all the research objectives and the obtained results. This chapter will propose recommendations for further work and application.

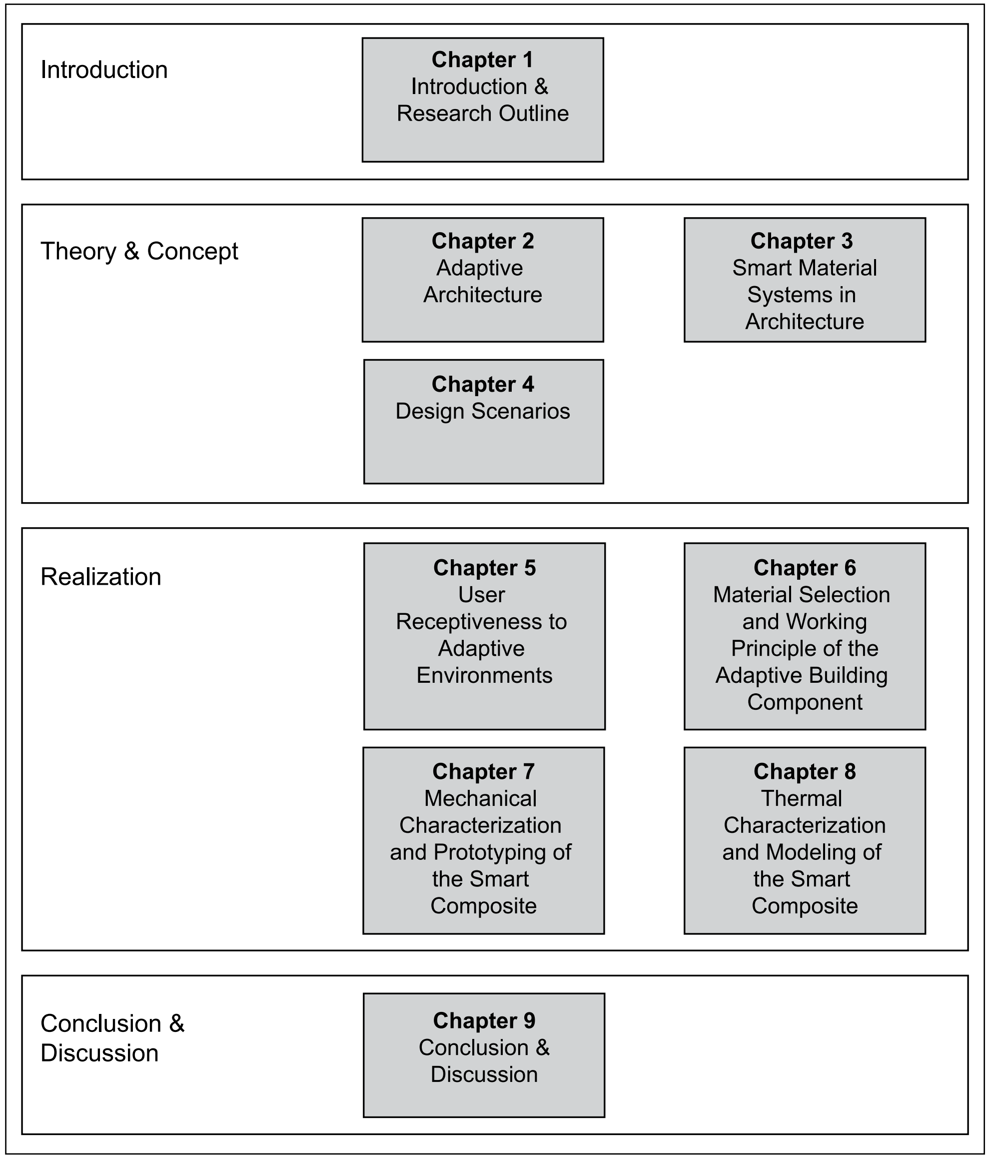

Figure 1.9 Outline of the dissertation

1.9 References

Ansari, F., Maji, A., et al. (1997). Intelligent civil engineering materials and structures a collection of state-of-the-art papers in the applications of emerging technologies to civil structures and materials. New York, ASCE.

Brand, S. (1994). How Buildings Learn; What Happens After They're Built. New York, Viking.

Breen, J. (2002). Design driven research. Ways to study and research urban, architectural and technical design. T. M. Jong and v. d. D. J. M. Voordt. Delft, DUP Science: 137-149.

Cook, P. (1972). Archigram. London, Studio Vista.

Corbusier, L. (1986). Towards a New Architecture. New York, Dover.

Eekhout, M. (2005). Delft Science in Design a Congres on Interdisciplinary Design, Delft, Delft University of Technology Faculty of Architecture.

Kendall, S. and Teicher, J. (2002). Residential Open Building. London, Spon.

Kolarevic, B. (2003). Architecture in the Digital Age Designing and Manufacturing. London, Spon.

Kolarevic, B. and Malkawi, A. M. (2005). Performative architecture beyond instrumentality. New York, Spon.

Kronenburg, R. (2002). Houses in Motion the Genesis, History and Development of the Portable Building. Chichester, Wiley-Academy.

Lelieveld, C. M. J. L. and Voorbij, A. I. M. (2007). The Application of Dynamic Materials in Adaptable Architecture. ManuBuild, The Transformation of the Industry– Open Building Manufacturing. M. Sharp. Rotterdam, The Netherlands, CIRIA, Classic House.

Lynn, G. (2008). Form. New York, Rizzoli International Publications, Inc.

Meredith, M. (2007). Never Enough (Transform, Repeat, Nausea). From Control to Design. T. Sakamoto and A. Ferre. Barcelona, Ingoprint SL: 6-9.

Motmans, M., Hartigh Den, M., et al. (1991). Flexibele HAT-woningen in Leiden; een onderzoek naar gebruik en waardering door bewoners van verplaatsbare ruimtescheidende kasten. Delft, Publikatieburo Bouwkunde.

ONL [Oosterhuis_Lénárd] (webpage) Retrieved 2012 from www.oosterhuis.nl.

Poelman, W. and Lelieveld, C. M. J. L. (2007). From Nano to Macro; Application of Dynamic Materials in Architecture. Shell and Spatial Structures: Structural Architecture -Towards the future looking to the past. Venice, Italy.

Poelman, W. A. (2005). Technology diffusion in product design towards an design process. Ph.D. Dissertation, S.n.

Rahim, A. (2006). Catalytic Formations-Architceture and Digital Design.

Sasaki, M. (2007). Mutsuro Sasaki. From Control to Design. T. Sakamoto and A. Ferre. Barcelona, Ingoprint SL: 68-116.

Srinivasan, A. V. and Mcfarland, D. M. (2001). Smart structures analysis and design. Cambridge, UK, Cambridge University Press.

Studer, R. (1970). The Organization of Spatial Stimuli. The Spatial Behavior of Older People. L. Pastalan and D. Carson. Ann Arbor, Mich, University of Michigan Press.

Toy, M. and Perrella, S. (1999). Hypersurface architecture II. London, Academy Editions.

Verweij, S. and Poelman, W. A. (2006). Evaluation of Flexibility Options in Different Housing Projects, an Exploration of Possible Flexibility for Second Users in Multi-storey Housing. IASS International Conference on Adaptability in Design and Construction. Eindhoven, The Netherlands. **1:** 2.38-32.42.

CHAPTER 2

ADAPTIVE ARCHITECTURE

2.1 Introduction

Adaptive architecture is defined as an architecture of which specific building components can adapt in response to changing stimuli, such as user input and environmental aspects (Lelieveld, et al. 2007). These adaptations can be found in different components of the building system. Additionally, adaptation can be envisioned on different technical levels. A door can be opened or closed. This performance can be executed by human power (manually control) or automatically by electric power (sensor detects approach and door opens). The levels of adaptive architecture are categorized to gain insight into the application of different techniques and performances in the building system. *Adaptive architecture* is utilized as a coordinating term for the different levels of architectural adaptation.

In literature, different connotations and definitions are given for architectural environments which show adaptive performances. In order to gain insight into the different connotations, an overview is given of the corresponding terms and definitions. Most definitions include the technical performance of the building. Therefore, these terms are used for the categorization of adaptive architecture. The presented categorization of adaptive architecture will be used for further analysis of the current adaptive building stock.

The state-of-the-art of adaptive architecture is studied. By analysing realized building projects, the current state of adaptive architecture can be analysed. The building system is classified into different components in order to determine the field of focus of this study. The classification will help to gain insight into the adaptive building components of the realized buildings.

Finally, the level of adaptive architecture is analysed which can be realized in the discourse of the current available technologies. Additionally, the results of this study will be implemented in the research goal.

2.1.1 Categorization of Adaptive Architecture

Various terms, such as dynamic, responsive, interactive, flexible and intelligent are used for architecture which has adaptive characteristics in some way. In order to gain a better understanding of these terms a short overview is given. It appeared that profound differences between these terms are based on the matter of complexity of the adaptation. Due to the ambivalent character of the definitions and connotations, a categorization of adaptive architecture will be presented to create clarity on this subject. The analysed literature will serve as the basis of this categorization.

2.1.2 Terminology

In literature, the term *dynamic* architecture or structure is used to define an environment which is able to adapt to the varying needs of the users, to changing environmental circumstances or to the designers desires and imaginations (Edler, et al. 2006). Here, the adaptation is set in a framework determined by parameters. Another term, *responsive,* is found as a definition of an intelligent environment, which has “purpose and intentions characteristics”, and can be indicated as a “self-reproducing autogenic environment” (Negroponte 1975). A concurrent difference between these connotations can be found in the executed performance of both systems. The definition of *dynamic* indicates a predefined performance, where *responsive* appears to dispose over self-initiative characteristics.

Another term is *interactive*, the term relates to a physical change of the architectural space as a result of embedded computation (Fox, et al. 2009). Additionally, the performance is recognized to be optimized by shifting from a mechanical (current) paradigm to a biological paradigm (future) (Fox, et al. 2009). Furthermore, the term *interactivity* is used as an “indicator of change in an installation or environment that a person can enforce, taking into account the mechanical, physical and psychological implications” (Dekker 2006).

In other work *intelligent* architecture refers to “built forms whose integrated systems are capable of anticipating and responsive phenomena, that affect the performance of the building and its occupants, whether internal or external” (Kroner 1997). *Intelligent* architecture responds to its occupants and the local and global environment in a sensitive, supportive and dignifying matter (Kroner 1997). This indicates that a different term is linked to similar performances. The integrated systems can be indicated as the initiator and controller of the alteration based on user performances and requirements, where in some cases the environment is added as a stimulator.

Similar building performance is attributed to *flexible* architecture. The ultimate *flexible* interior may be one that is completely “amorphous and transitional, changing shape, colour, lighting intensity, acoustics and temperature, as the inhabitants move through it-abandoning flat horizontal surfaces and demarcations between hard and soft, warm and cold, wet and dry” (Kronenburg 2002). Based on the avant-garde principles, a flexible floor plan is determined as an open space, which can be freely arranged based on the required or desired activities (Leupen 1997). The open floor plans and non-bearing façades stimulated a free use of space and enabled façade openings on every desired location.

This variety of definitions and connotations make it possible to identify different gradations of adaptive architecture. A completely amorphous environment requires more technical advances in order to realize adaptation compared to an installation or environment that change only within physical and mechanical possibilities. Therefore, the technological developments play an important role in the categorization of adaptive building components. In the following paragraph adaptive architecture is defined and categorized according to technical specifications.

2.1.3 Categorization and Definition

Figure 2.1 shows, the different levels of adaptive architecture. This division is based on the technological and performative parameters which indicate a specific character. The technological and performative advancements increase in terms of complexity from left to right.

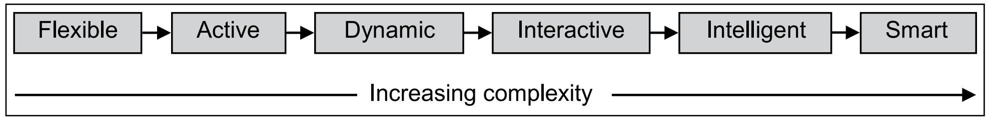

Figure 2.1 Levels of adaptation in order of sophistication

In Table 2.1, an overview is given of the specifications of the specific categories. The definitions of the different terms are explained in the following paragraphs.

Table 2.1 Overview of categories and specifications

	Control	Performance	Required technology
Flexible	Manual-Mechanical	Single-functional	Mechanical system
Active	Manual-Electric	Single-functional	Energy & system
Dynamic	Sensor	Single-functional	Sensor & system
Interactive	System & user interface	Single-functional, multiple options	Sensor & system & interface
Intelligent	System & user interface	Multi-functional	Ubiquitous system
Smart	Ubiquitous	Multi-functional	Artificial Intelligence

Flexible The first level of adaptive architecture is flexible architecture. Flexible architecture exploits the feature of a simple modification of specific building components. This modification is unilaterally controlled by the user. The building components are changeable and activated externally by human power. Flexible building components will only facilitate *one* adaptive function. An example of a flexible building element is a space divider; it can be opened or closed according to the user preferences and by human stimulation. In order to develop flexible systems the technical requirements are mainly mechanical techniques such as bearings, hinges, slides and rails.

Sliding mechanisms or bolt systems are widely used for flexible floor plans. With the use of sliding walls, new space configurations can be realized that meet the specific functions and requirements. The Rietveld-Schröder house in Utrecht, the Netherlands is a famous example of flexible architecture (Figure 2.2). In this project, the spaces can be reconfigured by the use of rotating and sliding walls.

Figure 2.2 Rietveld-Schröder house. Image courtesy unknown

Figure 2.3 Delfts blauw, Delft, De Architecten Cie., 1998

Active An active building component is fully controlled by the user, whereby a pre-set reaction is given to a specific command. The user is the initiator of a pre-set performance. The command can be, for example, given by the push of a button or via a touch screen. This means that push-button technology and user interfaces are important aspects for the realization of active architecture. System technology, such as actuating systems, plays an important role in the translation of the command into a certain action. Additionally, an energy source is required to execute the command.

An example is an automated door; the door can be opened by the use of an electric mechanism activated by the push of a button. It should be noted that the user is fully in control of the systems' performance, the system will not perform without active command of the user.

An active adaptive system is illustrated by the façade system of the Delfts Blauw apartment building in Delft, the Netherlands, from the architectural firm "de Architecten Cie." (Figure 2.3). The sun shading system is constructed as a sliding system. Within the sliding principle, different configurations are possible. The location of the shutters can be modified along the whole rails by a motorized control system. This performance is defined as an active system. The angle of the lamellas is controlled manually and can therefore be regarded as an active system. In appendix 1, a short description of this project is given.

Dynamic When a building component is dynamic, it has the ability to change its configuration without manual control of the user. The building component detects a certain change and reacts accordingly according to programmed systems. The adaptive performance of the building is confined in a framework and programmed in advanced. Advancements in computer and sensor technology are required in order to establish dynamic environments.

An electric sliding door can be considered *dynamic.* These systems detect the approach of a person by a sensor, after which the door opens automatically. After passing through the door, the door closes subsequently. The door can either be open or closed as a reaction to an input stimulus; either there is a person approaching the door or not. The system will only react to one input.

An example of dynamic building components are the windows of the Chabot College, by tBP Architects. The transparency of these windows can be adjusted according to amount of sun radiation. The window can be fully transparent or translucent to prevent heating and glare. The system is automated controlled by the use of sensors. However, the automated performance can be manually overruled by the users.

Interactive Interactive architecture instantly reacts on user performance or environmental changes. It can communicate with the user or environment on an immediate level (Oosterhuis 2002). When a certain situation reoccurs, the system will "remember" the user's preferences and react accordingly. The performance of the building is realized on a single-functional level. This indicates that only one performative aspect is facilitated. Developments on interactive architecture are related to the integration of advanced computer systems in the building system.

The door can illustrate the principle of an interactive system. An electric door can increase its performance speed, by detecting the approaching speed of the user. When approaching fast, the door opens fast. The user can hereby adjust the opening and closing performance. Additionally, the interactive system can determine that the door should open by a certain temperature, for ventilation purposes. Also, the system can determine whether the person approaching the door wants to go through the door, or only pass the door's location without actually entering. In terms of operation, the door only opens and closes, but the manner of opening and closing is based on variable input definitions.

Figure 2.4 Chabot College, with left the translucent window configuration and left the transparent window configuration. Image courtesy Eric Sahin.

An example of an interactive building project is the Saltwater pavilion by ONL [Oosterhuis_Lénárd] (Figure 2.5). In this project, digital models react on external stimuli, which are derived from environmental parameters such as user behaviour and weather conditions (ONL [Oosterhuis_Lénárd] webpage). The digital models are translated into real-time performance of projections and sound. The user can react on this projection and establish a relation with its environment (Figure 2.6). The performance is executed within a specific framework, which is set by a computer programming specialist.

Figure 2.5 Saltwater pavilion top view. Image courtesy (ONL [Oosterhuis_Lénárd] webpage).

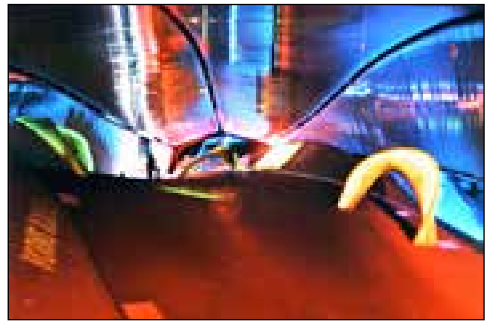

Figure 2.6 Interior view Saltwater pavilion. Image courtesy (ONL [Oosterhuis_Lénárd] webpage).

Intelligent Intelligent architecture is best explained by the definition of Collier and Thelen (Collier, et al. 2003); "*If the system adapts itself to the users' interests and interaction preferences and works cooperatively with the user to accomplish specific goals with the use of additional sources of knowledge to meet the needs of the user, a system is considered intelligent*".

The system interacts with the user and/or environment and reacts on a multi-functional level. The system can detect, process, decide whether to react, how it will react and when. The building system has the ability to take the initiative to adapt and how to adapt. An intelligent system can detect that the door is open, even when nobody is passing and can thereupon close the door. If the user wants the door to be opened, for example for ventilation purposes, the system can adapt and learn that the door should stay open during the specific situation. Simultaneously, the heater will be turned down and the sun-shading will be closed to control the indoor climate. The system will understand the purpose of the opened door and the door will remain open when such situation re-occurs. The door will hereby not only be a gateway, but also a control system for climate optimization. In the case of intelligent architecture, not only will the door be an adaptive element, but it will also be part of a system of related intelligent elements controlled by a ubiquitous computer system. In this example, the door, heater and sun shading system interrelate and are part of one system.

This illustrates that reactions on re-occurring situations will not necessarily lead to the same adaptation. The system has the ability to *learn* from its environment or user preferences.

Research on domotics, assistive technology and ambient intelligence is based on the concept that integrating technologies in our environment lead to a transformation from stand-alone products to embedded systems. These technologies support users in a variety of aspects such as safety, energy saving, caring, information, comfort and communication. Additionally, the function of entertainment is also facilitated at any given moment at every possible place (Aarts, et al. 2003; Lorente 2004). As all systems are integrated and controlled by one intelligent system, an optimized performance of the building system can be established. This could be illustrated by an example of indoor climate and comfort. By extensive sun radiation, the sun shading will close automatically, the light system tuned on and the heater dimmed. Additionally, the thermal energy can be stored and released during situations when the indoor temperature is low. Thus, all integrated systems collaborate and can be adjusted for optimum performance. The system should be able to learn from user behaviour and react on different situations by a determined performance.

In Ambient Intelligence a full integration of technology and knowledge will lead to systems which fully collaborate but have also the possibility to take over tasks when other systems drop out. Ambient Intelligence anticipates on user actions or environmental changes without conscious mediation (Collier, et al. 2003).

Smart Smart architecture has the ability to grow, evolve, adapt and learn. It shows self-initiative and has learning capabilities. In comparison to intelligent architecture, the system does not only learn by the actions of users or changes in the environment, but also evolves according to its own discretion. The smart system is completely integrated into the life and behaviour of the users and environment. As Vincent (Vincent 2001) describes it;” the ultimate smart structure would design itself”. The relationship between the building system and its user will become similar to human interaction; the building will become reactive to emotions. To create smart adaptive systems, new technologies are required that are not currently available. Knowledge transfer is an important aspect for the development of smart architecture. Developments in artificial intelligence and material technologies are important requirements for the realization of buildings which can perform on a smart level.

A smart system can be illustrated by a bio-mimicry system, which can function with a similar principle as biological processes. The pervasive systems can grow, evolve, breathe and think like living organisms. The complexity of biological processes is often not fully understood. Especially on the level of implementing this knowledge into smart building projects, there is still a long way to go. However, it offers inspiration for visionary architects who imagine growing buildings and evolutionary design. An interesting example is the work of John Johansen (Figure 2.7). He envisions a building that can grow out of a seed. The seed contains an integrated architectural code, which holds all information of the building’s features (Johansen 2002). The building can adapt itself spatially by reconfiguring its molecular system and can grow and recover, based on the behaviour of living organisms.

Figure 2.7 Nano-architecture, enables the growth of new spaces. From left to right, the evolution of a new set of spaces is illustrated. Image courtesy John Johansen (2002).

2.2 Building System Classification

In order to determine in what way and to what extend the adaptive characteristics are envisioned in realized adaptive building projects, the building system is classified into different types of building components. Subsequently, the building components can be subdivided into elements. In Figure 2.8, an overview is given of the building system classification. This classification is based on the work of Brand (1994). In his work, the building components are categorized by the life expectancy. The lifetime of the building component determines when renewal is required. By constructing the building components in such a way that alteration can be executed independently, without the demolishment of the other components, the building system can be optimized. This idea underlines the Open Building principle, where, among other things, the disentanglement of the building system in subsystems is an important issue for enhancing flexibility (Dekker 1998; Kendall, et al. 2002). In this research, the classification is used to determine the focus field. It is impossible to analyse the whole buildings system. It will help to clarify which building component enables adaptation.

The first component of the building system is the *structure* of the building, which establishes the shape of the building and ensures its stiffness. The lifetime of a building structure is direct related to the lifetime of the building and is generally between 50 and 300 years, although, most buildings do not exceed a lifetime of 60 years (Brand 1994).

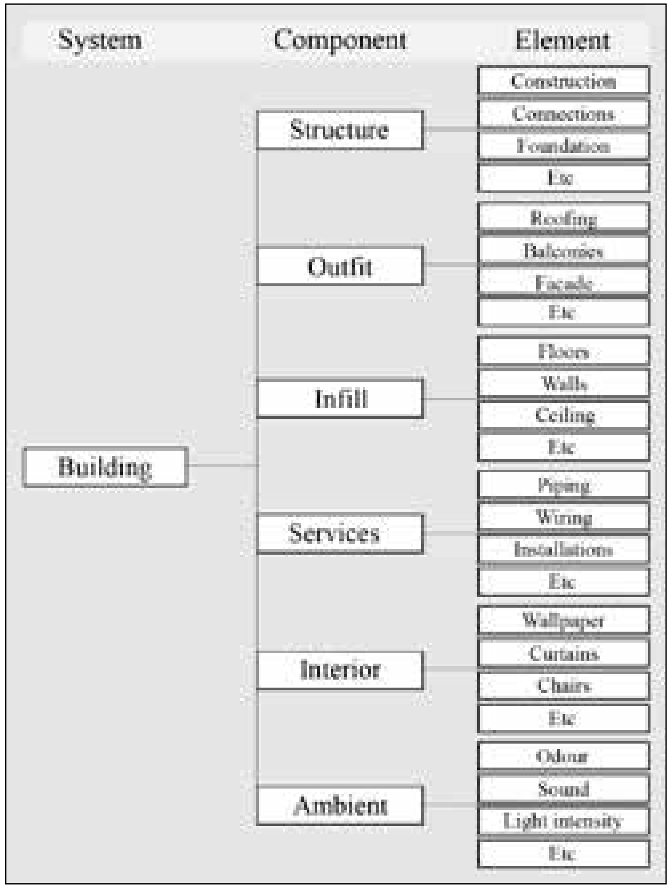

Figure 2.8 Overview of building system, category (components) and subcategory (elements)

The exterior finishing elements belong to the *outfit* category. All exterior elements attached to the building structure are part of the outfit of the building. This category includes the façade elements, the roofing and additive elements such as balconies. The lifetime of the outfit can be around 20 years (Brand 1994).

The next category is the *infill* of the building. The infill contains all finishing elements of the interior of the building. Examples of elements in this group are ceilings, floors and walls, including non-loadbearing walls. The lifetime of the infill is roughly 10 to 30 years.

The fourth component category encompasses the *services* of the building. This category includes the technical installations, such as central heating, air control and networks, such as wiring and piping. The lifetime of these services elements is around 7 to 15 years (Brand 1994).

The component *interior* comprises all elements which are used to decorate and make the building comfortable for living. Interior elements are considered attachment to the building and are relatively simple to renew. It includes furniture, products and finishing. Elements of this category include products such as chairs, desks, closets etc. Finishing like paints and carpeting are included in this group, as these aspects belong to the decoration of a house and can be renewed without considerable effort. The lifetime of this component is somewhere between days, months and years.

The last component category of the building system is the *ambient* aspect. The ambient component of the building focusses on the sensorial experience of the building system. Ambience is not a tactile component, but based on the experience of space. The ambient aspects are a result of the experience of the previously mentioned tangible components. An example of ambient elements is the intensity and colour of illumination, which influences the ambient atmosphere of a room. This component cannot be defined by its life expectancy, as it is dependent on the other building components.

2.3 Projects

To gain insight into the current state-of-the-art, realized adaptive architectural projects were analysed. This analysis focused on the method and the level of adaptation. The projects have been all realized and enabled an immediate, reversible and continuous adaptation. The analysis was limited to the *structure*, *outfit* and *infill* of the building system. *Services* and *interior* are more product related and are therefore excluded from this analysis.

The projects were selected based on the innovative usage of adaptive building systems. It is important to note that the presented list is by no means complete. In order to create an overview of the technological developments over time, the analysis started at the beginning of the twentieth century. Only one project is analysed based on any given technology and its specific application. Especially, with regard to the contemporary application of LEDs in façade elements, many examples can be found which have the same application purpose. Additionally, on the subject of revolving buildings various examples could be found (Randl 2008). Only three examples are included in this study, which all show different revolving performances.

2.3.1 Results and Analysis

In Table 2.2 an overview is given of different adaptive building projects. The projects are sorted based on their construction date. A short description of the presented projects is given in Appendix 1. It should be noted that on the level of *structure*, *infill* and *outfit* no current examples of intelligent and smart behaviour have been found. Currently, interactive architecture is mostly realized by projections, sound and illumination. As these systems mostly perform on ambient level these are excluded from this analysis.

Table 2.2 Overview adaptive architecture projects

	Architect/ designer	Name Project	Place	Year	Component	Method of adaptation	Level
A	Rietveld, Gerrit	Rietveld-Schröder House	Utrecht, The Netherlands	1924	Infill	Manually reconfigurable sliding walls.	Flexible
B	Rohe, Mies van der	Tugendhat house	Brno, Czech Republic	1930	Infill	Draperies on ceiling tracks.	Flexible
C	D'Angelo, Floyd	Aluminum House	Snow Creek, USA	1962	Structure/ outfit	House structure on motorized rotating pole. Activated by sun angle.	Dynamic
D	Holl, Steven	Fukuoka apartment building	Fukuoka, Japan	1992	Infill	Manually pivoting elements.	Flexible
E	De Architecten Cie.	Delfts Blauw	Delft, The Netherlands	1998	Outfit	Motorized configurable sliding shutters and windows.	Active
F	Atelier Brückner	Cyclebowl	Hanover, Germany	2000	Outfit / Structure	Pneumatic control of roof and façade transparency. Sensor controlled louver system.	Dynamic
H	Ban, Shigeru	Naked House	Tokyo, Japan	2000	Infill/ Interior	Manually movable units.	Flexible
N	Luigi Colani	Rotorhouse	Germany	2000	Infill/ Interior	Electrical rotation room.	Active
M	Bruno de Franco & Sergio Silka	Suite Vollard	Curritaba, Brasil	2001	Structure/ Outfit	Rotating floors	Active
I	Peter Marino Associates	Chanel Ginza	Tokyo, Japan	2004	Outfit	Adjustable translucency and image of façade. Possibility of motion pictures on the facade.	Dynamic
J	UNStudio	Galleria Department Store	Seoul, South Korea	2004	Outfit	Image on façade can be changed. Also movies.	Dynamic
K	Herzog & de Meuron	Allianz Arena	Munich, Germany	2005	Outfit/ Ambient	Pressure of façade can be adjusted to weather circumstances. Suspended ceiling. Adjustable colour of façade.	Dynamic
M	Environmental Design Institute	Shanghai Qizhong Centre	Shanghai, China	2005	Outfit	Retractable roof	Dynamic
P	Electroland	Enteractive	Los Angeles, USA	2006	Outfit/ ambient	Adaptive lighting and sound system	Interactive
L	dRMM	Sliding House	Suffolk, England	2009	Structure/ Outfit	Sliding walls	Active
N	tBP Architecture	Chabot College	Hayward, USA	2009	Outfit	Transparency of window changes for sun shading purposes	Dynamic
O	Hoberman Associates	POLA	Tokyo, Japan	2009	Outfit	Adaptive shading system	Dynamic

2.4 Conclusion and Discussion

By defining different levels of adaptive architecture, a clear classification can be made of the adaptive performance of the building. The role of the user changes through the different levels. Where flexible architecture requires human energy to initiate adaption, dynamic architecture is stimulated by sensor technology and activated by an energy source, such as electric power. In smart architecture, the performance of the building component is no longer consciously stimulated by the user, but has become a ubiquitous system with evolutionary characteristics.

Although the analysed projects are only a small selection of the realized adaptive buildings, the main conclusion can be drawn that most realized projects were found on flexible, active and dynamic adaptation level. Especially, after 2004 more dynamic projects were realized. This development is mostly attributed to the large scale availability and popularity of digital and LED technology. The adaptive building elements were in most projects integrated in the building system. Especially, adaptive outfit components were fully integrated in the façade system. However, when analysing the performative aspects, the specific building components were behaving individually. For example, at the POLA project of Hoberman Associates, the adaptive shading system reacts on the amount of sunlight. The energy use can be decreased and the indoor climate optimized by inherently connecting this system to the climate and light system.

A level of intelligence could be reached when the building system will be based on fully integrated elements, which are able to recognize and react mutually, that can give orders and take over tasks when other elements malfunction. Based on the currently available technology it should be possible to develop interactive and intelligent environments. For smart architecture, more technological advances are required.

2.5 Research Implementation

The discussed adaptive building projects show that innovation of adaptive environments is constantly emerging. With the current technological advancements, interactive and intelligent environments are realistic prospects. To enhance this performance, optimization of the control system and pervasive systems is necessary.

Current technological advancements are well developed in order to transform the static architectural environment into an adaptive evolving world (Corbusier 1986; Kroner 1997). With the current available technologies, tangible adaptive environments can be realized. Negroponte underlined this already in 1975, by referring to A. Johnsons work where he writes about walls that can move by touch, change colour or form according to the function based on the state-of-the-art technology (three pigs revisited, 1971 (Negroponte 1975)).

Interactive environments are no longer science fiction, but can be realized in real-time. With the emergence of material and control technologies and the integration of fast computer systems in the building system, tangible interactive environments are realistic. Knowledge diffusion forms the basis of innovation on this subject. Industries, such as automotive, aerospace and robotics have acquired a wide knowledge and experience on subjects as material innovation and digital technologies. Knowledge from these disciplines, among others, can be implemented, translated and integrated in order to enable realization of adaptive building components. By covering this interdisciplinary field of research and development, large advantages of the building performance can be established.

Electronic advancements and technologies have found their way into architectural installations. Interactive digital models have been translated into the real-time world by the use of projection and light visualizations (Bullivant 2006). Additionally, large mechanical installations demonstrated shape-morphing behaviour of architectural surfaces. With the use of pistons and pneumatics in combination with digital models, adaptive mechanical structures realize shape morphing tangible environments (dECOi webpage; Flare Facade webpage; Studio Roosengaarde webpage).

The projection and light visualizations as well as the mechanical installations bring us closer to the realization of an interactive environment that can adapt to our preferences spatially. Although, the projections and light installations can be translated to 3d mediums (Plane Scape by Wolfgang Bittner (Wolfgang Bittner webpage)), these installations are still less “tactile” compared to a building space or surface. A disadvantage of the mechanical installations is that these require large construction sizes, are considerable noisy and require high maintenance. These aspects have an important influence on the high costs of mechanical installations. Based on the current available technologies other solutions should be feasible and require investigation.

Smart material technology is a newly emerging knowledge field and shows promising application possibilities in the built environment. By realizing building components that can change, shape, emerge and adapt on material level, large advancement can be found in terms of weight and complexity. This thesis focusses on the implementation of smart material technology into a tangible adaptive environment. In the following chapter the advancements of smart material technology will be elaborated, together with the current available smart material technology in architecture.

Adaptive building systems will not only lead to an optimization in terms of functionality, but will also have the potential of contributing to a significant reduction of the energy consumption and material resources. Especially, when the building performance is optimized with respect to climate comfort, advantages on sustainability are found. The Chabot College, with adaptive window transparency, can serve here as an example. By dynamically controlling the window transparency, heat gain by solar radiation is reduced considerably. The application of these dynamic daylight systems reduces the overall energy consumption of a building (Platzer 2003).

2.6 References

Aarts, E. and Marzano, S. (2003). The New Everyday Views on Ambient Intelligence. Rotterdam, 010 Publishers.

Brand, S. (1994). How Buildings Learn; What Happens After They're Built. New York, Viking.

Bullivant, L. (2006). Responsive environments architecture, art and design. London, V and A Publications.

Collier, R. and Thelen, E. (2003). User-System Interaction Based on Spoken Dialogue. The New Everyday. E. Aarts and S. Marzano. Rotterdam, 010 Publishers: 78-83.

Corbusier, L. (1986). Towards a New Architecture. New York, Dover.

dECOi (webpage) Retrieved 2012 from www.hyposurface.org.

Dekker, A. (2006). The New Art of Gaming, or What Gaming can Learn from Installation Art. *Game Set and Match II: on Computer Games, Advanced Geometries and Digital Technologies*, Delft, The Netherlands, Episode Publishers.

Dekker, K. (1998). "Research information: Open Building Systems: a case study." Building Research & Information **26**(5): 311-318.

Edler, J. and Edler., T. (2006). Message vs. Architecture? Dynamic Media as a Continuation of Architecture. *Game Set and Match II: on Computer Games, Advanced Geometries and Digital Technologies*, Delft, The Netherlands, Episode Publishers.

Flare Facade (webpage) Retrieved 2010-04-07 from www.flare-facade.com.

Fox, M. and Kemp, M. (2009). Interactive architecture. New York, Princeton Architectural Press.

Johansen, J. M. (2002). Nanoarchitecture a new species of architecture. New York, Princeton Architectural Press.

Kendall, S. and Teicher, J. (2002). Residential Open Building. London, Spon.

Kronenburg, R. (2002). Houses in Motion the Genesis, History and Development of the Portable Building. Chichester, Wiley-Academy.

Kroner, W. M. (1997). "An Intelligent and Responsive Architecture." Automation in Construction **6**(5-6): 381-393.

Lelieveld, C. M. J. L. and Voorbij, A. I. M. (2007). The Application of Dynamic Materials in Adaptable Architecture. ManuBuild, The Transformation of the Industry– Open Building Manufacturing. M. Sharp. Rotterdam, The Netherlands, CIRIA, Classic House.

Leupen, B. (1997). Design and analysis. Rotterdam, 010 Publishers.

Lorente, S. (2004). Key issues regarding Domotic applications. International Conference on Information and Communication Technologies: From Theory to Applications.

Negroponte, N. (1975). Soft architecture machines. Cambridge, USA, MIT Press.

ONL [Oosterhuis_Lénárd] (webpage) Retrieved 2012 from www.oosterhuis.nl.

Oosterhuis, K. (2002). Architecture goes wild. Rotterdam, 010 Publishers.

Platzer, W. J. (2003). Switchable Facade Technology - Energy Efficient Offices with Smart Facades. ISES Solar World Congress. Goteborg, Sweden.

Randl, C. (2008). Revolving architecture-a history of buildings that rotate, swivel and pivot. New York, Princeton Architectural Press.

Studio Roosengaarde (webpage) Retrieved 2010-04-07 from www.studioroosegaarde.net.

Vincent, J. (2001). Smart by Nature. Lightness: The Inevitable Renaissance of Minimum Energy Structures. A. Beukers and E. Hinte van. Rotterdam, 010 Publishers: 42-47.

Wolfgang Bittner (webpage) Retrieved 2012 from www.wolfgangbittner.com.

CHAPTER 3

SMART MATERIAL SYSTEMS IN ARCHITECTURE

3.1 Introduction

The term *smart material* is widely used and smart materials are recognized as a specific material group. However, no general consensus on the usage of the term is defined. There is an active discussion regarding the linguistics of the term “smart materials”. In general, the following definition is applied: “smart materials are materials capable of automatically and inherently sensing or detecting changes in their environment and responding to those changes with some kind of actuation or action” (Ansari, et al. 1997). This action or actuation is based on a change in the intrinsic material properties.

Also the term *intelligent* material can be found to define similar material characteristics. In literature a clear distinction is made between *intelligent* and *smart* materials (Shahinpoor 1997; Addington, et al. 2005). More advanced material properties are attributed to *intelligent* materials in relation to smart materials. Here, intelligent materials dispose over the ability of reflection or reason, which will add to a certain survival strategy (Shahinpoor 1997). Intelligent materials, in this context should be able to learn and conscious about their performance. These are characteristics which in other literature are assigned to *smart* (Srinivasan, et al. 2001).

In general, it is debatable whether a material can be referred to as being smart or intelligent, since materials do not have cognitive capabilities (Srinivasan, et al. 2001). Cognition is a distinguishing characteristic for being smart or intelligent. Additionally, the *ability to learn* is an important aspect of being smart or intelligent (Srinivasan, et al. 2001). Smart and intelligent characteristics are assigned to living creatures such as humans, animals or plants. They can evolve, learn and optimize their performance. When applying this definition with to the performance of materials, it becomes clear that materials lack these characteristics. A material disposes over a set of characteristics which can only be edited chemically. A material can change its properties by changing environmental settings, such as temperature, but the material will always change along a similar transition path. The material cannot determine whether it would perform differently on certain circumstances. Besides, an external stimulus is always required to evoke this change. Looking at, for instance thermal-responsive materials, it becomes clear that these materials can only respond in a certain way to specific temperatures. Temperature is the external stimulus required to activate change. When the material should respond to a *different* temperature, this can only be realized by the adjustment of the molecular structure.

When smart materials only focus on one behavioural aspect, it is very hard to determine this as being smart. A single material could hardly ever be considered smart, as it mostly responds similar on only one stimulus. Only when the material is constructed out of hybrid material mixtures, in a system or a structure, it can specifically respond to a number of inputs and generate specific outputs (Culshaw 1996; Srinivasan, et al. 2001). When sensors, actuators and control mechanisms become part of the micro-structure of the material itself, materials can become smart systems (Anderson, et al. 1992). This means that materials become “smart” by the specific application in a system, this can be considered a smart material system.

It is recognized that a specific material group needs to be defined for materials with distinctive material characteristics such as sensing, processing and acting. Although the term *smart* does not meet the literal explanation, it defines a specific material group. Mostly, smart materials are embedded in a structure or system, e.g. *smart material systems or structures*. Miniaturization and material innovation enables smart material systems that almost reach a level of smartness due to multifunctional performance.

Smart materials react on external stimuli, such as light, temperature, pH and magnetic field. These materials can respond by, for example, changing their colour, shape or transparency (Figure 3.1). As these materials detect a stimulus and act accordingly, they have both sensory and actuation properties.

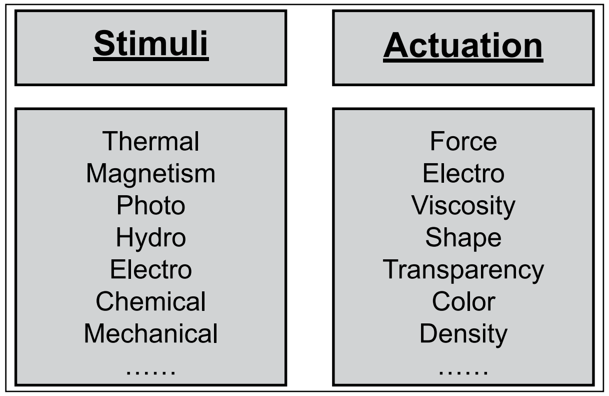

Figure 3.1 Different stimuli of smart materials and their output response

In some situations, the behaviour of the material is accidental and conflicts with the application purpose. Obviously, only performances that do not disrupt the component purposes are considered *smart*. This can be explained by the expansion behaviour of wood at high moisture levels. It is generally known, that the absorbing of moisture results in the swelling of the wood elements. This behaviour is not exactly an advantage when applied as a structural or interior finishing material in floors and walls. The warping of wood in these situations will lead to cracking and torsion. On the other hand, this characteristic can be used as a natural humidity controller of the indoor climate. Also, this behaviour is especially useful for the construction of water-proof surfaces, such as façades or boats. In this application, the material characteristic is used as intended performance ability and can therefore be considered *smart*.

3.1.1 Passive, Active and Hybrid Systems

Smart material systems can be used in active or passive systems. A system is referred to as *passive*, if the material system senses a certain stimulus change and responds to this directly with a kind of action or actuation (Figure 3.2). The required energy to initiate the activation is derived from environmental resources. This performance is a closed-loop system and cannot be interrupted.

A system is considered *active* when the performance of the material is fully controlled by a system. A sensor detects the change of the external stimulus, after which the control system processes this input and subsequently gives an impulse for activation (Figure 3.3). Energy input is required for the performance of the material system. The performance of the system can be adjusted when required. An automatic light system is considered *active*. The illumination will be turned on when the environmental light diminishes. The light level is detected by a light-sensitive sensor and the illumination is activated by an electric stimulus.

A *hybrid* system combines the characteristics of both active and passive systems. The material can perform on a passive level, but this performance can be overruled by an active system. An example can be given by an adaptive daylight system, when detecting high temperature loads by sun radiation, the passive system automatically shades the glass surface. In winter situations, however, high thermal loads can be an advantage. In this case, it is preferred that the shading is prevented by active control. Hybrid systems can lead to a higher level of performance, but will also lead to a higher level of complexity (Spencer, et al. 2003). In Table 3.1, the specific characteristics of the discussed systems are given.

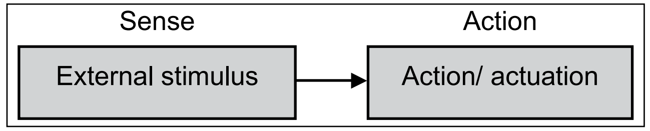

Figure 3.2 Passive system, senses input, and reacts instantly with a certain action

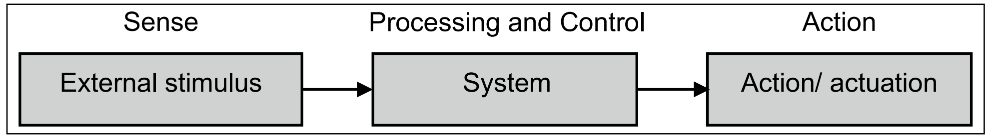

Figure 3.3 Active system: detects change, system processes input, defined action is executed. The user can interfere with the system, and control the output reaction.

Table 3.1 Specified characteristics passive, active and hybrid systems

	Passive	Active	Hybrid
Detection	Material sensor	System sensor	Material and System sensor
Output	One-on-one reaction	Variable output	Variable output
Reaction	Direct	Controlled	Direct and Controlled

3.1.2 Smart Material Systems in Architecture

The distinct smart material characteristic can be found in a wide range of materials. In essence organic material systems, such as wood and concrete, can be considered smart systems. Concrete seems to have some self-healing characteristics. When cracks appear, the mortar will repair under the influence of water. It should be noted that this recovery is not controlled and is therefore considered a passive system.

In this thesis, only material systems are considered smart, if the material is able to change inherently provoked by external stimuli. This excludes static materials with innovative characteristics or extreme performances, such as aerogel and holographic foils. Aerogel possesses substantially high insulation properties in relation to a very low density. This extreme insulation performance is not considered smart, as the material remains constantly in a similar condition.

Advances in smart materials have found their way into the architectural practice and experimental projects (Addington, et al. 2005; Ritter, et al. 2007). An overview is given of smart material systems which have found their way in building practice. It should be noted that only materials are presented which are found in practical application, this indicates that experimental examples are omitted from this overview. The smart materials systems are categorized by behavioural aspects:

- Structural performance
- Climate and energy performance
- Architectural performance

Every category will be discussed further by use of examples. The purpose of the examples is to provide an overview of the current state of smart material technology in the building environment.

3.2 Structural Performance

Smart material systems can be embedded in the building system to support and optimize the structural performance. Hereby, they take care of the rigidity of the structure and maintain a safe and healthy structure. Smart material systems can diagnose malfunctioning of the structure throughout the lifetime of the building and serve as a constant health monitor. Additionally, deviations cannot be only detected and prevented, but also be repaired to avoid calamities.

The degradation of the building structure can lead to extremely dangerous situations. Unfortunately, the collapse of a building or building parts is a worldwide issue. Full security of the structural quality is demanded, but considerably difficult to envision, as structural defects are difficult to detect. Preventing catastrophic failure due to structural malfunction can be diminished by the optimization of safety monitoring systems, the use of a recovery system or the prevention of the occurrence of irregularities. Continuous structural control and safety monitoring can be realized by embedding smart material systems in the building structure. However, it should be noted that instant failure due to design mistakes would still be difficult to prevent.

By implementing smart material systems in the building structure, a reduction of costs can be realized on the level of safety inspection, maintenance and energy usage. Embedded smart material systems can constantly check the structure quality and will communicate the current state to a control system. This can decrease the amount of safety checks and monitor irregularities much earlier. Smart materials have great advantages above conventional systems, due to the small material scale and the fast response time. As the materials are fully embedded in the structure, precise local monitoring and repair can be realized, during fabrication as well as the lifetime of the building.

3.2.1 Safety Monitoring

Safety monitoring of the structural integrity of a building can be realized by the integration of fibre optics in structural materials (Ansari 1997; Srinivasan, et al. 2001; Mrad, et al. 2008). Fibre optics can transmit light over long distances without signal loss. By sending pulses of light through the embedded fibres, cracks in the building structure can be constantly observed. Less light will be transmitted when the fibre is damaged or deformed, as this will scatter the light pulse. The amount of reflected and transmitted light is detected which makes it possible to determine the location of the irregularity. A similar principle can be found by the implementation of carbon fibres in concrete (Sun, et al. 2000). By applying current through the fibres continuous monitoring can be envisioned. Disturbances in the fibre indicate cracks or other irregularities.

With these monitoring systems, it is possible to enable a continuous safety monitoring of the inner building structure. Irregularities in, for example, concrete structures can be detected in an early stage, due to continuous monitoring. By implementing smart material systems for continuous safety monitoring in the building structure, a financial profit is perceived due to the reduction of material usage and inspection.

3.2.2 Self-Healing Properties

A disadvantage of safety monitoring is the subsequent manual repair after irregularities are detected, especially when the irregularities are located at a difficult place. In this situation, it is more advantageous to use materials which are able to detect the irregularities and induce subsequent recovery. Self-healing materials have such characteristics and enable intrinsic and invisible healing of irregularities. Based on biological recovery technologies, artificial self-healing systems have been developed which enhance recovery after rupture. The self-healing system has found its way into various material technologies, such as metals, concrete and polymers.

Two kind of self-healing systems can be distinguished; passive and active systems. Passive systems instantly initiate the healing process after rupture, while active systems require external activation to enable the healing process. It should be noted that the presented technologies are quite interesting for architectural application.

3.2.2.1 Passive self-healing systems

Passive self-healing systems show instant recovery after rupture. An example of such systems are polymeric materials with embedded microcapsules (White, et al. 2001). In Figure 3.4, a passive principle of a self-healing polymeric material is shown. The material is filled with microcapsules and catalysts. When a rupture occurs, the microcapsule breaks open and will initiate a reaction with the present curing agent (White, et al. 2001; Aïssa, et al. 2012). The material will regain its properties when the rupture is filled with the fully cured polymeric material. It should be noted that this is a finite process; once a capsule is used for recovery, a rupture at the same location will not be recovered. A scar will mark the rupture location. A similar performance could also be envisioned with embedded hollow fibres in polymer materials (Wu, et al. 2008).

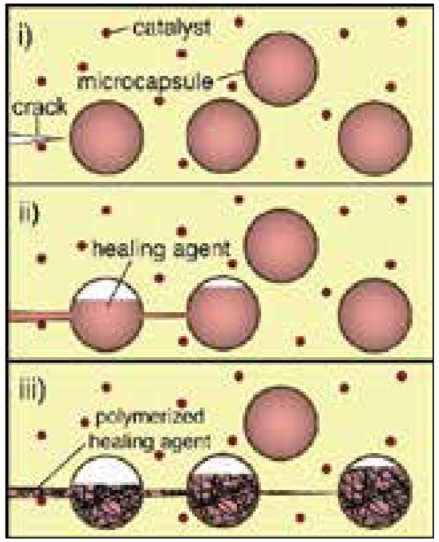

Figure 3.4 Passive self-healing system. Step 1) a crack occurs, step 2) microcapsule cracks open and gets into contact with catalyst, 3) curing of the polymer closes the crack. Image courtesy (White, et al. 2001).

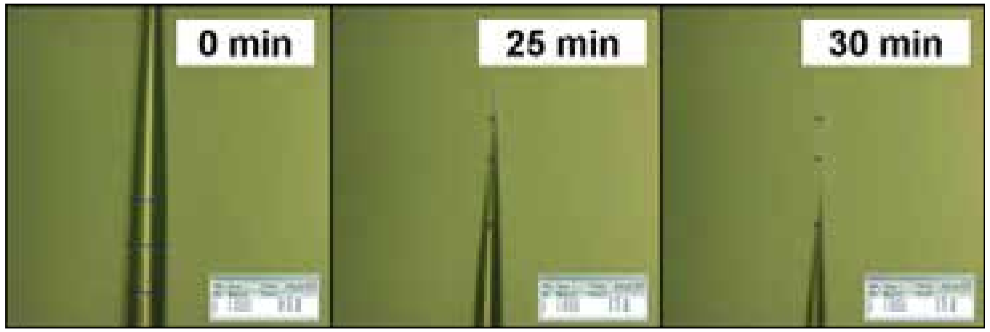

Figure 3.5 Time dependent crack closure in polymer. Image courtesy Fraunhofer UMSICHT

Another passive system is based on the integration of specific bacteria in concrete material. The bacteria forms calcite out of oxygen, carbon dioxide and calcium. Recovery is initiated when the calcite gets into contact with moisture and finally becomes fully rigid (Jonkers, et al. 2010). This means that ruptures can only be recovered located at places where moisture can reach and oxygen is provided. For intrinsic irregularities, this self-healing system is therefore not sufficient. As long as an optimal living environment for the bacteria is maintained, and contact with moisture is ensured, the recovery process is endless. An interesting example of the real-scale application of this self-healing concrete is a pavilion in Breda, the Netherlands (Figure 3.6).

Figure 3.6 Self-healing pavilion Breda, the Netherlands by Marcus Architecten, 2009. Image courtesy (Marcus Architecten webpage).

3.2.2.2 Active self-healing systems

Active self-healing systems require an active stimulation in order to initiate recovery after material failure. This means that a monitoring system is required that activates the recovery process. These processes are induced by chemical, photo, thermal or electric activation. By applying charged field to the material, recovery is facilitated by ion bonding. This is an infinite process and can be realized on every given location at the entire material component. Similar processes are initiated with photo and thermal induced process. These processes can also act passively, when applied in an outdoor application. By a sufficient raise of the (outdoor) temperature, recovery is realized without active interference. Recovery is based on molecular diffusion across the rupture (Aïssa, et al. 2012). Application can be found in coatings for corrosion protection (Aïssa, et al. 2012) or self-healing automotive paints.

3.2.2.3 Conclusion

It must be mentioned that for a durable large scale structural application of self-healing materials more research is required. When applied on a large scale, difficulties occur with the consistency of performance. Recoveries are not fully realized and finite recovery processes are considered relatively untrustworthy. Self-healing systems seem to present acceptable performance when applied on an esthetical level for the recovery of non-structural surfaces. Especially, the recovery of scratches or other surface irregularities have found their way to practice. Nevertheless, the presented technologies show promising application possibilities in future self-healing building components.

The development of self-healing concrete gains a great advantage in terms of durability and structural health monitoring. This will lead to a considerable reduction of monitoring and repairing costs (Wu, et al. 2008). Additionally, due to the self-healing capacity of concrete, less material is required. This is an improvement on sustainable level, as the use of concrete demands a high amount of energy due to transport and production.

3.2.3 Prevention

Prevention is always better than cure. An important aspect in damage control is the influence of environmental factors on the building structure. These can cause fatigue of the structure materials. Environmental factors can lead to oxidization, moisture, mould and structural failure, among others. Environmental loads can be instant and deliver relatively large forces on the building structure. The occurrence of seismic forces and strong wind loads on a building is a difficult issue. For functional purposes, a building structure is required to be rigid, inelastic. However, the problem with rigidity is that vibration forces cannot easily be dissipated, which will lead to cracks and failure. Ideally, a building structure behaves like a pudding under the influence of large external forces. By damping the experienced earthquake energy instead, the building structure stays intact.

The control of vibrations in the building structure by smart material systems is intensively studied in experimental projects. The emergence of smart material systems with actuation properties open up new frontiers on the subject of structural control. Smart material systems, such as shape memory alloys, rheological fluids and piezo-ceramics are studied to perform as actuator and damper material to avoid large deflections (Song, et al. 2006; Ozbulut, et al. 2011). However, from these promising material systems, currently, only rheological materials have found their way into the application field.

By using controllable dampers, the structural stiffness of a building can be adjusted based on the changing environmental parameters (Srinivasan, et al. 2001). In Figure 3.7, a magneto-rheological fluid damper is shown. The damping system is based on embedded magnetic particles in a fluid. The particles can move freely in the fluid when no field is applied. (Figure 3.8) In this state, the damper is considered flexible and can deform. By applying a magnetic field, the particles align and prevent flowing of the fluid (Lord Corporation webpage). The damper is fully rigid, as the fluid becomes nearly solid. The amount of magnetic field can be adjusted within milliseconds and thereby controlling the damper's stiffness (Spencer, et al. 2003). The damper remains stiff by normal conditions, but becomes flexible during seismic activity. This enables the building structure to transfer extreme forces, without breaking down. Experimental projects have been carried out with these devices and show promising results (Figure 3.9).

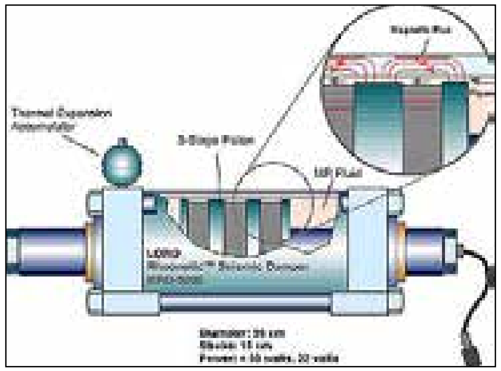

Figure 3.7 Section of magneto-rheological (MR) damper (Lord Corporation webpage) Image courtesy Lord Corporation.

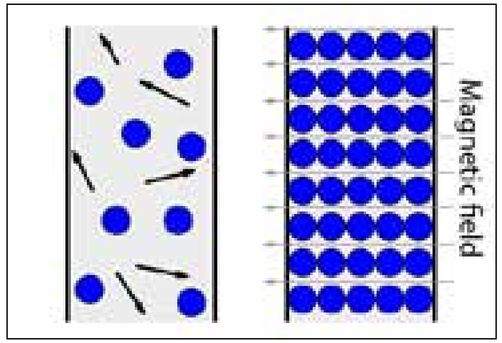

Figure 3.8 Magneto-rheological fluid principle. In the left image you can see that the fluid with the magnetic particles move freely when no field is applied. In the right image, the particles are aligned under applied magnetic field, which prevents the fluid from flowing. Hereby, the viscosity increases, obtaining a nearly solid consistecy. Note that a similar performance occurs under electric current.

Figure 3.9 MR damper in structural component, Nihon-Kagaku-Miraikan museum, Japan. Image courtesy unknown.

3.3 Climate and Energy Performance

The control of the indoor climate for the optimization of the user comfort requires a considerable energy usage. Advances on smart material systems for the optimization of the indoor climate will not only lead to an increase of user comfort, but also a decrease of energy consumption. Secure energy control systems reduce the energy consumption and maintain a comfortable climate during variable weather conditions. Additionally, integrated smart material systems in building components can be used for energy harvesting. By converting solar radiation into electric power, building systems can become fully autarkic on this level.

3.3.1 Latent Heat Storage

The control of a comfortable indoor climate is highly energy consuming due to variable weather conditions. Especially, in commercial and industrial buildings active comfort control requires large installations and lead to high energy usage. Ideally, thermal energy will be subtracted during warm periods and released during cold periods. By the use of latent heat storage, a passive system based on Phase Change Materials (PCMs) enables such a performance. The PCM technology is based on the phase transition from solid to liquid phase. This phase transition is equivalent to the phase transition process of water. When heat is extracted from a liquid, the material will become solid (ice). Subsequently, the substance will melt again by applying heat.

By high temperatures, the PCM melts, enabling latent heat storage. When the ambient temperature drops below a specific temperature, the thermal energy is released, increasing the ambient temperature. The ambient temperature will be kept within the comfort zone, preventing extreme temperatures. The transition temperatures of PCMs can be adjusted according to different ambient requirements. These temperatures can be determined accurately by selecting the correct material and composition.

The application of PCMs will decrease the energy consumption and maintain a comfort temperature level throughout various weather conditions. PCMs are especially effective in lightweight buildings and as a retrofit for energy unbalanced buildings. PCMs can be found as encapsulated salt hydrates (Salca BV webpage) or glycerol (BASF webpage). Glycerol-based PCMs have the disadvantage that these are highly flammable. PCM can be embedded in gypsum panels (Figure 3.10) or can be encapsulated in add-on elements (Figure 3.11).

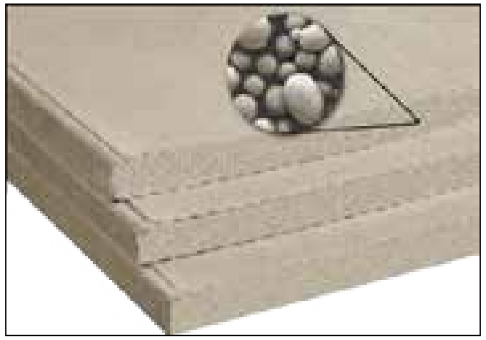

Figure 3.10 PCM integrated in gypsum board. Image courtesy Micronal BASF.

Figure 3.11 PCM capsules embedded in a flexible cover, which can be used for retrofitting. Image courtesy (Salca BV webpage).

3.3.2 Adaptive Daylight Systems

Another example is the application of smart material systems in adaptive daylight systems (Hellinga, et al. 2011). Also here, the performance is based on the control of the indoor climate and the reduction of the energy consumption. The application of large glass surfaces in the building system raises issues such as overheating of buildings and considerable energy loss. Efficient adaptive daylight systems will lead to considerable improvements with respect to user comfort and energy control. Currently, developments are found of smart material systems which are embedded in the glass surface as film layer or sandwiched between glass panels. The integration of these technologies does not influence the glass thickness. However, restrictions are found on large glass dimensions. Adaptive daylight systems can be controlled passively or actively.

3.3.2.1 Passive Daylight Systems

Passive daylight systems are based on photo-responsive[5] or thermo-responsive[6] systems. This category can be divided in chromic systems and tropic systems. Photo-chromic or thermo-chromic systems provide a tinted glass surface under the influence of ultraviolet radiation or temperature. The visual characteristics are preserved after activation. A glass panel with embedded thermo-chromic film is presented in Figure 3.12. Here, it can be clearly seen that the visual properties are maintained in tinted state.

Figure 3.12 Activated thermo-chromic daylight system, with low visual capabilities. Image courtesy by Pleotint.

Thermo-tropic systems consist of a small layer of material sandwiches between glass plates. This layer is changing to diffuse state at a threshold temperature (Lampert 2001). Here, the visual capabilities are faded, but the incidence of light is sustained. Thermo-tropic systems are based on phase changing performance.

The advantage of passive daylight systems can be found in the omission of wiring, control systems and extra energy usage. The limitation of these systems is defined by the inability of the user to control the performance. During winter time it might be advantageous to use the sun radiation for extra heating of the room; with passive systems the solar radiation will always be blocked. Due to the passive characteristics it might be possible that the transition does not cover the whole glass surface, creating an inhomogeneous tinted surface (Lampert 2004).

3.3.2.2 Active daylight systems

Next to passive systems, also active daylight systems have been developed with integrated smart material systems. In contrast, these systems are fully controllable by electric current. In Table 3.2, an overview is given of the different technologies with the related transmission values for visual light transmission and energy consumption.

5. Photo-responsive systems are acting by UV light.
6. Thermo-responsive systems react to temperature change.

Table 3.2 Overview of active daylight systems and transmission values.

Technology	Stimulus	Visual light transmission transparent	Visual light transmission translucent	Energy consumption
Electro chromic (EC)	Current	70-50 %	3,5-10%	1-5 V
Polymer Dispersed Liquid Crystal (PDLC)	Current	80%	30%	24-100V
Suspended Particle Device (SPD)	Current	80%	50%	100V

Actively controlled daylight systems are embedded as a thin film between the glass layers. The wiring is embedded in the framing and do not require larger glass or framing sizes. In most systems, the control of both LC and SPD requires a continuous energy input in order to maintain the transparent phase (Baetens, et al. 2010). However, systems are developed which only require an energy pulse during transition (Lampert 2001; Peer+ Glass webpage). EC systems have memory properties and can therefore maintain the transparent phase for about 14-48 hours. Occasionally, a pulse correction is required to preserve the transparent phase (Lampert 2003; Smart Glass webpage).

EC and LC can be fabricated in different tinted colours, but SPDs can only be provided in grey tints. In Figure 3.13 and Figure 3.14, LC and EC systems are shown in both tinted and transparent phase. Here, the visual transmittance characteristics in tinted state are clearly illustrated. The visual transmittance serves as a great advantage above conventional daylight systems.

Figure 3.13 Liquid Crystal system. Image courtesy by Peer+ glass.

Figure 3.14 Electro-chromic system. Image courtesy of Saint-Gobain.

A disadvantage of the EC systems is that the colour degrades over time. A checker effect may occur when multiple glass panels are used, as different glass elements degrade differently (Lee, et al. 2006). LC systems will become a bit yellow over time under the influence of UV light.

The transition time from clear to tinted phase depends on the dimensions and the ambient temperature. By increasing panel sizes as well as ambient temperatures, the switching time between the different states decrease considerably. At 10°C a switching time of 1-7 minutes is required for a full transition (Lee, et al. 2006), where by lower temperatures switching times of 85 minutes can be found (Baetens, et al. 2010). LC systems and SPD are known to have switching times of 10 milliseconds (Interpane webpage) to only a few seconds (Smart Glass webpage). The guaranteed life time of LC, SPD and EC is about 5 to 10 years (Baetens, et al. 2010; Saint-Gobain webpage). This is considerably lower compared to the use of regular glass surfaces.

The development of adaptive daylight systems with embedded smart material technology will lead to advancements on the level of energy consumption. Even when the systems are in tinted condition and thereby decreasing the glare and heat transmission values, the incidence of light is ensured. This will lead to considerable savings of artificial light use. Additionally, optimized control systems will prevent overheating and lead to savings on cooling costs. Substantial savings are found when the radiation load is controlled accurately.

Even though adaptive daylight systems with embedded smart material systems have found their way to practice, scaling and a long life time remain issues of concern. Further developments on these issues will be required.

3.3.3 Energy Harvesting

Photovoltaic technology can also be regarded as a smart material system. These systems convert solar radiation into electric power. Under the influence of solar energy, electrons are transferred to a different energy band, causing the release of electrons and producing electric current. In the early years, photovoltaic cells were mainly applied as additional elements onto existing building components. With the development of this technology the photovoltaic cells can now be integrated into the building envelope, as glass panels (Figure 3.15) and flexible panels (Figure 3.16).

Figure 3.15 Photovoltaic cells in insulating glass panel. Image courtesy Syracuse glass.

Figure 3.16 Sphelar voltaic cells encapsulated in flexible matrix. Image courtesy Kyosemi Corporation.

3.4 Architectural Performance

The architectural performance of the building system includes the functional and aesthetical aspects. The way the building communicates with the environment is an important aspect of the architectural performance. This communication can not only be envisioned on functional level or by the aesthetical representation, but also contains a certain entertainment value. The functional performance of the building system is related to the use and ambience. On an aesthetical level smart material systems can contribute to the ambience of the building and the communication with the user. The integration of smart material systems can influence the way the building is used and how it functions. Not only the relation with the user, but also the relation with the environment is included in the functional performance.

3.4.1 Lighting and Displaying Technology

In theory, lighting systems can be approached as smart material systems. LEDs are emitting light by the application of electric current. In chapter 2, examples of embedded lighting systems in façades are given. These lighting systems serve multiple purposes, such as; commercialization, displaying, illumination and entertainment. The adaptation of the lightened building surface will change the ambience of the environment. The widely used LED system demands considerable construction sizes and deliver pixelated presentations. Developments in the display technology show promising application possibilities.

Especially the development of Organic Light Emitting Diodes (OLEDs) offers great possibilities for adaptive building applications. Not only for advances in displaying technology, but also in the sense of illumination and colour effects. OLEDs require no backlighting during displaying, which saves substantially in terms of size and energy use. Additionally, it is a great advantage that the diodes can be printed on almost any substrate, including flexible materials (Figure 3.17). This enables the integration in glass facades without the addition of extra weight and large elements dimensions. Issues as large scale applications and life time are currently researched upon.

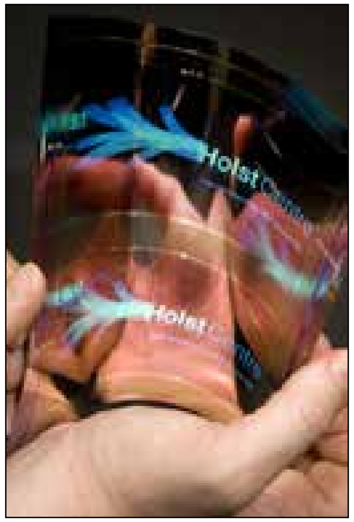

Figure 3.17 OLED can be wrapped and stretched without degradation. Image courtesy by Holst Centre.

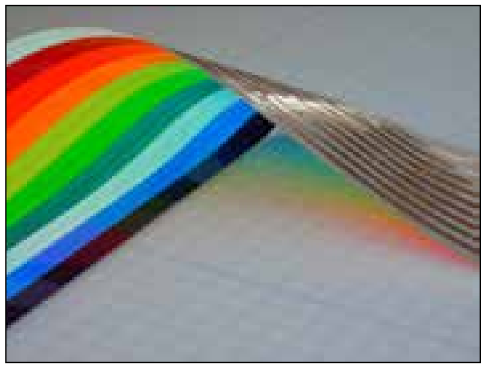

Figure 3.18 EL light strip. Image courtesy Earlsmann.

Electroluminescent lighting (EL) technology can be used for indoor and outdoor accent lighting purposes. Due to the flexible and thin character (0.5 mm) of the material, the application field is diverse. Less energy is required in comparison with LED lighting systems. Additionally, lengths of approximately 90 meters can be realized. The material can be manufactured with any print or customized shape (Figure 3.18).

3.4.2 Space Division

Adaptive daylight technologies cannot only be used for sun-shading purposes. They can also serve on a functional level for space division and concealment. In Figure 3.19, an example of space division purposes is shown, based on electro-chromic technology.

Figure 3.19 Left: Liquid Crystal System, transparent phase, Right: Translucent phase. Image courtesy Privalite, Saint-Gobain.

3.4.3 Aesthetical and Entertainment Adaptation

Thermo-chromic technology can also be applied on building surfaces for esthetical and colour changing purposes. Thermo-chromic paints can be implemented in many compounds. However, the application on the building envelope is restricted due to material degradations by constant UV exposure. In Figure 3.20 and Figure 3.21 examples are shown of thermo-chromic paints.

Figure 3.20 Thermo-chromic furniture. Image courtesy J. Mayer Architechts, Germany.

Figure 3.21 Touch me Thermo-chromic wall paper. Image courtesy Zane Berzina.

3.4.4 Self-Cleaning Technology

Due to the increasing urbanization and motorization of our transport network, airborne pollutants are becoming more and more a problem. This does not only reduce the air quality but also affects the wastewater. The development of self-cleaning surfaces with embedded titan dioxide crystals decreases these contaminations.

Titan-dioxide crystals can act as a natural catalyst to break up pollutants into non-toxic elements. The material surface is hydrophilic, which means that water will spread like a sheet over the surface (Figure 3.22). Grease, mould and bacteria are not able to adhere to the surface. When applied to outdoor surfaces the rainfall will take care of natural cleansing. As long as UV light can reach the crystals, the oxidation is an endless process.

Titan dioxide can be added into various compounds. Self-cleaning concrete surfaces or asphalt roads will initiate detoxification of air and surface pollution. Application on glass surfaces increases the glass vision and saves cleaning costs.

Figure 3.22 On the left self-cleaning glass is shown, as the glass surface is hydrophilic the water will form a film on the glass surface. On the right side is regular hydrophobic glass; the water forms small droplets.

Image courtesy Pilkington Activ.

3.5 Conclusion and Discussion

A considerable amount of examples are presented of embedded smart material technologies in the built environment. The performance of these systems are found on different performance levels and can be subdivided in structural performance, climate and energy performance and architectural performance. In some examples, such as adaptive daylight systems and safety monitoring, smart material systems replace conventional systems and methods. This will lead to the optimization of the conventional building performance. The reduction of construction size and energy usage, among others, will encounter financial benefits. In other examples, smart material technologies are adding new performances to existing building components, this example is illustrated by self-cleaning behaviour. By applying the titan-dioxide as an additive to the conventional building material, surfaces will also acquire cleansing functions.

One of the great advantages of smart material technology is the ability of integration these in existing building components. Due to the intrinsic material performance, smart material systems have generally small dimensions. By embedding smart material systems in the building structure, lightweight building components can be accomplished which envision multi-behavioural performances.

The application field of smart material systems covers a wide area, from medical and electronic application to robotics. Miniaturization is one of the key aspects within these disciplines. Smaller material systems will enhance the application possibilities in terms of lightweight and performance speeds. In general, developments occur between milli- and nano-scale (Table 3.3). On an architectural level smart material systems mostly require a larger scale of application and longer life-times. Building components are found in the range from milli- to kilo-scale. The scaling aspect limits the one-to-one application of smart material systems in architecture.

Some interesting performances of smart material systems can, in theory, lead to novel design solutions. However, large scale application and long life-times are mostly the bottle-neck to envision such implementations. Adaptive daylight systems can serve here as an example. Liquid crystal technology (LC) has shown a good operation in the display technology. A similar performance would be interesting in architecture for adaptive daylight systems.

The dimensions of electronic devices, such as cell-phones are around $10 \cdot 10^{-3}$ m^2, whereas for the application on glass surfaces large sizes of at least 10 m^2 are required. When envisioning the translation to the architectural scale, issues such as operation speed and degradation should be solved. This illustrates that translation from the small scale application to the larger building scale is an important challenge. A one-to-one scaling of all components will not specifically lead to optimal performance on large scale. Developments are in progress in order to overcome these scaling difficulties and to optimize the performance.

Table 3.3 Scale definition with level of magnitudes

Scale	Magnitudes in meters
Giga	10^9
Mega	10^6
Kilo	10^3
-	1
Milli	10^{-3}
Micro	10^{-6}
Nano	10^{-9}

The implementation of smart material technologies in building components requires a total different design approach. Instead of designing static environments, the designing has to deal with an immediate building performance. The performance of the building cannot be translated in drawings, as these cannot represent the transient performance of the immediate adaptive spaces. Adaptive building proposals should be presented by scenarios, the adaptive plan (Holland 1992). In this plan, the transient dimension of time plays a crucial role.

Although material innovation is evolving on a slow pace on the architectural field, the implementation of smart materials in trustful architectural applications has shown to be feasible. Restrictions such as scaling, performance optimization, reliability considerations, cost efficiency and certification cannot be neglected but can be overcome. The presented examples show that the implementation of smart material technology is feasible in practice.

3.6 Research Implementation

The presented smart material technologies are embedded in existing conventional building components. In this research project the objective is to develop a specific building component, which enables a shape-morphing performance. It is recognized that the full morphing of a building components is considered a large step in relation to the presented available technologies. However, in order to envision a fully transient, immediate, adaptive, tangible and expressive building component with available advanced smart material technologies an alteration of the current static building components is required. Especially, since the shape-morphing characteristic of building component has been a challenging issue in various experimental architectural projects. The realization of these projects is based on complex mechanical principles (Flare Facade webpage; Hoberman Associates webpage).

An inspiring example of a morphing architectural component can be found in the work of dECOi Architects with the Aegis Hypo-surface (dECOi webpage). This interactive wall represents a specific morphing performance as a reaction to external physical stimuli (Figure 3.23). The installation is based on a system of sensors and pistons, controlled and activated by large mechanical system and computers. This mechanical system requires large and heavy construction sizes and generates a considerable amount of noise. The complexity of the system demands for a better solution, based on advanced material technologies.

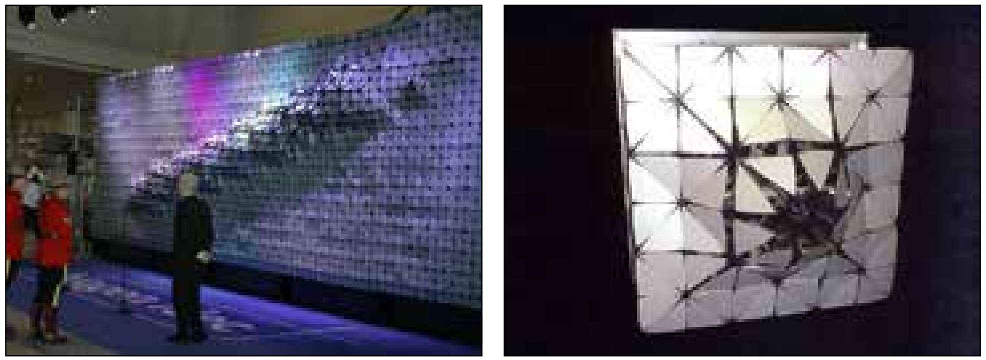

Figure 3.23 Aegis Hyposurface by dECOi Architects. Image courtesy dECOi Architects.

Given the proposition that the main reason for creating static architecture or complex adaptive building components is the lack of advanced technological solutions, it can be argued that infusion of these technologies will lead to disruptive innovations in architecture.

3.7 References

Addington, M. and Schodek, D. (2005). Smart Materials and Technologies. Oxfors, Architectural Press.

Aïssa, B., Therriault, D., et al. (2012). “Self-Healing Materials Systems: Overview of Major Approaches and Recent Developed Technologies.” Advances in Materials Science and Engineering **2012**.

Anderson, G. L., Crowson, A., et al. (1992). Introduction to Smart Structures. Intelligent Structural Systems. H. S. Tzou and G. L. Anderson. Dordrecht, Boston, London, Kluwer. **Vol. 13:** 453.

Ansari, F. (1997). Theory and Applications of Integrated Fiber Optic Sensors in Structures. Intelligent civil engineering materials and structures a collection of state-of-the-art papers in the applications of emerging technologies to civil structures and materials. F. Ansari, A. Maji and C. Leung. New York, ASCE: 2-29.

Ansari, F., Maji, A., et al. (1997). Intelligent civil engineering materials and structures a collection of state-of-the-art papers in the applications of emerging technologies to civil structures and materials. New York, ASCE.

Baetens, R., Jelle, B. P., et al. (2010). “Properties, requirements and possibilities of smart windows for dynamic daylight and solar energy control in buildings: A state-of-the-art review.” Solar Energy Materials and Solar Cells **94**(2): 87-105.

BASF (webpage) Retrieved 2011 from www.basf.com.

Culshaw, B. (1996). Smart structures and materials. Boston, Artech House.

dECOi (webpage) Retrieved 2012 from www.hyposurface.org.

Earlsmann (webpage) Retrieved 2012 from www.earlsmann.com.

Flare Facade (webpage) Retrieved 2010-04-07 from www.flare-facade.com.

Hellinga, H. I. and Lelieveld, C. M. J. L. (2011). “Intelligente daglichtsystemen: De toepassingsmogelijkheden van ‘Smart Materials’ “ Bouwfysica **2**: 17-21.

Hoberman Associates (webpage) Retrieved 2012 from www.hoberman.com.

Holland, J. H. (1992). Adaptation in Natural and Artificial Systems; An Introductory Analysis with Applications to Biology, Control, and Artificial Intelligence. Cambridge, Mass., MIT Press.

Interpane (webpage) Retrieved 2011-04 from www.interpane.com.

Jonkers, H. M., Thijssen, A., et al. (2010). “Application of bacteria as self-healing agent for the development of sustainable concrete.” Ecological Engineering **36**(2): 230-235.

Lampert, C. M. (2001). Progress in switching windows. Solar and Switching Materials San Diego, CA, USA, SPIE.

Lampert, C. M. (2003). “Large-area smart glass and integrated photovoltaics.” Solar Energy Materials and Solar Cells **76**(4): 489-499.

Lampert, C. M. (2004). “Chromogenic smart materials.” Materials Today **7**(3): 28-35.

Lee, E. S., Selkowitz, S. E., et al. (2006). Advancements of Electrochromic Windows. P. California Energy Commission. Berkeley.

Lord Corporation (webpage) Retrieved 2012 from www.lord.com.

Marcus Architecten (webpage) http://www.marcus-architecten.nl/.

Mrad, N., Li, H., et al. (2008). Fiber Optic Systems: Optocal Fiber Sensor Technology and Windows. Smart Materials. M. Schwartz, CRC Press.

Ozbulut, O. E., Hurlebaus, S., et al. (2011). “Seismic Response Control Using Shape Memory Alloys: A Review.” Journal of Intelligent Material Systems and Structures **22**(14): 1531-1549.
Peer+ Glass (webpage) Retrieved 2010-04-07 from www.peerplus.nl.
Pleotint (webpage) Retrieved 2011-04 from www.pleotint.com.
Ritter, A. and Müller, A. (2007). Smart Materials in Architecture, Interior Architecture and Design. Boston, Birkhäuser.
Saint- Gobain (webpage) Retrieved 2009-11-10 from www.quantumglass.com.
Salca BV (webpage) Retrieved 2012 from www.salcabv.nl.
Shahinpoor, M. (1997). Intelligent Civil Engineering Materials, Structures and Systems Revisited. Intelligent civil engineering materials and structures a collection of state-of-the-art papers in the applications of emerging technologies to civil structures and materials. F. Ansari, A. Maji and C. Leung. New York, ASCE: 44-61.
Smart Glass (webpage) Retrieved 2011-04 from www.smartglass.com.
Song, G., Ma, N., et al. (2006). “Applications of shape memory alloys in civil structures.” Engineering Structures **28**(9): 1266-1274.
Spencer, J. B. F. and Nagarajaiah, S. (2003). “State of the Art of Structural Control.” Journal of Structural Engineering **129**(7): 845-856.
Srinivasan, A. V. and Mcfarland, D. M. (2001). Smart structures analysis and design. Cambridge, UK, Cambridge University Press.
Sun, M., Li, Z., et al. (2000). “A study on thermal self-diagnostic and self-adaptive smart concrete structures.” Cement and Concrete Research **30**(8): 1251-1253.
White, S. R., Sottos, N. R., et al. (2001). “Autonomic healing of polymer composites.” Nature **409**(6822): 794-797.
Wu, D. Y., Meure, S., et al. (2008). “Self-healing polymeric materials: A review of recent developments.” Progress in Polymer Science **33**(5): 479-522.

Chapter 4

Design Scenarios

4.1 Introduction

In chapter 1, the deflecting performance of the ABC is presented. There, the application of the component in the building system was not considered. However, it should be clear that the main interest of this project is the performance and realization of the ABC.

To gain insight into the application possibilities of the ABC different design scenarios are described in this chapter. The adaptive performance can be realized on different levels of the building system. As the proposed adaptive building component does not have structural characteristics, the application of the ABC is restricted to the *outfit*, *infill* and *interior* elements. The performance of one design scenario is studied in more detail. The adaptive performance on building scale is analysed by the use of simulation tools. Insight is given into the aerodynamic performance of an immediate adaptive building envelope. This chapter serves as an inspiration for the application of the ABC.

The level of adaptation is mostly determined by the operating system of the adaptive building components. This aspect is not included in the presented design scenarios. The operation and control of the components is considered a specific knowledge field and lies outside the scope of this research. The design scenarios will only focus on the performance of the components, e.g. how the adaptive behaviour is realized.

4.2 Outfit

The outfit of a building system is constantly encountering environmental influences. These environmental parameters are highly variable and dynamic. Sun radiation, thermal load, wind, light and precipitation can serve as an example of such parameters. The building system is designed to maintain a satisfying functional performance while enduring these environmental influences. The environmental aspects do have a considerable influence on the user comfort. The outfit of the building as well as the service elements are designed to meet an acceptable indoor climate. Current solutions, such as installations and interior and mechanical appliances (e.g. sun shading, curtains, heating, and HVAC systems) help to control the indoor climate by dynamic environmental parameters.

The implementation of smart material systems can establish an immediate adaptation of the building system to the dynamic environmental parameters. Due to the intrinsic performance of these systems, reactive and lightweight elements can be integrated in the building system.

4.2.1 Adaptive Daylight System

The current popularity of all-glass facades will result in large heat gains and losses and thereby an increase of energy usage in order to maintain an acceptable indoor climate. The use of sufficient sun-shading will result in a reduction of energy usage for heating and cooling systems. Studies that have been performed on the manual operation of daylight systems (flexible level) showed that users did not alter the settings frequently in order to match an optimal indoor climate by a changed environmental situation (Rubin, et al. 1978). Users appeared to have their general preferred settings which seem to be independent from the daily routine and climate conditions (Rubin, et al. 1978). By improper use of these systems the actual mentioned energy reduction is not obtained. Logically, the manual controlled systems are only operated when users are present, although a considerable gain could be reached during times when users are absent. For example, unused spaces can deliver high temperatures to the rest of the building when the sun shading remains unused by extreme sun radiation. Automated control off the whole building will help optimize the building performance.

A considerable gain on the energy reduction by means of lighting and climate control systems can be established by actively adjust to the amount of sun transmittance. Automated motorized control of daylight systems (active level) has shown satisfactory performances, especially by the use in office buildings (Lee, et al. 1998). In most cases, a hybrid control system is applied here, which means that an automated system can be overruled by a manual control system. The performance of these systems is based on the detection of the sun radiation, after which, for example louvers, are opened or closed. Extended studies on automated blind systems show an considerable increase of the user comfort and a reduction of the energy consumption of approximately 7-15% (45º blind angle) and 17-32% (0º blind angle) in contrast to a static blind system (Lee, et al. 1998). However, operational problems such as maintenance and noise generation are profound issues. Thereby, large structural dimensions of the motorized systems will increase the building construction sizes. Studies with automated electro-chromic window systems (see chapter 3) showed that users did not overrule the automated system frequently and the available blinds were hardly used (Lee, et al. 2012). An advantage of electro-chromic windows above blinds can be found in the fact that an outdoor view is maintained, silent control is envisioned and the system is fully integrated in the glass panel.

In the first design scenario an external adaptive daylight system is presented, based on the ABC performance. This scenario is based on a similar performance of an external mechanical daylight system. The ABC's deflecting performance will replace the mechanical hinge system of a sun shading system. Adaptive elements are able to open and close according to the measured sunlight incidence.

The façade is constructed out of strips material of which particular parts can be controlled (see Figure 4.1). When sunlight is allowed to enter the building, the elements will be found in bent configuration. Subsequently, the sun is blocked after the ABC is recovered into its initial straight shape. In order to enable protection against high sun radiation, the component should be fabricated from opaque material.

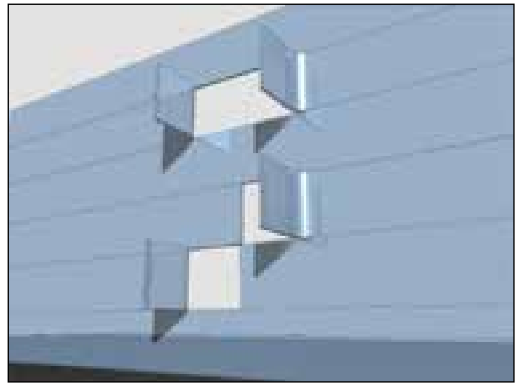

Figure 4.1 Adaptive daylight system, randomly opened.

4.2.2 Ventilation

4.2.2.1 Façade Tessellation

A similar principle can be used for the application of the ABC as façade tessellation (Figure 4.2). By controlling the individual components, the ventilation of the building is enabled by airstream. This principle can also be realized as a hybrid system, where both the wind load and the temperature are activation sources. A control system will detect the indoor and outdoor temperature and defines the façade configuration. With this method it is possible for the users to overrule the system and define the preferences and settings manually.

This principle can be optimized by the integration of a sun shading performance. By opening the upper side of the element, direct light can come in during ventilation (Figure 4.3). When opening the lower side, ventilation is enabled while simultaneously reflecting the direct sunlight. The activation of the façade elements always entails ventilation. This system can be applied externally on the building envelope, to enable the shading capacity while eliminating ventilation. The façade tessellation can be executed by different shape variations of the adaptive elements (Figure 4.4).

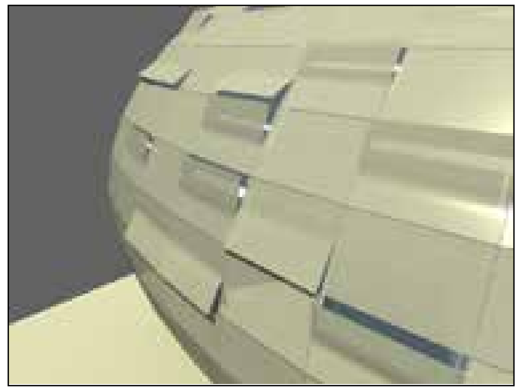

Figure 4.2 Facade tessellation for ventilation or sun-shading purposes.

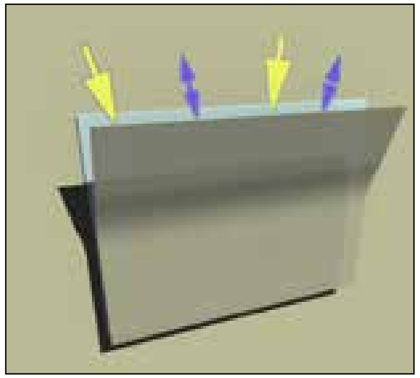

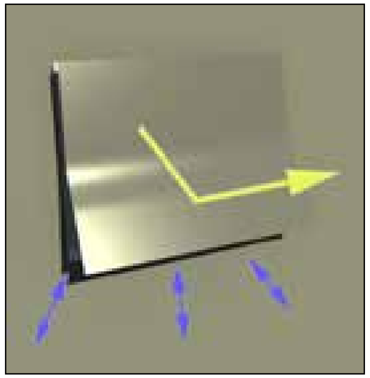

Figure 4.3 Left: Element opens at the top, enabling a free flow of air and light. Right: the lower side of the element is opened, the light is blocked and ventilation is enabled.

Figure 4.4 Variation of façade tessellation for ventilation and sun accession

4.2.2.2 Lamellas

The initial performance of the ABC is based on a recoverable one-way bending performance. The application area can be enlarged by introducing multiple bending behaviour. In Figure 4.5, a lamella system is presented which enables ventilation by the multiplication of the ABC principle. These lamellas are able to immediately open and close congruously to the amount of required fresh air. In the presented figure the lamellas are vertically oriented. Likewise, one could also think about a horizontal oriented lamellas system (Figure 4.6). The scale of the lamellas can vary and is related to the determined fabrication and performance characteristics.

A variation of a lamella can be envisioned, which is able to open at one side of the ABC slab (Figure 4.7). This performance is related to the gill cleft of a fish, mimicking the breathing performance. Although, it should be mentioned that the morphing performance is found at a slow pace.

Figure 4.5 Facade constructed out of ABC, initiating ventilation

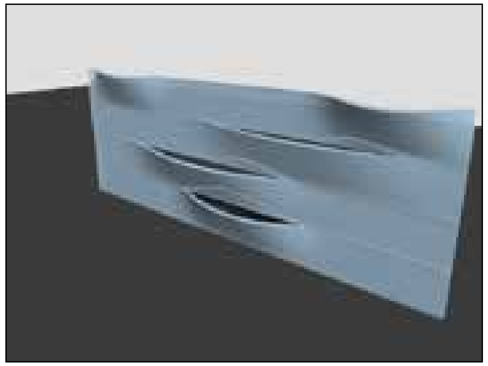

Figure 4.6 Facade elements, which can open and close for ventilation purposes

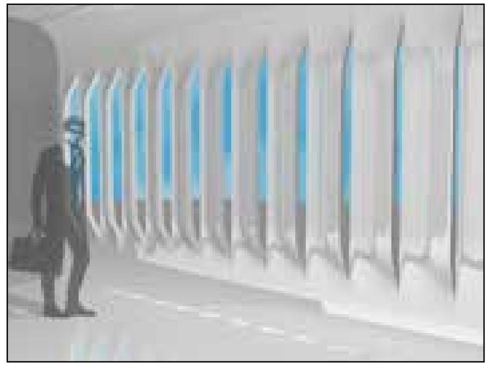

Figure 4.7 Vertical lamella system for ventilation purposes

4.2.3 Wind

High rise buildings experience considerable wind loads on high altitudes. This causes strict requirements for the installations that use natural ventilation input. Additionally, this prevents the opening of windows for ventilation purposes on high altitudes. By controlling the wind vortices on the building surface, a decrease can be found of the large wind loads. The small ABCs are used for adaptive façade tessellation, facilitating aerodynamic surface control. In Figure 4.8, the design concept is presented for an elementary building envelope. The small elements are able to open and close according to the wind velocity and direction. Every element can be controlled individually, leading to a diverse surface texture. The purpose of these elements is to lead the wind around the building envelope for better control of the wind-flow and thermal control. This principle enables the guidance of the wind from shadow parts of the envelope to parts where sun radiation can lead to a high heat load. Additionally, the purpose of these adaptive elements is a decrease of wind velocity and pressure. In order to generate such behaviour, the adaptive elements should be able to deform both in horizontal as vertical direction (Figure 4.9). Within this adaptive system, different configurations of the building envelope can be established when the aerodynamic optimization is required (Figure 4.10 and Figure 4.11).

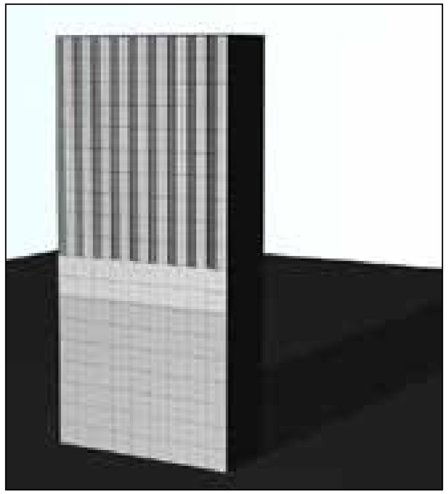

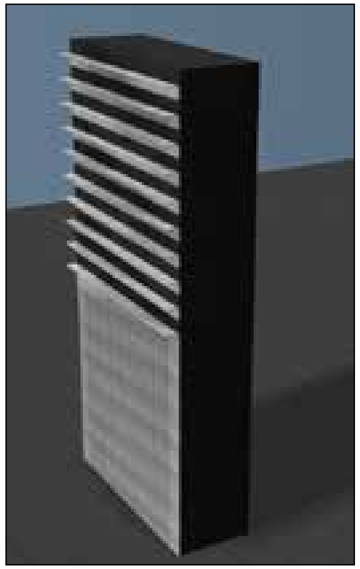

Figure 4.8: Model of adaptive façade tessellation, vertical and horizontal deformation of the smart elements enables aerodynamic optimization of the building surface.

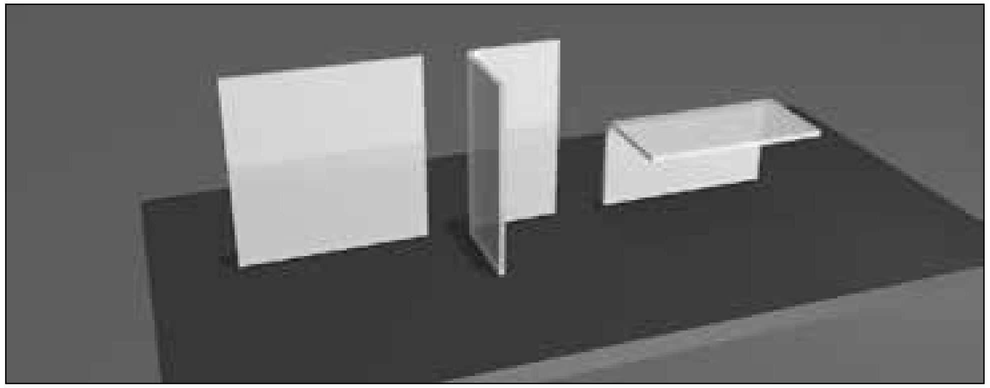

Figure 4.9 Schematic representation of shape morphing facade element. Left: flat surface, middle: vertical deformation, right: horizontal deformation.

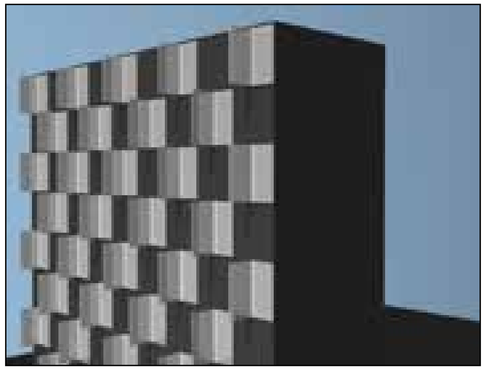

Figure 4.10 Vertical deformation detail.

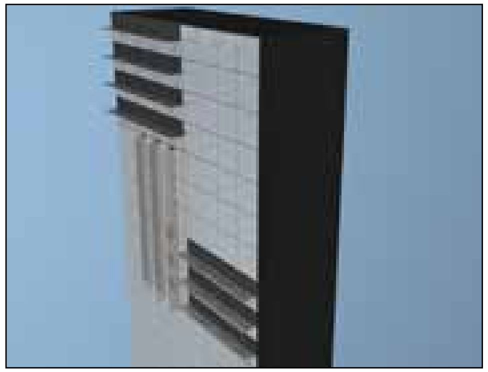

Figure 4.11 Deformation variations for wind conduction.

4.3 Infill

Currently large amounts of buildings remain unoccupied during a considerable amount of their lifetime. In general, utility buildings are unoccupied during the night-time, whereas other buildings, such as houses and theatres remain unoccupied during the daytime. Besides, a considerable amount of vacancies can be found due to a decreasing use in the functional segment or by functional decay. In this day and era, with a shortage of space in high urbanized areas and a decrease of material resources, such a high amount of unused space is not acceptable.

A possible solution for this problem could be found in the spatial adaption of the building space according to specific use and functions. In this vision, room sizes will be able to adapt their shape, size and configuration to the amount of occupants and the appropriate activity. Large spaces do not need to be heated when only used by a single person: it will shrink and morph to fit the user and activity requirements. Naturally, this prospect is highly conceptual and futuristic.

Adaptive infill elements for space division purposes have been found in various realized projects. In chapter 2, different adaptive infill systems have been presented, from sliding walls, to pivoting elements and draperies on ceiling tracks. The adaptive character of the floor plan configuration will enhance the functional use of a space. Based on user studies, the reconfiguration of the floor plan is highly preferable (chapter 5 and Hofman, et al. 2006). The application of smart material technology will show various advantages above mechanical adaptive wall elements, as is discussed in chapter 3.

Based on a similar bending principle of the presented lamellas, an adaptive space division concept has been developed. By scaling the lamellas, possible application in a non-bearing interior wall could be envisioned. In Figure 4.12 (left), a schematic of the straight configuration is shown. By activating the ABC slabs a functional space is created (Figure 4.12, right). The configuration of the space is determined by the precise control of the bending angle of the ABC. It is recognized that such a large scaling application is highly experimental. However, it is interesting to think about such large scale performances of the ABC.

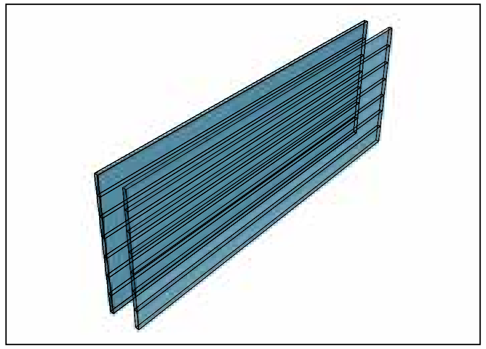

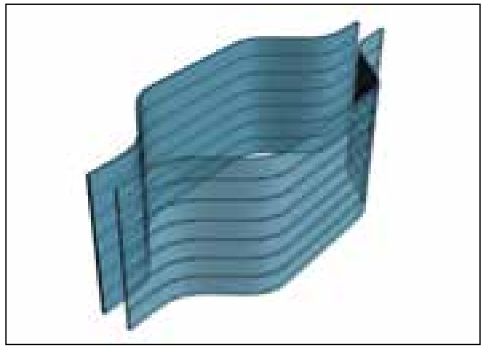

Figure 4.12 Left: Straight configuration; hallway Right: Strips are deformed creating an extra space, when required.

4.4 Interior

The current urbanization and the thereby related decrease of user space, demands for a multifunctional use of the building stock. A space can be designed based on the flexible floor plan and thereby guarantee a flexible use of the space. However, the functional use is highly dependable on the present elements. Specific furniture elements are required to perform certain functions. In order to enable multi-functional use of space, either all required elements should be present, covering a considerable amount of unused floor space, furniture has to be (re)moved or furniture with multifunctional use should be present. An example of multifunctional interior elements is a studio couch. These furniture elements can be transformed into beds when the function sleeping is appears. To prevent constant moving of furniture and other elements, an adaptive interior design would be an interesting solution.

In this design scenario an interior design is presented, which enables an adaptive configuration of space. The furniture elements can dissolve in the floor or walls when use is not required (Figure 4.13). By constructing a space out of strips, the ABC can be used for the generation of furniture elements. The room can react on the amount of visitors by erecting and dissolving furniture elements (Figure 4.14). For the application of furniture element, the ABC should deliver enough stiffness. As the material erects out of the floor, the material should be stressed at other places in order to maintain the room size. Here, a similar problem arises compared to the envelope lamellas, which require stretching to prevent shrinkage of the space during performance.

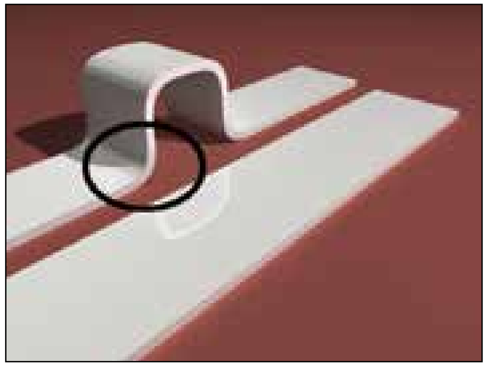

Figure 4.13 Furniture element based on the presented performance of the ABC. The encirceled part is the required performance of the ABC.

Figure 4.14 Interior view of adaptive furniture and façade system.

4.5 Case study Aerodynamic Optimization of the Building Envelope[7]

4.5.1 Introduction

Wind is a phenomenon which is highly dynamic by nature and thus is a challenging design driver for architecture. The aerodynamic performance-oriented optimization of shapes is a rather common technique in the turbo machinery, aerospace, naval, wind turbine and automotive industries. The operating conditions of components and vehicles are characterized by a flow direction, which is constant or varying within a small range. The optimization process, allows the maximization of the aerodynamic performance. In aerospace, mechanical adaptation of the shape is characterized by a changed fly direction. Additionally, wind turbines are able to rotate in relation to the wind direction. It should be noted that adaptive aerodynamic optimization by the use of smart material technology is an upcoming aspect in these industries (Chopra 2002; De Rossi, et al. 2004; Carpi, et al. 2005; Hulskamp 2011; Icardi, et al. 2011). However, fully functioning application of smart material elements in practice have not been realized yet.

Buildings, as static elements, endure dynamic wind loads. Especially, at high altitudes considerable wind loads can be found. By the use of adaptive building systems, which are able to adjust the large scale geometry to external conditions, the building can react to these adaptive parameters (Irwin 2009; Teuffel, et al. 2009; Tse, et al. 2009). Studies of geometrically morphing building skins for high-rise towers, which are wind responsive (i.e. the overall structural geometry can respond to external conditions), have already been carried out (Teuffel, et al. 2007).

A second option for modifying the aerodynamics of the building is to act at a smaller scale, by changing the roughness of the envelope. It is demonstrated that effects of reduction of wind pressures are considerable for walls with surface roughness such as balconies, louvers, canopies and any kind of appurtenances (Chand, et al. 1998; Maruta, et al. 1998). Adding external elements to the building envelope can reduce the local forces on the building façade. Obviously, by actively modifying the external flow field it is also possible to act on the natural ventilation and the heat exchange between internal and external environments. In fact, the heat transfer coefficient from the building surface to the environment is strongly correlated to the air velocity. External roughness elements, which are able to change orientation, can strongly modify the velocity field, for example, by making a more uniform pattern on the facade or canalizing the airflow and moving it in different zones. These external elements should be able to move and adjust themselves assuming different apertures and directions in different areas of the building façade according to the wind characteristic and the current needs (e.g. cooling energy demand). Therefore, an adaptive façade system, based on the ABC performance is presented which can divert the wind flow.

The wind load of a high-rise building with a locally geometrically morphing façade is analysed by numerical simulation. The focus lies on the influence of the surface texture on the wind pressure and velocity fields. The attributes are controlled individually, to enable a full control of the building surface.

4.5.2 Wind

The aerodynamic and hydrodynamic characteristics of a smooth body are not necessarily better than the ones of a rough body, as it might be naturally expected. Surface roughness does indeed increase the friction between the flow and body, but it has also a positive influence on other phenomena. The increase of the

7. This study is based on a published paper co-authored by L. Lignarolo and P. Teuffel (Lignarolo, et al. 2011).

surface roughness could paradoxically be the enhancement of the aerodynamic characteristics of the body. Various examples of this apparent inconsistency, where the surface roughness is exploited for enhancing the aerodynamic characteristic of a body, can be found in different fields, such as sport and nature. The extremely rough skin of a shark reduces friction when it glides through water, resulting in fast and efficient swim capabilities (Shark Skin Coating webpage). This principle is affected by a multitude of V-shaped bumps that cover the shark's body. The bumps channel water along the grooves in the skin fabric, allowing the water to spiral in microscopic vortices (small tornado-shaped water formations). The forming of eddies is hereby prevented as water passes over the skin. This effect has been mimicked in sportswear for optimized performance.

Another interesting example of aerodynamic optimization is the random-looking bumps on the humpback whale's flippers (Peacock, et al. 2008). A sort of tubercles is enhancing the hydrodynamics performance of the fins, enabling fast turning manoeuvres. By translating similar design strategies to wind turbines, the reduction of drag and the increase of lift can be realized. This feature will enable the generation of energy under low wind conditions (Whale power webpage).

Also, in the design of golf balls roughness is used for the reduction of the drag force (Aoki, et al. 2010; Smith, et al. 2010). The dimples on the surface of a golf ball cause the air flow on the upstream side of the ball to transit from laminar to turbulent (see Figure 4.15). The turbulent boundary layer is able to remain attached to the surface of the ball much longer than a laminar boundary and so creates a narrower, low pressure, wake and hence less pressure drag. The reduction in pressure drag causes the ball to travel further.

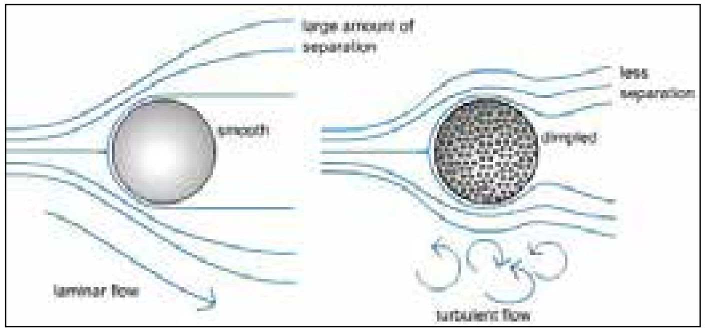

Figure 4.15 Flow field around a golf ball. Image courtesy unknown.

In the field of architecture, research has been performed on how the façade roughness can affect the wind distribution on the building surface. Experimental data indicated that for a 25 meter square section high-rise building, wind pressures are remarkably affected by the surface roughness (Maruta, et al. 1998). This effect was particularly found near the leading edge of the side wall on which local severe peak pressures decreased with increasing roughness. It is demonstrated by wind-tunnel experiments that an increase of the roughness length from 0 to 1.2 meter established a reduction of the under-pressure of approximately 25% to 30% close to the building upwind edge (Maruta, et al. 1998). Thereby, the surface roughness influenced the fluctuation of pressures produced by the disturbance of separated flows and separation bubbles. An increase of the roughness length from 0 to 1.2 meter reduced the oscillation of about 70%. These roughness attributes can be realized by the addition of, for example, balconies on the building envelope.

In other research, the pressure distribution on the windward wall of a low rise building by balcony-like roughness elements was analysed (Chand, et al. 1998). The different pressure distribution on the façade of a low rose building with and without balconies was calculated (Chand, et al. 1998). It was demonstrated that large differences occurred, especially close to the top and the bottom floors of the building. Naturally, this phenomenon was affecting the overall driving force of wind-driven natural ventilation. The balconies can be approached as very large roughness tubercles. It was shown that provision of balconies altered the wind pressure distribution on the downwind wall. Balconies produced a reduction of the wind pressure over the entire upwind wall on the ground floor and also at points covered by the balcony at the top floor. The wind pressure increased at the intermediate floors. This effect can be used for modifying the ventilation magnitude through openings located at opposite walls or for enhancing the stack effect of openings located at different heights above one floor.

4.5.3 Design

The given that the surface texture of a body can manipulate the aerodynamics of this body forms the basis for the design of a building envelope. The change of the surface texture for the control of the wind pressure and velocity is an important design condition. The large wind forces on the building envelope are used as a performative stimulus. The morphing building envelope must be able to change its surface roughness in order to control the indoor climate by natural ventilation. This principle can also be found in biology by the fur of mammals and the feathers of birds. By adjusting the thickness of their "coat" the thermoregulation of the animal is exploited.

The presented design in paragraph 4.2.3 enables the aerodynamic optimization of the building envelope. In relation to the fur of a mammal, the airflow can be meander controlled over the building envelope. This will reduce the high wind velocities and enabled natural ventilation on large altitudes. This performance is studied successively by simulation models.

4.5.4 Performance Study

The performance of the adaptive elements for enhancing the air-flow of high-rise buildings is studied using computational fluid dynamics (CFD). A series of CFD simulations has been conducted of some simple case studies. The purpose of these simulations was to analyse the actual influence of external roughness elements on the wind flow field close to the surface of a building. The code OpenFOAM 1.7x has been used for this purpose. This software has been chosen because it is a reliable general purpose code, open source and contains solvers especially suited for the wind analysis.

As a first step to assess the validity of the method and the tool, the case analysed by Chand (1998) has been reproduced. Figure 4.16 shows the geometry of the low rise building with dimensions 10 by 7.5 by 15 meters. Balcony-like appurtenances are added on the front face (upwind facade). The following two cases have been simulated:

A1. smooth wall
B1 . wall with balconies

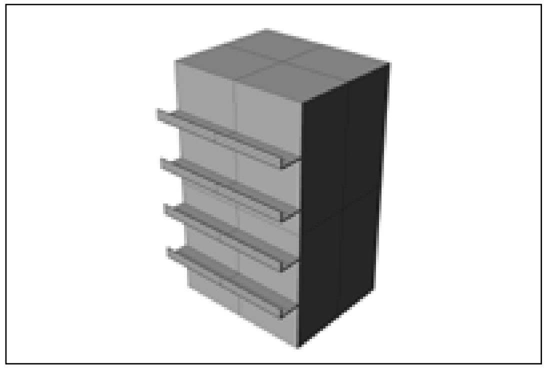

Figure 4.16 Low rise building with balconies (B1)

After the validation of the simulation tool, the aerodynamic performance of the design concept is studied. A simple box-shaped high-rise tower is used for this purpose, with dimensions of 30*30 meter and a height of 100 meters. The roughness elements are positioned along the entire building surface in vertical and horizontal direction (see Figure 4.17). The vertical appurtenances are covering the entire floor height. Hence, the following cases have been simulated:

A2. smooth surface
B2. horizontal roughness elements on the side wall
C2. vertical roughness elements on the side wall

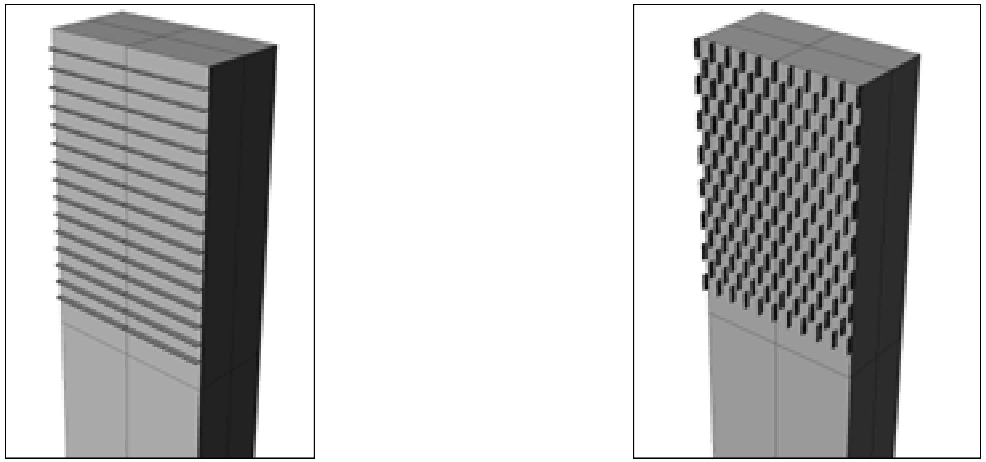

Figure 4.17 High-rise building with roughness elements (Left: case B2 and right: C2)

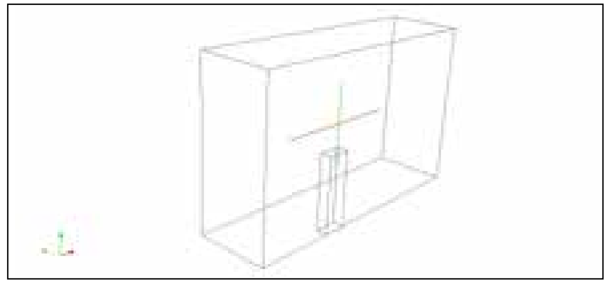

Figure 4.18 Computational domain

Figure 4.18 shows the computational domain which is used for the simulation. It is a simple rectangular box with a length of 360 meters, a height of 220 meters and a width of 100 meters. The building is positioned 100 meters after the inlet. Due to the symmetry of the chosen geometry, only half of the domain has been taken into account and a symmetry plane boundary condition has been applied at the central wall. The mesh is constructed out of 1,500,000 points. Each simulation has been performed with the Reynolds Average Navier Stokes method using the *k-ε* turbulence model. At the inlet, a velocity profile with the classical shape of an Atmospheric Boundary Layer (ABL) has been introduced.

4.5.5 Simulations Results and Discussion

The comparison between the two sets of data is shown in Figure 4.19. The first simulation shows a rather agreeable match between Chand's results and the CFD results. The matching between the two sets of data is not perfect but can be improved by further refinement of the mesh. At this stage of the study, the current data is considered satisfactory. The purpose of this study is to generate insight in the performance of the adaptive façade elements, more than creating an advanced simulation model.

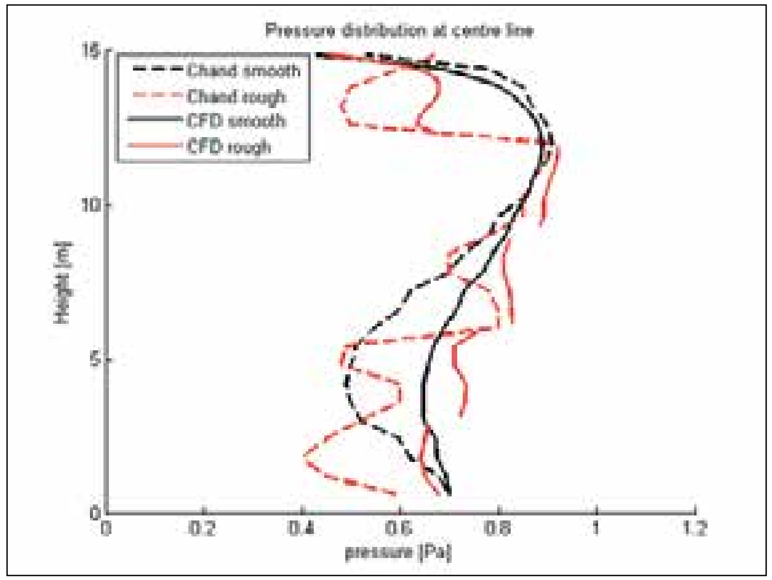

Figure 4.19 Comparison with the simulation results of Chand's experimental data.

Figure 4.20 shows the comparison between the pressures fields of the smooth building (case A1) and the building with appurtenances (case B1). Only the values of the front side (the one facing the wind, the upwind façade) are reported. The differences between the two fields due to the presence of the balconies are rather evident, especially at the locations on the top and the ground floors.

After the validation of the methods, the second case study has been analysed. It has been noticed that the difference in the pressure fields for the case of a smooth and a rough facade are much less evident for high rise buildings. However, the influence of the roughness elements is much stronger on the velocity field.

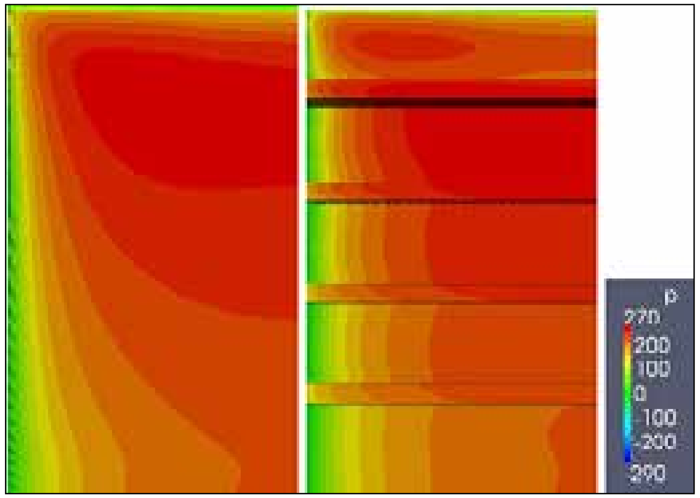

Figure 4.20 Pressure field on the upwind façade of the low-rise building (Case A1 and B1)

In Figure 4.21, the velocity fields of case A2, B2 and C2 are compared (wind approaching from the right hand side of the picture). The values of velocity are taken along a plane located at 0.5 meters away from the façade surface; this corresponds to the plane which intersects the roughness elements at their centre point. Notice how much the flow field is affected by the presence of the roughness elements. Along the smooth façade (case A2), velocities are mostly within the range 5 – 9 m/s and up to 15 m/s close to the top and the upwind corner. Right after this corner, there is an area where the velocity is almost equal to zero. Moving the roughness elements in a vertical direction (case C) provides a larger uniformity of the flow field. As a matter of fact, they offer a big resistance to the wind, decreasing the air velocity close to the façade. This effect can be exploited when there is need to decrease the heat exchange between the indoor and outdoor environment, for example at winter time in the case of strong wind. Turning the roughness elements into a horizontal direction provides a sort of canalization of the air that can be exploited for moving the zone at a higher velocity where desired. For example the areas of the building at higher insolation, where there is need to enhance the natural heat exchange.

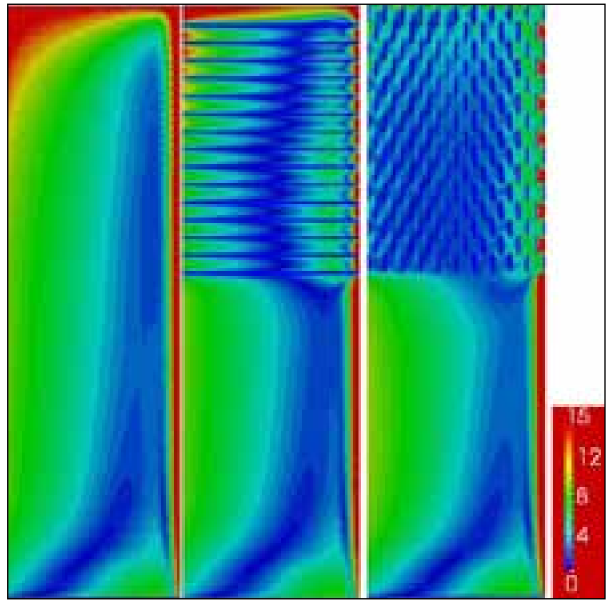

Figure 4.21 Velocity field on the side wall of the high-rise building (case A2, B2 and C2). The wind is approaching from the right-hand side.

Another minor, but still positive effect obtained by adding roughness elements on the façade is the decrease of vortices close to the upwind corner. Figure 4.22 shows the different pressure distributions on the lateral side of the building (wind coming from the right hand side of the picture) with (case A2) and without (cases B2 and C2) the roughness elements on the side wall. The zones characterised by a strong under-pressure and therefore by a strong suction on the façade elements (e.g. windows or double skin elements) are coloured in red. It is evident in Figure 4.22 that close to the building corner in the upwind zone there is a strong under-pressure area. This is due to the presence of a corner vortex, which is almost completely eliminated.

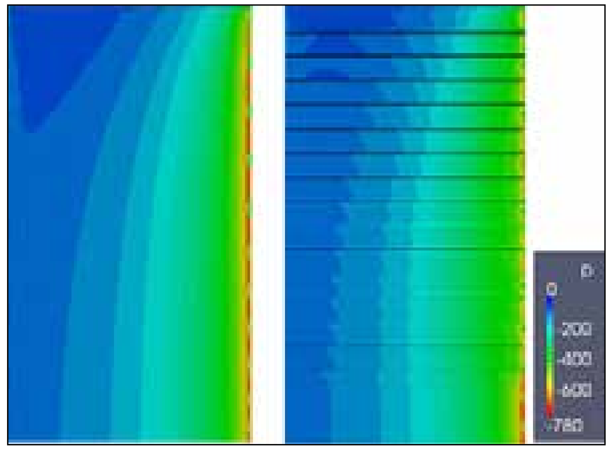

Figure 4.22 Detail of pressure field on the top region of the side wall of the high-rise building (case A2 and B2). The wind is coming from the right-hand side.

4.5.6 Conclusion and Discussion

It has been demonstrated both by past wind tunnel tests and CFD simulation that the texture of a building façade has a strong effect on the wind flow field. This phenomenon can indeed be exploited for the modification of the natural ventilation inside the building, the heat exchange through the envelope, as well as for reducing the effect of strong vortexes on the façade elements. The difference in the pressure field is much more evident for low rise buildings in relation to high-rise buildings. However, for high-rise buildings the velocity field is much more affected by the presence of façade elements.

It is recognized that the adaptive building systems meet large wind forces, especially on higher altitudes. When the elements are subject to large wind forces during transition to other configurations, larger deformation forces are required. Further research is important to study these adaptive elements in wind and outdoor situation. The relation between the deflection size and the effect on the wind velocity is an important aspect for further study.

The presented performance of the ABC is limited to a single directional deformation, although, in the design proposal elements are presented that can be deformed in more directions for an optimal regulation of the wind flow field. The shown design scenario elucidates the application of the smart composite as a façade tessellation. Further development of the ABC will show the feasibility of the proposed design concept for wind conduction purposes.

4.6 Conclusion

In this chapter a diverse presentation of design proposals is given, based on the presented deflecting performance of the ABC. The application field of the ABC has been found in *infill*, *outfit* and *interior* components of the building system. The design scenarios are based on the presented performance of the ABC. Different scales are used to broaden the field of application. It should be noted that further optimization of the ABC is required to meet the presented scaling and performances.

In order to analyse the performance of the ABC for aerodynamic envelope optimization, the wind load is studied for different design scenarios. Corresponding studies on the performance for ventilation and sun shading purposes present the advantages of adaptive elements. Further research on immediate adaptive façade tessellation will show the optimization of the indoor climate in relation to the energy gain of such a façade optimization. The discussed simulations show advantages of this adaptive envelope system.

The presented design scenarios are based on a functional performance of the building components. Other performance based possibilities can be envisioned with the presented design scenarios. Especially the façade tessellation scenario could also be operated for entertainment purposes. By controlling the components individually patterns can be formed.

Overall, different application solutions based on the ABC performance have been presented. Future shape-morphing building components do show promising performances. However, the fabrication and operation of the shape-morphing building components remains an interesting challenge. In the following chapters these challenges will be tackled.

4.7 References

Aoki, K., Muto, K., et al. (2010). “Aerodynamic characteristics and flow pattern of a golf ball with rotation.” Procedia Engineering **2**(2): 2431-2436.

Carpi, F., Sommer-Larsen, P., et al. (2005). Electroactive polymers: new materials for spacecraft structures. European Conference on Spacecraft Structures, Materials and Mechanical Testing K. Fletcher. Noordwijk, The Netherlands.

Chand, I., Bhargava, P. K., et al. (1998). “Effect of balconies on ventilation inducing aeromotive force on low-rise buildings.” Building and Environment **33**(6): 385-396.

Chopra, I., University of Maryland (2002). “Review of State of Art of Smart Structures and Integrated Systems.” AIAA Journal **40**(11): 42.

De Rossi, D., Carpi, F., et al. (2004). Electro-Active Polymers For actuation and sensing in space applications. 55th International Astronautical Congress Vancouver, Canada**:** 1-11.

Hofman, E., Halman, J. I. M., et al. (2006). “Variation in Housing Design: Identifying Customer Preferences.” Housing Studies **21**(6): 929 - 943.

Hulskamp, A. W. (2011). The smart rotor concept on wind turbines actuator Dissertation, Delft University of Technology.

Icardi, U. and Ferrero, L. (2011). “SMA Actuated Mechanism for an Adaptive Wing.” Journal of Aerospace Engineering **24**(1): 140-143.

Irwin, P. A. (2009). “Wind engineering challenges of the new generation of super-tall buildings.” Journal of Wind Engineering and Industrial Aerodynamics **97**(7-8): 328-334.

Lee, E. S., Claybaugh, E. S., et al. (2012). “End user impacts of automated electrochromic windows in a pilot retrofit application.” Energy and Buildings **47**(0): 267-284.

Lee, E. S., Dibartolomeo, D. L., et al. (1998). “Thermal and daylighting performance of an automated venetian blind and lighting system in a full-scale private office.” Energy and Buildings **29**(1): 47-63.

Lignarolo, L., Lelieveld, C. M. J. L., et al. (2011). Shape Morphing Wind-Responsive Facade Systems Realized With Smart Materials. Adaptive Architecture. F. Stacey and M. Stacey. Londen, UK.

Maruta, E., Kanda, M., et al. (1998). “Effects on surface roughness for wind pressure on glass and cladding of buildings.” Journal of Wind Engineering and Industrial Aerodynamics **74-76**: 651-663.

Peacock, T. and Bradley, E. (2008). “Going with (or Against) the Flow.” Science **320**(5881): 1302-1303.

Rubin, A. I., Collins, B. L., et al. (1978). Window Blinds As a Potential Energy Saver - a Case Study. U. D. o. Commerce, N. B. o. Standards and U. States**:** 85.

Shark Skin Coating (webpage) Retrieved 2011-02-10 from www.sharkskincoating.com.

Smith, C. E., Beratlis, N., et al. (2010). “Numerical investigation of the flow over a golf ball in the subcritical and supercritical regimes.” International Journal of Heat and Fluid Flow **31**(3): 262-273.

Teuffel, P. and Ajdarpasic, D. (2007). Development of a Shape Morphing Building Envelope. IASS 2007 Structural Architecture; Toward the Future Looking to the Past. Venice, Italy.

Teuffel, P., Plomp, H., et al. (2009). Computational Morphogenesis Using Environmental Simulation Tools. International Association for Shell and Spatial Structures (IASS) A. Domingo and C. Lazaro. Valencia, Italy.

Tse, K. T., Hitchcock, P. A., et al. (2009). “Economic perspectives of aerodynamic treatments of square tall buildings.” Journal of Wind Engineering and Industrial Aerodynamics **97**(9-10): 455-467.

Whale power (webpage) Retrieved 2011-02-10 from www.whalepower.com.

CHAPTER 5

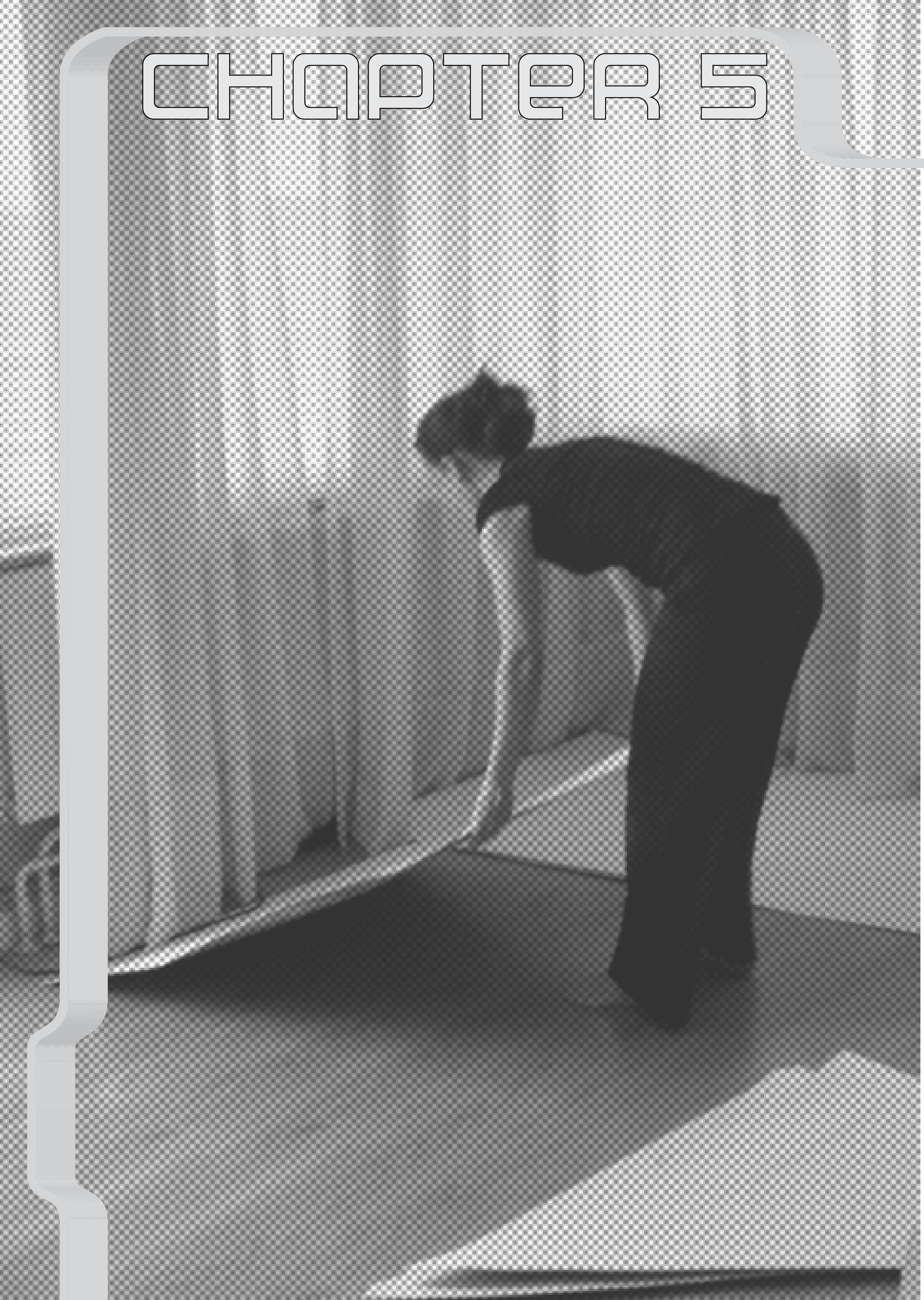

USER RECEPTIVENESS TO ADAPTIVE ENVIRONMENTS

5.1 Introduction

In the previous chapters the concept of adaptive architecture has been analysed. Additionally, the translation of shape morphing components into tangible environment has been explored. The application of smart material technology can lead to the realization of an adaptive environment on a dynamic or, with the implementation of advanced systems, interactive level. The realization of dynamic environments will not only lead to profound changes in terms of functionality and performance, but will also change the relation between the environment and the user. With the introduction of a new vision in architecture it is important to connect with the values of the users. As Weiser states: “What matters is not technology itself, but its relation to us” (1996).

Dynamic environments require a different user approach. The interaction between the dynamic environment and the user is realized immediately and sometimes even initiated by the building itself. This can be illustrated by an adaptive sun-shading system. The system can initiate a performance during high sun radiation. The user can adjust this performance and thus will become actively involved in the performance of the system. Ideally, the system will register these adjustments and will act accordingly during the following occurrence. As discussed earlier, adaptive building systems can be found in the current building situation. These systems are mostly considered flexible or active. By taking the step to a dynamic or interactive environment, a new paradigm of buildings will evolve. This will influence the relationship between the user and his environment considerably, as well as the versatility of user space.

In the course of the development of this new paradigm, a study has been conducted on the receptiveness of users on adaptive environments. It is crucial to perform research on user experience, not only to gain insight into the success or failure off adaptive architecture, but also to analyse the ideas and preferences of the user for the design of an adaptive environment. The collaboration with users can lead to more pragmatic ideas. It will ensure that the technology meets the need of the user through appropriate design.

The user preferences based on functionality have been examined in relation to the instant adaptation of a residential environment; the home. Through the use of case studies, the user preferences of adaptive spaces have been analysed. As the technology is often not yet available, mock-ups were used in order to solve the technological discrepancy. The analysed case studies in this chapter are pushing the adaptive building concept towards a full ambiguous building system which can be adapted according to specific activities.

5.1.1 User Experience and Acceptance of Adaptive Architecture

The user experience of the built environment is a widely studied subject. However, on the subject of dynamic or interactive environments, the user requirements and preferences are still largely unknown. Most sources focus on the current state of the building environment, whereby immediate adaptive architecture is mostly ignored. When focusing on specific products, such as adaptive daylight systems, see chapter 3 and 4, research has been performed, but usually discusses the operation and control, rather than the user experience and receptivity.

The experience of a space is crucial for the acceptance of a space and is related to the success factor of a building. Naturally, a positive building experience will add to the success of a building. People's relationship to buildings is an ever-changing phenomenon. These are influences by different parameters such as politics, rituals, economics, social and cultural conditions, conscious and unconscious experiences (Proshansky 1978; Manzo 2003). The parameters which influence the relationship with a building are connected to the parameters which determine the form of a building. Rapoport (1969) defines that the socio-cultural factors as well as the physical factors, are influential parameters on the form of the building. The socio-cultural parameters (which include the ritual, economic and political factors) are the primary forces which determine the form and use of the building. The physical factors are the secondary forces and are determined by the climate conditions, construction method, available materials and advances in technology (Rapoport 1969; Ittelson, et al. 1974).

Technological developments play a large role in the socio-cultural development of society. The embedded technological innovations have changed the way of living enormously. Communication with and transport to the other side of the world remained expensive and time consuming 50 years ago. Now, our current personal and information network has spread immensely on a global level. This has resulted into an extensive globalization of knowledge and information. Due to globalization, unification of socio-cultural aspects between countries and continents has led to a standardization of the built form.

5.1.2 Adaptation of the Home Environment

This study is focusing on receptiveness of the user to adaptive *home* environments. Home is the place of the occurrence of multiple activities, compared to other spaces, such as utility buildings among others. The home is the embodiment of the self and also expresses the relation of the self to a broader society (Feldman 1990). If this society is under a constant change and embedded in the technological world, the effects of a static and outdated house on the inhabitant could be two-fold. Either the users are longing for safe predictable times and traditional houses (nostalgia), or this could lead to a discrepancy between the user and the place they live in, as the users live in houses that do not meet their requirements.

According to Relph (1976) home is the central reference point of the human existence. Feldman (1990) emphasizes this when she defines the home environment as a "unique place of familiar, known, and predictable activities, people, and physical elements". An interesting question would be how people will react if this focal point of predictable activities would be subject to immediate change, even when this change is under full control of the user. This will be a subject of research in this chapter.

There is hardly any literature on the subject of the appearance of the home and the wish for redecoration and reconfiguration the existing setting. Mostly, user research is focussing on emotions and situations for the analysis of the psychological relationship between place and user (Manzo 2005). On the relationship between the ever changing and developing user and its environment, Rapoport points out that we must look for a "loose" framework whereby the interplay of the constant and changeable aspects of man can find expression."(1969). This theory is supported by Studer (1970) who defines an "open" environment that should be "adaptive" to the behaviours it supports (Ittelson, et al. 1974), which is very closely related to the "plan libre" of Le Corbusier (1986).

Although these definitions are not very specific about the physical form and performance of a space, it can be concluded that the space should be open to changes. The ever-changing character of the user is recognized and translated to the built environment. Rapoport (1995) underlines the problem of the negligence of the physical aspect in the environmental psychology. Rapoport does not go further than stating that a house should be an "environment best suited to the way of life of a people" (1995).

Norberg-Schulz defines that the concept of place requires rich possibilities of identification (1988). With the term *genius loci*, Norberg-Schulz describes the spirit of the place, which is based on its character. This can be clarified in relation to the place-identity theory of Proshansky, in which he states that users generate a place-identity, which is based on the dimensions of the self, related to the personal identity and physical environment (1978). The place-identity is a sub-identity of the self-identity of a human being, in which both influence each other. It must be noted that the place-identity is based on individual experiences as well as social experiences from a whole groups living under the same circumstances and situations. Identity is a dynamic organism even if it is in a state of equilibrium (Breakwell 1986). A building's success is based on the relationship between the building and its users, and how the users can identify themselves with the building. This relationship and identification can alter through the years. The self-identity is under constant change and the place-identity will develop coincidentally.

The change from the static building representation to the constant adaptive building concept will require a shift in the user identity. Breakwell (1986) created an identity model, which is based on two processes; the process of assimilation and accommodation and the process of evaluation. By assimilation, new components are absorbed into the identity structure of the user. Accommodation is used for the process in which new elements are fit in the identity structure by means of adjustments. The new elements are accommodated in the identity structure. The process of evaluation induces the "allocation of meaning" and values both the old and new identity content. Both the old and new elements will constant evaluate to a satisfied identity balance. In the model of Breakwell both processes are interrelated and influence each other. As Breakwell states; "The interplay of both processes across time will produce the content and value dimensions of identity" (1986).

Even though Breakwell did not study interactive buildings it should be credible from his theory that the user can become accustomed to the changing physical and changing environment, as the self and the related place-identity are able to respond to these changes (Proshansky, et al. 1983).

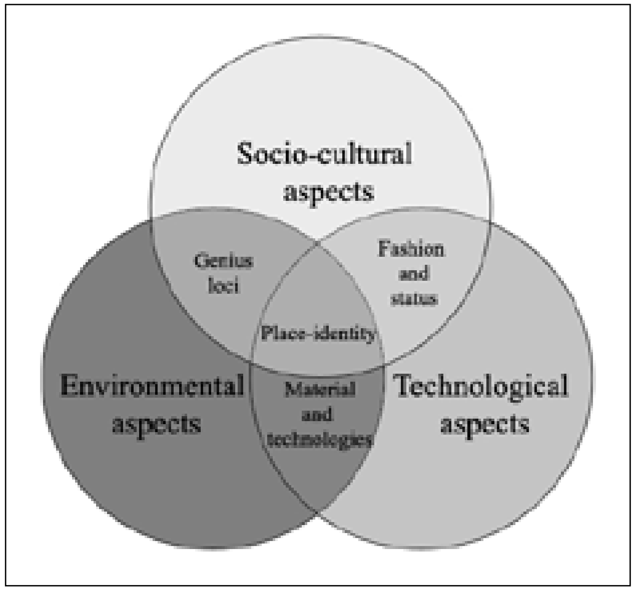

Figure 5.1 Model of influential aspects on places based on the place-identity of the user.

Based on the literature of Rapoport (1969), a model of the influential parameters on the place-identity is developed. In Figure 5.1, the influential aspects on the place-identity are illustrated. The visualization of the home is strongly related to the place-identity of the users (Breakwell 1986). The place-identity is influenced by the socio-cultural aspects (Rapoport 1969; Proshansky 1978; Manzo 2003), physical aspects and environmental aspects. The environmental aspects are linked to the geographical location, which include climate, vegetation and soil, as well as the (urban) location. Fashion and status are determined by physical aspects such as existing technologies and are characteristic for the time period and customs. Fashion and status have changed from national scale to international scale, supported by the current technological advancements. This has clearly influenced the perception on the world and its translation to the built environment. The genius loci, as explained earlier, describes the relationship between the location and the socio-cultural aspects. The genius loci are the characteristics of the place and determine the appearance of the building (Norberg-Schulz 1980).

The building material and technologies are influenced by the geological location as well as the current state of knowledge. An example is the construction of North-American houses out of wood and the West-European houses out of stone and bricks, as these materials are more available on the respective locations.

The influential parameters are constantly changing and evolving and subsequently influencing the place-identity. This will lead to a change of the home requirements as well as the building performance, shape and use. Changing influential parameters which relate to immediate adaptive buildings are discussed in chapter 1. The last century the building location has concentrated to higher urbanized areas, with rare floor space and privacy. Additionally, physical developments such as the personification and customization of electronic products based on technological advancements are an important development. The place-identity has been influenced according to these parameters. Immediate adaptive buildings are presented in this research as a reaction on these fast developments.

In this research project, the receptiveness of the users on adaptive environments is analysed in relation to the home, based on distinctive activities. People distinguish places on the basis of behaviour (Genereux, et al. 1983). Behaviours are related to a place in such a way that they happen more frequent in relation to other behaviours at that specific place. A set of rules is determined by the user for every specific activity to which the place should comply with.

5.1.3 Customization of the Interior

Related research on the subject of the home customization can give an insight into which attributes the user would like to change within the current building system. A study executed on the customization preferences of new house owners, stated that the priorities of customization were found at the attributes for interior finishing (importance of 30%), house volume and exterior (26%) and floor plan (23%) (Hofman, et al. 2006). Other tested attributes, such as technical systems (12%) and environment (9%), scored relatively lower. Naturally, it is recognized that in this cited study adaptive building attributes were not an issue of interest. The main interest was about which attributes the participants would prefer to change at the moment they move into a new house. However, the study gives an indication of which home attributes prefer customization. These attributes will be studied further in an adaptive building context.

5.1.4 Research

An inventory is made of the users' visions on adaptive architecture in relation to a specific activity. Three different kinds of studies were conducted in order to collect information on these user aspects. First, an exploratory research was conducted to gain insight on the receptiveness to adaptive architecture by the users, using an internet inquiry. The second part consisted of an interview. The purpose of this interview was to analyse what users would like to adapt according to predefined activities. In the last part of this user research, specific adaptive attributes were explored. Here, physical models were used to illustrate the adaptive performance. These studies were also conducted by use of interviews.

The research is based on a qualitative approach; due to the lack of prior research on this subject, this will lead to a better understanding of the results. As an adaptive environment is not a familiar setting, it is important to keep in mind that the participants mostly base their vision on the current situation and what they are familiar with (Valkenburg, et al. 2008). The participant has to break with the conventional ideas of the static environment. To help the participants develop a mind-set whereby everything was possible, a scenario was read preliminary to the inquiry. The participant had to imagine living in the year 2030 where no restrictions on technological level would border any imaginary ideas. The scenario of both the survey and the interview were identical.

The main questions of this research are:

1. How receptive are users to adaptive environments?
2. How do users want to adapt their home related to different activities?
3. Which building attributes should be adaptive?

5.2 Internet Inquiry

5.2.1 Research Method

The internet inquiry consisted of general questions to attain information about the participant, followed by research questions formulated on a visual analogue scale and ended with open questions on the subject of interactive architecture. The participants had to respond how receptive they were to the proposed scenarios of adaptive building attributes. The participants had the possibility to give their answer on a 1 to 5 scale basis, with the scaling value 1 as very negative, 2 as negative, 3 as no opinion, 4 as positive and value 5 as very positive. Examples of the given scenario were: the possibility of changing the colour of a wall, changing the inner wall to reconfigure the amount of rooms, the opening of the roof or adapting the position of the windows and the change of transparency. The questions of the internet inquiry are presented in Appendix 2. The proposed scenarios were based on a brainstorm session executed by students.

The internet inquiry was spread by email to approximately 200 people of Dutch nationality, of which a number of 70 people participated; 42 female and 28 male. The 200 people were randomly chosen out of the acquaintance database of the students who collected the data.

5.2.2 Results

In Figure 5.2, an overview is given of the adaptive examples and the resulted score. In general, a high score is found for the specific adaptive attributes. Scores higher than 4 are found for:

- Wireless electric socket
- Disappearance of interior elements
- Change of ambience by colour
- Change the transparency of windows
- Furniture in floor
- Windows move with sun
- Change of interior walls

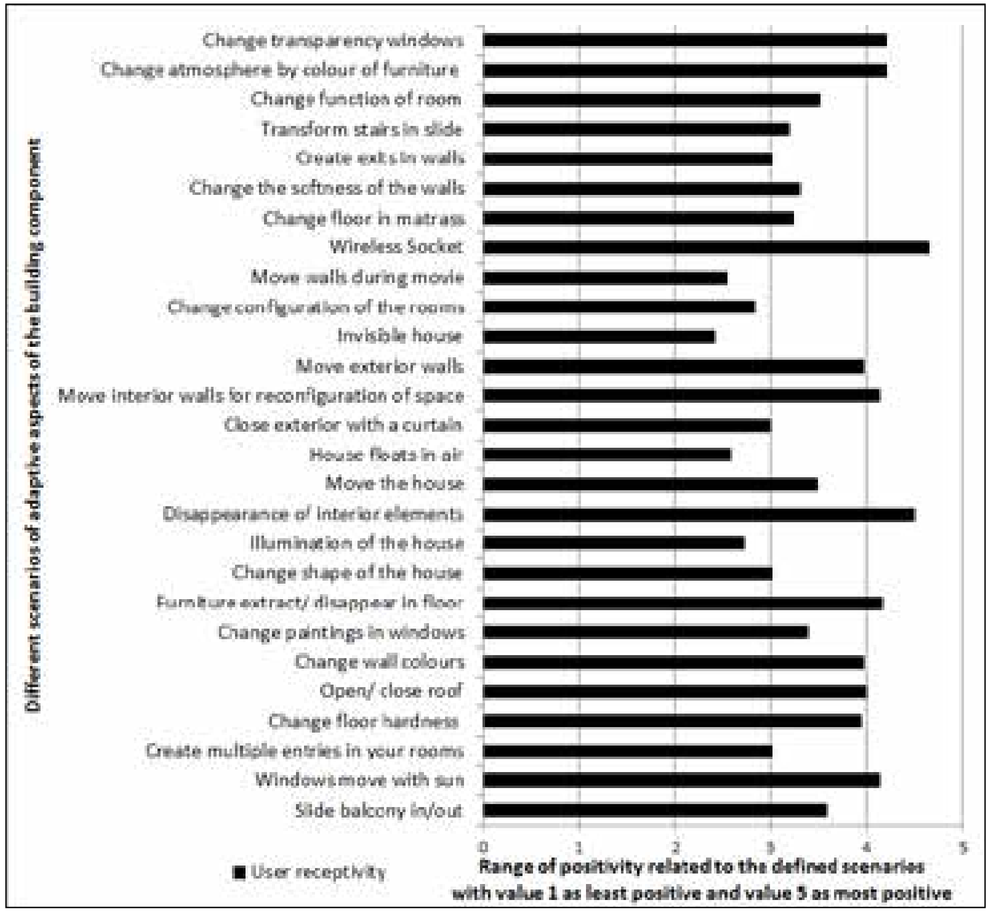

Figure 5.2 Receptivity of adaptive attributes

In order to determine the overall opinion of the participants on adaptive architecture, the mean outcome of all the questions were taken per participant. The mean score of each participant is plotted together with the age of the participants. The outcome is shown in Figure 5.3.

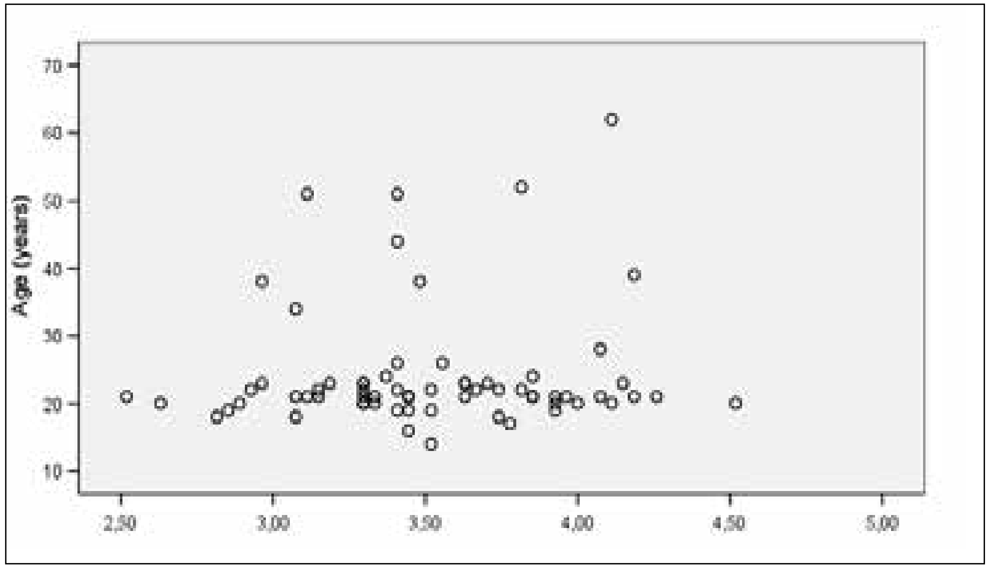

Figure 5.3 Overall score acceptability adaptive attributes related to age.

Based on the data in Figure 5.3, it can be concluded that no significant relation is found between the age of the participant and the overall score on the acceptability of adaptation. The mean of all the participants is widely spread, with a concentration between the value 3 and 4.

5.3 Interview

5.3.1 Research Method

An interview was performed to analyse the vision of the users on adaptive environments in relation to different activities. A total of 20 people participated in the interview.

During the interview each participant was asked to describe the setting of their preferred apartment configuration according to different daily activities. Sketching was allowed to illustrate the ideas. A scenario was presented to create a mind-set. An important aspect was that the apartment was made of flexible material and that any preferred configuration could be realized. By the use of this research method, the participants required a certain amount of imagination to reflect on the proposed adaptive situations, or come up with their own solutions.

The following activities were used in this research: morning activities, such as washing and eating breakfast, working or studying, cleaning, having visitors over, dining and sleeping. The activities were based on a daily routine.

During the interview the following questions were posed for every determined activity;

- What is the shape of your house? (think about, walls, windows, doors, size and the amount of rooms)
- Where is your furniture located and what kind of furniture is this?
- Where are your electronic devices located and what is their purpose?
- How do you want to illuminate your house? (think about artificial light, or sunlight and atmosphere)
- What colour composition do you have in mind? (think about the colour of the walls, furniture and floor)
- From which material is the floor made of? (hard, soft, materialization)
- What kind of climate do you prefer? (humidity, temperature, scent)
- What is the view from your house?

The interview was executed at the home of the participant or at the Delft University of Technology. The average time of the interview was set around 30 minutes. The inquiry was executed by two interviewers; one asked the questions and the other interviewer recorded the answers. Every change in the apartment situation made by the participant was noted. A scoring system was developed to determine the level of adaptability in order to generalize the outcome of the interviews. The scoring system was based on 9 questions;

- Did the participant present large changes according to the different activities?
- Did the participant change the amount of rooms according to different activities?
- Did the participant change anything on the exterior of the house? (e.g. facade, view)
- Did the walls change (e.g. colour, shape, size)
- Did the floor change (e.g. colour, material)
- Did the window(s) change? (e.g. shape, size, height, quantity)
- Did the participant change the illumination in certain situations?
- Did interior components change? (e.g. furniture)
- Did the participant have outstanding ideas?

It is acknowledged that the first and last question were rather subjective, however it is very hard to generate an overall score based on this interview technique. For the purpose of gaining insight into the perception of the user, this scoring method was considered sufficient. For every change according to the questions one point was given. The overall score was based on the total of all points.

The participants of the interview were divided in two groups. The first group, the student group, existed of 10 students. The students were between 19 and 25 years old. All these students studied at the faculty of Industrial Design of Delft University of Technology, The Netherlands. Half of the participants of this group were male. The other group was the middle aged group. This group contained 10 people in the age of 40 to 60 years old. Four participants of this group were men. All participants were of Dutch nationality.

5.3.2 Results

In Figure 5.4 and Figure 5.5, the results of the interview are presented. In these figures the percentage indicates the number of participants who changed the attributes during any of the activities. These figures imply that the students in general were more receptive to changes. It is recognized that question 1 on the determination of large changes is subjective, but in relation to the other questions it can be assumed that the scoring is valuable. For almost all questions, more than 60% of the students proposed a change for all different activities. Only for the amount of rooms 40% of the students proposed a change. In general, a score of 90% is found for the amount of large changes. In contrast to the students, the middle aged only attained a score higher than 50% for the change of the lighting conditions. None of the middle aged participants changed the amount of rooms according to the proposed activities.

All participants of the middle aged group considered the initial configuration of the apartment as a space with multiple rooms. In contrast to this, 70% of the students considered the initial configuration as one large space. Hereto related, 85.7% of this student group changed the amount of rooms for every activity. Subjects who considered multiple rooms did not change the amount of rooms, but more the shape and size of the apartment. Unused rooms were imagined to become smaller when no activity was found in that room. It could be stated that participants who considered a large open space scored higher on the level of adaptability of spaces in general. This indicates that more changes were proposed during the activities.

The interview gave insight into the ideas of the participant on the subject of adaptive environments. The lack of windows during sleeping was a frequent returning aspect; however, in the morning the windows needed to be present. This is very well related by the fact that a few participants wanted to have light colours in the bedroom while waking up, but dark and warm colours, like orange and brown, when going to sleep. During the activity "visiting" the shape and size of the room was changed by the students. Mostly, the colours changed according to the activities, in a few cases the softness of the floor was an aspect of change.

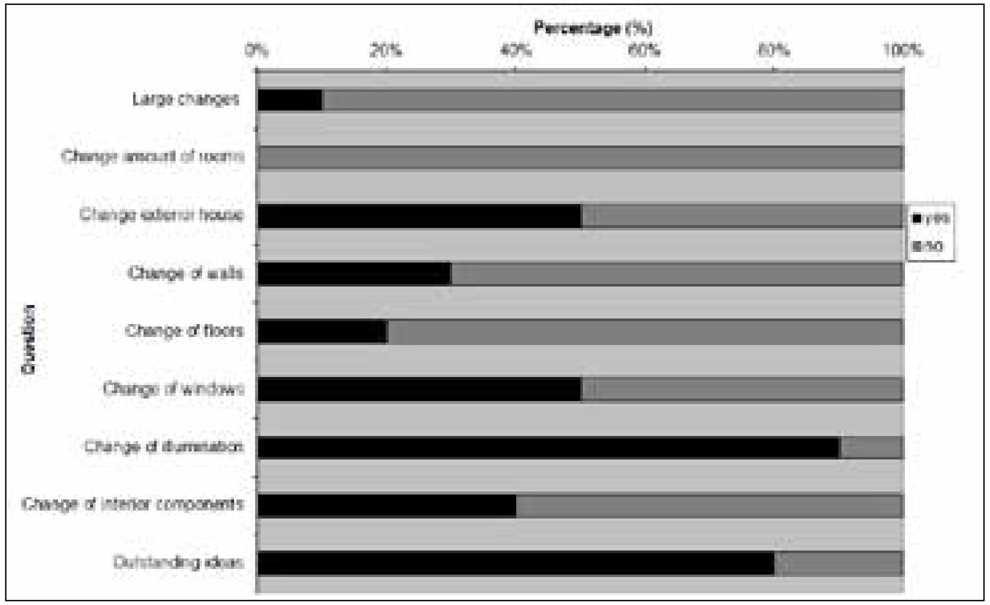

Figure 5.4 Results of middle aged group based on determined scoring system for interview.

Most outstanding ideas were found in terms of cleaning solutions. One of the suggested solutions was that the house must decrease in size during cleaning, resulting in less cleaning surface. Less window surface was also a given cleaning solution. Another interesting proposition colour coding for dirty places or attributes with red, and clean places or attributes with green, was an interesting proposition. Floating furniture for easy vacuuming was found as the perfect cleaning solution. Another interesting idea was the rotating of the house according to the sun. It should be noted that most ideas mentioned resulted from the group of students. The ideas of the middle aged were mostly based on electric devices, such as a universal remote control for all devices. These are not considered design-related attributes, which influence the building performance.

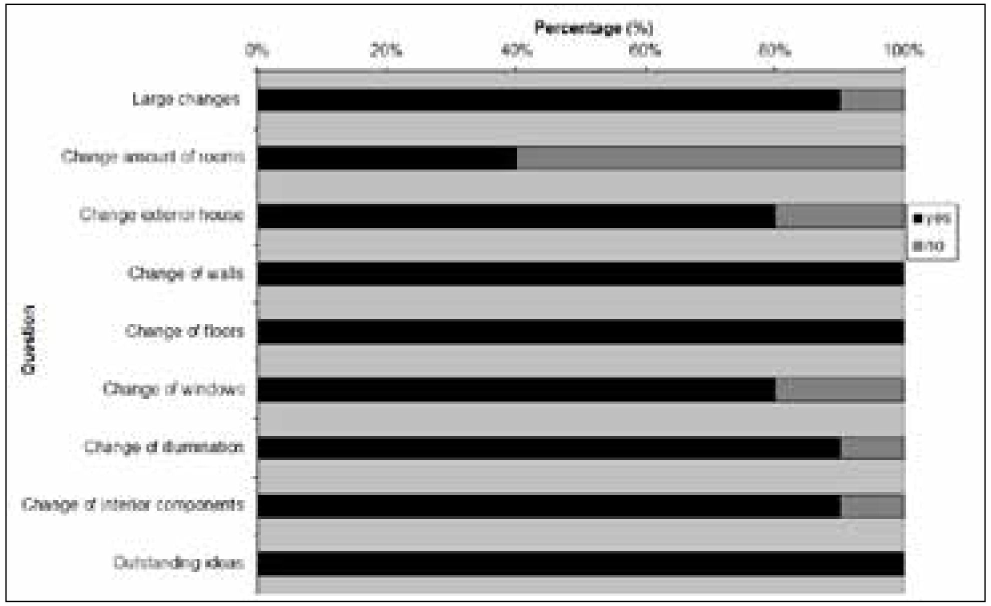

Figure 5.5 Results of student group based on determined scoring system for interview.

5.4 Prototype Inquiry

Descriptive scenarios might lead to a different interpretation or a lack of imagination to visualize this scenario. Based on past experiments on the user-environment relationship it can be concluded that this research preferable should be executed in the context which they occur (Ittelson, et al. 1974). Therefore, it is recommended that subsequent research should focus on a different kind of representation, for example: model representations (scale models of different scenarios, or working prototypes), pictorial representation (image of different scenarios) or real-time representation (full-scale environment). Real-time study of adaptive environments will add to a better understanding of the users' reaction to these environments. Therefore, it is important to work with physical models and context to elicit the users' reaction (Ross, et al. 2007).

The experimental nature of adaptive environments and the related challenges of the technical translation in tangible adaptive environments made it difficult to test a working prototype. With the use of (scaled) prototypes, different adaptive architectural performances were tested in terms of user receptiveness. The adaptive building attributes were selected based on the results of the exploratory studies. Here, the highest scores of both studies were used to determine the users' receptiveness and preferences on this specific adaptive concept. The wireless socket, the (dis) appearance of furniture and the change of colour gained the highest scores at the internet inquiry, where the movable walls, the change of the location of the window and adaptive lighting settings were a popular adaptive aspect at the interview. Based on these findings, the following parameters were determined for the specified prototype study:

- Adaptive floor plan, the adaption of space configuration and furniture arrangement
- Adaptive window settings, e.g. location and transparency

5.4.1 Adaptive Floor Plan

5.4.1.1 Research Method

The subject of research was the configuration of the floor plan of a studio apartment related to specific activities. The participants were asked to configure his or her preferred floor plan. Full scale predefined floor elements were used to configure the room outline (Figure 5.6). When the desired outline was determined, the room was furnished with full-scale furniture to experience the space scale. The participant could select the following furniture elements: bed, table, couch, TV and chairs.

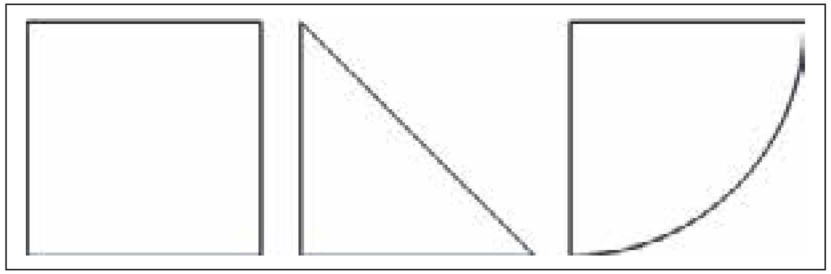

Figure 5.6 Three different floor tiles, which could be selected for the floor configuration. The square tile is 1m²

The participants had to determine their room configuration according to the following activities: sleeping, relaxing, studying and dining. Additionally, a general room configuration had to be defined, which had to be suitable for all activities. In order to prevent infinite size spaces, the maximum room size was 14 m^2. This number is based on the average student room size in Delft.

Between the different activity assignments, all furniture was removed from the floor plan, after which the last floor configuration had to be adjusted to the preferred setting for the current activity.

With this study, the intention was to explore the amount of changes to the floor plan. Additionally, it was analysed whether the participant always used the maximum floor plan size or if smaller dimensions were related to specific activities. As furniture elements were included in this study, the usage of the furniture was analysed.

This study was conducted with eight participants, all were Dutch students from the Delft University of Technology. Half of the participants were male. The student

ranged in age between 19 and 27 years.

5.4.1.2 Results

Every participant configured a floor plan for the five activities and a general floor plan. In Figure 5.7, different results of one participant are shown. First, the floor panels were configured and the furniture was placed. Following, the participant could experience the space and decided if the configuration met his preferences. Note that the furniture usage changed for every activity. In appendix 2, the floor plan settings of all participants are shown.

Figure 5.7 a-c Configuration of the floor plan for the activities sleeping (b), studying(c), relaxing (d).

Table 5.1 Overview of the amount of changing space configurations and the amount of participants making those changes

Amount of different configurations	Amount of participants
0	0
1	0
2	2
3	0
4	5
5	1

In Table 5.1, an overview is given of the amount of changes made by each participant. Only one participant changed the floor plan for every activity as well as the general setting. Most participants made four different configurations. There was no general consensus on which activities required similar spatial configuration. Only the activities *sleeping* and *studying* required the least amount of surface area, respectively 11 and 10 m^2. Additionally, the shape of the floor plan for these activities was in most cases rectangular (6 out of 8 participants). The general setting and the *relaxing* activity were determined with a surface area of around 13 to 14m^2. In these situations the maximum amount of floor elements were used.

When analysing the arrangement of the furniture for the different activities, it could be concluded that specific furniture elements are related to specific activities. Additionally, specific furniture elements were removed from the room configuration. This means that when the specific activity did not require the furniture element it was not considered relevant to position the "unused" element. The bed element was only placed during the activity "sleeping" and for the general setting. Only one participant also placed the bed element during the activity "relaxing".

Most participants noted that it was difficult to configure the space from scratch. They would prefer predefined configurations of which they could choose. Additionally, all participants preferred an automatic adaptive system. This implies that they did not want to physically adapt the space.

When the participants used the rounded floor elements, they implicated that rounded spaces relate to a certain amount of cosiness. However, no general conclusion could be drawn about the space configuration and the related activity.

5.4.2 Adaptive Window Settings

5.4.2.1 Research Method

During this study, the participant had to determine whether the window settings of a small scale prototype required adjustments according to different activities. Three aspects were taken into consideration; the location, transparency and shape of the window. For this study a transparent box was representing a small- scale studio space. The space was furnished with small-scale white interior elements (Figure 5.8). Every participant had to imagine a similar outdoor view (Figure 5.9). This view was randomly chosen and was not considered influential.

Figure 5.8 Research setup

Figure 5.9 View

The purpose of this study was to investigate whether the participant would like to change any of the window attributes according to a certain activity. The specific window configuration was not a subject of research, but was more focussing whether the window configuration was changed or not. The participant had to place window elements on the transparent prototype. A selection could be made from rectangular, square, round and oval shaped window elements. Every window shape came in four different sizes. For every window four different gradients of transparencies were available. Prior to the study, the participant had to specify his or her preferred general window setting. This setting was not related to any activity and was considered the initial window setting.

In order to avoid giving the impression that the adaptation of the window was compulsory for every activity, the initial window setting was set between every activity. If the participant wanted to change the settings, this was a conscious decision.

The activities were divided into day and night activities. For the first 5 activities, the space was illuminated from the outside, mimicking daylight. The last 3 activities were illuminated from above, indicating night-time. The activity *reading* was selected as an activity which took place both during day- and night-time to compare the window settings during different lighting situations.

1. Having breakfast
2. Studying or working
3. Reading
4. Cleaning
5. Having guests
6. Dining
7. Reading
8. Sleeping

day (1–5)

night (6–8)

After the prototype inquiry, every participant was asked to fill in a questionnaire with general questions. These questions had to give insight into subjects such as: when the window attributes should be adjusted and whether the adaptation of the window shape, transparency and location was something they would envision and use in their current home environment.

For this study 13 participants were interviewed. Eleven participants were Dutch students from the Delft University of Technology at the Faculty of Industrial Design, two followed a non-technical study. Eight participants were male.

5.4.2.2 Results

Every participant had to indicate after the study whether he or she would be receptive for the adaptive window principle in practice. In Table 5.2, the preferences of the participants are shown related to the adaptable attributes. Although, the adaptive principle scores relatively high in this small research group, the adaptive *shape* attribute does not give a convincing score.

Table 5.2 Score of participants on the adaption of different adaptive window attributes. The percentage of the positive or negative score is indicated.

	Location		Shape		Transparency	
Answer	Freq.	Perc.	Freq.	Perc.	Freq.	Perc.
Yes	10	77	9	69	11	85
No	3	23	4	31	2	15
Total	13	100	13	100	13	100

In Figure 5.10, a preference setting of a participant is shown. The explorative character of this experiment is illustrated by the small-scale prototype.

Figure 5.10 Window setting of prototype

In Table 5.3, the amount of changes per participant for all activities is given. The scores are divided by the different types of adaptation; the location, shape, transparency and the addition/subtraction of an extra window. The last attribute was not specifically tested, but during the interview it occurred that the participant would like the option to add or subtract a window.

Table 5.3 Amount of activities during which the participant changed the window attributes

	Location		Shape		Transparency		Add window	
Amount of changes	Freq.	Perc.	Freq.	Perc.	Freq.	Perc.	Freq.	Perc.
No	3	23.1	10	76.9	3	23.1	4	30.8
One	2	15.4	2	15.4	2	15.4	2	15.4
Two	6	46.2	-	-	3	23.1	4	30.8
Three	2	15.4	-	-	2	15.4	1	7.7
Four	-	-	1	7.7	2	15.4	1	7.7
Five	-	-	-	-	-	-	1	7.7
Six	-	-	-	-	1	7.7	-	-
Total	13	100	13	100	13	100	13	100

When comparing the results of the interview with the questionnaire regarding the receptiveness to the adaptive windows, a large discrepancy was found between the scores of the shape of the window. 9 out of 13 participants indicated in the general questionnaire that they were positive towards the adaptation of the window shape. During the experiment, 10 participants did not change the window shape, whereas 3 participants did execute a change in shape. The attributes *location* and *transparency* gave corresponding scores for the interview and the questionnaire. The discrepancy could be related to the fact that the adjustment of window attributes is not solely induced by the given activity parameter.

The participants indicated in the questionnaire that the location of the window was highly dependable on the location of the furniture. The low score regarding the repositioning of the window could be related to a similar furniture arrangement throughout the study.

When posing the question to the participants in which situation they would prefer to change the window settings, they responded that the preferences are mostly related to the daylight parameters. In Table 5.4, an overview is given of the situations in which the participants would prefer adaptation of the window attributes. These results indicate that the expected activity dependency was not correct. However, it could be expected that the adjustment of the window attributes are related to a set of parameters. Some participants also indicated that they would change the window settings for entertainment purposes. This aspect was only mentioned by 3 of the 13 participants.

Table 5.4 Parameters on which the window attributes should be adapted according to the participants, multiple answers were allowed.

	Number of participants
Daylight	10
Time of day	5
Weather	4
Entertainment	3
Activity	2

In Table 5.5, the amount of participants who changed the window settings during the activity *reading* is listed. During day- and night-time 7 out of 13 participants did not change any of the attributes. This means that the general window settings were considered suitable for the proposed activity. The location of the window was more important during daytime, whereas the transparency was changed more during night-time. When comparing the results with the results in table 3, the amount of changes (6 participants) are closely related to the number of participants who would like to change the window attributes according the time of the day.

Table 5.5 Change of window setting for the activity reading during daytime and night-time.

	Daytime	Night-time
Location	5	1
Shape	-	1
Transparency	1	4
No changes	7	7
Total	13	13

It should be noted that 8 out of 13 participants indicated that they would prefer curtains above the change of transparency during night-time, or a combination of both. They indicated that direct sunlight would be a parameter for changing the window transparency, while maintaining the view.

When posing the question whether the adaptive system should be able to act autonomous, 8 of the participant answered that they would prefer such a system, but that they would like to overrule this system. Additionally, the system should be able to use the participant’s preferences as pre-set configuration. Four of the participants indicated that they only wanted their own pre-set configuration, and 1 participant only wanted to adjust the window settings manually.

5.5 Conclusion and Discussion

The objective of this study was to explore on which level the user is receptive to adaptive architecture. Explorative research has been performed on the adaptive building performance of the home environment. Firstly, defined adaptive attributes were validated by the user. The user had to give an indication whether the proposed attribute was considered something the user preferred to adapt. Secondly, the user was interviewed and had to determine which building aspects required adaptation according to different indoor activities. Here, the user had to propose the adaptive attributes. Subsequently, two studies have been conducted on adaptive wall systems and adaptive window settings. The technical translation of these adaptive attributes was not included in this research. By the use of prototypes the adaptive performance of the attributes was simulated.

It is known that adaptability on building level will lead to more complexity of the place-identity of the user. It should be taken into account that during the development of an adaptive environment that the changes should be introduced tactfully. The user should be able to identify with the building in some way. The relation between the user and the environment is dynamic in that sense that the user creates his/her own place, and that the place influences the users-self (Cooper 1974). This means that the environment does not need to be perfect. It is important to stay related to the current form of the home, as this appearance is well related to our traditions and culture. A sudden change with all what went before should be prevented, even though large alterations could be achieved by the technological developments (Rapoport 1969). Large changes could lead to uprooting and to a disconnection with the house. Next to that, the interface and technology used for the realization of adaptive environments should focus on the experience of the user and their understanding of the system. This aspect also appeared during the prototype study on the adaptive window system. Almost two thirds of the participants preferred curtains instead of the transparency adjustment during night-time. This is a blinding method that they are familiar with and can relate to. The participants indicated that the technological translation of the adaptive window system was something they could not conceive as feasible in practice. Although, advanced daylight systems are available that do meet the presented performance. However, this technology has not been widely applied yet.

5.5.1 Internet Inquiry

A reasonable high score is found for the proposed adaptive building attributes. A point of critique on the internet inquiry can be found on the fact that the participant had to give their opinion on given examples of adaptive home situations. A possibility exists that the participant did not fancy the given examples, which does not necessary mean that the person is not positive towards adaptive architecture in general. The follow-up study of the interview gave the opportunity to gain a better understanding of the preferences of the participant on the subject of adaptive environments.

In general, the preference of the participants was focused on *interior* elements, such as wireless socket, adjustments of the furniture and interior and adjustment of the interior colour. The adjustment of the interior colour can also be considered an *ambient* element. Additionally, the change of the indoor walls (*infill*) and transparency and location of the window (*outfit*) also gained high scores.

5.5.2 Interview

During the interview the participant had to give his or her vision on the most optimal configuration of an apartment according to different daily activities. This test was performed without insinuated configurations, as given in the internet inquiry. This means that the adaptability of the house was solely based on their own vision regarding the subject of adaptability, their acceptability and creativity. However, it appeared that the given solutions and descriptions of the participant, especially the middle aged, were based on what they thought was possible based on current available technologies. The given scenario which has to change the mind-set at the beginning of the interview did not influence the participants.

The large difference between the middle aged and the students on the scoring of the questions can be explained by the fact that the students were mostly students of the Faculty of Industrial Design. The students are trained to think outside the box and are skilled in brainstorming and design method. Therefore, it should be easier for the students to imagine the possibilities of an adaptive environment. Further research with similar age groups should point out if this issue is funded or not. Additionally, the interview method should be adjusted. The conceptual subject will be much more supported by models, sketches or figures.

5.5.3 Prototype Inquiry

5.5.3.1 Adaptive floor plan

For every activity the participant had to start with an empty setting and configure a floor plan for the specific activity. This might have resulted that the participant reconfigured a different the floor plan for every situation. Further research on the reconfiguration of the floor plan should pay attention to this issue.

In this study, the meaning of play became a new aspect in the reconfiguration of the space. The reconfigurable floor plan released the participant from the current static floor plan settings. In some situations this has led to interesting floor configurations, which by no means could be related to the current rectangular floor plans we are familiar with. In some situations asymmetrical and irregular floor configuration were proposed (Figure 5.11). Here, the participant was completely released from the rectangular static floor plan of our current environment. The participant started to play with the possibilities. Although, the configuration possibilities were limited, creative floor solutions were found.

Figure 5.11 Left a proposed floor plan for relaxation activity. Right: general arrangement. Both floor plans are from the same participant.

Not only the floor plan configuration gave interesting results on the use of the space by the participant, also the use of furniture elements led to insight into the user preferences of adaptive space use. Furniture elements were removed from the scene, when the activity did not require the specific furniture element. Especially when living in a limited space, redundant furniture elements lead to unnecessary space use. This space could be better used during the preferred activity. When the possibility was given that the specific elements could be placed and removed when required, the participants made extensive use of this.

The participants responded that the use of the floor elements together with the full-scale furniture enhanced their spatial experience. However, the lack of windows and walls was considered a restriction in this study.

All participants indicated that the concept of an adaptive floor plan was interesting and challenging, however the practical execution of the concept raised some questions. They indicated that they would use the adaptive aspect of the room configuration, only not frequent for every different activity.

5.5.3.2 Adaptive window settings

During this research different window attributes were studied in relation to different activities. The results indicated that the receptiveness to changing window settings in general scored positive. However, during the study, the shape of the window was often not changed. Only 3 out of 13 participants adjusted the window shape. This could be explained by the fact that the window settings were only studied according to a change in activity. During one assignment, the daylight settings were subject of change. During daytime the location of the window was changed more often, whereas during night-time the transparency was changed more. In general, 7 out of 13 participants did not change any of the attributes during the activity *reading*. Further research on the influential parameters will be necessary to draw conclusions. It could be argued that the user preferences are related to a set of parameters.

The small scale prototype gave a spatial impression of the window settings and was therefore much more related to the participants' perception in comparison to the interview. However, further research with full scale models is advisable to gain insight into the real-scale perception of adaptive windows. More extensive research on this subject with a larger participant group and more defined parameters will lead to a better understanding of the user receptiveness on the subject of adaptive window systems. Additionally, the control and performance of such a system must also be studied.

5.5.4 General

The participants in this research were rather receptive to adaptive environments. During all studies high scores were found when adaptive building attributes were proposed. Although, the technical realization was unclear for the participants, the concept was considered interesting.

The realistic technical translation of the proposed adaptive scenarios created some difficulties for the participants' imagination. Therefore representation is an important aspect when studying adaptive environments. The importance of a tangible prototype is acknowledged as this will enhance the user experience and the interactive relation with space. The user could generate a more clear perception of the adaptive aspects. Especially the middle aged group had problems to visualize adaptive floor plans and interior walls. By using (scaled) models the proposed scenarios could be experienced better.

It is acknowledged that user research is rather subjective. Not only the user' preferences and experiences are rather subjective, but also the defined rating system. The perception of the participant is highly dependent on experiences, background and situation. Every participant interprets the assignment differently and even then the interpretation and expression will vary when tested at different times. This subjectivity is difficult to generalize, and is a recognized issue in user studies. The subjectivity of the rating system is narrowed by generalizing the options in the case of the interview. Therefore, not the specific adaptive propositions of the participant were rated, but the given that something was changed. In this case, how it was changed was eliminated from this research. By generalizing the adaptive proposition of the participant the results of the different test cases could be compared

The interview was considered to be an inventory research, to indicate *if* the participant would change settings according to certain situations. Thereby it was specified *what* was the proposed adjustment. With the follow-up study on the specific adaptive building attributes, an impression could be made on *how* the settings would change. By using this research method, the subjectivity of the rating system was not completely solved, but delivered a tool for comparison.

The amount of participants for all studies is recognized to be a considerable small group. However, to attain a better understanding of the topic on an explorative way the amount of participants was sufficient.

The participants indicated that they would very much prefer to change a combination of building attributes during both prototype studies. Thereby, the relation between the location of the furniture and the window settings were considered valuable. During the adaptive window study, the participants indicated that they would consider the adjustment of the window settings according to the furniture location. Likewise, during the adaptive floor plan study, the participants pointed out that they would like to have an indication of the wall configuration.

This research can be used to gain a first insight into the design methodology of adaptive environments. By designing with adaptive aspects, the relationship between the user and the building and the translation of the performance into a tangible component are important issues. When transferring from a background of static building design to adaptive and interactive environment, the design principles change considerably.

The user receptiveness to adaptive spaces is rather positive. However, it should be prevented that adaptive spaces adds to complexity. The participants pointed out that a full carte blanche made it difficult to define their preferences. Therefore it should be kept in mind during the design of adaptive environment that the adaptive behaviour should be realized in a certain framework. Hereby, the operation of the adaptive component as well as its performance should be clear to the user.

5.6 References

Breakwell, G. M. (1986). Coping with Threatened Identities, Routledge.

Cooper, C. (1974). The House as Symbol of the Self. Designing for Human Behavior: Architecture and the Behavioral Sciences. J. Lang, C. Burnette and W. Moleski. Stroudsburg, Dowden Hutchinson and Ross. **6:** 130-146.

Corbusier, L. (1986). Towards a New Architecture. New York, Dover.

Feldman, R. M. (1990). “Settlement-Identity: Psychological Bonds with Home Places in a Mobile Society.” Environment and Behavior **22**(2): 183-229.

Genereux, R. L., Ward, L. M., et al. (1983). “The behavioral component in the meaning of places.” Journal of Environmental Psychology **3**(1): 43-55.

Hofman, E., Halman, J. I. M., et al. (2006). “Variation in Housing Design: Identifying Customer Preferences.” Housing Studies **21**(6): 929 - 943.

Ittelson, W. H., Proshansky, H. M., et al. (1974). An Introduction to Environmental Psychology. New York, Holt Rinehart and Winston.

Manzo, L. C. (2003). “Beyond house and haven: toward a revisioning of emotional relationships with places.” Journal of Environmental Psychology **23**(1): 47-61.

Manzo, L. C. (2005). “For better or worse: Exploring multiple dimensions of place meaning.” Journal of Environmental Psychology **25**(1): 67-86.

Norberg-Schulz, C. (1980). Genius Loci; Towards a Phenomenology of Architecture. London, Academy.

Norberg-Schulz, C. (1988). Architecture: Meaning and place; selected essays. New York, Rizzoli.

Proshansky, H. M. (1978). “The City and Self-Identity.” Environment and Behavior **10**(2): 147-169.

Proshansky, H. M., Fabian, A. K., et al. (1983). “Place-identity: Physical world socialization of the self.” Journal of Environmental Psychology **3**(1): 57-83.

Rapoport, A. (1969). House Form and Culture. Englewood Cliffs, Prentice-Hall.

Rapoport, A. (1995). A Critical View of the Concept “Home”. The Home: Words, Interpretations, Meanings and Environments. D. Benjamin and D. Stea. Avebury, Aldershot**:** 25-52.

Relph, E. (1976). Place and Placelessness. London, Pion.

Ross, P. and Keyson, D. (2007). “The case of sculpting atmospheres: towards design principles for expressive tangible interaction in control of ambient systems.” Personal and ubiquitous computing **11**(2): 69-79.

Studer, R. (1970). The Organization of Spatial Stimuli. The Spatial Behavior of Older People. L. Pastalan and D. Carson. Ann Arbor, Mich, University of Michigan Press.

Valkenburg, R., Vos-Vlamings, M., et al. (2008). Basisboek Human Technology Interaction, Wolters-Noordhoff.

Weiser, M. and Brown, J. S. (1996). “The Coming Age of Calm Technology.” PowerGrid Journal **1.01**.

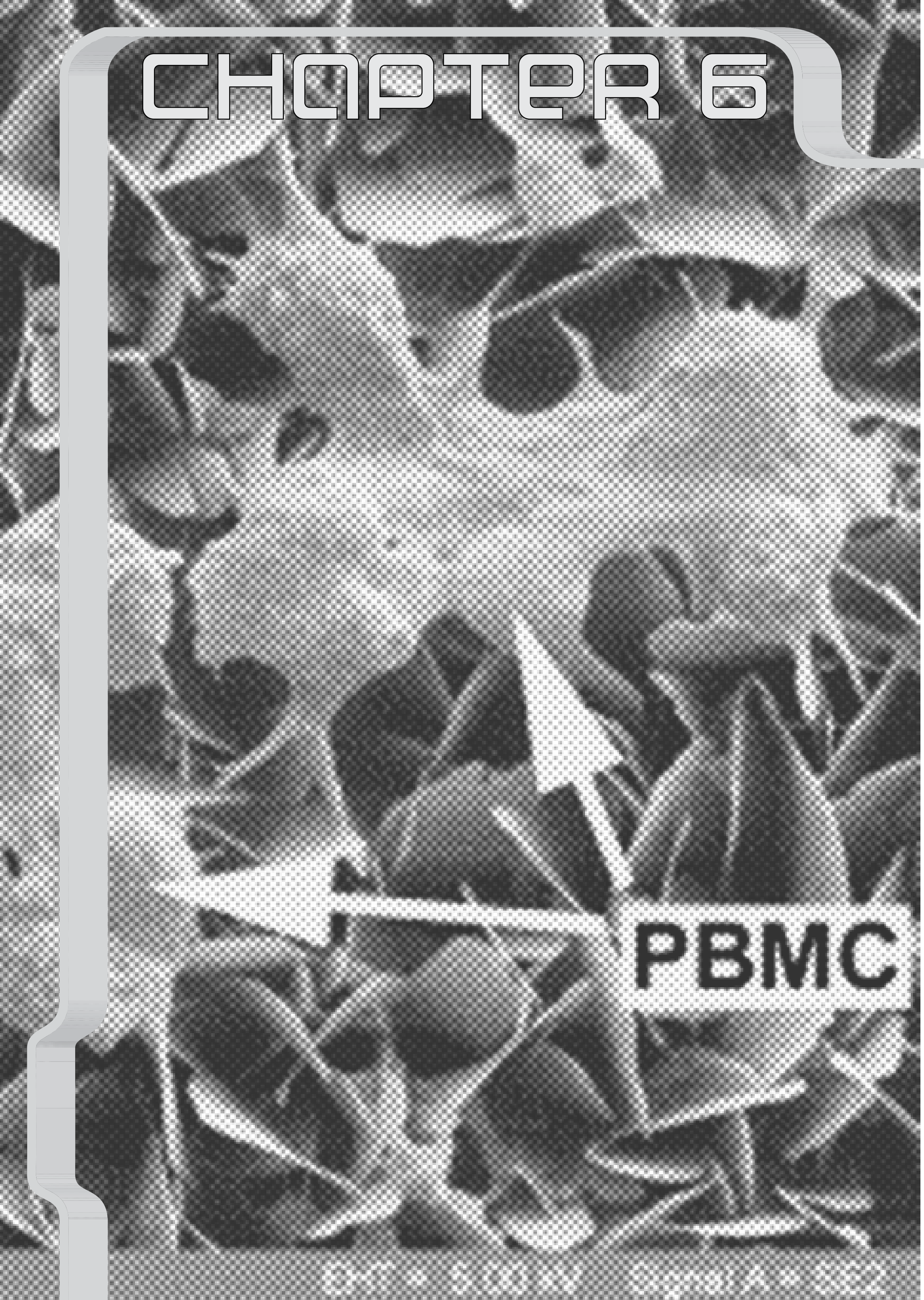

Material Selection and Working Principle of the Adaptive Building Component

6.1 Introduction

In this chapter, the material selection for the realization of the adaptive building component (ABC) is presented. A smart material analysis is executed in order to gain insight into the performance of shape-morphing smart material systems. A general overview is given of the material properties and performance parameters. These parameters are analysed in relation to the design requirements. The material characteristics are validated after which the most suitable materials are selected for the application in the ABC. Subsequently, the characteristics of the selected materials are discussed more in depth.

Based on the material properties and application techniques, the performance of the adaptive building component is described. The ABC will be composed out of different smart material systems. In order to realize a full working prototype, the composition of the ABC is studied. Finally, the functional principle is presented, which will form the basis of the fabrication and analysis in the following chapter. Aspects such as the activation and control of the ABC are described here.

6.2 Adaptive Performance

As is explained in chapter 1, the ABC should enable a hinge-like deformation, retain this deformation without constant energy input and subsequently recover to its initial shape. In order to enhance the application in the building system, the ABC should be able to realize a considerable amount of cycles. Ideally, at least 10.000 cycles should be possible. This amount is based on a 5 year performance of at least 5 cycles daily. Additionally, the ABC should enable immediate adaption, within minutes.

The challenge is to obtain such a deformation without large mechanical devices. The presented two-dimensional deformation has a relatively small construction size for the required deformation. It is preferable that the activation energy should be as low as possible and is energy efficient.

In order to demonstrate the principle of the ABC, a small-scale prototype will be fabricated and analysed. The component should have a length of around 100 mm. This dimension is related to the available tools and machinery for the fabrication and testing of the ABC. For the realization of shape-morphing *infill* and *outfit* components, the proposed deformation should be feasible on scale sizes of around 500 mm. To enable such performance, smart material systems are required, which have the characteristics to deliver large deformations. Additionally, the materials should show reasonable scaling potential.

6.3 Literature Review on Shape Morphing Materials

An inventory has been carried out on the subject of shape-morphing smart material systems (Lelieveld, et al. 2008). The smart material systems are analysed according to the determined design requirements, discussed in Chapter 1. Only material systems that can change their physical dimensions in response to external input are considered in this review. Smart material systems are extensively researched upon in other knowledge fields. Especially in robotics, shape-morphing smart material systems have been studied thoroughly (Shahinpoor, et al. 1998; Mavroidis, et al. 1999; Bar-Cohen, et al. 2007). For this reason, the literature analysis has been performed in other knowledge domains, such as robotics.

It should be noted that not all smart material technologies with shape-morphing characteristics are discussed. This is due to the fact that some material systems deliver small strains to begin with, such as carbon nanotube actuators (Bekker, et al. 1998). These systems find their application on micro- or even nano-scale. These developments do not show scaling abilities to macro scale.

Even though, the ABC is focusing on a two-way deformation, (deflection and recovery) an analysis has been executed on all shape-morphing performances. This also included one-way performance. For this application large work output and recovery forces are required. Next to that, the actuator should be able to deform a considerable amount of times. Continuous control is not necessary; if the deformation is met, the material system does not need to give constant work output. Low performance frequencies are acceptable, as long as this is found within activation scales of minutes. Obviously, low energy activation will be an advantage. It is desirable to use lightweight material systems.

A short description is given of each smart material system currently known to shape morphing material science. However, this will not provide a detailed discussion of the mechanical and chemical performance of these materials. For a full review of shape morphing materials, with inclusion of specific material properties, the reader is referred to the work of (Gandhi, et al. 1992; Tzou, et al. 1992; Culshaw 1996; Huber, et al. 1997; Otsuka, et al. 1998; Madden, et al. 2004; Shahinpoor, et al. 2008).

6.3.1 Shape Memory Alloys

The shape memory effect in alloys was first discovered in 1932 and can be found in various alloys. Shape Memory Alloys (SMAs) have two phase conditions in solid-state. Commonly known phase transformations are from liquid to gas or from solid to liquid. But SMAs have the characteristic of a diffusionless solid-state phase transformation. The material properties differ between these phases, while maintaining the solid state.

At low temperatures the SMA is in its weaker phase: the martensite phase. During this phase the SMA can be easily deformed, due to the low modulus of elasticity and tensile strength. When heated above a specific transition temperature, the alloy transforms into a stronger phase: the austenite phase (Duerig 1990). During this transition, the crystalline structure of the alloy will recover to its original stiff configuration after deformation in the low temperature area.

SMAs are able to generate a high recovery force while under constrain. This indicates that the alloy delivers a higher recovery force than required to recover itself during free recovery. This enables the application of the SMA as an actuator[8] material. In order to maintain the “strong” austenite state, a continuous energy input is required. Due to its “weak” material characteristics at low temperatures, the SMA will deform when forces are applied in this phase. However, when no external forces are applied at the SMA in the low temperature region, the initial shape is maintained. SMAs can deliver high stresses in relation to the delivered strain. SMAs are available with different activation stimuli, such as light, temperature, moisture. Thermo-responsive SMAs are more developed and deliver higher actuation forces.

A large disadvantage of the SMAs is the high fatigue rate. The memory effect degrades by large strains, high temperatures, large constraining forces and repeated thermo-mechanical cycling (Loughlan, et al. 2002).

6.3.2 Thermostatic Materials

Thermostatic elements are bimetallic strips consisting of two or more materials with different thermal expansion coefficients (Ohkata, et al. 1998). By heating the composite material it will bend in the direction of the material with the smallest thermal expansion. The thermostatic elements deliver a small deflection with relatively low forces. Continuous energy input is necessary to maintain the induced deformation. When thermal load is removed, the thermostatic element will recover to its initial shape. The deformation speed is depending on the thermal conduction characteristics of the materials, as well as the thermal expansion coefficient and is commonly rather low.

6.3.3 Shape Memory Polymers

Shape Memory Polymers (SMPs) were introduced in 1984 in Japan (Dietsch, et al. 2007). In general, SMPs have thermo-responsive characteristics. Shape Memory Polymers have, like most polymers, a transition temperature at which the polymer transforms from a solid glassy state into a rubbery state. This specific temperature is the glass transition temperature (T_g)[9]. SMPs have relatively low glass transition temperatures of around 50 to 100°C. The material has a low tensile strength in the rubbery phase. This enables large deformations by the application of appropriate external forces. In the rubbery state, the material can be elongated 200% without the occurrence of plastic deformation (Corner Stone Research Group Industries webpage). The deformation can be fixated by reverse transition from rubber to rigid state upon cooling. The original shape or configuration can be recovered by subsequent unconstrained heating above the glass transition temperature (T_g). The SMP will hereby recover back to its “remembered” initial shape.

Shape Memory Polymers can recover strains of approximately 100-400% by thermal activation (Otsuka, et al. 1998; Leng, et al. 2011). The thermo-mechanical cycle of deformation and shape recovery can be repeated numerous times without degradation of the material performance (Dietsch, et al. 2007; Corner Stone

8. An actuator is able to induce the activation of another medium with the appliance of work output. An actuator will perform by the different input power, e.g. electric, thermal, and magnetic.
9. Glass transition temperature of a polymer material. This temperature indicates the material transformation from glassy to rubbery phase. Below this temperature, the polymer is glassy state, which is considered the rigid phase. Above this temperature the polymer is rubbery and easy to deform.

Research Group Industries webpage).

6.3.4 Electro-Active Polymers

Electro active polymers deliver morphing behaviour under the influence of an electric current. Electro active polymers can be divided into two groups; ionic polymers and dielectric polymers. The performance of ionic polymers is based on the movement of ions in a gel-like substrate (Shahinpoor, et al. 1998). Upon electric activation, all the ions are concentrated at the activated side of the substance, showing a bending behaviour. Low activation energy is needed for activation (Shahinpoor, et al. 1998). By switching the electric field, the deflection is inverted. The shape morphing performance can be controlled very securely by varying the electric activation. Continues electric field is required in order to maintain the deformation. As the polymer constituency is based on a gel-like substrate, the actuator will run dry after a certain time. Large deformations are possible, but small forces are related to increased deformation (See Figure 6.1). Ionic Polymer Metal Composites (IPMCs) are an example of ionic polymers.

Dielectric polymers are based on elastomer material sandwiched between two conductive layers, these deliver compression forces due to attraction upon electric activation. This system can deliver large strains, but require large activation potentials (typically around 1000 Volt (Madden, et al. 2004)). For architectural application this might lead to difficulties. The deformation is retained without continuous activation. The dielectric polymers encounter large fatigue, which shorten the life time considerably.

6.3.5 Piezoelectric Materials

Piezoelectric materials have reversible electromechanical characteristics. This means that mechanical work output is induced by electric current. On the other hand, by mechanical deformation an electric current is delivered (Tzou, et al. 1992). Therefore, this material can be used for sensor and actuator purposes. Only the actuator properties are interesting for this study. The deformation of the material is depended on polarity. The principle of deformation is similar to that of dielectric polymers. By applying electric current the material expands. Large forces can be attained by stacking different layers of piezo-material. However, it should be noted that this will lead to small deformations. For bending deformations, piezoelectric fibres can be embedded in polymer material, creating Micro Fibre Composite (MFC) actuators. MFC's typically deliver high stresses, but require high voltages for activation. Minor degradation is found up to 10^8 cycles (Nuffer, et al. 2007). Different materials have piezo-electro characteristics, but the PZT (zirconate titanate alloy) is the most developed material and delivers higher strain performance (see Figure 6.1).

6.3.6 Wax Actuators

Wax actuators exist of waxes or fluids in a sealed container which can give large volume expansions or contractions by increasing temperature (Duerig 1990). This behaviour is based on a phase change performance. Due to the sealed container and the thermal conductivity of the material, the reaction time is very low (Ohkata, et al. 1998). Wax actuators are considered smart, as the performance is based on the expansion of a fluid material resulting in a deformation. Since the actuator size is considerably large due to the container, it can be compared to mechanical actuators, such as hydraulic or pneumatic systems.

6.3.7 Comparison

In Figure 6.1, an overview is given of the stress-strain relation of different actuators. For analysis purposes, mechanical actuators and human muscle are also included in this overview.

The material properties are derived from literature. In all cases, the maximum values are used for analysis; this means that the values can be considerably lower depending on the application and material characteristics. Nonetheless, this graph is considered a good indication of the actuators' performance.

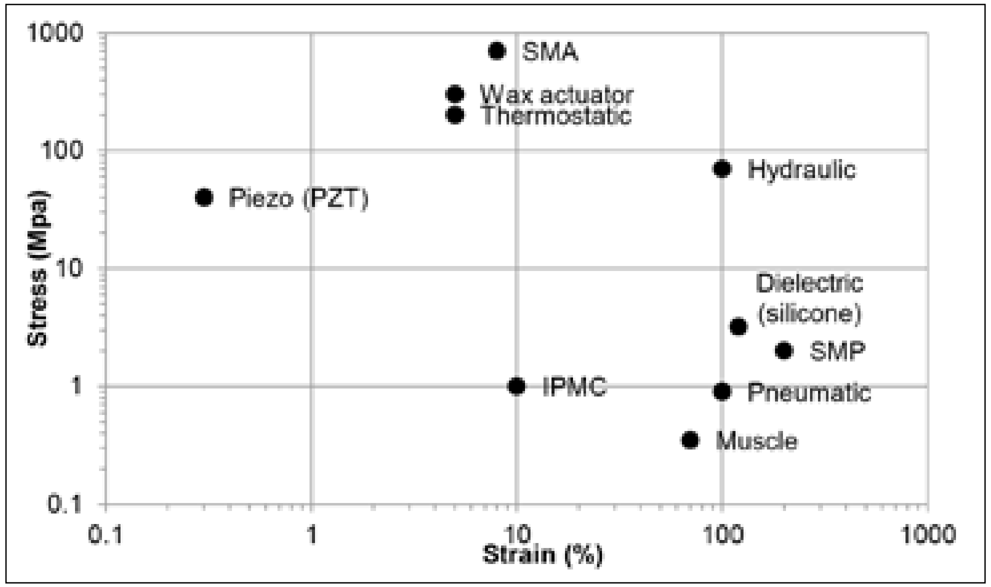

Figure 6.1 Stress strain relation actuators (Huber, et al. 1997; De Rossi, et al. 2004; Madden, et al. 2004; Carpi, et al. 2005)

In Table 6.1 the discussed smart material systems and their properties in relation to the design requirements are presented. The strain, actuation stress, actuation energy, the amount of cycles and the required bending behaviour are validated for all discussed materials. When the score is negative, it indicates a significant discrepancy between the properties and the design requirements. A negative/ positive score refers to acceptable material properties. Whereas a positive score, indicates that a good match is found.

In general, shape morphing smart material systems possess over actuator characteristics. This means that these materials can be used to deform other materials. Only SMPs deliver just enough force for their own recovery and can therefore not be used for actuating purposes. To initiate the deformation of the SMP, external force is required, after which the material is able to recover itself. Some of the discussed smart material systems show two-way morphing behaviour by reversing the activation stimulus, such as EAPs and piezoelectric materials. For the presented application this is an advantage, but by using antagonist behaving actuators two-way performance can also be realized. Two-way behaviour is therefore not a specific requirement.

Table 6.1 Comparison different smart material systems

Material	Strain	Stress	Activation Energy	Cycles	Deformation	Size	Two-way
SMA	+-	+	+	+-	+	+	+
Thermostatic	-	+-	+	+-	+	+-	+-
SMP	+	-	+-	+	+	+	-
IPMC	+-	-	+	+-	+	+	+
Dielectric (silicone)	+	-	-	-	+	+	+
Piezoelectric ceramic	-	-	-	+	+	+	+
Wax	-	+	+-	+	+-	-	+

6.3.8 Discussion

The reviewed smart material systems all have different shape morphing material characteristics. Some materials have some characteristics that meet the design requirements, but other characteristics conflict with the desired application. In some cases the material properties do not meet the requirements by far, which means that the material is unsuitable for the desired performance. The human muscle can deliver considerable forces when embedded in a bone system, but show small forces when actuated alone.

SMPs deliver just enough force to enable recovery after deformation, while the applied deformation stress and recovery stress are similar. SMPs can therefore not be used as an actuator material. This also indicates that it is not possible to use antagonists shaped SMP, to enable a reversible shape deformation. This material needs to be deformed by external force, after which the SMP guarantees recovery. An advantage of these materials is that the deformation can be fixated structurally, without continuous energy input. But when considering a reversible deformation performance, these materials do not meet the design requirements.

For deformation purposes, Shape Memory Alloys (SMAs) deliver the highest actuation stress in relation to actuation strain (Huber, et al. 1997). However, equal work output for each cycle cannot be guaranteed due to the nonlinear character of the SMA's performance. Dielectric elastomeric actuators find relatively large strains in relation to stresses. A disadvantage of these materials is the required high voltages for activation, which leads to high costs and large dimensions for power supply (Madden, et al. 2004). Additionally, the aspect that high voltages are required gives serious problems concerning safety and usage.

Ionic Polymer Metal Composites do not meet the performance requirements due to the disadvantageous stress/strain relation. In order to deliver large output stresses, small strains are found and vice versa. This hinders the optimization of the IPMC performance for architectural application. However, when considering the activation energy, only a small voltage input is required, which is considered an advantage of these materials (Shahinpoor, et al. 1998).

An important aspect is the dimension of the smart material in order to enable deformation. Wax actuators show similar dimensions as conventional mechanical actuators such as hydraulic and pneumatic devices. Wax actuators therefore fail to meet the design requirements of lightweight and small size components. Additionally, wax actuators are linear motion devices, which narrows the possibilities of application (Otsuka, et al. 1998).

The deformation of thermostatic elements is limited to bending, but does have the quality to respond on cooling, which is not possible with SMAs (Tautzenberger 1990). However, a continuous energy input is required in order to maintain the deformation of the thermostatic elements. Upon cooling, the thermostat will deform to the initial shape, delivering actuation stress. This behaviour hinders the fixation of the shape deformation considerably. Although the SMA characteristics do show a low elasticity modulus at low temperatures, the initial shape is retained. SMA actuators show more advantages on the subject of force and motion, compared to thermostatic elements. Even more, the actuation speed and response is much faster (Ohkata, et al. 1998).

SMAs have relatively small sizes compared to other actuators with large deformation output. A disadvantage of thermally activated materials is the low performance frequency. The actuation time of SMAs can be decreased by resistive activation, but is still considered slow in comparison to electro active materials such as piezoelectric materials. Fortunately, the fast performance is not a design requirement and the low response time of the SMA is therefore acceptable. It is recognized that the thermo responsive behaviour is a disadvantage in terms of practical use in architecture. Most materials show linear deformation behaviour, but SMAs show a range of application possibilities and can deliver tension, compression and torsion.

To conclude, SMAs show the most optimal performance to enable shape-morphing behaviour:

- Large recovery forces
- Considerable strain deformations
- Small dimensions in relation to work output
- Favourable ratio of delivered force/ weight density enables lightweight actuator system
- Noiseless performance
- Low activation energy
- Multiple motion solutions

It should be mentioned that SMAs have poor structural conditions at low temperatures and is therefore not suitable for structural application. As is mentioned earlier, SMPs can be deformed in rubbery phase, after which the deformation is fixated in rigid condition without continuous energy input. Therefore, it is decided to combine these materials in a composite material, in order to take advantage of both materials' characteristics.

In general, commercially available SMPs have thermo-responsive properties. Additionally, other activation stimuli can be found for SMP activation. These methods of activation are considerably new developments and are not widely available yet. Below, a brief overview of these activation methods is given. Different reviews give a more complete overview of research on activation of SMP (Behl, et al. 2007; Leng, et al. 2011).

One method of activation is inductive heating, which provides remote and wireless control. Inductive heating is based on a magnetic field, which dissipates heat through hysteresis in magnetic particles (Schmidt 2006; Leng, et al. 2008b). Super-paramagnetic particles are dispersed within the SMP matrix, providing shape transitions by electromagnetic field and inducing magnetic heating (Schmidt 2006; Liu, et al. 2009). The basic material properties such as thermal and mechanical behaviour are comparable with SMPs without magnetic particles (Schmidt 2006). However, the modulus of elasticity increases considerably compared to SMPs without fillers, which decreases the potential strain (Schmidt 2006).

Developments on photo-responsive SMPs enable remote activation. Light can be used as a stimulus for fixating and releasing the deformation (Jiang, et al. 2006; Behl, et al. 2007). Different photo-responsive systems can be found. The polymer is thermally stimulated by using irradiation with infrared light (Jiang, et al. 2006). As with stimulation by ultraviolet light, the material responds to different wavelengths, avoiding the effects of thermo-responsive activation (Lendlein, et al. 2005). This system gains great advantages above thermo-responsive SMPs in terms of energy loss and practical application. Remote activation is possible with photo-responsive SMPs.

Photo-responsive SMPs can either enable a shape memory effect, which fixates the user-defined shape and initiate recovery, or initiate a two-directional movement. In the latter case, a deformation can be obtained by irradiating parts of the sample, activating specific pre-set shape configurations. Another method is the application of different wavelengths. Different initial shapes are related to specific wavelengths. By subsequent activation with the specific wavelengths a two-directional movement can be realized. Naturally, the deformation is restricted by the polymers' initial shape and the method of activation.

A disadvantage of the photo-responsive stimulation method is that the activation time is relatively long; around 60 minutes for a sample with a 0.5 mm thickness. This could be decreased by increasing the light intensity, decreasing the sample thickness (Jiang, et al. 2006) or the integration of carbon black (Leng, et al. 2009). Carbon black will increase the diffusion of the light. But this would not fit the application scale of this project, as larger dimensions are required. Photo-responsive SMPs show promising possibilities for advancements and further development is required in order to enlarge the potential of this material.

Another possible performance principle is used by hydro sensitive SMPs. Hydro sensitive SMPs react to fluids, which enable diffusion of moisture in the polymer and act as a plasticizer (Yang, et al. 2005; Behl, et al. 2007). Another reaction is initiated when the SMP is immersed in water below T_g. After deformation the SMP will exhibit recovery upon saturation (Huang, et al. 2005). The actuation speed depends on the saturation properties of the polymer and is considered relatively low. The limitations of this system are clear for architectural applications. Hydro sensitive SMPs do not meet the application profile for remote activation since it will lead to considerable difficulties regarding implementation.

The most commonly used SMPs are thermo responsive and are activated by external heaters. Interesting research has been done on the subject of integrated conductive heating methods by means of resistive heating, i.e. electric current. Solutions with the integration of conductive fillers in the polymer matrix are found. However, upon cycling, degradation is found in the conductive properties. The aggregation of carbon nanotubes, Nickel chains or carbon black will increase the properties such as strain and stiffness (Koerner, et al. 2004; Leng, et al. 2008a; Liu, et al. 2009), but have the tendency to decrease the glass transition temperature (Yang, et al. 2005; Leng, et al. 2008b).

As thermo-responsive SMPs show the most optimal performance and are conveniently commercially available, it was decided to focus on thermo-responsive polymers. External heating will not be adequate in terms of functionality and practicality of the intended architectural application. Therefore, an intrinsic heating method should be developed that enables local heating of the SMP body, without the obstruction of the desired performance. Integrated conductive elements are necessary in order to realize active control of the adaptive building component. The integration of conductive elements will be studied in the following chapter.

In accordance to the presented heating methods of the SMP, the thermal energy required for SMA actuation can be delivered by various methods. Such as increasing ambient temperatures, radiant activation by infrared light, inductive heating by magnetic field or conductive heating by electric current (Jinhao, et al. 2000). It should be mentioned that SMAs exists which perform by magnetic response. These Ferromagnetic Shape Memory Alloys (FSMAs) react much faster and more efficiently compared to temperature-induced responses. This is a logical consequence of the absence of the heating and cooling of the material. However, due to the considerably small actuation stresses of around 9 MPa (Madden, et al. 2004), these materials are not sufficient for the presented application (the thermo-responsive SMAs deliver stresses of around 700 MPA). Thermo-responsive SMAs deliver high actuation forces and are commercially available. These materials are the most suitable for the presented application.

Most SMAs possess over a one initial shape at the high temperature range. By training, SMAs can remember a determined shape at both a high and a low temperature range (Liu, et al.). These two-way SMAs can be very effective for minimum cycling. Compared to the one-way SMAs these actuators deliver a lower transformation strain and show a higher fatigue, which means a decrease of cycling and stability (Huang 2002). Additionally, the fixation of the memory shape will lead to difficulties for the ABC application. These issues are similar as the discussed thermostatic elements. As the two-way SMAs have two transition temperatures, the high temperature can only be maintained by continuous thermal activation. When cooling down, the SMA will transform into the low temperature shape. Therefore, two antagonists *one-way* SMAs are used to fulfil the presented design requirements.

6.4 Working Principle of Smart Composite

A smart composite (SC) will be constructed out of SMA strips embedded in a Shape Memory Polymer (SMP) matrix (Figure 6.2). The initial shape of the Smart Composite is in flat configuration. The SMA delivers the deformation of the composite, while the SMP fixates this deformation. Three SMA strips are used for the reversible deformation. SMA_{1+3} provide the deformation performance and SMA_2 will initiate recovery. Since the SMP consists over shape memory characteristics, less force is required for recovery in comparison to deformation. After the deformation of the SMP, the recovery is realized by both the SMP and the SMA_2 strip.

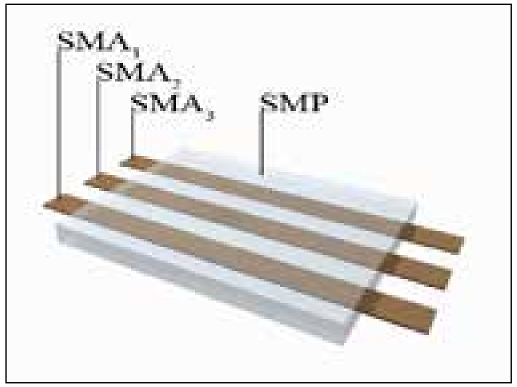

Figure 6.2 Smart Composite

The SMA_1 and SMA_3 strips, which induce the deformation, are first annealed in bent position. The strips are flattened at room temperature and then embedded in the SMP matrix. Upon thermal activation, the SMAs initiate recovery into their initial bent position. Both the SMP and SMA_2 strip are deformed during this recovery, realizing the forward movement. It should be noted that the SMP is heated before the SMA_{1+3} strips are initiating deformation. For the recovery, the backward movement, of the SC, the SMP is heated until a full rubber condition has been reached after which the SMA_2 strip is activated. This material is also deformed at room temperature and will initiate recovery into the flat initial shape.

In Figure 6.3a-j, the principle of performance of the smart composite is illustrated in detail. Here, it is assumed that the initial shape is in flat configuration.

- Figure 6.3a: The SMP is heated above T_g to exhibit full rubber characteristics.
- Figure 6.3b: To induce deformation, the SMA_{1+3} strips are activated above A_f, initiating full recovery into their original bent state.
- Figure 6.3c: The recovery of the SMA strips causes the deformation of the SMP body together with the SMA_2, which is in martensite phase.
- Figure 6.3d: When the deformation criteria are reached, the SMP is cooled down to fixate the deformation. The strain energy is stored.
- Figure 6.3e: When the deformation is fixated, the SMA_{1+3} strips will be cooled until fully martensite. The composite will regain its full stiffness.

For the backward movement, both the polymer and the SMA_2 are heated in order to realize the recovery. Hereby, the composite will return to its flat configuration.

- Figure 6.3f: The SMP body is heated until a full rubbery phase is reached. The SMP exhibits some recovery, but this is not sufficient for full recovery of the SMC.
- Figure 6.3g: SMA_2 is heated to induce full recovery.
- Figure 6.3h: The SC is fully recovered into its initial flat configuration.
- Figure 6.3i: The SMP is cooled to retain the current configuration
- Figure 6.3j: SMA_2 is cooled, after which the primary shape is fixated.

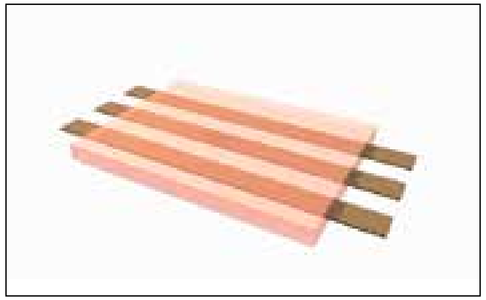

Figure 6.3a SMP is heated until it is fully rubbery

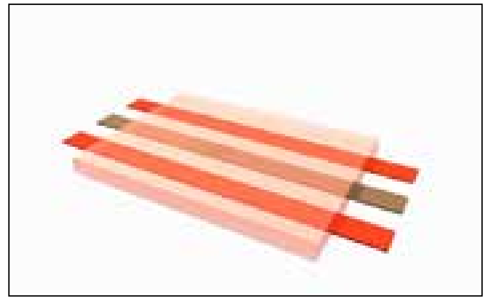

Figure 6.3b Both SMA_1 and SMA_3 are heated

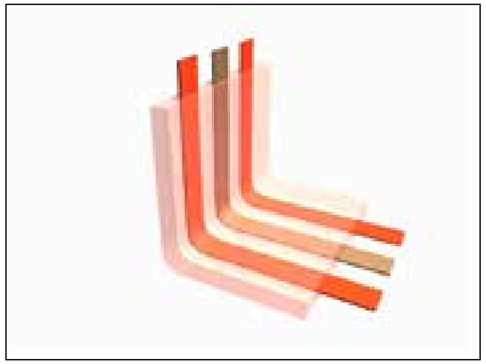

Figure 6.3c Full deformation of the SC, the forward movement.

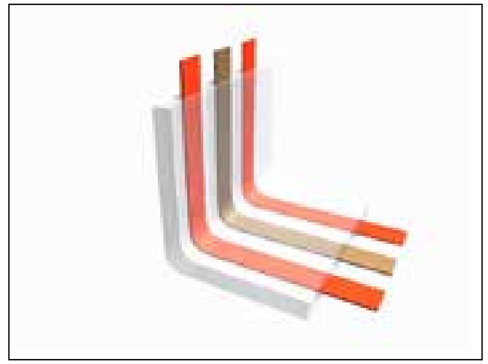

Figure 6.3d SMP is cooled to fixate the deformation

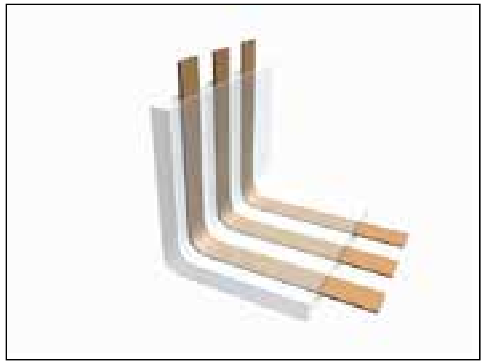

Figure 6.3e SMA_1 and SMA_3 are cooled

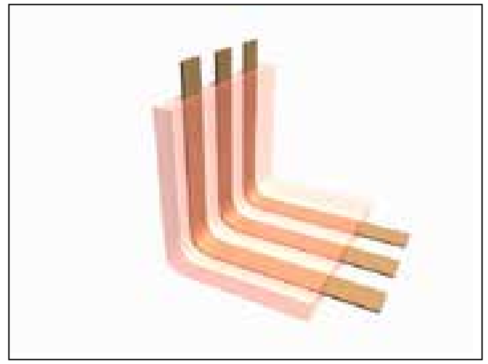

Figure 6.3f SMP is heated, until it reaches the fully rubbery state

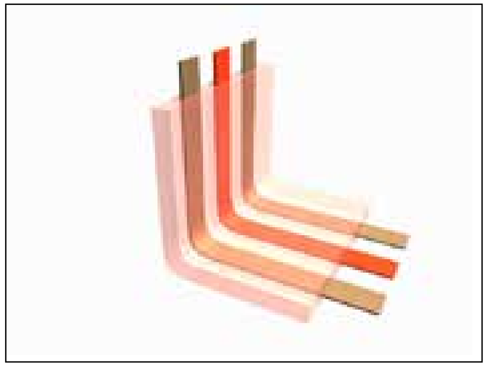

Figure 6.3g SMA_2 is heated to initiate recovery

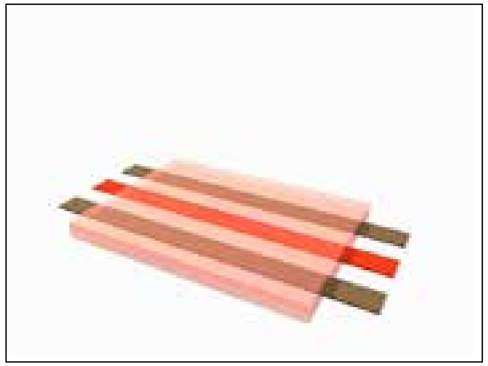

Figure 6.3h SC is fully recovered, the backward movement

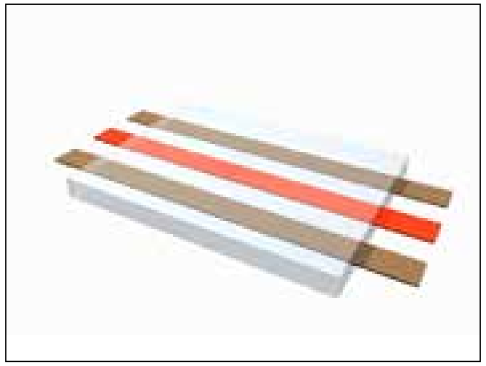

Figure 6.3i Recovery is fixated by cooling SMP body

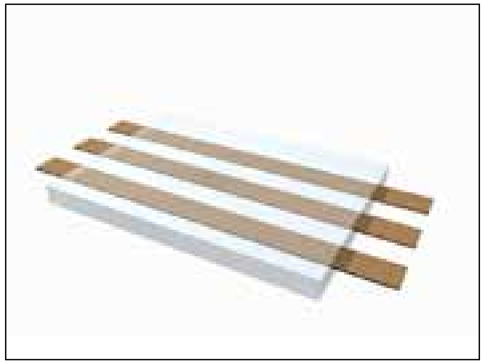

Figure 6.3j Initial shape is recovered

After having discussed the working principle of the SC, the specific materials will be discussed more in detail.

6.4.1 Matrix Material: Shape Memory Polymer

Shape memory characteristics are found in both thermoset and thermoplastic polymers. Thermoset polymers have stronger chain links, which relate to stronger material properties. Additionally, the thermoset polymer cannot be melted after it is cured, in contrast to thermoplastic polymers which can be reused. When heated above its melting point, thermoplastic SMPs allow reprogramming of the original shape.

Recent developments show shape memory characteristics in biopolymers. These polymers are based on natural resources, such as polylactic acid (PLA). These thermoplastic materials can be melted and reshaped (Inoue, et al. 2005; 2007). The SMP can be recycled for other purposes. Next to the fact that the material is manufactured out of natural resources, recyclability makes the material more durable (NEC webpage). Unfortunately, this material has not been commercially available yet.

The initial shape of the thermoset polymer is fixed once these are fabricated. Thermoplastic SMPs deliver relatively poor thermal and mechanical performance (Leng, et al. 2011). Thermoset polymers are more suitable for architectural components as they give high environmental durability and better mechanical performance (Abrahamson, et al. 2003). Additionally, the manufacturing of thermoset SMPs with embedded components for electric heating is less complicated. In this research thermoset styrene based SMP will be used for the matrix material.

A considerable amount of polymers have shape memory characteristics. However, normally the T_g covers a large temperature range, which leads to slow recovery times and high energy sources. Specific SMPs show a sharp transition range at which the Young modulus drops considerably. The transition temperature (T_g) can be adjusted by chemical composition to meet the application specifications.

6.4.2 Actuator Material: Shape Memory Alloy

As is discussed earlier, the shape memory behaviour of SMAs is based on a reversible solid-state phase transformation. This indicates that no atomic bonds are broken or formed, which is mostly the case with phase changes (e.g. solid to liquid). The transformation is based on the distortion of the atomic lattice (Langelaar 2006). In Figure 6.4, the molecular structure of the shape memory effect in SMA is presented. In the high temperature region, the austenite phase, the SMA molecules are ordered in a crystal structure. This is considered the initial shape of the SMA. When cooled to a lower temperature, the SMA will transform into the martensite phase. The SMA maintains the initial configuration, but the atoms will configure in a twinned position generating a herringbone structure (see image Figure 6.4; initial shape martensite). This structure enables the deformation of the SMA. By applying an external stress, the material will deform. This will result in the detwinning of the molecular structure. The stored strain is released upon heating, initiating recovery to the symmetrical crystal structure (Hodges, et al. webpage). This lattice structure is highly static and has only one configuration, in contradiction to the variable martensite phase (Duerig 1990).

Although a significant amount of alloys exhibit the shape memory behaviour, only the alloys that deliver high recovery stresses are of interest. The material characteristics and performances vary considerably between the different alloys. Both nickel-titanium (NiTi) and copper-based alloys are widely available. However, NiTi alloys show a more optimal performance and have favourable characteristics in relation to copper-base alloys (Huang 2002). NiTi alloys have a higher shape memory strain (up to 8% versus, 4-5% for the copper-based alloys), are more thermally stable, have better corrosion resistance and show better ductility (Duerig 1990). Additionally, NiTi alloys have a lower fatigue and have therefore a longer life-time than copper-based alloys (Huang 2002). On the other hand, copper-based alloys are inexpensive and have a wider range of potential transformation temperatures. The production of the copper-based alloys is less complex since this material can be melted and extruded in air. This gains remarkably in production costs (Hodges, et al. webpage). Titanium is considered a reactive metal; therefore melting must be executed in vacuum or in an inert atmosphere. Due to the advanced mechanical characteristics of NiTi SMAs above the copper-based SMAs, NiTi-alloys are used in this research project.

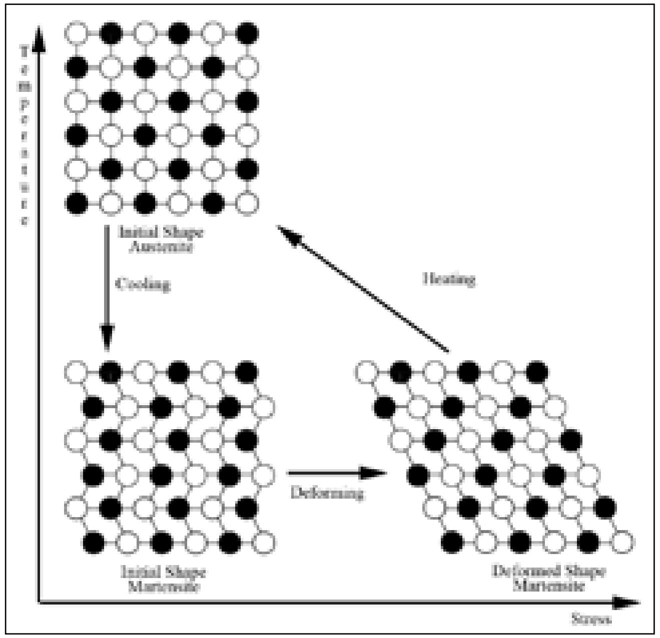

Figure 6.4 Process of Shape Memory Effect (Chopra 2002)

The actuation force depends on diverse factors, such as the geometry of the actuator (most common actuators are wires or springs), cross section of the used SMA and the amount of stress in the actuator. Larger dimensions will lead to higher forces. Nevertheless, the stress-strain relation should be kept into account. Large dimensions will initiate large forces, but will prevent substantial deformation in the low temperature area. Repeated use of the SMA will lead to degradation of the shape memory effect. The functional properties related to the lifecycle of the SMA actuator are depending on a various amount of parameters (Ikuta 1990; Otsuka, et al. 1998; Loughlan, et al. 2002). Manufacturing parameters, such as composition, cold-work and heat treatment are important for the performance of the actuator. Additionally, the loading conditions are of considerable influence. Lower transformation strains will lead to an increase of the cycling performance of the actuator. Fatigue increases by uncompleted transformation cycles and high loads during constrained recovery. Maximum constrained recovery forces as well as maximum deformation strain should be prevented, as this will shorten the operation time. SMAs must be protected from overheating to prevent degrading, which results in a decrease of the performance. The SMA performance will be restricted by the amount of required cycles (Table 6.2).

Table 6.2 Relation amount of thermo-mechanical cycles and stress and strain relation for NiTi SMAs (Stoeckel 1992; Memory Metalle GmbH webpage).

Cycles	Max. Strain (%)	Max Stress (MPa)
1	8	500
<100	4-5	275
<10.000	2	140
>100.000	1-2	70

In general, the maximum amount of strain recovery that is still heat recoverable can be found at 4%. Above this point plastic deformation occurs, leading to un-recoverable deformations (Duerig 1990). The precise strain recovery is dependent on the alloy characteristics, with its thereto-related mechanical processing, deformation mode and cycling.

As described earlier, the SMA shape memory effect is based on thermo-mechanical performance. The transformation temperature is not a strictly defined point, but rather a range. In Figure 6.5, the temperature dependent phase transformation is illustrated. The austenite start temperature (A_s) is the temperature at which the alloy will start the transformation from martensite to austenite phase. The temperature at which the alloy is 100% transformed into austenite phase is indicated as the austenite finish temperature (A_f). By cooling, the phase transition from austenite to martensite phase starts at the martensite start temperature (M_s). The SMA is fully martensite above the martensite finish temperature (M_f). Due to the transformation hysteresis, the cooling and heating paths are not identical. It is important to note that the heat flow in the alloy is influenced by the changed material characteristics (Chopra 2002).

The transformation temperatures are related to the Nickel-Titanium proportions in the alloy. A change in composition of 1% will change the transformation temperature with 100^{o}C (Hodgson, et al. 2000; Morgan, et al. 2004).

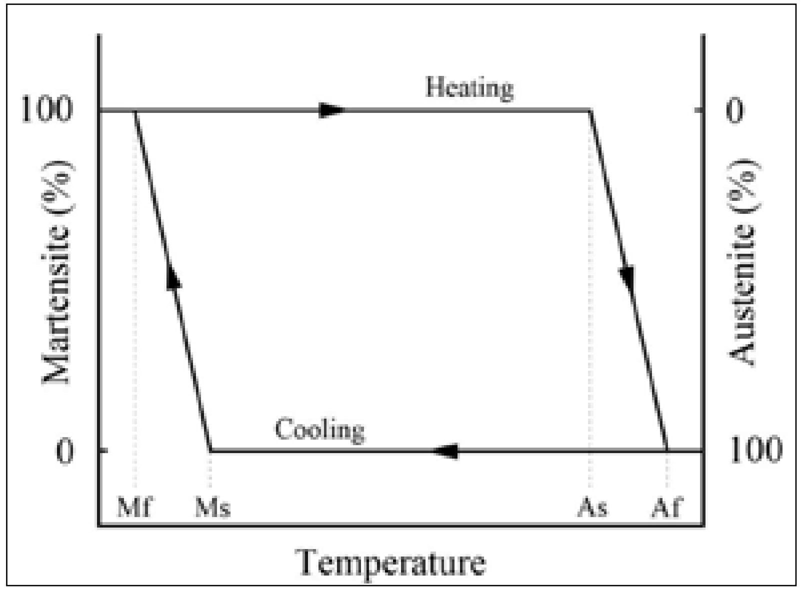

Figure 6.5 Schematic presentation of the phase transformation of SMA (Chopra 2002)

6.5 Smart Composite Specifications

6.5.1 Activation and Control

As discussed previously, both SMA and SMP are thermo-responsive. Therefore, uniform heating of the composite cannot be executed since this will lead to simultaneous activation of both material systems. The different components are heated by electric current in order to enable successive activation. The heating settings are depending on the resistance of the materials, therefore this heating method is called resistive heating.

The electric resistance properties of the SMA show acceptable values through both phases in order to enable resistive activation. However, resistive heating will cause some difficulties on the aspect of temperature control. Continue application of electric power will results in an increasing temperature which may activate the other components (W=J/s). Further investigation is required to determine the desired control parameters; this issue is studied in chapter 8.

As SMPs do not have electrical conductive properties (Huang, et al. 2005), heating wires will be embedded in the heating zone of the SMP matrix to enable thermal activation. Constantan wires have considerably high resistance values, and can therefore generate high temperature by low currents. Furthermore, the material properties of constantan material are particularly stable in a large temperature range. This is a great advantage of a heating element.

The heating wires are only located at a dedicated heating area where the bending occurs. By configuring the wires parallel to the bending direction, the deformation stress will not increase considerably. The technical specifications are further investigated in chapter 7.

In Figure 6.6, the thermal-mechanical activation system of the Smart Composite (SC) is illustrated. The SMP is heated above its threshold temperature by applying an electric current. Continuous monitoring of the material system is necessary in order to prevent overheating. When the control system notes that the SMP surface temperature is raised above the T_g, either $SMA_{1\&3}$ or SMA_2 is activated by resistive heating until a full austenite state has been reached. Subsequently, the SMP will be cooled by switching off the electric current. When the SMP reaches the glassy state, the SMA will be deactivated, initiating ambient cooling.

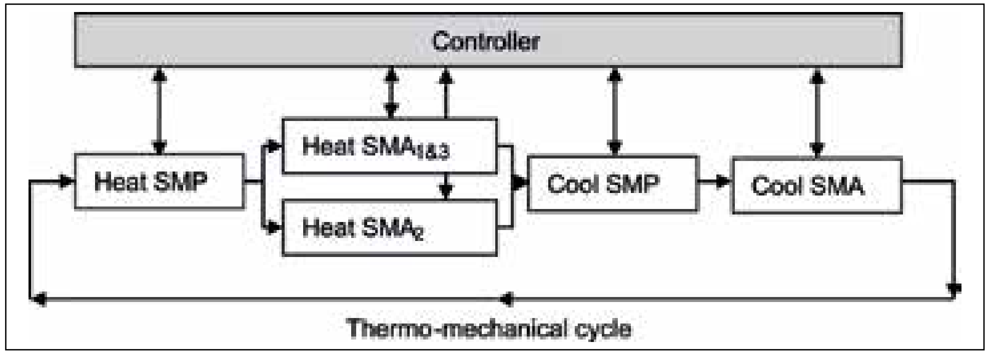

Figure 6.6 Thermo-mechanical cycle of SC performance

6.6 Conclusion and Discussion

After the inventory of smart material systems, it can be concluded that not one specific material met all the design requirements. Therefore, a composite material is presented which is composed of both SMA and SMP material. By combining both materials, the required performance specifications are met. The smart composite can realize a shape morphing performance and can be actively controlled.

Both SMA and SMP are thermo-responsive and will be activated by resistive heating. Therefore, constantan heating wires will be integrated into the SMP matrix to enable local heating of the SMP. By increasing the SMP body temperature, the material will transform into rubbery phase and can then easily be deformed. The SMP matrix will take care of the fixation of the deformation, whereas the SMAs will perform as actuators. By embedding antagonist SMA strips in the SMP matrix, a deformation (forward movement) and recovery (backward movement) of the SC can be realized.

Further research on the fabrication of a SC prototype must gain insight into the real-time performance. Realization of the SC will indicate if the desired performance will be met. Some critical aspects which have been discussed in this chapter might lead to performance difficulties of the selected material systems. Due to the complex stress-strain behaviour, designing with SMA will be quite challenging. Aspects such as electrical, thermal and mechanical behaviour need to be optimized simultaneously. Therefore, further investigation is necessary. The following chapter will outline the fabrication, optimization and mechanical analysis of a small scale prototype.

The materials used during this research are all commercially available. Although optimization of materials on chemical level, such as molecular proportions, could benefit the performance of the materials and the result of the research considerably it would go far beyond the scope of this research.

6.7 References

Abrahamson, E. R., Lake, M. S., et al. (2003). "Shape Memory Mechanics of an Elastic Memory Composite Resin." Journal of Intelligent Material Systems and Structures **14**(10): 623-632.

Bar-Cohen, Y., Kim, K. J., et al. (2007). "Electroactive polymer materials." Smart Materials and Structures **16**(2).

Behl, M. and Lendlein, A. (2007). "Shape-memory polymers." Materials Today **10**(4): 20-28.

Bekker, A. and Brinson, L. C. (1998). "Phase Diagram Based Description of the Hysteresis Behavior of Shape Memory Alloys." Acta Materialia **46**(10): 3649-3665.

Carpi, F., Sommer-Larsen, P., et al. (2005). Electroactive polymers: new materials for spacecraft structures. European Conference on Spacecraft Structures, Materials and Mechanical Testing K. Fletcher. Noordwijk, The Netherlands.

Chopra, I., University of Maryland (2002). "Review of State of Art of Smart Structures and Integrated Systems." AIAA Journal **40**(11): 42.

Corner Stone Research Group Industries (webpage) Retrieved 2008-07-09 from www.crg-industries.com.

Culshaw, B. (1996). Smart structures and materials. Boston, Artech House.

De Rossi, D., Carpi, F., et al. (2004). Electro-Active Polymers For actuation and sensing in space applications. 55th International Astronautical Congress Vancouver, Canada**:** 1-11.

Dietsch, B. and Tong, T. (2007). "A Review - Features and Benefits of Shape Memory Polymers (SMPs)." Journal of Advanced Materials **39**(2): 10.

Duerig, T. W. (1990). Engineering Aspects of Shape Memory Alloys, London, Butterworth-Heinemann.

Gandhi, M. V. and Thompson, B. S. (1992). Smart materials and structures. London, Chapman and Hall.

Hodges, D. E., Wu, M., et al. (webpage) "Shape Memory Applications, Inc.".

Hodgson, D. and Russell, S. (2000). "Nitinol melting, manufacture and fabrication." Minimally Invasive Therapy & Allied Technologies **9**(2): 61-65.

Huang, W. (2002). "On the selection of shape memory alloys for actuators." Materials & Design **23**(1): 11-19.

Huang, W. M., Yang, B., et al. (2005). "Water-driven programmable polyurethane shape memory polymer: Demonstration and mechanism." Applied Physics Letters **86**(11): 114105.

Huber, J. E., Fleck, N. A., et al. (1997). "The Selection of Mechanical Actuators Based on Performance Indices." Proceedings of the Royal Society A: Mathematical, Physical and Engineering Sciences **453**(1965): 2185-2205.

Ikuta, K. (1990). Micro/miniature shape memory alloy actuator. Robotics and Automation, 1990. Proceedings., 1990 IEEE International Conference on.

Inoue, K., Serizawa, S., et al. (2007). Highly Functional Bioplastics (PLA compounds) Used for Electronic Products. Polymers and Adhesives in Microelectronics and Photonics, 2007. Polytronic 2007. 6th International Conference on.

Inoue, K., Yamashiro, M., et al. (2005). "Thermo-Reversibly Cross-Linked Polylactic Acid Acting Rewritable Shape Memory." Polymeric Materials: Science & Engineering **93**: 967.

Jiang, H., Kelch, S., et al. (2006). "Polymers Move in Response to Light." Advanced Materials **18**(11): 1471-1475.

Jinhao, Q., Junji, T., et al. (2000). "High-speed response of SMA actuators." International Journal of Applied Electromagnetics and Mechanics **12**(1): 87-100.

Koerner, H., Price, G., et al. (2004). "Remotely actuated polymer nanocomposites: stress-recovery of carbon-nanotube-filled thermoplastic elastomers." Nature Materials **3**(2): 115-120.

Langelaar, M. (2006). Design Optimization of Shape Memory Alloy Structures. PhD. Dissertation, Delft University of Technology.

Lelieveld, C. M. J. L. and Voorbij, A. I. M. (2008) "Dynamic Material Application for Architectural Purposes." Advances in Science and Technology **56**, 595-600.

Lendlein, A., Jiang, H., et al. (2005). "Light-induced shape-memory polymers." Nature **434**(7035): 879-882.

Leng, J., Lan, X., et al. (2011). "Shape-memory polymers and their composites: Stimulus methods and applications." Progress in Materials Science **56**(7): 1077-1135.

Leng, J., Wu, X., et al. (2009). "Infrared light-active shape memory polymer filled with nanocarbon particles." Journal of Applied Polymer Science **114**(4): 2455-2460.

Leng, J. S., Huang, W. M., et al. (2008a). "Significantly Reducing Electrical Resistivity by Forming Conductive Ni Chains in a Polyurethane Shape-Memory Polymer/Carbon-black Composite." Applied Physics Letters **92**(20): 204101.

Leng, J. S., Lan, X., et al. (2008b). "Electrical conductivity of thermoresponsive shape-memory polymer with embedded micron sized Ni powder chains." Applied Physics Letters **92**(1): 014104-014103.

Liu, Y., Lv, H., et al. (2009). "Review of electro-active shape-memory polymer composite." Composites Science and Technology **69**(13): 2064-2068.

Liu, Y. and Mccormick, P. G. "Two-Way Shape Memory Effect in NiTi " Materials Science Forum **56 - 58**: 585-590.

Loughlan, J., Thompson, S. P., et al. (2002). "Buckling control using embedded shape memory actuators and the utilisation of smart technology in future aerospace platforms." Composite Structures **58**(3): 319-347.

Madden, J. D. W., Vandesteeg, N., et al. (2004). "Artificial Muscle Technology: Physical Principles and Naval Prospects." Oceanic Engineering, IEEE Journal of **29**(3): 706-728.

Mavroidis, C., Pfeiffer, C., et al. (1999). Conventional Actuators, Shape Memory Alloys, and Electrotheological Fluids. Automation, Miniature Robotics and Sensors for Nondestructive Testing and Evaluation. Y. Bar-Cohen.

Memory Metalle GmbH (webpage) Retrieved 2008-04-16 from www.memory-metalle.com.

Morgan, N. B. and Broadley, M. (2004). Taking the Art Out of Smart!- Forming Processes and Durability Issues for the Application of NiTi Shape Memory Alloys in Medical Devices. Material & Processes for Medical Devices Conference. Anaheim, California, The United States.

NEC (webpage) Retrieved 2008-07-14 from http://www.nec.co.jp/rd/Eng/innovative/E4/05.html.

Nuffer, J., Schönecker, A., et al. (2007). Reliability Investigation of piezoelectric

Macro Fibre Composite (MFC) Actuators. Adaptronic Congress. Göttingen, Germany: 23 - 24 May.

Ohkata, I. and Suzuki, Y. (1998). The Design of Shape Memory Alloy Actuators and their Applications. Shape Memory Materials. K. Otsuka and C. M. Wayman. Cambridge, USA, Cambridge University Press: 240-267.

Otsuka, K. and Wayman, C. M. (1998). Shape memory materials. Cambridge, UK, Cambridge University Press.

Schmidt, A. M. (2006). “Electromagnetic Activation of Shape Memory Polymer Networks Containing Magnetic Nanoparticles.” Macromolecular Rapid Communications **27**(14): 1168-1172.

Shahinpoor, M., Bar-Cohen, Y., et al. (1998). “Ionic Polymer-Metal Composites (IPMCs) as Biomimetic Sensors, Actuators and Artificial Muscles - a Review.” Smart Materials and Structures **7**(6): R15-R30

Shahinpoor, M. and Schneider, H.-J. (2008). Intelligent materials. Cambridge, Royal Society of Chemistry.

Stoeckel, D. (1992). Status and Trends in Shape Memory Technology. Actuators ‘92. Bremen, Germany: 97-84.

Tautzenberger, P. (1990). Thermal Actuators: a Comparison of Shape Memory Alloys with Thermostatic Bimetals and Wax Actuators. Engineering aspects of shape memory alloys. T. W. Duerig, K. N. Melton, D. Stöckel and C. M. Wayman, Butterworth-Heinemann: 207-218.

Tzou, H. S. and Anderson, G. L. (1992). Intelligent Structural Systems. Dordrecht, Kluwer.

Yang, B., Min Huang, W., et al. (2005). “Effects of moisture on the glass transition temperature of polyurethane shape memory polymer filled with nano-carbon powder.” European Polymer Journal **41**(5): 1123-1128.

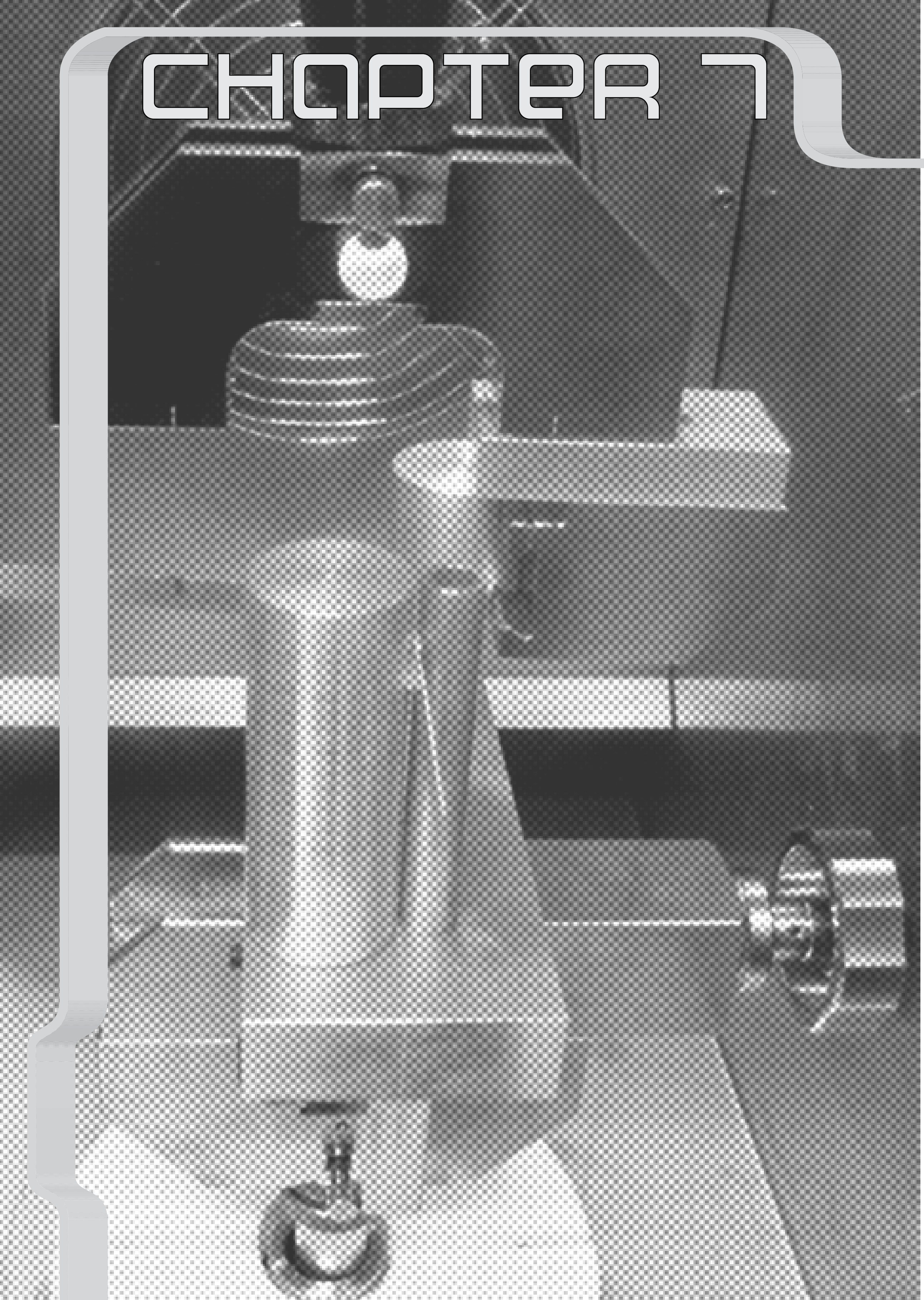

Chapter 7

Mechanical characterization and prototyping of the smart composite

7.1 Introduction

An Adaptive Building Component (ABC) based on smart material technology has been discussed in chapter 6. The desired performance will be realized by a composite material from shape memory materials. In this chapter, the fabrication and performance of the smart composite (SC) is subject of research. The performance and properties of the required materials are analysed and characterized. First, the material components are analysed separately, after which the performance of the SC is tested with a small-scale prototype.

In general, the SC should be able to establish the desired deformation of a 90° angle. This deformation should be maintained without constant energy input or constrain. Subsequently, the deformation should be recovered into the initial flat configuration. The deformation angle of the SC is related to the memory shape of the SMA strips. Different initial angle settings of the SMA strips are analysed in order to determine the most optimal performance.

In Figure 7.1, a schematic of the SC is shown. The required settings for the realization of the forward deformation are given in Table 7.1. The active components (SMA_1 and SMA_3) should deliver sufficient force for the deformation of the passive components (SMP and SMA_2). In Table 7.2, the settings of the components for the recovery (backward deformation) are presented. The SMP and the SMA_2 should deliver sufficient force for the recovery of the deformation. Before the SMA strips are activated for the realization of the deformation, the SMP must be fully rubbery.

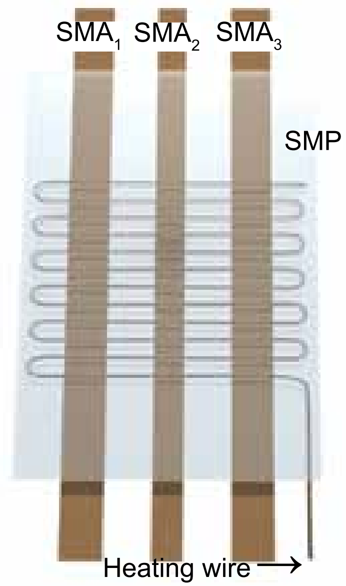

Figure 7.1 Schematic of SC with heating wires.

Table 7.1 Specific settings of the SC components in order to enable the forward deformation.

Component	Performance	State	Condition
SMP	body	rubbery (heated)	passive
SMA_1 and SMA_3	actuators	austenite (heated)	active
SMA_2	antagonist	martensite (cold)	passive

Table 7.2 Specific settings of the SC components in order to enable the backward deformation.

Component	Performance	State	Condition
SMP	body	rubbery (heated)	active
SMA_1 and SMA_3	antagonist	martensite (cold)	passive
SMA_2	actuator	austenite (heated)	active

It is assumed that the force required for the deformation of the SC is equal to the sum of the required forces for the deformation of the individual components (see Equation 7.1). This means that the SMA strips facilitating the deformation should deliver sufficient force for the deformation of both the SMP in the rubbery phase and the antagonist SMA strip in martensite condition. Additionally, the sum of the delivered force by the SMP in the rubbery phase and the SMA strips initiating recovery should be equal or larger than the force required for the deformation of the antagonist SMA strips in martensite condition (Equation 7.2). Note that the SMA strips can move freely in the SMP matrix, which is expected to minimize the friction between the SMA and SMP.

For deformation:

$$F_{SMA_{ant,mart}} + F_{SMP,rubbery} \leq F_{SMA_{def,aust}} \qquad \text{Equation 7.1}$$

For recovery:

$$F_{SMA_{rec,aust}} + F_{SMP,rubbery} \geq F_{SMA_{ant,mart}} \qquad \text{Equation 7.2}$$

$F_{SMA,ant,mart}$ defines the required force for the deformation of the SMA strip found in martensite condition. This is the antagonist SMA of the SMA strip that initiates deformation. This SMA provides the recovery of the SC after deformation (SMA_2).

$F_{SMP,rubbery}$ defines the required force for the deformation of the SMP in rubbery phase; this is equal to the unconstrained recovery of the SMP.

$F_{SMA,def,aust}$ defines the delivered force of the SMA which facilitates the deformation of the ABC. This SMA is performing in austenite phase (SMA_1 and SMA_3).

$F_{SMA,rec,aust}$ defines the delivered recovery force by the SMA strip while in austenite phase (SMA_3).

$F_{SMA,ant,mart}$ defines the required force for the deformation of the SMA in martensite phase. This SMA is programmed to initiate the deformation of the ABC, and is considered the antagonist of the SMA that facilitates recovery (SMA_1 and SMA_3).

Experiments will be conducted in order to analyse the deformation performance of the individual components. SMA_{1+3} should deliver enough force for the deformation of the SMP body in rubber condition and the SMA_2 in martensite condition. Therefore, the required force for the deformation of both components will be analysed. For the backward movement, the SMP must recover to the initial configuration and the SMA_2 should be able to deform the martensitic SMA_{1+3}.

Both materials show thermo-responsive behaviour. Therefore, the threshold temperatures should be determined for the determination of the exact transition temperatures.

The following aspects require analysis for the performance of the smart composite:

- Transition temperature of the SMP
- Deformation force of the SMP. Determine the force required for the deformation of the SMP in full rubbery phase.
- Deformation force of the antagonist SMA. Determine the force required for the deformation of the SMA in martensite phase.
- Recovery force of the SMA. Determine the delivered recovery force of the SMA in austenite phase.
- Determine programmed shape of the SMA, for the realization of a 90° deformation
- Analyse the performance of the SC.

After the experiments with the individual components, the shape morphing performance of the SC is tested with the fabrication of a small scale prototype. Additionally, Equation 7.1 and Equation 7.2 will be validated by analysing the performance of the SC together with the outcome of the individual components.

The fabrication of the SC prototype requires specific attention. Both the SMA strips as the heating wires should be embedded in the SMP matrix. The two component SMP resin will be cured in a mould by heat ramping. The heating wires can be integrated in the SMP matrix during curing. However, it is not possible to integrate the SMA strips during curing, as these will show shape-morphing performance at the curing temperature. Therefore, the SMP matrix will be fabricated out of two components. The SMA strips will be embedded in the SMP matrix after curing and the two SMP components will be connected by adhesion bonding.

The initial shape of the SMA strips will be programmed by heat treatment. The SMA must be annealed at high temperatures before attaining the memory shape. The settings of this heat treatment, such as temperature and heating time, will be determined experimentally.

For the fabrication of the smart composite the following aspects will be studied:

- Adhesion bond SMP
- Curing method SMP with integrated heating wires
- Annealing settings SMA

It should be noted that the purpose of the experiments is to gain information on the material performance for the presented application.

7.2 Mechanical Characterization of the Shape Memory Polymer

As is explained earlier, the performance of the SMP is based on thermo-responsive characteristics. Therefore, the specific transformation temperature needs to be determined. The required deformation force of the SMP in rubbery phase will be determining the actuation force of the SMA strips. It should be noted that the required deformation force in the rubbery phase is equal to the unconstrained recovery force of the SMP.

7.2.1 Transition Temperature and Young modulus

The SMP should be heated until it reaches the full rubbery state before the deformation of the SC can be initiated. The temperature at which the SMP will transform from solid to rubber condition will be determined experimentally.

7.2.1.1 Research Method

The glass transition temperature can be determined by Dynamic Mechanical Analysis (DMA). This method analyses the viscoelastic behaviour of the polymer. A viscoelastic material has both elastic and viscous characteristics. This means that, under stress, it partly dissipates energy (viscous characteristic) and it partly stores energy (elastic characteristic). By DMA, oscillated stress or strain is applied on a small polymer sample, resulting in a stress/ strain relation. By increasing the sample temperature, the viscoelastic characteristics changes accordingly, showing a considerable change around the T_g region. The storage modulus measures the stored elastic energy during deformation. This energy will be fully released at the moment the stress is released. The loss modulus characterizes the viscous behaviour of the polymer, which is associated with the dissipated energy. The damping coefficient, Tan delta, is defined as the loss/storage modulus ratio and indicates how well the material can dissipate energy.

The T_g can be determined by different methods. This is either the specific point where the curve of the storage modulus shows a large drop or the position of the peak on the tan delta curve. Additionally, the onset of the storage modulus can be used as an indication of the T_g (Menard 1999). It is important to realize that the glass transition of a material is in fact not a specific temperature point, but is a temperature range between approximately 20 to 50 °C.

The T_g will vary for different oscillation frequencies. At low frequencies, the polymer has more time to relax between the load cycles and therefore shows lower elasticity (storage modulus).

The young modulus (E) can be derived from the DMA results by the following equation (Menard 1999):

$$E = \sqrt{(E'^2 + E''^2)} \qquad \textbf{Equation 7.3}$$

In Equation 7.3, the E' indicates the storage modulus and the E" the loss modulus.

The applied specimen dimensions are 34.6 x 9.3 x 1.1 mm, derived from manufactured SMP material. When extracting the clamping, the specimen length measures 24.36 mm. The temperature has been increased from 25°C to 130°C at a rate of 1°C per minute. Measurements have been executed at frequencies of 3.2, 10 and 32 Hz. The DMA used for this analysis is the Q800 from TA-Instruments.

7.2.1.2 Result and Discussion

The results of the DMA tests by different frequencies are shown in Figure 7.2. The modulus is independent of the frequency (e.g. is elastic) at room temperature and has a value of about 800 MPa. Between 50 and 100°C, the material is viscoelastic (frequency dependent). The Tan delta has a maximum value in this temperature range. Above 110°C, the material is rubbery elastic and has a modulus of about 0.5 MPa. The material is also frequency independent at this high temperature range. In the prototype, the SMP motion is relatively low; therefore the data of the lowest frequency of 3.2 Hz is used for further analysis.

In Figure 7.3, the storage modulus at a frequency of 3.2 Hz is shown. Based on this it can be concluded that considerable differences are found between the onset of the storage modulus curve and the tan delta peak. Therefore, it is decided that the transition temperature (T_g) will be determined here as the temperature where the SMP material reaches a certain rubber level which enables deformation. On the whole, rubber has a typical Young modulus of 10 to100 MPa. The storage modulus of the tested SMP will drop below 100 MPa at a temperature of 58°C. This temperature is therefore chosen as the minimum SMP body temperature before deformation is initiated. This value is in agreement with the T_g of 62°C provided by the supplier of the polymer (Corner Stone Research Group Industries webpage).

It should be addressed that in the elastic ranges, the storage modulus can be directly used as Young modulus. It can be clearly seen in Figure 7.2 that the loss modulus gives low values in relation to the storage modulus. When calculating the Young modulus with Equation 7.3, the loss modulus has such a small contribution that it is negligible. Therefore, the Young modulus is determined by the storage modulus in Figure 7.3. The Young modulus by temperatures below T_g can be determined as 797 MPa and by temperatures above T_g as 0.5 MPa.

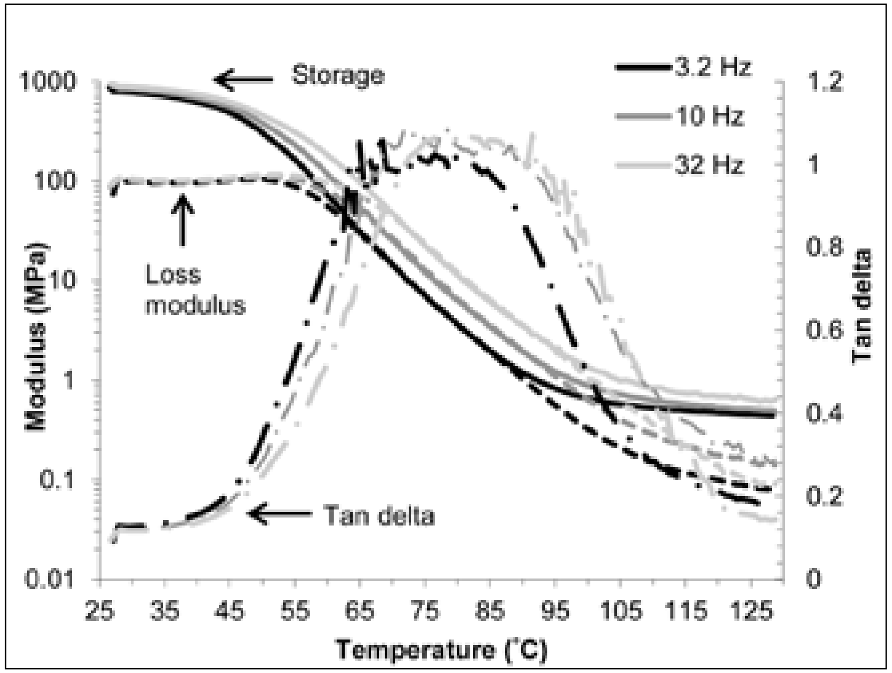

Figure 7.2 Storage modulus, loss modulus and Tan delta versus temperature. The solid line is the storage modulus, the dotted line the loss modulus and the dashed-dotted line the Tan delta. The different colours refer to different frequencies. Note that the modulus curve is on a logarithmic scale.

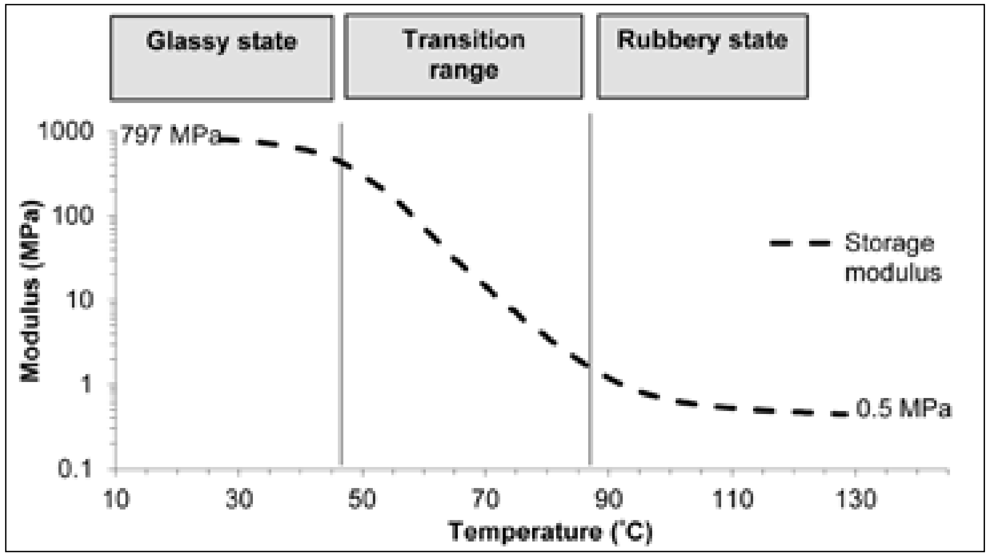

Figure 7.3 Storage modulus at 3.2 Hz with the specific material conditions.

7.2.2 Deformation force of the SMP in Rubbery Phase

This paragraph discusses the deformation of the SMP in rubber condition. The specific deformation from the initial straight configuration into a bent angle of 90° is analysed. This data can be used for the specification of the required actuator force of the SMA strips. The required force for the deformation of the rubbery SMP from straight configuration into an angle of 90° (e.g. the forward movement) is considered equal to the recovery force of the rubbery SMP (e.g. the backward movement). This means that the deformation force during loading is equal to the recovery force during unloading. This is the basic memory characteristic of SMP.

7.2.2.1 Research Method

The deformation force of the rubbery SMP will be determined by torsion experiments (Figure 7.6). To ensure that the SMP is in full rubber condition, this experiment is executed at a uniform temperature of 110°C. In practice, the SMP will be deformed by the SMA actuators, which are annealed with a radius of 15 mm. In order to obtain a deformation with a similar radius, the SMP will be rolled over a cylindrical attachment with the required radius. By rotating the grip head of the torsion bench, the sample is rolled over the cylinder until a deformation of 90° is met. In Figure 7.4, a schematic representation of the research setup is given. Note that different rotation angles are used for the grip head and the SMP sample. The grip head angle is obtained from the test bench data file and is 0° at the start of the experiment and 180° at the end. The deformation angle of the SMP sample is 180° when the sample is flat and 90° when the material is bent, as is illustrated in Figure 7.4.

The torsion bench determines the torsion of the grip head. Actually, the deformation angle of the SMP is required for further analysis. Therefore, the deformation of the SMP is recalculated to meet the correct data. The rotation path of the grip head follows torsion angle from 0° to 180°. Whereby, the SMP deforms from 180° to 90°. Furthermore, the actual deformation force must be recalculated in order to determine the force in the direction of the deformation.

The required deformation force is calculated by dividing the arm through the obtained torque. The torque arm is the distance from the clamp to the point of deformation.

$$M = F * a \qquad \text{Equation 7.4}$$

M= torque in Nmm
F= Force in Newton
a= arm in millimetres

As the SMP is rolled over the cylinder by the grip head, the contact point is constantly changing. This will result in an increase of the arm. For this reason, the arm should be calculated for every deformation angle. The increase of the arm length can be calculated by the use of the basic calculation for the arc of a circle;

$$l = \frac{\pi r \gamma}{180} \qquad \text{Equation 7.5}$$

l=arc length in mm
r=radius of the cylindrical attachment in mm
γ= angle between the initial force incitement point and the current force point in degrees

This experiment is executed five times with the same material sample. The dimensions of this sample are 125*60*7 mm. The grip head rotates with 50° per minute.

The experiments are executed with a Zwick/Roel Z005 torsion bench (Figure 7.5). The setup is enclosed in an oven in order to enable operation at a high uniform temperature. The research setup is shown in Figure 7.6

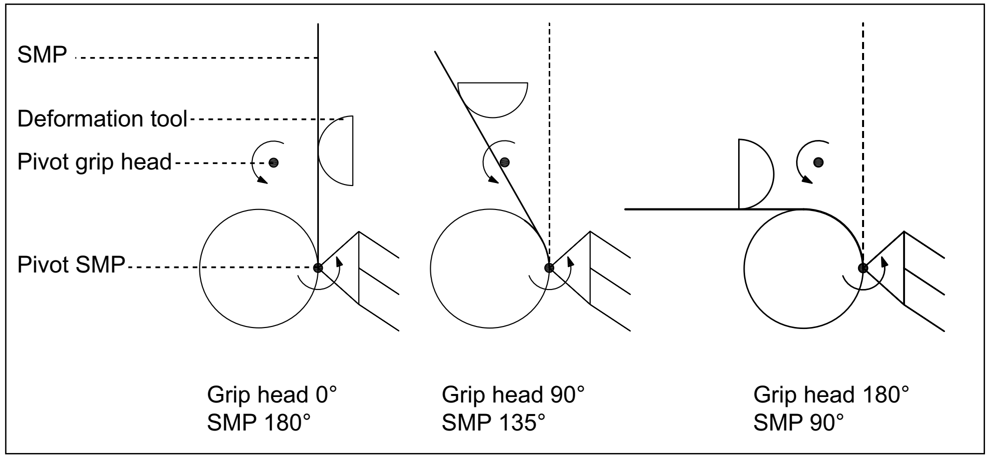

Figure 7.4 Schematic top-view of the research setup. By torsion of the grip head, the SMP will be rolled over a cylinder with a radius of 15 mm. The deformation tool is clamped in the grip head of the torsion bench.

Figure 7.5 Zwick Roell Z005 torsion bench with heating chamber.

Figure 7.6 Torsion bench with SMP sample.

7.2.2.2 Result and Discussion

In Figure 7.7, the obtained results of the torsion experiments are plotted against the deformed angle. All experimental data overlap, which indicates that the experiments are reproducible.

The increase of required force with decreasing deformation angle can be attributed to the compression and tension forces at respectively the inside and outside of the SMP material. Around a torsion angle of 110°, the force curve shows a considerable increase of inclination. This can be explained by a shortcoming of the research setup. After a certain bending deformation, the grip head is touching the cylinder during the rolling of the SMP material. This will lead to a considerable increase of the deformation force. By omitting this final data part, a clear indication is found of the required deformation force of the SMP. The included trend-line extrapolates the torsion/force curve of the small torsion area. The recorded forces for the SMP are low and range from approximately 0.1 to 0.35 Newton after the correction.

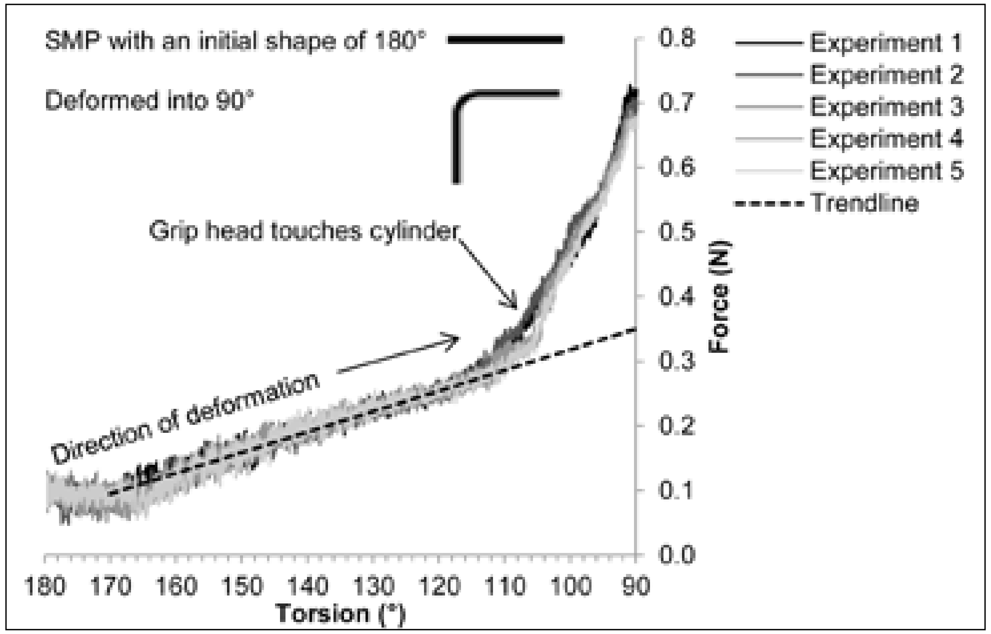

Figure 7.7 Deformation force SMP in rubbery phase at a temperature of 110°C. SMP is deformed from 180° to 90°. Dimensions: 7*60*125 mm.

7.3 Mechanical Characterization of the Shape Memory Alloy

7.3.1 Transition Temperature

The performance of the SC is based on the deformation of the SMP material in the rubbery phase by the SMA actuators, which occurs in a temperature range of 58 to 65°C (Figure 7.3). It should be noted that the SMP should be fully rubbery before the deformation is initiated. Since the SMAs are embedded in the SMP matrix, this means that the activation temperature of the SMA strips should be well above the glass transition temperature of the SMP. Otherwise, the SMA strips will start the deformation before the SMP is fully rubbery. This can lead to cracks on the SMP surface.

Based on the activation requirements and the commercial availability of the SMA, a transition temperature of 95°C is chosen. The transition temperatures are affected by the thermal treatment during the annealing of the initial shape. The given activation temperature of the supplier therefore should be seen as an indication and the actual transition temperatures will be determined experimentally.

7.3.1.1 Research Method

The characterization of the phase transition points are determined by Differential Scanning Calorimeter (DSC) analysis. The Differential Scanning Calorimeter is an instrument which measures temperature related material properties. Upon thermal treatment of a sample, the threshold temperature of the phase transition can be determined. Thermally induced phase transitions are based on endothermic (absorption of energy) or exothermic (release of energy) processes. The DSC analyses the amount of absorbed or released heat during heating. A Perkin Elmer DSC 7 is used for this analysis.

The sample is heated from 0°C to 120°C with 10°C per minute. Subsequently, the temperature is decreased with similar speed. The analysis is repeated twice, as during the first cycle some atomic dislocation may lead to deviations (Loughlan, et al. 2002). After the second cycle, the material stabilizes. For this reason, the second cycle has been used for the determination of the transition temperatures.

7.3.1.2 Result and Discussion

In Figure 7.8, the results of the DSC experiment are shown. During heating, the SMA absorbs the heat (endotherm) and the sample releases heat during cooling (exothermal). The phase transition from martensite to austenite starts at a temperature of 92°C. The SMA is fully transformed at an austenite finishing temperature (A_f) of 106°C. The activated strips should reach a temperature above the austenite finish temperature (A_f=106°C) in order to establish a full transformation of the SMA. The activation of the antagonist SMA strip in the composite is prevented when the local temperature does not exceed the austenite start temperature (A_s) of 92°C. Fatigue at high temperatures will be avoided when the maximum temperature of the SMA does not exceed 150°C (Loughlan, et al. 2002).

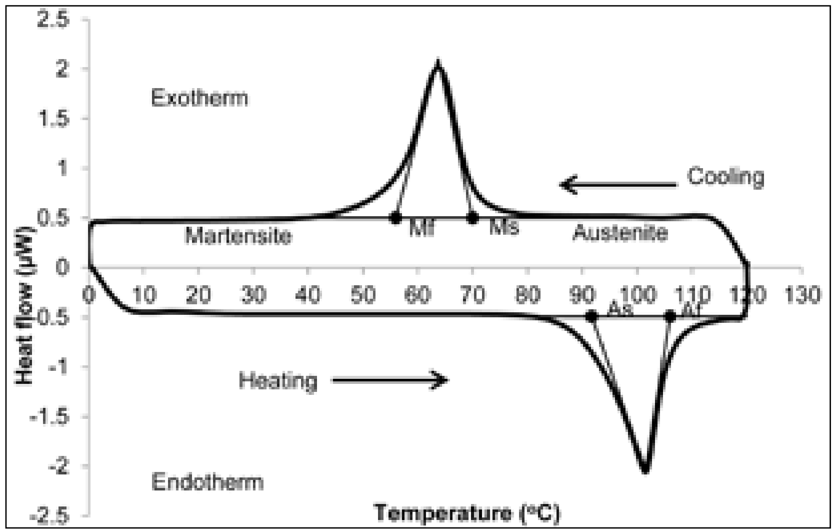

Figure 7.8 Transition temperatures derived by DSC experiments. During heating, the transformation from martensite to austenite phase starts at a temperature of 92°C (A_s). The SMA is fully austenite at a temperature of 106°C (A_f). By cooling, the SMA transforms to martensite phase starts at 70°C (M_s). The SMA is fully martensite at a temperature of 55°C (M_f). During the phase transition from martensite to austenite, heat is absorbed (endotherm). During the cooling from austenite to martensite, heat is released (exothermic).

7.3.2 Recovery in Austenite Phase

After the determination of the required deformation force of the SMP body in rubbery condition, the force capacity of the SMA will be determined. As the SMA strips enable the deformation of the SC as well as the recovery, both aspects will be analysed. The force capacity of the SMA strip for the initiation of a deformation from a straight strip into a 90° angle is analysed. Additionally, the force capacity of the antagonist SMA strip is determined. This strip initiates a recovery from a 90° angle deformation into the initial straight configuration (the backward deformation).

7.3.2.1 Research Method

In correspondence with the SMP experiments, torsion experiments are executed with the Zwick/Roell Torsion bench Z005. The samples are annealed at different deformation angles, in order to determine the optimum performance-shape relation. The SMA strips are annealed at angles of 0°, 45°, 90° and 225° with a radius of 15 mm (Figure 7.9 and Figure 7.10). These dimensions are defined at the inner angle of the SMA strip.

Figure 7.9 Moulds for annealing the SMA strips in an angle of 0°, 45°, 90°, and 135°.

Figure 7.10 SMA strips after annealing.

7.3.2.2 SMA Actuation Force for Forward Deformation from 180° to 90°

The SMA samples with a programmed angle of 0°, 45° and 90° are tested for the deformation of the SC from initial straight configuration (180°) into a 90° angle. The research method is illustrated in Figure 7.11. In order to test the force capacity, the SMA strips with a programmed angle of 0°,45° and 90° are first straightened (angle of 180°) and then clamped in the torsion bench. The temperature is raised until it is well above the austenite finishing temperature ensuring a full austenite condition. By increasing the temperature of the SMA strip above the transition temperature, the strip will initiate a recovery into its annealed shape. This recovery is prevented by a small pin (Figure 7.12). With this pin, the recovery force can be measured by the torsion bench. The recovery force of the SMA strip is measured while slowly changing the torsion angle with a speed of 10° per minute until a recovery of 90° is reached. The SMA strip is in constant contact with the pin. In Figure 7.12, an image of the research setup of the torsion bench is shown. Here, the SMA strip has been recovered into a 90° angle.

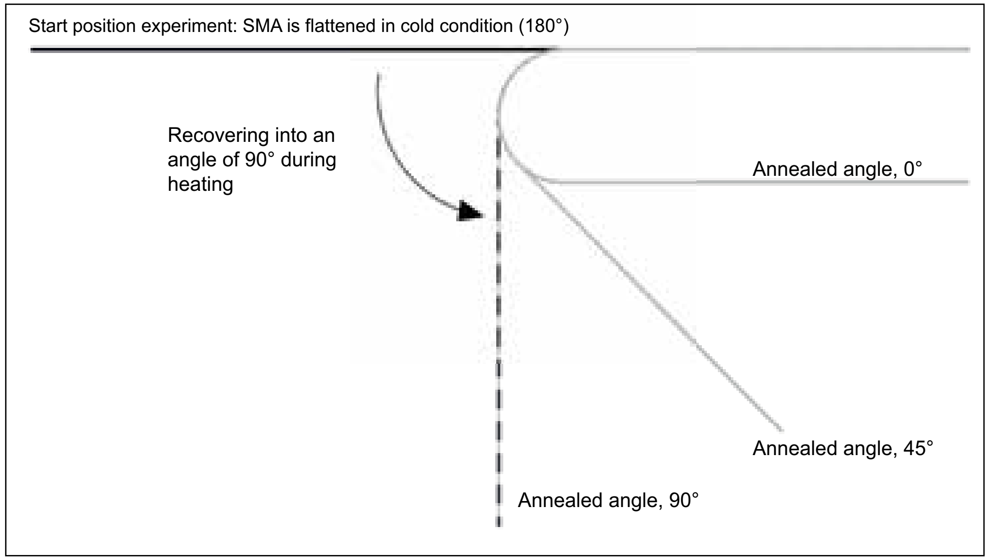

Figure 7.11 Schematic top-view of the deformation test for the determination of the force of the SMA. The SMAs with a programmed angle of 0°, 45° and 90° are flattened in cold condition before the recovery tests are executed. The recovery force is measured until the SMA strip reaches 90°.

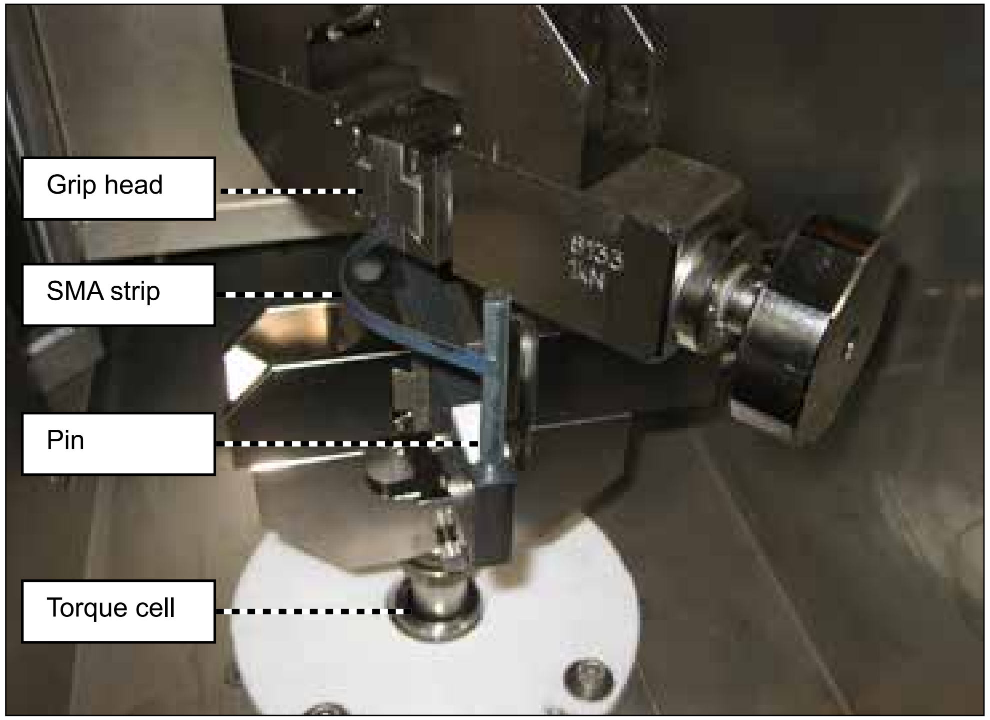

Figure 7.12 Research setup of torsion bench

7.3.2.3 SMA Actuation Force for Backward Deformation from 90° to 180°

The recovery force from a 90° deformation angle into the initial flat shape of 180° is analysed for a SMA sample with a programmed angle of 225°. In Figure 7.13, the principle of this experiment is presented. The SMA sample is bent in a 90° angle while in cold condition (martensite). After heating above the threshold temperature, recovery occurs until the SMA reaches the initial shape of the SC (180°). The material thickness is 0.5 mm and the width 10 mm. Every experiment is cycled three times, whereby the third cycle is used for further analysis.

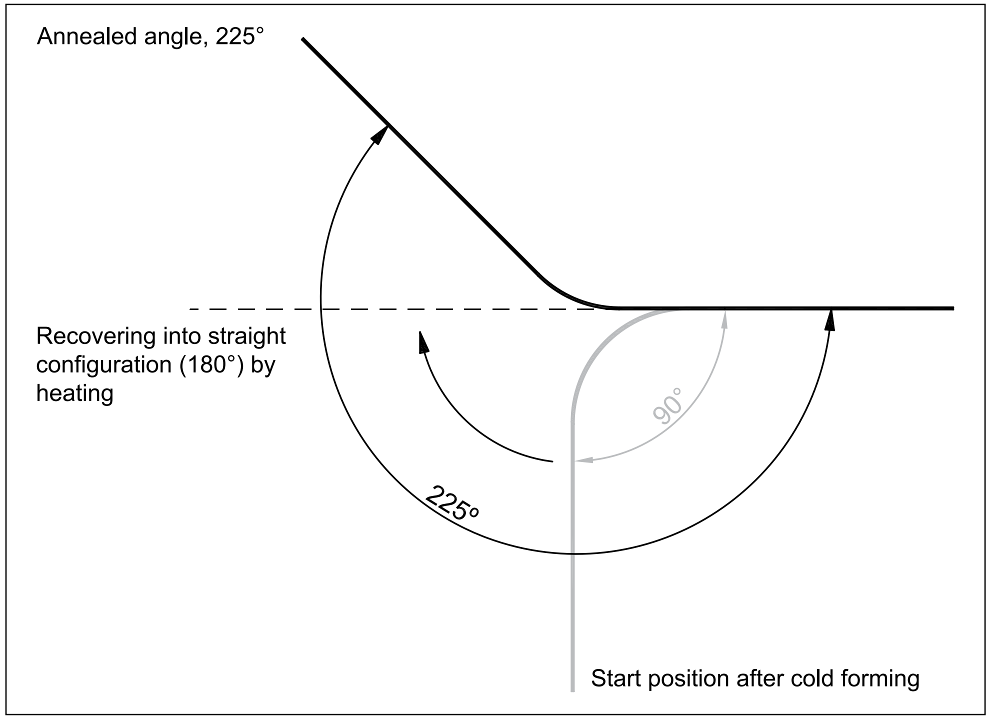

Figure 7.13 Schematic of top-view of the backward deformation. The SMA with a programmed shape of 225° is deformed in martensite state into a 90° angle. Recovery is measured until the SMA reaches a straight configuration.

7.3.2.4 Data Evaluation Procedure

The torsion bench delivers the torsion and the torque with respect to the torsion axis. The deformation of the SMA strips and the related force at the location of the contact point is required for further analysis. This means that the results should be converted in order to obtain the desired data. In Figure 7.14 and Figure 7.15, a schematic is given of the top-view of the research setup. In Figure 7.14, the start position of the torsion bench is illustrated. The grip head will rotate with an angle of β, allowing the SMA a recovery until it reaches the contact point, while the delivered torque is measured (Figure 7.15).

In these schematics the relation between the torsion angle of the grip head and the recovered angle of the SMA strip is shown. By the use of the determined parameters, the given torque can be converted into the force capacity of the SMA strip. The used symbols are explained in Table 7.3.

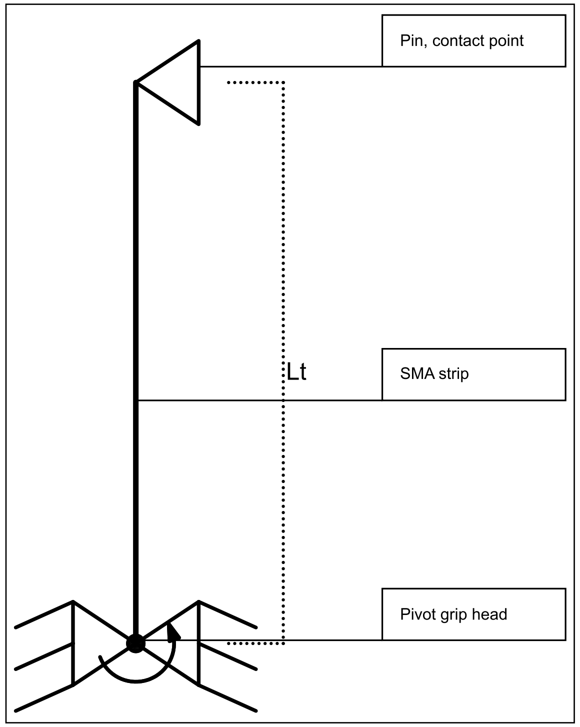

Figure 7.14 Schematic top-view of SMA torsion test in austenite condition.

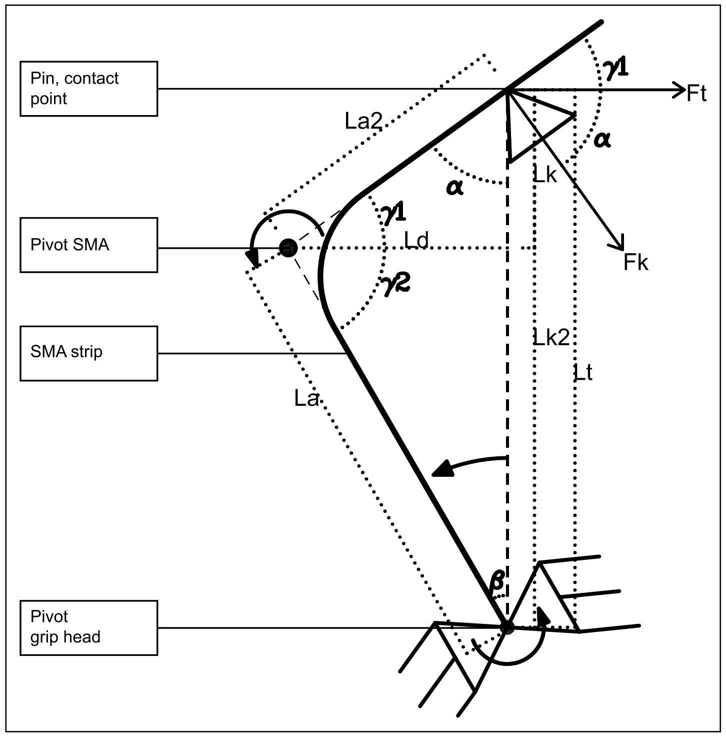

Figure 7.15 Schematic top-view of SMA during torsion test. The grip head rotates counter clockwise with an angle of β. The SMA strip deforms with an angle of γ1+ γ2.

Table 7.3 Specifications of the indication points

Symbols	Explanation
L_t	Distance from torsion axis to the pin. With this arm, the torque is calculated by the torsion bench.
L_a	Distance from torsion axis to the rotation point of the SMA.
β	Rotation angle of the torsion bench
γ	Recovered angle SMA strip, this angle is the sum of γ_1 and γ_2.
α	Angle between the measured force (F_t) and the required force (F_k)
M_t	Determined torque by torsion bench
F_t	Force perpendicular to torsion arm (L_t)
M_k	Required torque delivered by SMA strip
F_k	Required force perpendicular to torsion arm (L_{a2})
L_{a2}	Torsion arm SMA strip

The recovered angle (γ) of the SMA strip is calculated with the following equations:

Equation 7.6
$$\gamma = \gamma_1 + \gamma_2$$

Equation 7.7
$$\gamma_2 = 90 - \beta$$

Equation 7.8
$$\gamma_1 = a\tan\left(\frac{\left(L_t - L_a\cos(\beta)\right)}{\left(L_a\sin(\beta)\right)}\right.$$

The force delivered by the SMA strip at the location of the contact point is determined by the following equation:

Equation 7.9
$$F_k = \left(\frac{M_t}{L_t\cos(\alpha)}\right)$$

The angle between the forces F_t and F_k ( ) is calculated with:

Equation 7.10
$$\alpha = 180 - \beta - \gamma$$

For every experiment the variables L_t and L_a need to be determined. The variables M_t and β are measured by the torsion bench.

In order to validate these calculations, the experiments are captured by video from top view. By the use of a tracking program, the actual deformation angle of the SMA strip could be analysed (see Figure 7.16).

In Figure 7.17, the relation between the torsion of the grip head and the torsion of the SMA strip is presented for the calculated and the tracked data. It should be noted that especially at the low angle area, a difference of approximately 10° is found. This difference could be attributed to the fact that during heating the SMA already delivers a considerably high force on the contact point. The SMA will initiate recovery before the grip head has been rotated. This causes the SMA to initiate recovery in the start position. The start position of the calculated angle is determined by the grip head. When the grip head has an angle of 0°, the related angle of the SMA (γ) should be 180°. When analysing the tracker data, an angle of 170° is found. This initial recovery is a shortcoming of this test set-up. Since this recovery could not be prevented, it will be considered a measuring error. The difference between the calculated and the tracking results decreases with increasing torsion. This is caused by the decrease of the recovery force, which prevents the SMA strip to deform more than is prevented by the contact point.

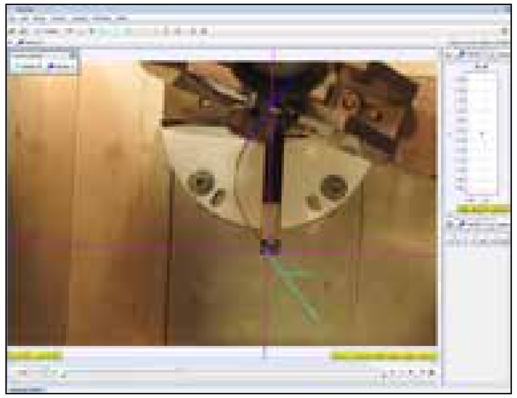

Figure 7.16 Screen capture of tracking program.

The calculated results correspond quite well with the measured tracking data. Therefore, this recalculation method of the data according to the equations above is used for further analysis.

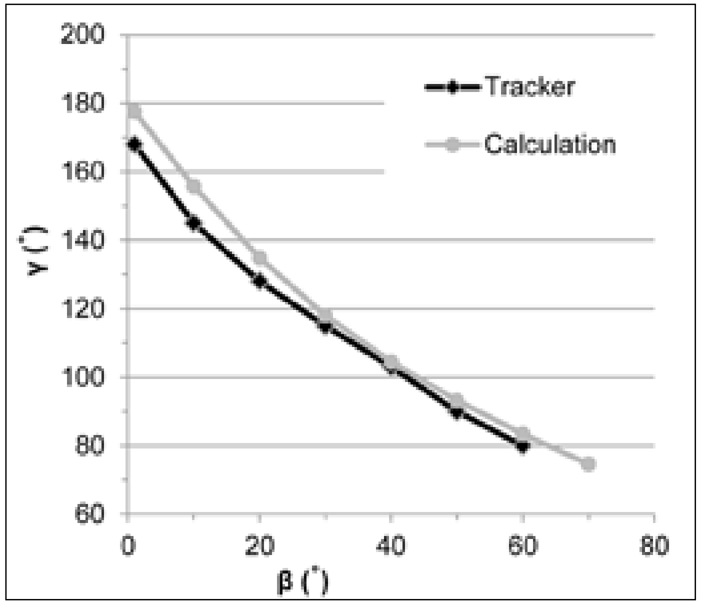

Figure 7.17 Relation between the torsion angel of the clamp head (β) and the torsion angle of the SMA (γ), calculated by the given equations and the results of the tracker.

7.3.2.5 Result and Discussion

7.3.2.5.1 SMA Actuation Force for Forward Deformation from 180° to 90°

In Figure 7.18, the relation between the recovery angle and the delivered force is presented for different programmed angles. The results show that during the recovery of the SMA with a programmed angle of 90° only an angle of 104° has been realized. The SMA did not deliver sufficient force for deformation to 90°. As can be expected, the SMA with a programmed angle of 0° delivered the highest recovery force. Where the curves of the SMA with a programmed angle of 45° and 90° are following a similar slope, the data of the 0° shows some deviations. Especially, in the region between 180 and 160°, the slope of the curve changed considerably in contrast with the other data. This could be attributed to the fact that the cold formed deformation of the 0° SMA strip is considerably large compared to the other SMA strips. The SMA strip with the programmed angle of 0° experienced the largest constrain in the start position compared to the other strips, which might explain the deviation in the large angle region. After 160°, all the curves show similar slopes.

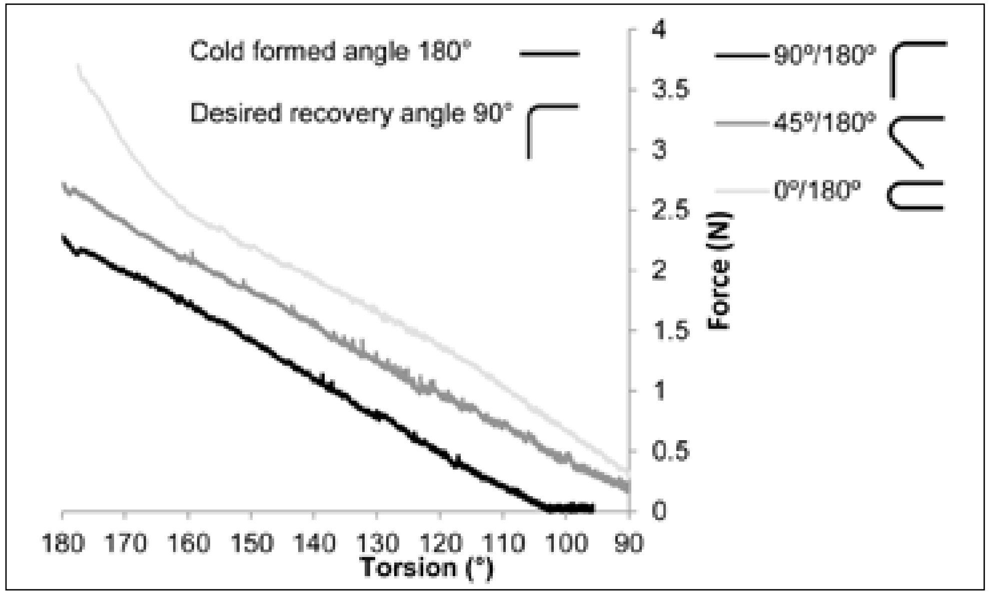

Figure 7.18 Recovery force in austenite condition for the different annealed angles. After cold forming in an angle of 180°, recovery is initiated into the desired 90°. The SMA strips have a thickness of 0.5 mm and a width of 10 mm.

7.3.2.5.2 SMA Fatigue Tests Forward Deformation from 180° to 90°

In Figure 7.19, the recovery is presented for the SMA sample with a programmed angle of 0° for 4 consecutive tests. The results indicate that some fatigue is found during the recovery tests. By the cycling of the SMA sample, the decrease of recovery force between experiment 1 and 4 is 0.4 Newton by 90° torsion. It is considered critical that recovery forces are reducing during cycling of the performance. However, it should be addressed that in the SC prototype, the SMAs are not fully constrained during the performance of the SC. This will lead to higher recovery forces and lower fatigue. The characterization of the SMA fatigue and the relation with the maximum deformation angle and the recovery performance is considered beyond the scope of this research. The obtained data will be used as a prospect of the SMA performance.

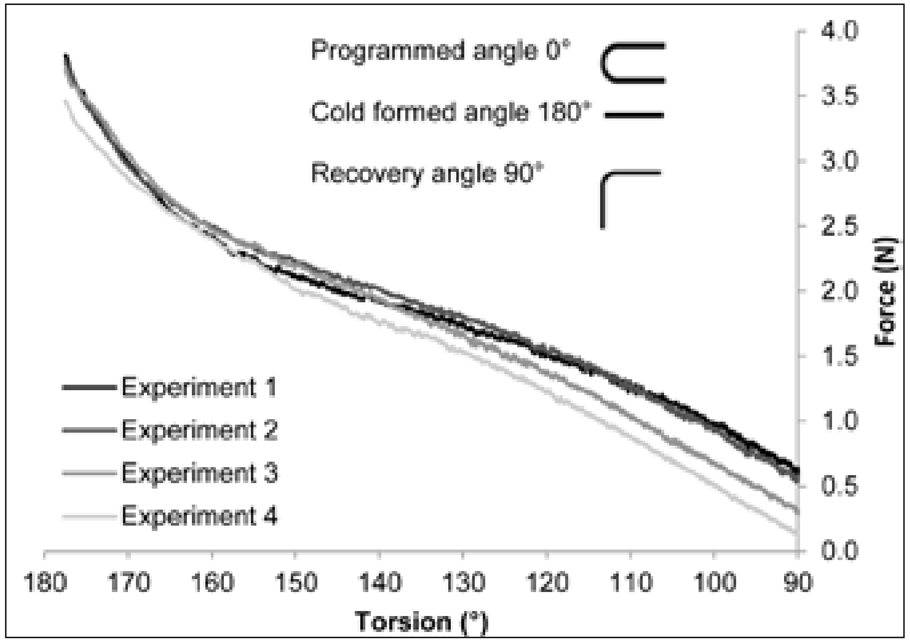

Figure 7.19 Austenite recovery of a SMA strip from 180° to 90° with a programmed angle of 0°. This experiment is repeated four times. SMA thickness is 0.5 mm, width is 10mm.

7.3.2.5.3 SMA Actuation Force for Backward Deformation from 90° to 180°

The recovery force of an SMA strip with a programmed angle of 225° is illustrated in Figure 7.20. The SMA strip is allowed recovery from a start position of 90° to a straight configuration of 180°. The material thickness of the sample is 0.5 mm with a width of 5mm.

In theory, the recovery force should be comparable with the force of a SMA strip with a programmed angle of 45°, initiating a recovery with torsion from 180 to 90°. Both SMA strips initiate a similar recovery path of 225°. In order to verify this, the results of the first cycle of the SMA strip with a programmed angle of 45° recovering from 180 to 90° are presented together with the results of a SMA strip with a programmed angle of 225° recovering from 90 to 180° (Figure 7.21). For this purpose, the data of the SMA strip with a programmed angle of 225° is multiplied by two, since the analysed sample had a width of 5 mm instead of 10 mm. When analysing the results of both experiments, it can be concluded that the curves are indeed close related with a maximum deviation of around 0.4 Newton. Note that the slopes of the curves are different, whereby the curves cross at the point around an angle of 115°. However, the trend and magnitude of both curves are comparable. It is assumed that the force could be multiplied in order to obtain the required force for specific SMA dimensions. This issue is not analysed in depth and the recalculation method is not fully justified. However, based on the obtained results the multiplication of data is acceptable.

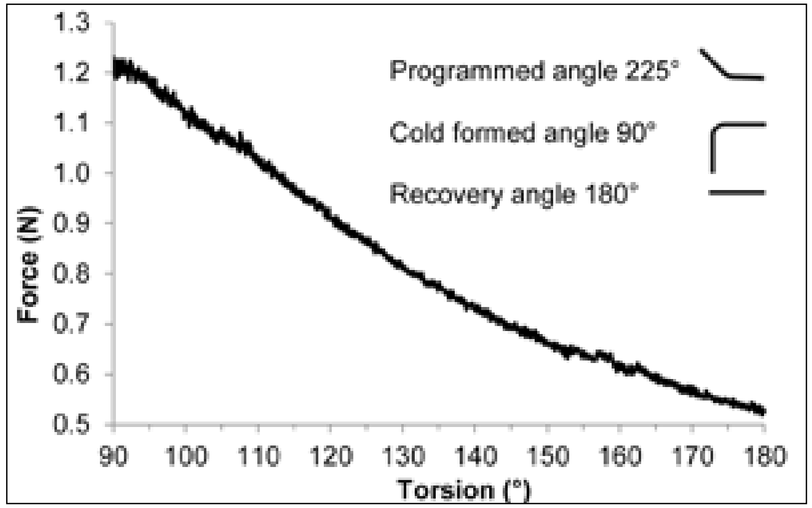

Figure 7.20 Austenite recovery of a SMA strip with a programmed angle of 225° from a start position of 90° into the flat configuration of 180°. The SMA thickness is 0.5 mm and the width 5 mm.

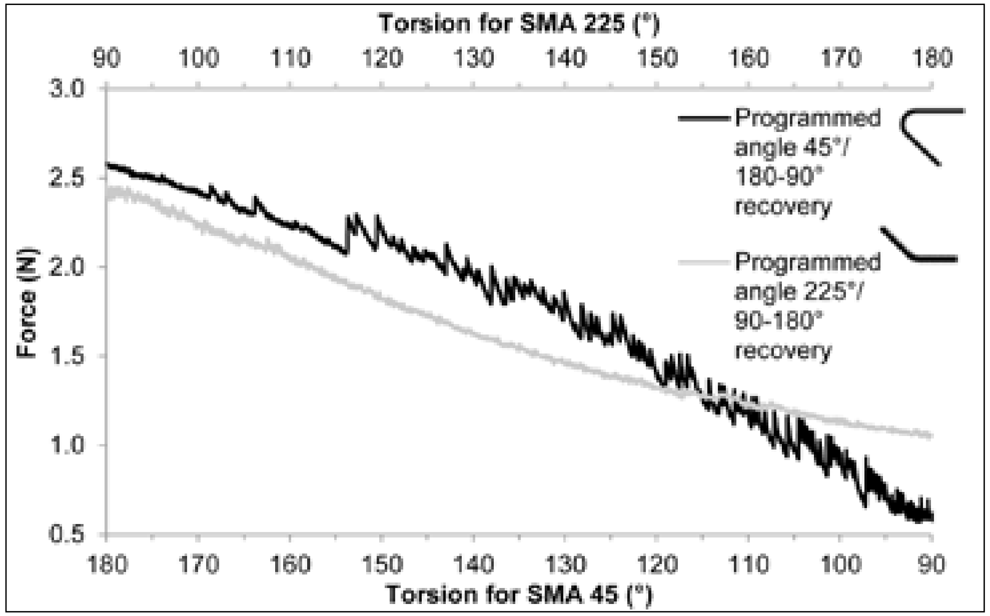

Figure 7.21 Comparison of austenite recovery between SMA with a programmed angle of 45°, recovering torsion of 180 to 90°, and a SMA with a programmed angle of 225°, recovering a torsion of 90° to 180°. Thickness 0.5 mm and width 10 mm.

7.3.3 Cold deformation of the SMA Strip in Martensite Phase

In order to enable the deformation of the SC, the SMA not only needs to deform the SMP but also the antagonist SMA strip. Therefore, it is important to conduct research on the deformation force of the SMA strip in martensite condition. The research method is comparable to the research method of the deformation of the rubber SMP.

7.3.3.1 Research Method

An SMA strip with a thickness of 0.5 mm and a width of 5 mm is placed in the torsion bench in straight configuration. The SMA strip is constrained into an angle of 90°. The programmed angle is 225°. By rotation of the grip head, the SMA strip will be bent along a cylinder with a radius of 15mm. The dimensions of this cylinder are related to the radius of the programmed angle of the SMA strips. The composite will follow this path during deformation. Also here, the data is recalculated in order to obtain the deformed angle of the SMA strips with the related deformation forces. This experiment is executed four times with the same material sample. The median of these experiments is used for further analysis. As this deformation will take place when the SMP is in the rubbery phase, this experiment is performed at a constant temperature of 70°C. This temperature lies well below the determined A_s of 92°C. The rotation is executed with 70° per minute. The research set up is shown in Figure 7.22.

Figure 7.22 Research setup martensite deformation SMA strip

7.3.4 Result and Discussion

The median of the force related torsion of the four experiments is given in Figure 7.23. The increase of the required force with an increasing deformation angle can be addressed to the compression and tension forces at respectively the inside and outside of the material's bending deformation. The increase of inclination around 110° can be attributed to the research setup, since at that point the grip head starts to contact the cylinder. This deviation is also found in the data of the rubbery deformation of the SMP material. This is a disadvantage of the current research setup. Nonetheless, the data gives a good indication of the deformation force of the SMA strip in martensite phase and will therefore be used for further analysis. A correction is made by extrapolating the curve from the large angle area.

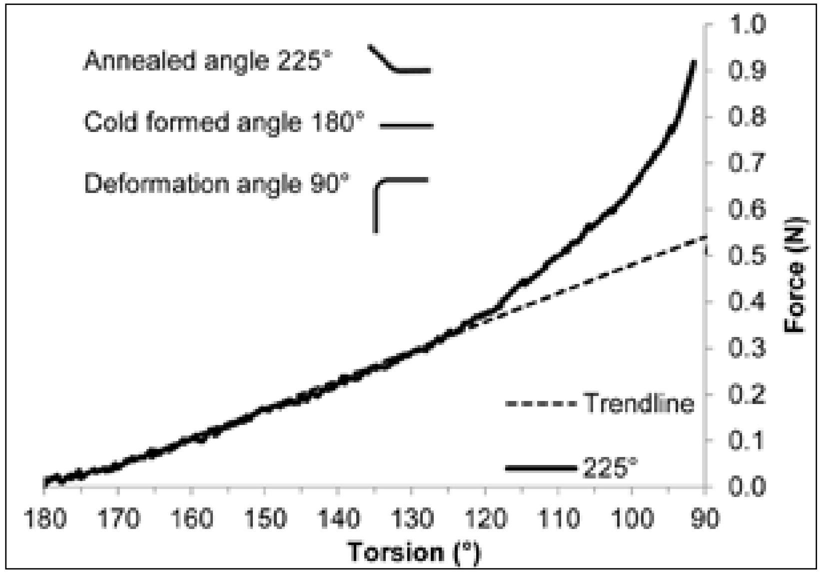

Figure 7.23 Cold deformation of a SMA strip with a thickness of 0.5 mm and a width of 5 mm and an annealed angle of 225°. Deformation is initiated from 180° to 90°.

7.4 Force Analysis of the Composite

By superimposing the data of the individual experiments, an insight can be created of the SC behaviour. First, the deformation from 180° to 90°, the forward deformation, is analysed. Second, the recovery of the SC is analysed from 90° to 180°; the backward deformation.

7.4.1 Forward deformation of the Smart Composite

In Figure 7.24, the deformation force of the SMP in rubber condition and the martensite SMA is given, together with the recovery force of two SMA strips. In theory, the following equation should be true for the deformation of the SC (see also section 7.1):

$$F_{SMA_1} + F_{SMA_3} > F_{SMP} + F_{SMA_2} \quad \text{Equation 7.11}$$

The F_{SMA1} and the F_{SMA3} are shown in Figure 7.24 as the black data line, whereas the F_{SMP} and F_{SMA2} are indicated by the grey data line. The SMA strips performing the hot recovery have a programmed angle of 0°. The third data cycle is used for this analysis. Initially, the SMA actuator forces are much higher (7 Newton) than the force required for the deformation of the antagonist SMA and the polymer (below 1 Newton). However, around an angle of 100°, the required deformation forces of the polymer and antagonist SMA exceed the actuation forces of SMA_{1+3} strips. Based on this graph it can be concluded that the SC will at least reach a bending angle of 100°. The SMA actuators (SMA_1 and SMA_3) do not deliver enough force for deforming both the SMP and SMA_2 into a deformation of 90°. By assembling a composite with components with similar dimensions as tested, the performance of the composite should be comparable with the results in Figure 7.24.

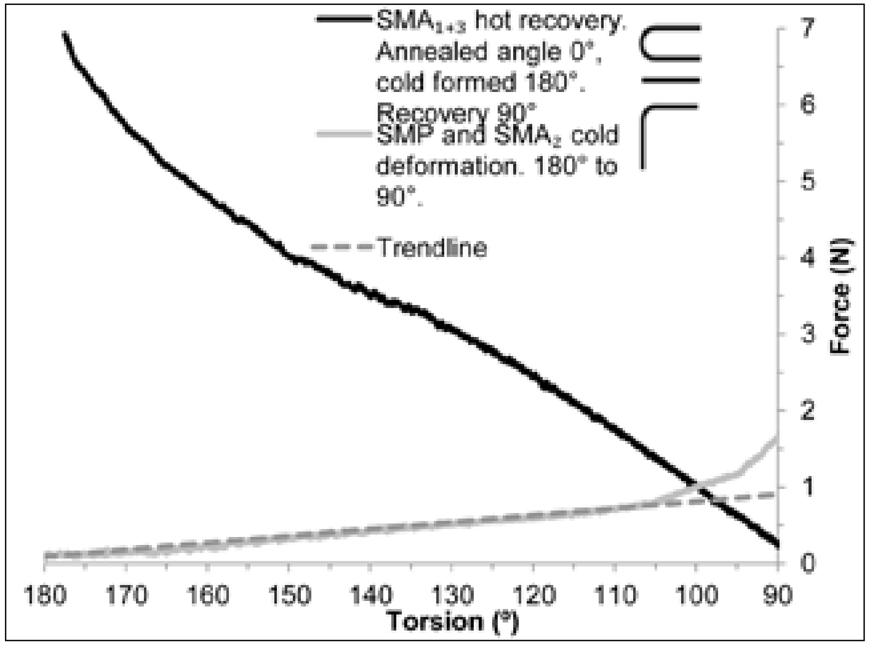

Figure 7.24 SMA deformation from 180 to 90° of two SMA strips with dimensions 0.5*10 mm, together with the sum of the deformation force for SMP in rubbery condition (dimensions: 7*60) and SMA in cold condition (dimensions: 0.5*5 mm).

7.4.2 Backward deformation of the Smart Composite

The experimental data can be used for gaining insight into the performance of the SMA and SMP from 90° to 180° with current dimensions. The two SMA strips which enabled the forward deformation have the following dimensions: 0.5*10 mm (SMA_1 and SMA_3). These strips should now be cold deformed from 90° to 180°. The experimental data of the SMA strip with dimension 0.5*5 are used multiplied by four. The data of the SMA_{1+3} for the cold deformation is recalculated with the data of Figure 7.23.

The austenite recovery data of the SMA strip with dimensions 0.5*5 mm is obtained by torsion testing (Figure 7.20). The recovery performance of the SMP is kept outside this analysis, as the SMP will facilitate only its own recovery. The SMA_2 actuator should therefore only take care of the deformation of the martensite SMA_{1+3} strips from 90° to 180°. In Figure 7.25, the cold deformation of SMA_{1+3} and actuation force of SMA_2 is presented for the recovery from 90° into a flat configuration of 180°. Initially, the actuation force of the SMA_2 strip is sufficient to enable the backward deformation. However, after a 125° recovery, the SMA_{1+3} forces exceed the actuation forces. Based on this data, it can be clearly stated that the current dimensions do not meet the desired performance for a full recovery. In the current condition, a recovery angle of 125° is the maximum recovery. Further study is required in order to improve the recovery characteristics.

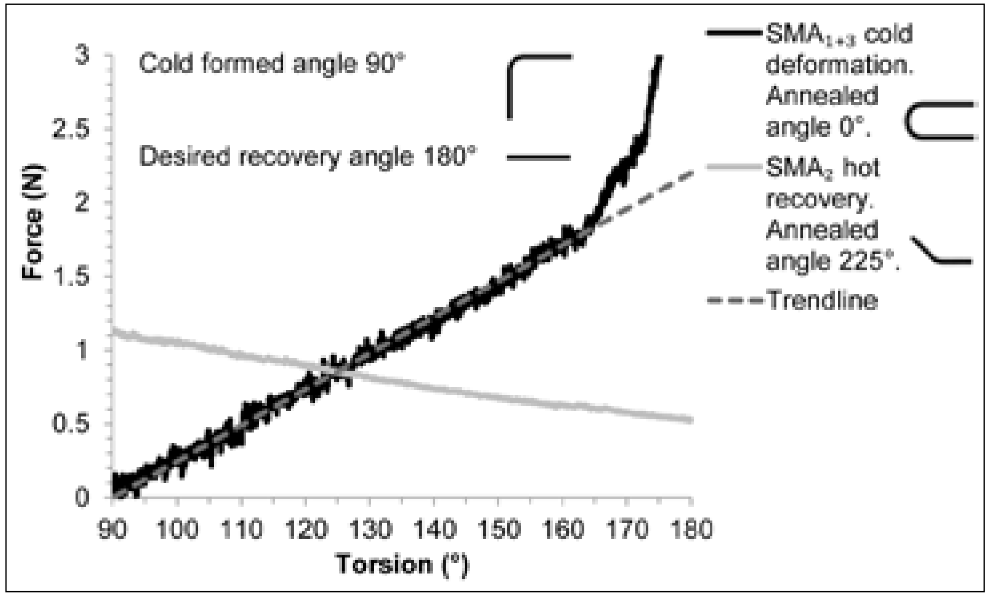

Figure 7.25 The recovery of the SC from 90° to 180° (backward deformation). The SMA_2 strip should deliver sufficient force for the deformation of the cold antagonist SMA_{1+3} strips.

7.5 Manufacturing of the Smart Composite

After the characterization of the individual components, small-scale prototypes are produced for the monitoring of the performance and manufacturing aspects. With this prototype, the predictions based on the experiments of the individual components can be validated.

Different heating methods are used for the analysis of the small scale prototype performance. The uniform heating method is used for the comparison with the data of the individual components. Next to this, the resistive heating method is used in order to analyse the intended operation. Not only is the presented single bending deformation analysed, but also a double bending deformation (Figure 7.26). A prototype is fabricated which enables the deformation on two locations of the composite strip, realizing an s-shaped deformation.

Figure 7.26 Smart Composite that facilitates the deformation at two locations of the component body

The experimental analysis of the SC performance is preceded by the manufacturing process. First, the fabrication and optimization of the SMP matrix is elaborated. Subsequently, the programming of the SMA strips is discussed. This chapter will finalize with the performance of the smart composite.

7.5.1 SMP

The SC consists of a SMP body with the integrated heating system and the embedded SMA strips (see Figure 7.27). In order to obtain the desired dimensions, the SMP is moulded for this specific application. The manufacturing of the SMP body with the integration of the heating wires requires attention. Functionally, the wires should be able to heat the SMP body in order to reach a full rubbery phase. The activation of the wires should be executed without the disturbance of the SC performance. The integration of the wires should also be aesthetically pleasing. Likewise, the integration of the wires should also be practically for manufacturing purposes.

Furthermore, the embedded SMA strips in the SMP matrix will also raise issues for the fabrication of the composite. The threshold temperature of the SMA strips, initiating the recovery, is found close to the temperature range of the SMP curing program. Since the SMA strips are embedded in the SMP matrix under constrain, the SMAs will start recovery during curing. This will result in undesired deformations during the curing process. For this reason it is decided to embed the SMA strips in the matrix after the curing of the SMP resin. This indicates that the SMP body should have small canals where the SMA strips can be embedded after curing. The SMP matrix will be fabricated out of two halves. Spacing for the SMA strips will be obtained by milling the cured SMP. The two SMP elements will then be connected by adhesion bonding. In order to ensure an optimal performance, these elements should be connected without the disturbance of the bending deformation. By conducting tensile experiments, the structural durability of this connection is tested.

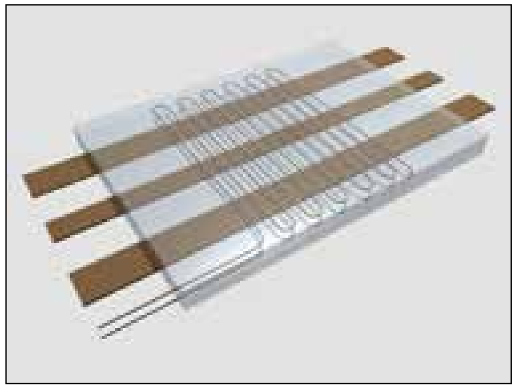

Figure 7.27 Schematic of SC. The SMP body with integrated heating wires and SMA actuators.

7.5.1.1 Casting of SMP

The SMP material is manufactured by casting the SMP resin in a mould. Due to chemical reactiveness of the SMP resin, the mould should preferably be made of glass or aluminium (Figure 7.28). After the casting in the mould, the resin is polymerized by a thermal treatment. The SMP should be cured for 36 hours at 75°C, or ramped to 75°C with 1°C per minute, soaked for 3 hours, then ramped to 90°C in 3 hours and ramped to 110°C in 2 hours (Corner Stone Research Group Industries webpage). Both curing methods give similar material characteristics.

Figure 7.28 Glass mould with cured SMP.

Figure 7.29 Milling of the SMP body.

Due to the shrinkage of the polymer during curing, some irregularities are found at the SMP surface. The SMP surface is equalized by milling the cured polymer (see Figure 7.29). This will ensure an equalized surface for optimized adhesion bonding.

7.5.1.2 Integrated Heating system

A heating system is integrated in the SMP body, which will ensure the heating at the desired bending location. The wires are heated by electric current. In order to prevent any disturbance of the deformation, the wires are configured parallel to the initiated bending direction.

The material *constantan* is used for the activation of the SMP; this material can endure high temperatures, without considerable changes of the material properties. It is possible to integrate the wires during the curing of the SMP.

The SC should be heated uniformly over the bending area. During operation, the temperature around the SMA strips should not exceed the specific transition temperature (A_f). Additionally, the heating time should also not be excessively long. Because of this, the wires are located at the centre of the two separate SMP parts. In Figure 7.30, the principle of the two SMP parts and the integrated heating wires is illustrated. The wires should be aligned accurately in the SMP matrix. Connections between the wires will lead to electric short-circuiting and related temperature peaks.

Figure 7.30 Exploded view SC components

The wires are stretched in the SMP mould before the resin is infused (Figure 7.31 a-b). With this method, the wires are aligned neatly, without connection between the wires. The wires are connected externally after curing and are protected with silicone rubber (Figure 7.32). The external connection of the wires will lead to a higher risk of damage. Additionally, this is not an optimal solution, esthetical as well as practical. However, to test the heating performance of the wires, this manufacturing method is considered relatively fast and simple.

Figure 7.31 a-b First fabrication method of integrated heating wires before casting.

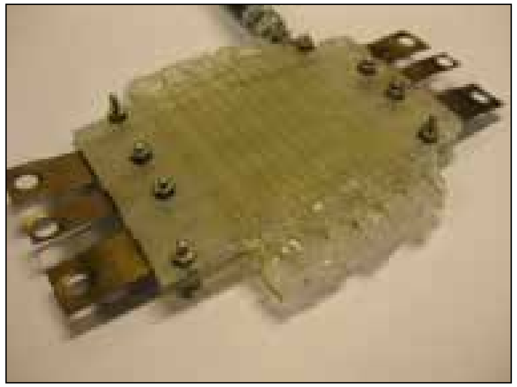

Figure 7.32 SC with externally connected heating wires. Due to the delamination of the SMP, the SMP elements are connected mechanically by the use of bolts. The adhesion problem is discussed in the following paragraph.

In order to realize a full integration of the heating wires without the need of external connections, first one part of the SMP is casted and partly cured until the liquid resin becomes semi-glassy. Then, the wires are glued on the half-cured SMP in undulating pattern (Figure 7.33). Subsequently, the mould is fully filled with SMP resin, integrating the wires in the SMP matrix (Figure 7.34). Lastly, a full curing cycle is run ensuring the full polymerization of the resin.

This fabrication process is considered relatively laborious. The wires are glued by hand and should be positioned precisely. However, functionally and aesthetically, this method gains a considerable advantage. For prototyping purposes, this is acceptable. But improvements are required for further large scale manufacturing.

Figure 7.33 Second fabrication method for the integration of the heating wires in the SMP matrix. First, one part of the SMP is partly cured. Then the wires are glued in the required pattern. Third, the other part of the SMP is casted and the whole SMP is fully cured.

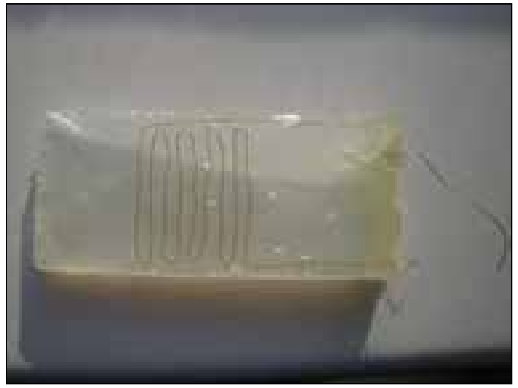

Figure 7.34 SMP with embedded heating wires, some shrinkage marks are visible.

7.5.1.3 Selection of Adhesive

After the milling of the small canals for the embedment of the SMA strips, the two SMP parts are connected by adhesion bonding. During the deformation of the SC, the SMA strips deliver a considerable amount of force on the adhesion bond. In order to prevent delamination, a sufficiently strong connection is required. Since the properties of the SC differ during operation and in fixated position, the adhesion should be able to attain the performance criteria constantly. During operation, the temperature of the SMP will rise above the T_g of 58^{o}C, to a maximum of 90^{o}C. The adhesive should maintain its characteristics during this temperature increase.

Moreover, the adhesion should support the deformation of the SMP without the occurrence of delamination.

The failure of the connection bond is based on three aspects: the strength of the adhesion material, the delamination of the adhesive or the rupture of the material.

After an analysis of adhesion materials, three kinds of glues are selected. A regular Super Glue (Bison) is selected based on its universal performance and transparency. The temperature region of optimum performance is between the 40°C and 80°C. The maximum temperature performance could lead to difficulties. The material is chemically resistant and has fast adhesion capabilities.

Araldite 2015 has a T_g in a similar temperature range as the SMP; between 67-80°C. This indicates that the adhesion will become rubbery during deformation. The adhesion will therefore not disrupt the deformation performance. However, it should be mentioned that the adhesion strength will decrease above the T_g. Araldite 2015 is a two-component adhesion and dries as a colourless pasta.

Araldite 2011, has a T_g in a temperature zone between 65-100°C. Compared to the Araldite 2015, the material has a higher tensile strength in the low temperature zone, but a considerable lower strength at temperatures around 90°C. The adhesion bond will remain yellowish after curing.

7.5.1.3.1 Research Method

The adhesion experiments are performed by tensile testing at a constant temperature of 90°C. This temperature lies well above the T_g of SMP. The experiments are executed with the Zwick/Roell Z005 tensile bench. For the experiment of the force in de direction of the adhesion bond, two hooks are positioned in a sample and will endure tensile forces (Figure 7.35).

The SMP will become rubbery in the high temperature region, which will result in large strains and eventually rupture of the SMP material. Ideally, the SMP material will show rupture before the adhesion connection failures. This will indicate that the connection is stronger than the SMP. The use of angular shaped specimens and tensile arms, will lead to an increase of the SMP rupture. For this reason, the tensile arms and spacing are circular shaped.

The adhesion surfaces connected with the Super glue and Araldite 2011 measure 14 mm by 19 mm and the adhesion surface of the araldite 2015 measures 14 mm by 16 mm. The dimensions differ due to inaccuracy of the manufacturing process. A similar adhesion thickness is ensured by the addition of 10% glass balls to the glue substances. The glass balls have a diameter of 0.1 mm, indicating the thickness of the adhesion bond.

The tensile strength is tested with a vertical displacement of 0.1N per second.

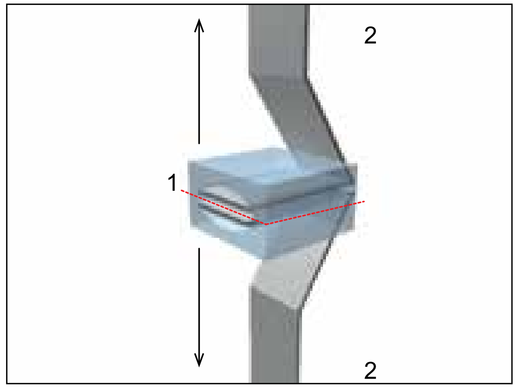

Figure 7.35 Tensile testing of adhesion bond. 1: the SMP sample, where the red line is the connection surface. 2: the hooks enabling tensile in the direction of the arrows.

7.5.1.3.2 Result and Discussion

In Figure 7.36, the results of the tensile experiments are presented with a stress related strain curve. The maximum force capacity of the SMA strip can be used as an indication of the amount of stress executed by the hooks at the adhesion bond. Hereby, the stress is calculated by dividing the maximum force capacity with the bonding surface. This will result in a stress of 0.03 MPa.

The Araldite 2015 shows rupture of the adhesion bonds at a stress of around 0.04 MPa during both experiments (Figure 7.37). This indicates that the adhesion barely meets the standards. Both the super glue and the Araldite 2011 meet tensile values of approximately 0.06 MPa. During the experiments with the Araldite 2011, the adhesion bond shows delamination (Figure 7.38). The experiments with the super glue do not give any indication of delamination, but show rupture of the SMP material (Figure 7.39).

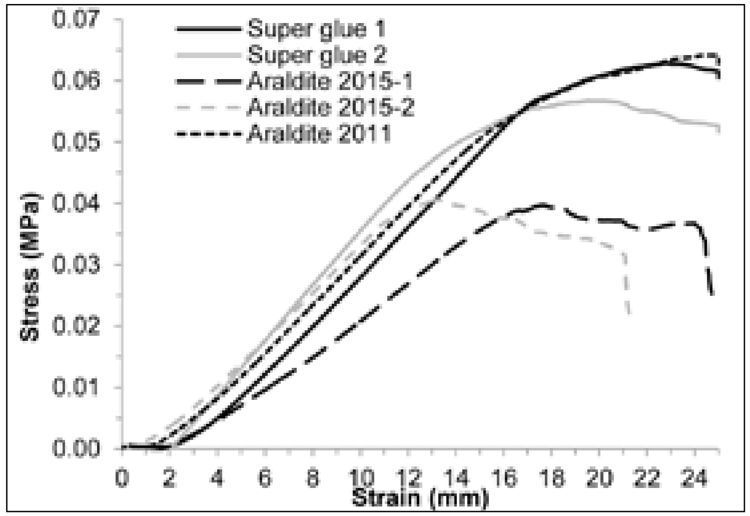

Figure 7.36 Tensile test of adhesion bond of SMP. The testing temperature is 90°.

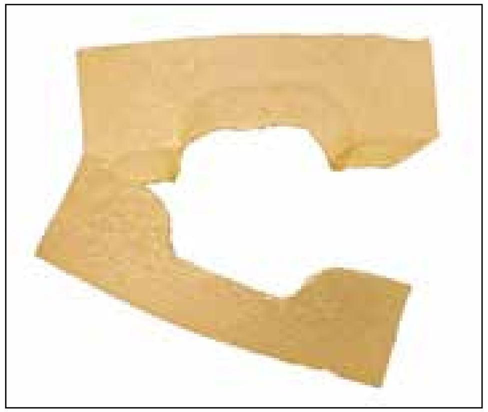

Figure 7.37 SMP specimen. The Araldite 2015 shows rupture of the bonds.

Figure 7.38 Tensile testing with the Zwick/ Roell workbench, failure of the adhesion bond is found during the experiment with the Araldite 2011.

Experimentation with the Super Glue has led to a satisfactory indication that this material will be sufficient for the connection of the SMP material. This material is widely available, transparent and low in costs. Because of this, this adhesion method will be used for further assemblage of the SC.

Figure 7.39 SMP specimen. The super glue gives a strong bond and the SMP ruptures.

Only the elongation forces are considered in these experiments. Other forces such as shear and torsion are not included in this experiment. The encountered forces during these experiments at the bonding surface are related to the SC performance. As the SMP is found in rubber condition during the deformation, aspects such as delamination by peeling delivered by shear stress are difficult to test. Standard peeling tests will lead to more extreme strains on the SMP body and lead to elongation of the material, which prevents the analysis of the adhesion bonding. Even with the current testing method, the rubbery condition of the SMP sample delivered some problems. The large encountered strains on the SMP body led to the stretching of the sample

and eventually, when the adhesion bonding was strong enough, rupture (Figure 7.39). Further experimenting with the SC will determine empirically if the Super Glue is suitable for this application.

7.5.2 SMA

7.5.2.1 Determination of the Annealing Settings

SMAs are manufactured by a well-defined process. The material is vacuum-melted, hot-worked, cold-worked and then heat-treated to achieve the shape memory properties (Hodgson, et al. 2000). When the SMA is cold-worked in martensite state the yield stress[10] increases, but the shape memory properties decrease subsequently. Heat treatment by annealing is required in order to set the shape memory properties and increase the recoverable strains. Annealing will restore the memory effect, but decreases the yield stress considerably (Duerig 1990). The heat treatment cycle is a very critical process. The settings of this process will be determined experimentally.

7.5.2.1.1 Research Method

The annealing settings are determined by the use of a Differential Scanning Calorimeter (Vokoun, et al. 1999). With this instrument, the transition temperatures during thermal treatment can be monitored. The operation of the DSC is explained earlier in this chapter. The thermal behaviour is monitored with the Perkin Elmer DSC 7. When the SMA is not annealed correctly, the temperature related specific heat curve will show some deviations. When annealing at a low temperature, the A_f will decrease and consequently a larger transition area between A_s and A_f will be found. When annealing at a high temperature, the A_f will shift to a higher temperature area.

The SMA samples are annealed for 1200 seconds by 500 and 600°C. After the annealing, the samples are quenched with water at room temperature. The optimum annealing settings can be determined, when a clear peak has been found for the martensite and austenite transition curve. Although the full heating and cooling cycle has been executed, only the results of the heating cycle are used for analysis.

7.5.2.1.2 Result and Discussion

The DSC tests are repeated twice, since after annealing dislocations in the molecule lattice are found (Loughlan, et al. 2002). These defects will stabilize by thermal cycling.

Higher temperatures and heating settings will increase the height of the actuation temperature of the SMA and often deliver a sharper thermal response. However, it should be prevented to heat the SMA above its recrystallization temperature. Heating above the recrystallization temperature will lead to a shift in the transition temperature (Liu, et al. 1997). In Figure 7.40, the DSC results of SMA material with an A_f of 95°C are presented. Here, a shift in the A_f is found when annealing in the high temperature region (600°C).

10. Yield stress is the specific point where the elastic deformation becomes a plastic deformation. After this point, the deformation will become permanent and non-recoverable.

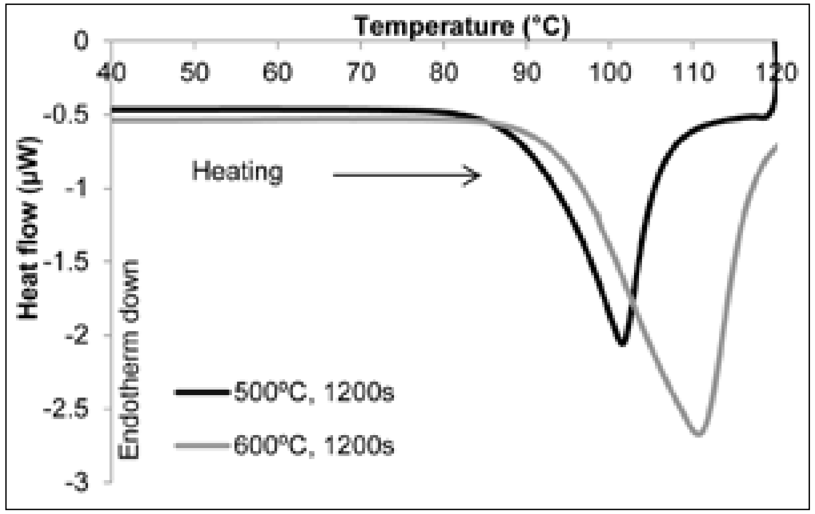

Figure 7.40 Specific heat flow by increasing temperature. The effect of the high temperature annealing can be clearly seen.

It can be concluded from the above graph that annealing temperatures of 500°C with a heating time of 1200 seconds will give good results. Higher temperatures will lead to recrystallization and a shift of the A_f. It should be noted, that during these experiments annealing occurred with small amounts of SMA material. When using moulds for the shape programming, the annealing time should be increased so that the full construction reaches the specific annealing temperature for a sufficiently long time.

7.6 Performance of the Smart composite

In order to gain insight into the performance of the SC, different prototypes have been developed. First, the deformation performance of the SC is tested. A similar test set-up is used as for the experiments of the individual components. The force capacity of the SC will be compared with the deformation results of the individual components. Subsequently, the performance of the SC is analysed by resistive heating. At last, the SC is lengthened in order to meet the deformation of two bending angles in reverse direction; the s-shaped shape deformation.

7.6.1 Deformation Experiments

The deformation performance of the SC is studied for the validation of the deformation predictions based on results of the individual components. A composite prototype has been manufactured with similar dimensions as the material characterization experiments. As these experiments are executed with uniform heating by a heating chamber, this heating method is also used for this experiment. For this reason, the heating wires are not integrated in the SMP body of this prototype.

By using uniform heating for the activation of the SC, it is not possible to embed both antagonist SMA strips. Simultaneous heating of the antagonist SMA strips will lead to conflicting performances. Therefore, only the deformation of the SC from 180° to 90° will be tested. In order to simulate the deformation force of the SMA strips in cold condition, a dummy strip will be embedded in the composite. This dummy strip requires a similar deformation force as the SMA strips. In Figure 7.41, the deformation force of a dummy strip from aluminium material is shown. The deformation force of a SMA strip in cold condition with dimensions 0.5*5 mm, is included for comparison reasons. It should be noted that the dummy strip requires larger dimensions in comparison with the SMA strip to meet corresponding deformation forces. The dummy strip measures a thickness of 0.4 mm and a width of 7 mm, against a thickness of 0.5 mm and a width of 5 mm for the SMA strip. The deformation force of the dummy is presented as the median of the four test cycles of the SMA strip in cold condition.

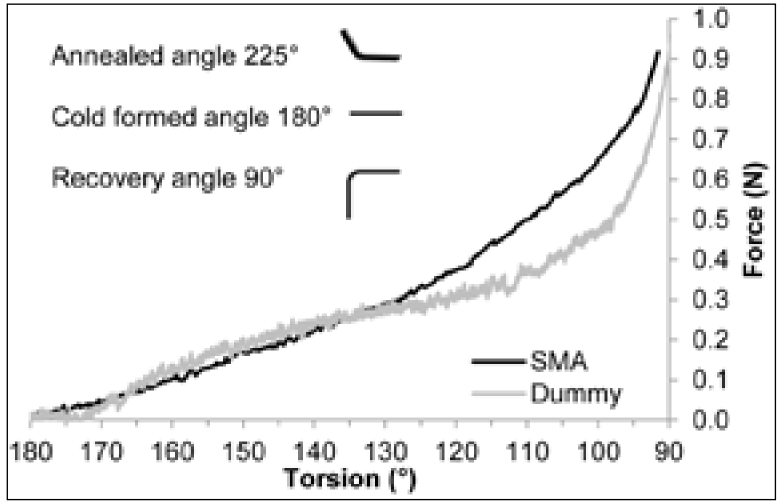

Figure 7.41 Deformation force of the SMA strip with a programmed angle of 225° with a thickness of 0.5 mm and width of 5 mm, together with the deformation force of an aluminium dummy strip with a thickness of 0.4 mm and a width of 7 mm.

7.6.1.1 Research Method

In order to test the torsion performance of the Smart Composite, a similar research set-up has been used as the austenite recovery experiments for the SMA strips. Here, the SC is placed in the torsion bench in straight configuration. Likewise, the SMA strips are placed in the SMP body in straight constrained configuration. The SC is inserted in a heating chamber. The temperature is raised to 110°C, which is considered well above the threshold temperature of the SMA. Following, the SC is allowed a recovery of 70° a minute, until a deformation of 90° is reached. This experiment is repeated four times.

The SMP measures a thickness of 7 mm with a width of 60 mm, the SMA strips are 0.5 mm by 10 mm and the dummy 0.4 mm by 7 mm.

7.6.1.2 Result and Discussion

In Figure 7.42, the results of the deformation of the SC from 180 to 90° are presented. In relation to the hot recovery experiments, also here full constrain is used during experimentation. This will result in a considerable fatigue, which can be concluded from the four data curves. The curves in the torsion region from 180° to 165° do not show coherent performances. This might be explained by the fact that the SMA actuators will initiate recovery, even when the SMP does not meet a full rubbery state. This is a disadvantage of the uniform heating method.

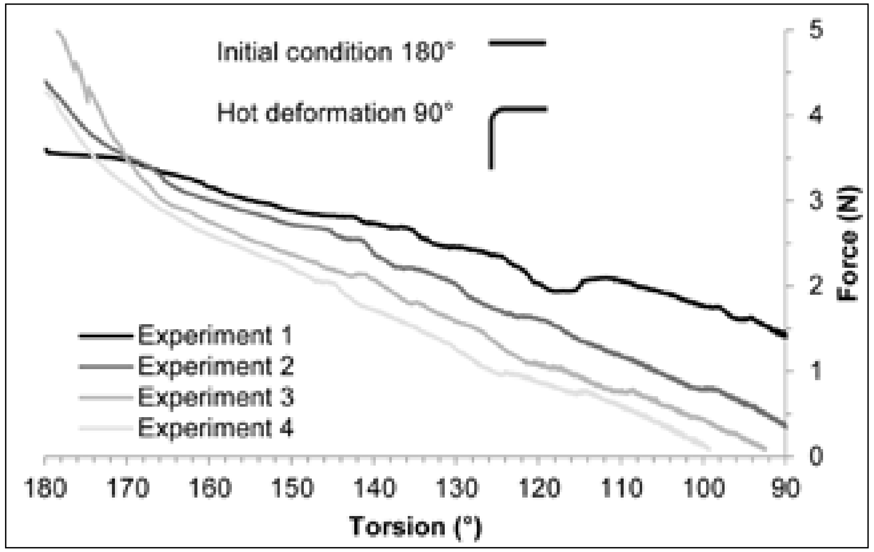

Figure 7.42 SC forward deformation from 180° to 90° with dummy antagonist strip. This experiment is repeated four times.

In Figure 7.43, the results of the composite experiments are compared with the results of the experiments of the individual components. The curve line of the individual components is based on Equation 7.1:

$$\left(F_{SMA_1} + F_{SMA_3}\right) - \left(F_{SMP} + F_{SMA_2}\right) = F_{deformation} \qquad \text{Equation 7.12}$$

F_{SMA1} and F_{SMA3} define the delivered force by hot actuation ($F_{SMA\ def,aust}$) and F_{SMA2} the required force for cold deformation ($F_{SMA\ ant,\ mart}$). In the SC this force is required for the deformation of the aluminium dummy strip. The resulted force should be equal to the force delivered by the Smart Composite.

The trend lines of both curves are plotted in order to give an impression of the obtained data. When comparing these data curves, it can be seen that at the start position a difference of around 2.5 Newton is found. By superposition of all the data of the individual components, aspects such as friction of the SMA strips in the SMP and the fact that the SMA are situated at the centre of the SMP are neglected.

The experimental data of the individual components could be used as an indication of the composite performance, but due to the large differences it is difficult to use this data as an exact guideline. In spite of this, the individual experiments delivered insight of the performance of the materials. Both curves give a similar indication of the deformation angle of 100°. When only focusing on the performance of the SC, this is the actual required information. However, superposition of the data requires more precision and the optimization of the research set-up.

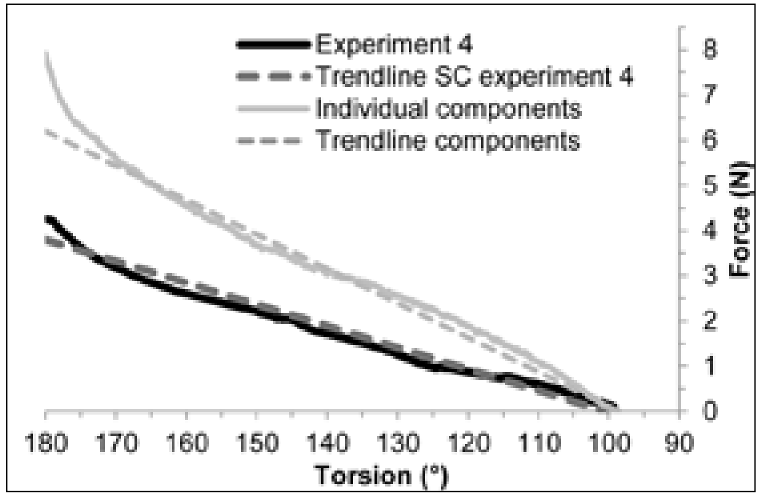

Figure 7.43 Delivered force of the composite for the fourth deformation cycle versus the predicted performance of the individual components, obtained from experimental data. A deformation from 180° to 90° is analysed, only a deformation of 100° has been reached.

7.6.2 Single Bending Performance

7.6.2.1 Version 1

The performance of the composite without maximum constrain is tested with a composite sample with integrated heating wires. The SC is fully activated by resistive heating. The heating wires are connected externally in this prototype. The deformation from 180 to 90° and the subsequent recovery is analysed. The SMP dimensions of this prototype are 7*40*70 mm. SMA_1 and SMA_3 have dimensions of 0.5*10 mm and are annealed in an initial angle of 0°. The dimension of SMA_2 is 0.5*6 mm and is annealed at 360°. The prototype is shown Figure 7.44.

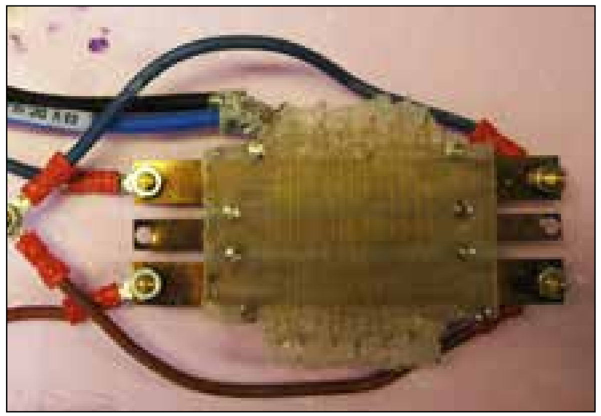

Figure 7.44 SC prototype with externally connected wires and electrical wiring

In Figure 7.45, the forward deformation of the SC is illustrated. During the deformation an angle of 93° has been reached. When the deformation is fixated, the SC recovers into an angle of 110° (see Figure 7.46). This indicates that the control of both the SMP and the SMA strips requires further investigation. The SMP should cool down before the SMA strips are deactivated. The bolts, required for the connection of the electric wires, measured considerable dimensions and weight. It can be argued that the weight of the bolts will add to the recovery before the fixation of the deformation is established. Additionally, the weight of the bolts requires extra deformation force.

Figure 7.45 and Figure 7.46 illustrate the deformation of the first cycle. Figure 7.47 shows the SC data from the first cycle of the torsion experiments. The delivered force of the composite is shown, together with the calculated outcome of the individual tested components. The results of the composite indicate that a 90° deformation is feasible. On the other hand, the results of the individual components only reached an angle of 92°. The performance of the SC is considered in good agreement with results of the experimental data. It should be addressed that during this experiment, the SC is not maximally constrained. Therefore, a larger deformation angle is to be expected. This was not the case, which indicates that other influential parameters played a role here, such as the bolts.

By optimizing the prototype, a deformation of 90° is feasible. The presented performance of the prototype is acquired after one cycle. Presumably, the SMA strips will show significant fatigue upon cycling. However, the performance is expected to improve with the optimization of the prototype.

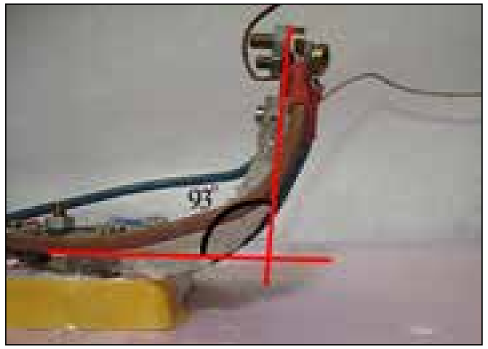

Figure 7.45 Deformation of SC prototype reaches 93°.

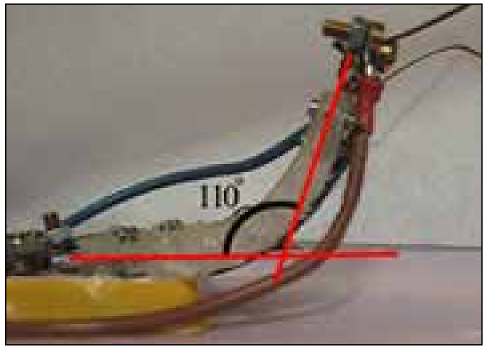

Figure 7.46 The deformation is fixated at an angle of 110°.

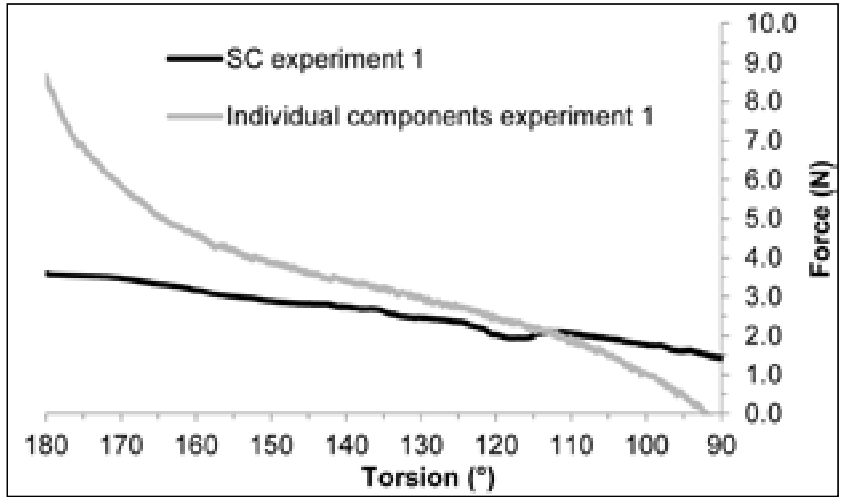

Figure 7.47 Delivered force for the first deformation cycle of the composite versus the predicted performance of the individual components, obtained from experimental data. A deformation from 180° to 90° is analysed. Note that the experiments with the SC obtained a deformation into 90°, whereas the individual components predicted a maximum deformation of 94°.

After the fixation into a 110° angle, the backward deformation has been realized. First the SMP is heated, after which the SMA_2 is activated in order to initiate recovery. A recovery of 165° is established (see Figure 7.48). The experimental data indicated that a recovery could be reached of 125° (see Figure 7.25). In relation to this, a considerable larger recovery is obtained by the prototype. It can be assumed that the bolts might have helped with the downward recovery.

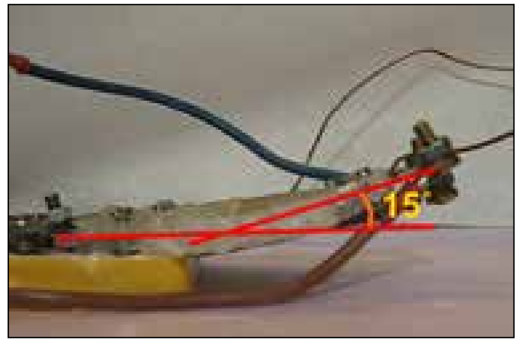

Figure 7.48 A recovery of 165° is established.

7.6.2.2 Version 2

The integration of the heating wires is optimized in prototype version 2. Externally connected heating wires are proven to be very delicate and broke relatively easily. Additionally, in terms of aesthetics full integration of the wires was necessary. In Figure 7.49, the deformation of the prototype is shown. During activation of the SC it is observed that not only the strips facilitating the deformation are activated, but also the antagonist strip initiated recovery. In Figure 7.49, the conflicting behaviour of this situation has been illustrated. Since the SMP body temperature is considered too high, the SMA_2 strip transformed from martensite to austenite phase and recovered to its annealed angle. Further analysis of the control of the SC and the thereby related activation settings is required. In chapter 8, this aspect will be studied further.

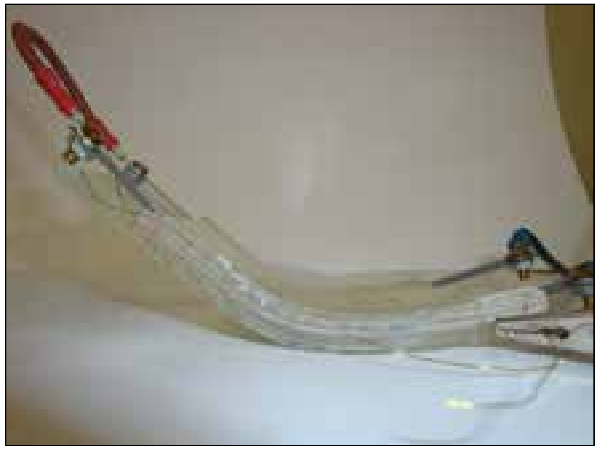

Figure 7.49 Prototype with full integration of heating wires. The SMP is 80*60 mm, the SMAs maintain similar dimensions. A recovery of 135° is reached.

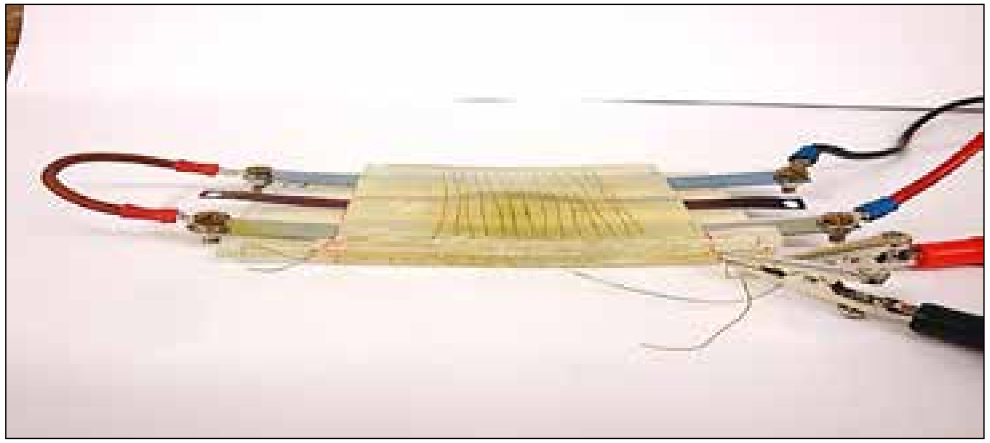

Figure 7.50 SC deformation, the SMP body temperature is considered too high, as the antagonist SMA also start recovering. Image courtesy Eelke Dekker.

7.6.3 Multiple Bending Performance

The application possibility for integrating two bending angles in one prototype is studied empirically. In Figure 7.51, the deformation principle is presented. In general, the prototype is based on the elongation of a single bending deformation. This principle is based on the positioning of the two bending angles in opposite direction. Variation on this principle is possible.

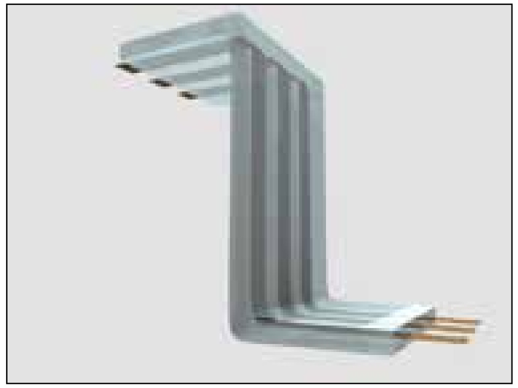

Figure 7.51 SC with two bending angles

The dimensions are similar as the small scale prototype with one-angle bending performance. The SMA strips initiating deformation are programmed in a 0° angle. The SMA strip facilitating recovery is programmed in a 225° angle. The SMP became fully rubbery with the activation of the serial circuited heating wires with values of 2.5 Ampere and 24 Volt. The serial circuited SMA strips are activated with 2.5 Volt and the related 13 Ampere. The SC is clamped at one side, enabling the desired deformation. It should be noted that in this configuration the SMA strips must be able to lift more weight.

In Figure 7.52 the deformation of the prototype is presented. Although two nearly 90° angles are found, not a full deformation is met. The activation of the SMP body and the SMA strips did not meet the correct activation settings. Because of this, the antagonist SMA providing recovery was also activated. A further analysis is required to meet the correct activation standards. Since the antagonist SMA strips encountered activation during the deformation of the SC, recovery of the SC cannot be realized.

Figure 7.52 SC with two-point bending deformation

7.7 Discussion and Conclusion

7.7.1 Experiments

The conducted experiments gave a good insight into the performance of the SC. The experiments with the SC showed that a deformation into a 90° angle can be realized. Additionally, the concurrent recovery to the initial shape is achieved. However, optimization of the prototypes is required in order to fully meet the desired deformation. Although a deformation of 90° has been found, after 3 cycles the SC performance degraded remarkably. Fatigue remains an important aspect for further product development. The large fatigue of the SMA actuator was clear during the experiments with the SC (paragraph 7.6.1.2). The performance of the SC is degraded with 2 Newton after 4 cycles. Optimization is crucial for enabling multiple cycles. The performance of the SC can be optimized when the relation between the different components is analysed. Further research should focus on the relation between the material dimensions and the delivered forces.

An empirical study has been performed on the integration of two bending angles. By connecting two SCs with opposite angles, an s-shaped deformation has been realized. The performance of this prototype gave satisfying results. The s-shaped deformation is reached. However, the 90° angles are not fully met. It should be mentioned that this performance gave a hopeful prospect on the realization of the design scenarios from chapter 4.

The sum of the forces of the individual components did not correspond with the delivered force of the SC. This could be attributed to the differences between the experimental set-up and the method of application. The SMA strips were not fully covering the entire width of the SMP body. The SMP body should be fully deformed, even though the SMA strips are only located at the outside edges. This required different deformation forces compared to the tested forces. During the experiments, it was assumed that the deformation force was delivered over the entire surface of the SMP. In practice, the SMA strips delivered a different kind of deformation. Not only point force, but torque over the entire length of the SMA strip. This difference of deformation may explain the disturbances in performance. Although some deviations are found between the experiments with the individual components and the SC, the order of magnitude was correct. When comparing the fourth deformation cycle, the sum of the individual components and the SC gave a similar prospect of the obtained deformation angle. It should be noted that the ultimate goal of these experiments is to gain knowledge of the deformation angle and concurrent recovery. For these parameters the experiments were very valuable.

Based on the experimentation and the prototype study, it could be stated that the desired performance of the SC is realistic. However, optimization in terms of fatigue and dimensions is required.

7.7.2 Fabrication

With the proposed fabrication process it is very well possible to manufacture a functional prototype. The conceptual performance of the SC is translated into a prototype which realized the deformation and the subsequent recovery. The fabrication of the SC is a laborious process, but it did enable the realization of an optimal performing prototype. The heating wires were able to heat the SMP body, into a fully rubbery state. Additionally, the resistive heating of the SMA strips did meet the intended performance. However, during the heating of the SMP body, the general temperature did exceed the A_s. This initiated the recovery of the SMA strips. This behaviour is undesirable, as this will prevent the concurrent recovery of the SC. This aspect will be studied further in the following chapter.

The SMA strips are activated by electric wiring, which are connected to the strips by bolts. Although this is considered a safe activation method, this does obstruct the optimal performance of the SC considerably. Preferably, the SC should deform freely, and must therefore be activated only at one edge of the SC.

7.7.3 General

It is vital to develop a numerical model that can simulate the behaviour of the SC. With this model, the performance of the SC can be optimized. The relation between the SMA dimensions and the force capacity should be determined in order to establish the best SMA performance. Additionally, the deformation force of the SMP in rubbery phase as well as of the SMA in martensite phase and the relation with variable dimensions are issues of interest. When including parameters such as slip and shear, a reliable model can be made. This model could then be used as a design tool for the application of the SC on architectural scale. This model will contribute to the understanding and optimization of the SC with smart material technology.

The development of this design tool is outside the scope of this research. This research is performed from a designer point of view. By crossing the border to material experimentation, an inquiry is made of the material performance. However, further research should be performed on a more fundamental level. Here, collaboration between material specialist and the designer is crucial.

7.8 References

Corner Stone Research Group Industries (webpage) Retrieved 2008-07-09 from www.crg-industries.com.

Duerig, T. W. (1990). Engineering Aspects of Shape Memory Alloys, London, Butterworth-Heinemann.

Hodgson, D. and Russell, S. (2000). “Nitinol melting, manufacture and fabrication.” Minimally Invasive Therapy & Allied Technologies **9**(2): 61-65.

Liu, Y., Van Humbeeck, J., et al. (1997). “Some Aspects of the Properties of NiTi Shape Memory Alloy.” Journal of Alloys and Compounds **247**(1-2): 115-121.

Loughlan, J., Thompson, S. P., et al. (2002). “Buckling control using embedded shape memory actuators and the utilisation of smart technology in future aerospace platforms.” Composite Structures **58**(3): 319-347.

Menard, K. P. (1999). Dynamic Mechanical Analysis a Practical Introduction. Boca Raton, CRC Press.

Vokoun, D. and Stalmans, R. (1999). Recovery Stresses Generated by NiTi Shape Memory Wires. Smart Structures and Materials 1999: Mathematics and Control in Smart Structures, Newport Beach, CA, USA, SPIE.

CHAPTER 8

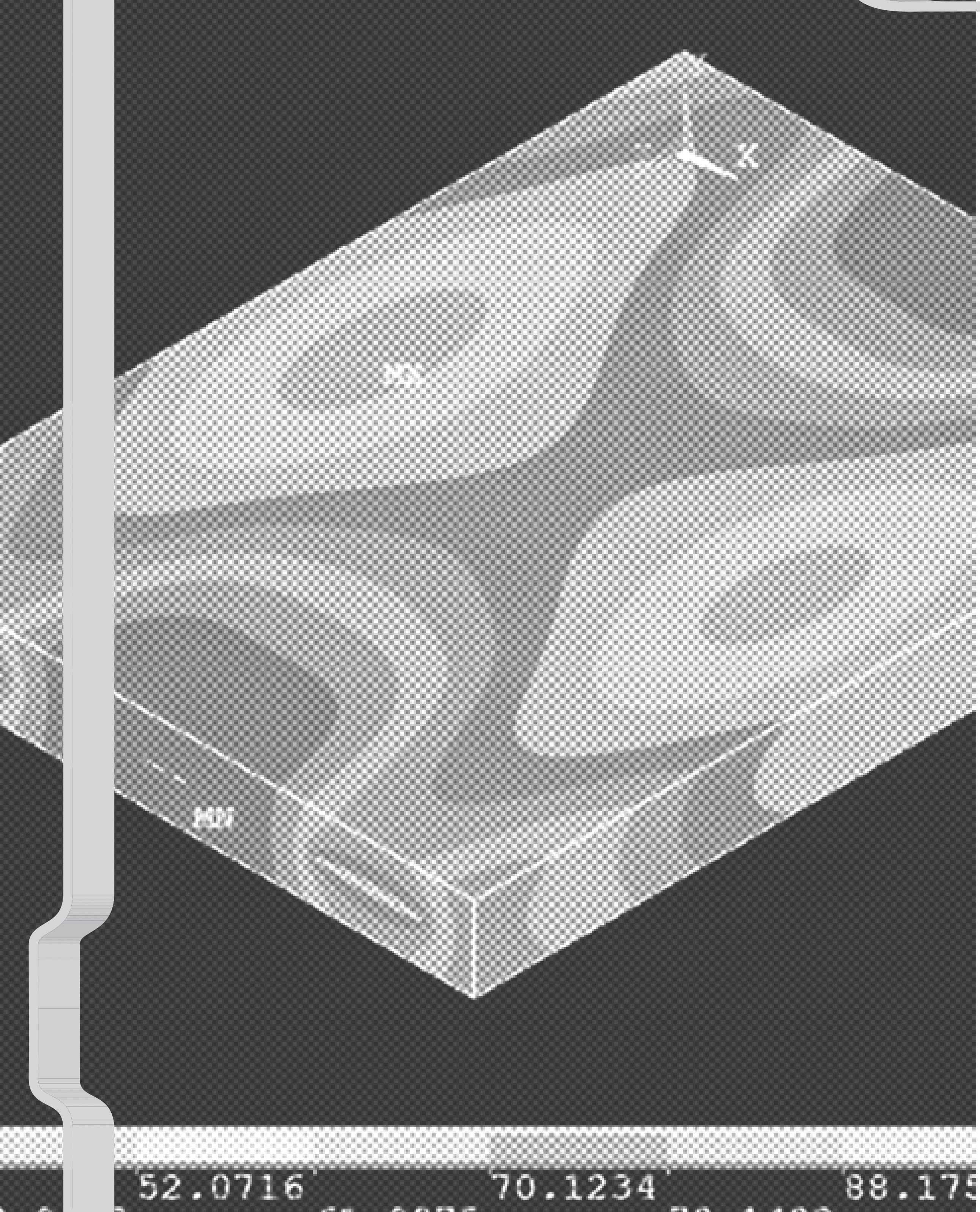

THERMAL CHARACTERIZATION AND MODELING OF THE SMART COMPOSITE

8.1 Introduction

The shape deformation of the smart composite is controlled by thermoelectric activation. As explained previously in chapter 7, the smart composite structure studied in this thesis consists of three SMA strips embedded in a SMP matrix. Heating the two outer strips (Number 1 and 3 in Figure 8.1) causes bending, whereas heating of the antagonist strip (Number 2 in Figure 8.1) will initiate recovery of the strip into the flat starting position. During these deformations, the polymer matrix is softened by embedded heating wires, presented as number 4 in Figure 8.1. It is clear that for proper operation the timing of the activation and the chosen heating powers are crucial in order to prevent simultaneous activation of the materials. It is of great importance that the SMA strips should not be activated before the SMP is fully rubbery. Due to the large force delivery of the SMA strips, the brittle SMP will show cracking when not fully transformed into rubber condition. Whereas during heating of SMA_3, the antagonist SMA strips should remain in the low temperature phase. Simultaneous activation will lead to undesirable performances of the composite.

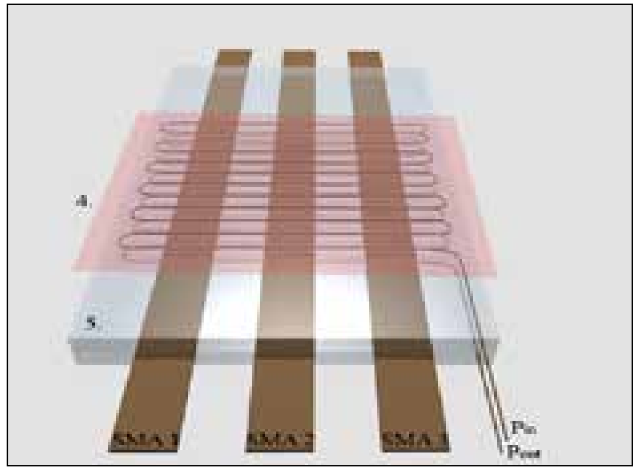

Figure 8.1 Schematic layout of smart composite, where SMA 1 and 3 indicate the strips providing bending deformation, SMA 2 is the antagonist SMA strip enabling recovery, number 4 is the heating zone of the SMA body (5) with embedded constantan heating wires. P_{in} represent the constantan wires located at the top layer of the SMP matrix, whereas P_{out} indicate the constantan wires located at the lower SMP layer.

Particular attention has to be drawn to the optimization of the activation parameters, such as current, potential and heating time. In order to determine an optimized control strategy, a finite element model[11] (FEM) of the smart composite is created. With this model, the thermal heating is simulated during activation of the smart composite. This is of particular importance since the finite element model can be used as a tool for determining the actuation parameters for different composite configurations (scales and compositions).

Validation experiments are conducted with a thermal imager in order to create

11. Finite Element Method (FEM) is used for numeric approximation of complex calculations. By dividing the structure in many small elements the problem is simplified.

reliable simulations of the thermoelectric behaviour of the composite. Therefore, the surface temperatures predicted with the FEM will be compared to temperature measurements from the experiments. In that way, both the modelling of the thermal activation of the SMP by heating wires and the SMA strips could be validated. The thermal performance can be analysed and adjusted in order to meet the optimal activation settings.

This chapter describes the finite element model simulation, experimentation and validation of the activation settings of the Smart Composite. Additionally, the optimal activation settings will be determined using the finite element model. The activation parameters such as time and electrical power input will be determined. As it is only required to activate the SMP in the area where the bending occurs, the heating wires are only located in this area (Number 4 in Figure 8.1).

8.2 Material Properties and Dimensions

The activation parameters of the SMA and SMP materials are determined in chapter 7. The SMA will initiate recovery above a temperature of 92°C. The SMP body temperature should thus remain below 92°C in order to prevent the activation of the SMA. The SMP will become fully rubbery above a temperature of 58°. In Figure 8.2, a schematic cross-section of the Smart Composite (SC) is presented. In this schematic, the temperature requirements are presented per component.

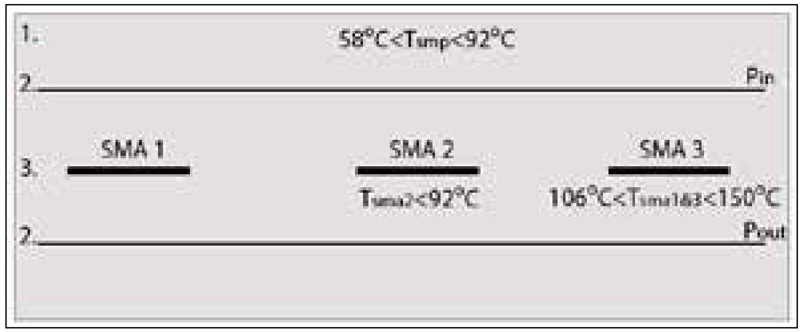

Figure 8.2 Schematic cross section of smart composite with the thermal requirements for the specific components. Number 1 is the SMP body, which required a minimum temperature of 58°C and should not exceed 92°C to prevent activation of the SMA strips. Number 2 represents the integrated heating wires for the activation of the SMP. Number 3 shows the SMA strips, which should locally reach a minimum temperature of 106°C for activation, the antagonist SMA should not be activated and should therefore be kept below 92°C.

The following parameters need to be defined:

1. The electric power and activation time for the activation of the heating wires. The SMP body temperature should at least reach a temperature of 58°C. The temperature around the antagonist SMA strips should be kept below the A_s of 92°C.
2. The required electric power and activating time of the SMA strips to achieve the A_f temperature of 106°C in the SMA strip. The SMA body temperature should remain below 150°C.

The electric power and the activation time are coupled activation settings. With higher power values, lower heating times are required in order to meet the activation parameters and vice versa. For the fixation of the deformed smart composite, the SMP should regain its stiffness before the SMA can be deactivated.

Both the FEM model and the thermal imager will deliver temperature data along the full surface for each moment in time. The amount of data is reduced by the selection of three representative points of interest, which presumably will encounter the highest influence of the thermal activation. One point is located at the centre of the heating zone and right above SMA_2. Two points are located at the sides of the smart composite, right above the SMA_1 and SMA_3 strips, as is illustrated in Figure 8.3. The points are located at the top surface of the SMP body.

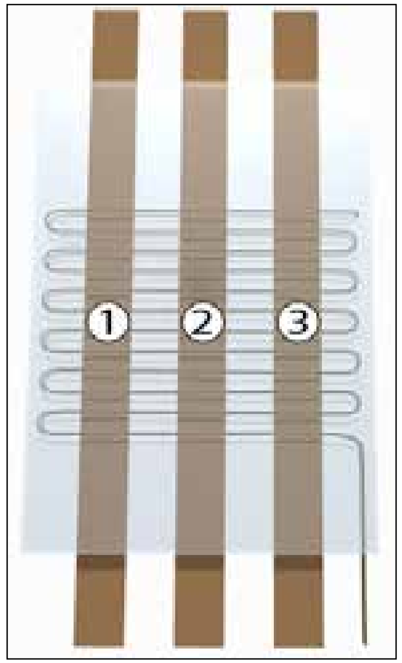

Figure 8.3 Schematic of smart composite with three data points; 1 left, 2 middle, 3 right.

The SMP used in this research project is from the Corner Stone Research Group (Corner Stone Research Group Industries webpage). This SMP is a thermoset styrene-based monomer. Thermoset styrene-based SMPs show good a performance in terms of shape recovery, shape fixation, and fatigue (Leng, et al. 2011). The SMP is cast from a two component resin, where one component (benzyl peroxide) is used as a hardener. The heating wires are constantan wires, from Isabellenheutte Heusler. The SMAs are provided by Memory Metalle (Memory Metalle GmbH webpage).

The material properties are given in Table 8.1; these have been provided by the material supplier or acquired from materials with similar characteristics. An important consequence of the phase transition of the SMA strips is the thermal dependency of the material properties. The SMA supplier provides different values for the elasticity modulus in austenite and the martensite phase.

For the SMP, only the thermal conductivity was provided by the supplier. Therefore, material data for the density and heat capacity was used of a polystyrene material with similar material characteristics. From the temperature dependent material property graphs it can be concluded that the thermal conductivity is hardly temperature dependent, whereas the specific heat capacity shows considerable changes in relation to temperature. Hence, temperature dependent specific heat data is used.

Table 8.1 Material properties of the smart composite components

Property	Unit	SMP		$SMA_{martensite}$	$SMA_{austenite}$	Constantan
Thermal conductivity	W/mK	0.17 [12]		9 [13]	18 [13]	22 [14]
Density	kg/m^3	1050 [15]		6450 [13]		8900 [14]
Specific heat capacity	J/kgK	25°C	1300 [15]	322 [16]		$0.41\cdot10^3$ [14]
		50°C	1400			
		62°C	1870			
		95°C	1900			
		200°C	2243			
Specific electric resistivity	Ωm	$10\cdot10^{14}$ [15]		$50\cdot10^{-8}$ [13]	$110\cdot10^{-8}$ [13]	$0.49\cdot10^{-6}$ [17]

The dimensions of the smart composite are related to the physical prototype and are presented in Table 8.2.

Table 8.2 Dimensions of smart composite materials

Dimension	Unit	SMP	SMA_{1+2}	SMA_3	Constantan
Length	m	$8\cdot10^{-2}$	$1.6\cdot10^{-1}$	$8\cdot10^{-2}$	1.50
Width	m	$6\cdot10^{-2}$	$1\cdot10^{-2}$	$5\cdot10^{-3}$	$R=1.25\cdot10^{-4}$
Height	m	$8\cdot10^{-3}$	$5\cdot10^{-4}$	$5\cdot10^{-4}$	
Cross section Area	m^2	$4.8\cdot10^{-4}$	$5\cdot10^{-6}$	$2.5\cdot10^{-6}$	$4.9\cdot10^{-8}$
Volume	m^3	$3.8\cdot10^{-5}$	$8\cdot10^{-7}$	$2\cdot10^{-7}$	$7.4\cdot10^{-8}$

8.3 Estimation of Required Heating Power

8.3.1 Required Heating Power of SMP

In order to obtain a first idea of the required power input of the heating wires and SMA strips, a rough estimation is made below.

The formula of heat generation is used for this estimation:

Equation 8.1

$$E = P * t = m * C_p * \Delta T$$

Where E indicates the energy in Joule (J), P the power in Watt (W), t time in seconds (s), m mass in kilograms (kg), C_p the specific heat capacity (J/kgK) and ΔT the temperature difference, T_x-T_0 (°C).

The initial temperature (T_0) of the smart composite is 25°C and the heating wires (T_{hw}) must reach at least a temperature of 58°C. This results in a temperature difference (ΔT) of 33°C. The mass of the SMP can be calculated by the use of the data from Table 8.1 and Table 8.2 and is $4\cdot10^{-2}$ kg. A specific heat capacity of 1400 J/kgK is used in this calculation. When applying Equation 8.1, energy of at least 1848 Joule is required to heat the SMP body to the desired temperature. This energy should be delivered by the heating for the activation of the SMP. The desired heating time of the SMP body is estimated between 60 and 300 seconds. This is considered a realistic heating time in terms of usage and operation of the SC. Within this timespan, the full SMP body should meet the transformation temperature. This means that the power generation of the wires should be between 31 and 6 Watt (Equation 8.1). The required electric potential can be calculated by the use of Joule's law.

Equation 8.2

$$P = \frac{V^2}{R}$$

P is the power in Watt (W), V the electric potential in Volt (V) and R the resistance in Ohm (Ω).

The resistance of the heating wires is calculated with:

Equation 8.3

$$R = \rho \frac{l}{A}$$

In this equation, l is the length in meters (m), A the cross-section area in square meters (m^2) and ρ the resistivity in ohm*meter (Ωm). When using the data of Table 8.1 and Table 8.2, a resistance of 15Ω is calculated for the wires.

An electric potential between 9.5 and 22 Volts is required in order to meet the desired heating times. For the validation of the numerical model three different activation inputs will be tested. Based on the calculated electric potentials, the validation experiments will be executed with activation inputs of 10, 15 and 20 Volt. The related current and power values can be calculated using Ohm's law.

Equation 8.4

$$U = IR$$

In Table 8.3, the heating settings for the wires are calculated by a resistance of 15Ω.

Table 8.3 Calculated current and power settings for heating wires

Potential (V)	Current (A)	Power (W)
10	0.66	6.6
15	1	15
20	1.33	26.6

8.3.2 Required Heating Power of SMA strips

In relation to the calculation described above, the activation settings for the

12. (Corner Stone Research Group Industries webpage).
13. (Memory Metalle GmbH webpage).
14. (Verkerk, et al. 1992).
15. (Moore 1989).
16. (TiNi Alloy Company webpage).
17. (Conrad Electronic webpage).

simultaneous activation of the SMA 1 and 3 strips are determined. As is discussed earlier, an intended activation temperature (T_{sma}) of 106˚C is required for the realization of a full phase transformation of the SMA strips. The mass for both SMA_1 and SMA_3 is $5.16 \cdot 10^{-3}$kg is calculated with the dimensions of Table 8.2.

The surrounding polymer can now be regarded as an insulation material and only the heat capacity and mass of these SMA strips are taken into account. Using the given Equation 8.1, with a specific heat capacity of 322 J/kgK in combination with a ΔT of 81˚C; a specified energy of 135 Joule is required for the heating of the SMA strips. This results in a required power of 2.25 Watt for a temperature increase within 60 seconds. When a resistance of 0.016 Ω and 0.035 Ω is calculated for respectively the austenite and martensite phase, 12 Ampere is required for martensite activation and 8 Ampere is required for austenite activation. In relation to this outcome, the SMA activation settings are determined to be 10, 12 and 15 Ampere. In Table 8.4, the activation settings are listed for all experiments.

Table 8.4 Overview experiments with activated component and desired activation setting.

Experiment	Activated component	Activation setting
1	Heating wires	10 Volt
2	Heating wires	15 Volt
3	Heating wires	20 Volt
4	SMA strips	10 Ampere
5	SMA strips	12 Ampere
6	SMA strips	15 Ampere
7	Heating wires & SMA strips	15 Volt/ 12 Ampere

8.4 Thermoelectric Experiments

The thermal performance of the physical prototype can be evaluated with thermal imaging by infrared detection. The Fluke thermal imager, Ti55 IR flexcam, with a 10.5 mm lens is used for this analysis (see Figure 8.4). The infrared camera captures the frequency of radiation at the surface of the prototype. This information is transferred to data which presents temperature variations in degree Celsius on the surface of the prototype. An important characteristic of this camera is the ability to capture a sequence of images over time. This enables the implementation of a time dependent temperature model.

Figure 8.4 Fluke thermal imager, Ti55 IR flexcam. Image courtesy by Fluke.

Although the fluke thermal image file contains time data with a second of accuracy, due to technical limitations it is not possible to transfer this time data with the related transfer software (SmartView 3.1). The capturing sequence is set to be every second, but because of automatic calibration of the camera during the capturing process, the time between the images ranges between one to three seconds. It should be pointed out that this will lead to irregularities with the actual time and limits an accurate time dependent thermal model. This is solved by determining the activation times of the experiments after every experiment and use similar times for the simulation, enabling the comparison of the data.

An emission value of 0.9 is calculated with the following equation (Thirumaleshwar 2006):

$$1/\varepsilon_{res} = 1/\varepsilon_1 + 1/\varepsilon_2 - 1 \quad \textbf{Equation 8.5}$$

ε_{res} is the resulting emission coefficient, ε_1 the emission coefficient of the material (0.95)[18] and ε_2 the emission coefficient of air (0.95). Emission defines the ratio of radiation emitted by a body in relation to the emission of radiation by a black body. A value of 0.9 indicates that the material is 90% efficient in emitting thermal radiation.

The data output of the thermal imager delivers the x and y coordinates of every pixel and the related temperature. In Figure 8.5, an example of a thermal image is presented. Here, the heating area can be clearly observed. The location of the three validation points is marked (A). As the heating wires are activated at the short side of the prototype (point B), a heating trail between the activation point and the dedicated heating area is visible.

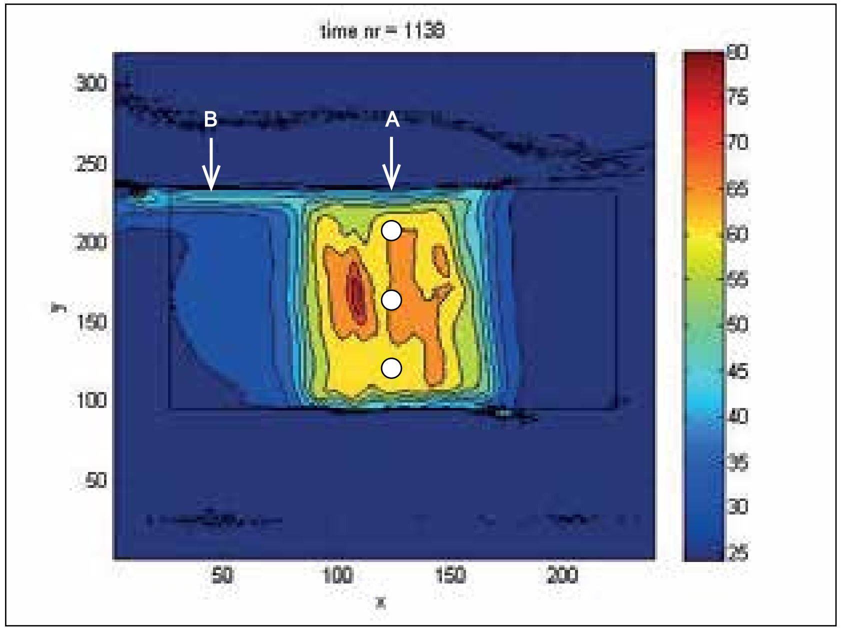

Figure 8.5 Temperature capture of thermal imager, the white dots indicate the data points (A), B indicates the point of activation. Image of sample 1 with activation setting of 15V at t=120s.

18. The emission coefficient is based on the thermal emission of the polymer material.

8.4.1 Research Method

The specimen is clamped in a setting in such way that free convection and radiation around the specimen is possible (see Figure 8.6). The experiments are carried out at ambient temperatures of approximately 24 to 25°C. It is important to note that the ambient temperature is slightly raised after every experiment. Therefore, a cooling time of at least 15 minutes is set between every experiment.

Experiments are subsequently performed with the embedded constantan wires and the SMA strips. After the camera is turned on, the heating elements are activated with the predefined activation settings. When the power supply is turned off, the cooling phase of the specimen is captured so the cooling curve could be analysed. Not every cooling curve is measured for every heating setting.

Four different specimens are manufactured. However, specimen 2 experienced a defect of the heating wires, which prevented a proper activation. This defect illustrates the delicate structure of the heating wires.

In order to acquire a good understanding of the thermal behaviour, the thermoelectric activation of the heating wires and the SMA strips are tested separately. For the final use of the smart composite, first the heating wires will be activated followed by the heating of the SMA strips. In order to validate the numerical model for the intended use, the final experiment is performed with the activation of both the heating wires and the SMA strips, successively.

The thermal performance of the prototype for the activation of the heating wires is tested for every specimen with the settings of 10, 15 and 20 Volt. Subsequently, the temperature is captured during the activation of the SMA strips. The two SMA strips which will provide the bending deformation are connected in series and activated with 10, 12.2 and 15 Ampere. The SMA strips are straight annealed preventing any deformation.

For comparison, the experiments with the activation of the constantan heating wires are executed with three different samples. The experiments with the SMAs are executed with one sample only.

Figure 8.6 Research set-up of the thermoelectric activation of the SMP

8.4.2 Results

In Table 8.5, an overview is given of the different activation settings for each sample. Experiments 1 to 3 consider the activation of the constantan wires. Experiments 4 to 6 cover the SMAs activation settings. During experiment 7, first the constantan wires are activated for 156 seconds, followed by the activation of the SMA strips for 410 second. The electric potential of experiment 4 to 7 is an estimation, as the resistance of the SMA is temperature dependent and leads to variable values along the heating cycle. The values are read from the variable power supply, but were constantly fluctuating. The average of this fluctuation is used in this table. Note that some heating settings are not round numbers, but for example, 10.1 V or 12.2 A. This is due to the variable power supply that is controlled manually.

Table 8.5 Activation settings for validation experiments including related heating time. Experiment 1-3 refer to the activation of the heating wires, experiment 4-6 to the activation of the SMA strips, experiment 7 the activation of both components. Activation setting such as 10.1 V and 12.2 A are used due to the manual control of the variable power supply.

Exp	Activated component	Sample 1		Heating time	Sample 3		Heating time	Sample 4		Heating time
		V	A	s	V	A	s	V	A	s
1	wires	10.1	0.62	506	10	0.62	506	10	0.62	470
2	wires	15	0.93	460	15	0.94	420	15	0.94	454
3	wires	19.5	1.22	280	20	1.24	280	20	1.26	540
4	SMA				~0.86	10	942			
5	SMA				~1.21	12.2	208			
6	SMA				~1.43	15	210			
7	wires				15	0.94	154			
	SMA				~1.23	12.1	254			

8.4.2.1 Activation of the Heating Wires

In Figure 8.7a-h the heating cycle of sample 1 is shown during the activation of the constantan wires by an electric potential of U=15 Volts. These images are generated by the thermal imager. The images indicate an inhomogeneous temperature in the heating region related to the positioning of the heating wires. The difference in temperature right above the heating wire and in between the wires is typically about 19˚C. Between 30 and 240 second the surface temperature increases from approximately 55˚C to 103˚C with activation settings of 15 Volts and 0.93 Ampere.

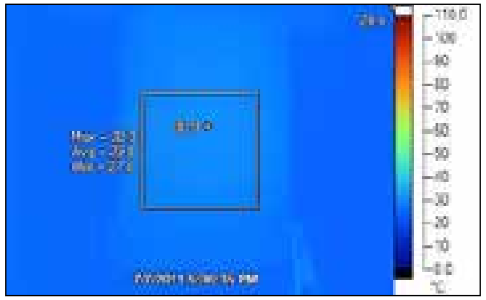

Figure 8.7a Thermal image activation constantan, U=15V t=0s

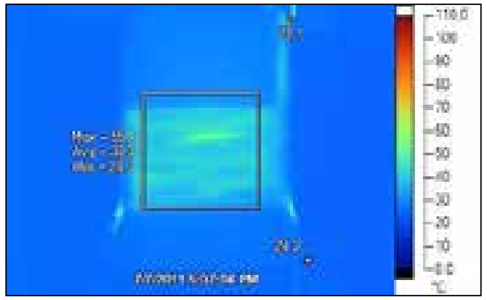

Figure 8.7b Thermal image t=30s

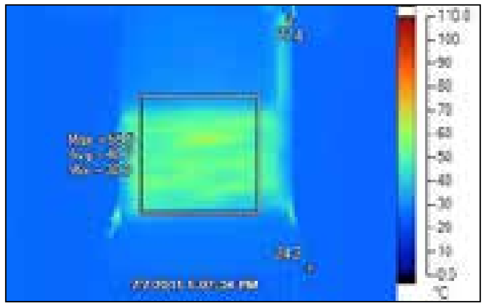

Figure 8.7c t=60s

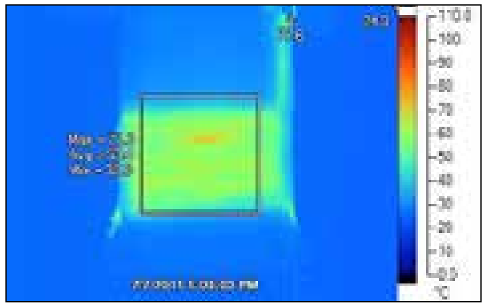

Figure 8.7d t=90s

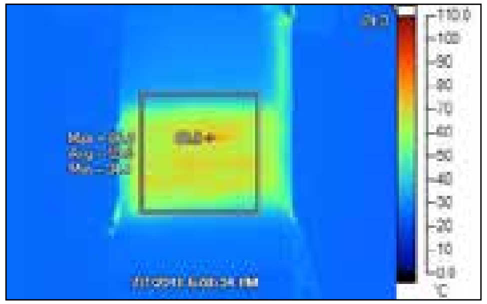

Figure 8.7e t=120s

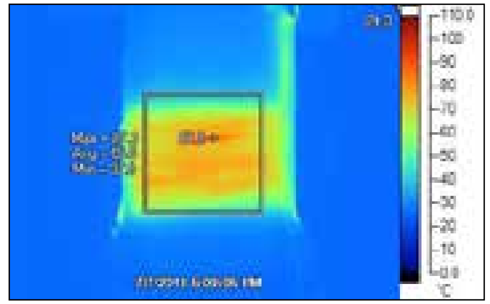

Figure 8.7f t=150s

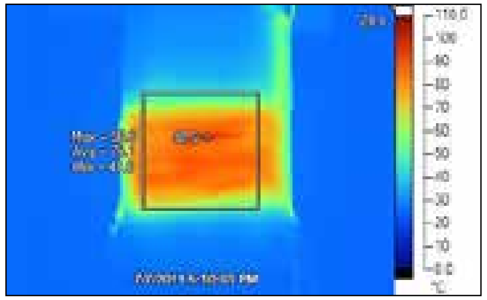

Figure 8.7g t=210s

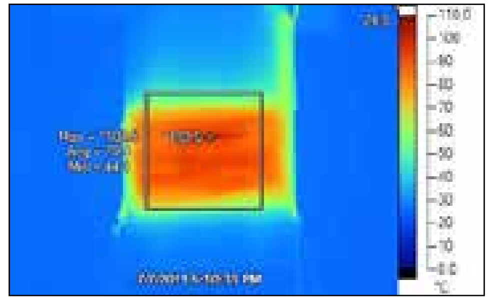

Figure 8.7h t=240s

In Figure 8.8a-c, the experimental results of all three samples are shown for the activation of the constantan wires with 15 Volt. The temperatures of the three data points are shown separately in the different figures; in Figure 8.8a, the data of the outer left point is given, in Figure 8.8b the data of the midpoint and in Figure 8.8c the data of the outer right point. A difference can be found between the surface temperatures of the different samples during the activation of the heating wires. When analysing the data of the left points (Figure 8.8a), it can be clearly seen that the temperature difference between sample 3 and 4 at the left side is negligible at t=400 seconds, but the difference between sample 1 and 4 is 6.7˚C. Whereas in Figure 8.8b (midpoint) the difference in temperature at t=400 seconds increases with 16.4˚C between sample 1 and 4, and 7.6˚C between sample 3 and 4. In Figure 8.8c (right point), a similar temperature difference is found. The temperatures of sample 3 and 4 are more related and again a higher temperature difference is found between sample 1 and sample 3 and 4.

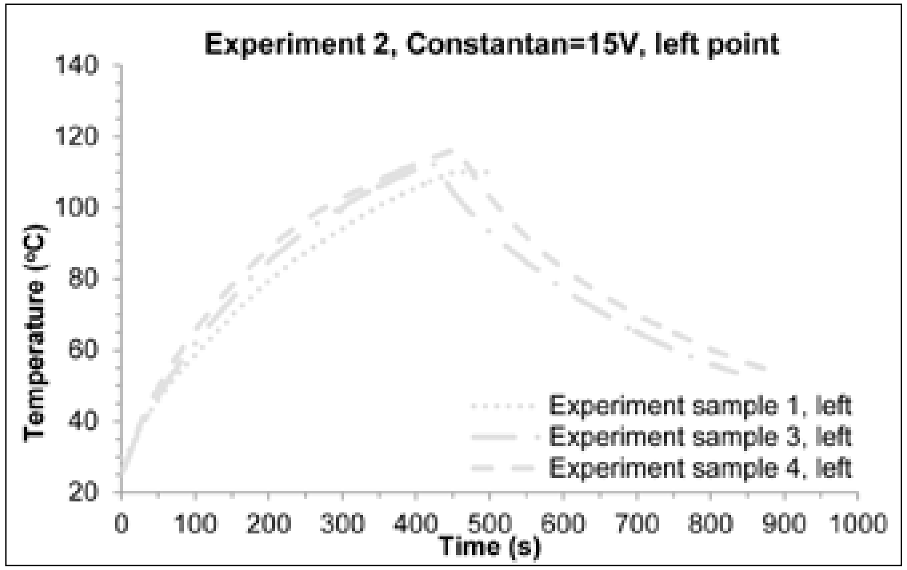

Figure 8.8a Temperature versus time for an activation setting of 15V, data of left (1) points of sample 1, 3 and 4.

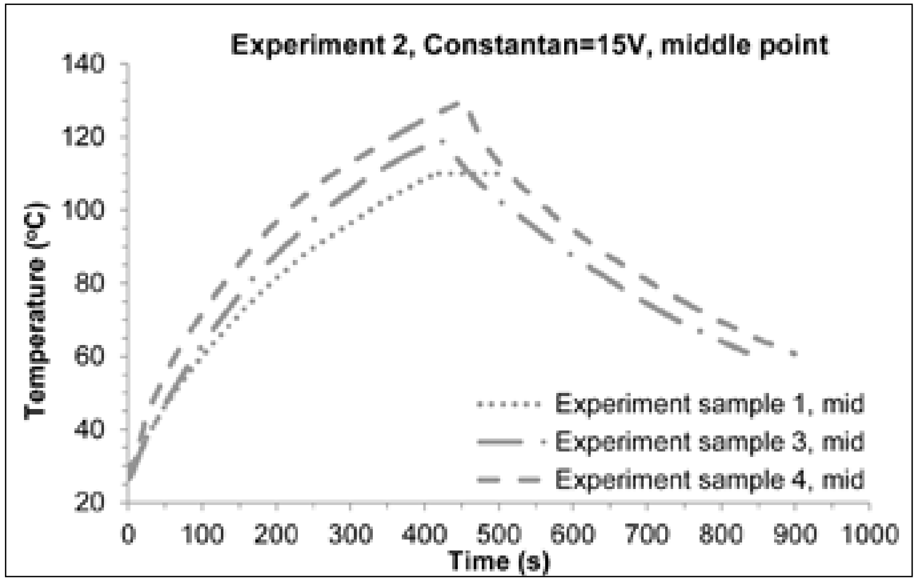

Figure 8.8b Temperature versus time for an activation value of 15V, middle (2) data points

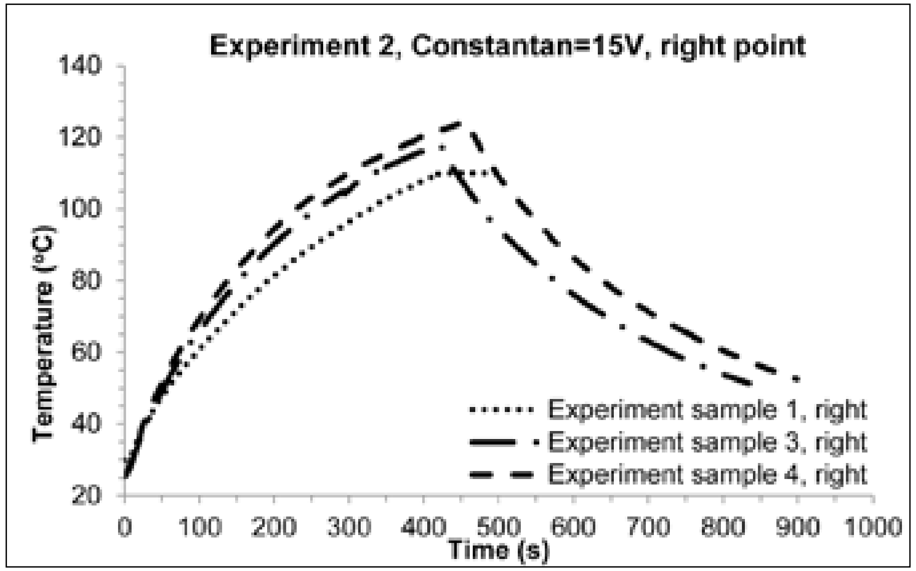

Figure 8.8c Temperature versus time for an activation value of 15V, right (3) data points

In theory, the temperatures of the left and right data points should be similar for each sample, however it can be concluded that is not the case (Figure 8.9). The difference between the left and right data point in sample 1 is 2.4˚C, as the differences in sample 3 and 4 are 5.5˚C and 7.8˚C respectively. The discrepancy is increasing at higher temperatures. On the SMP surface considerable temperature differences can be found. This can be illustrated by comparing all the data points for sample 2 (Figure 8.9). A maximum temperature difference of 7.5°C is found between the left and the midpoint

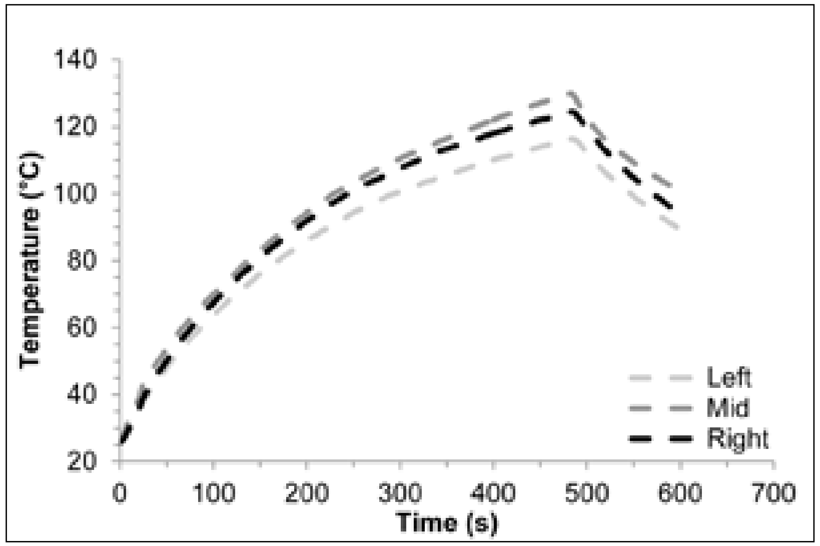

Figure 8.9 Data experiment 2, sample 4: constantan is activated with 15 Volt.

The location of the data points has an arbitrary character. A small shift of the data point may lead to different data output. In Figure 8.10, the temperature differences are shown when the data points are moved by a few millimetres. Temperature variations of about 4°C are found. As is shown earlier, the considerably large temperature variations can be attributed to the heating method. The heating wires provide high temperatures locally, instead of a homogenous body temperature. The poor conductive characteristic of the SMP prevents a proportional temperature distribution. When analysing the previous given results in Figure 8.8, the deviations between the data points are of a similar order. Further analysis of these three points is unnecessary. The deviation is recognized. For further analysis of the activation settings, only the midpoints are used for validation purposes during the activation of the heating wires.

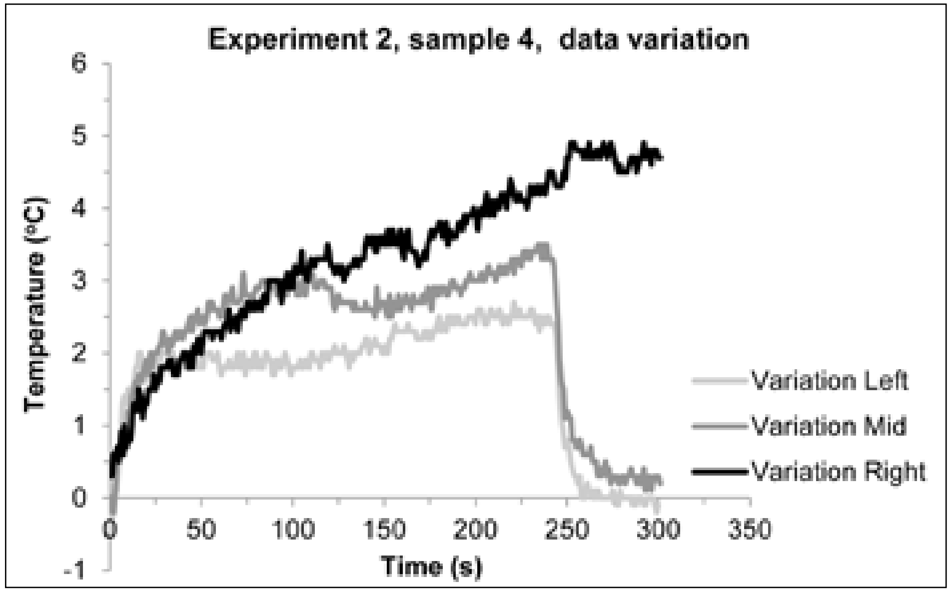

Figure 8.10 Temperature variation between three data points over time for experiment 2, sample 4. Note that the maximum temperature difference is only 5°C.

In Figure 8.11 and Figure 8.12, the data of respectively experiment 1 (heating wires activation with 10 Volt) and experiment 3 (heating wires activation with 20 Volt) are shown. The results indicate that the differences between the temperature data of the different samples increase with increasing electrical potential. The maximum temperature difference between the midpoints of samples 1 and 4 is 16.4°C. In experiment 3, a maximum temperature difference of 28.8˚C is found at the midpoint values between sample 1 and 4. The temperature curve of sample 3 and 4 are much more related.

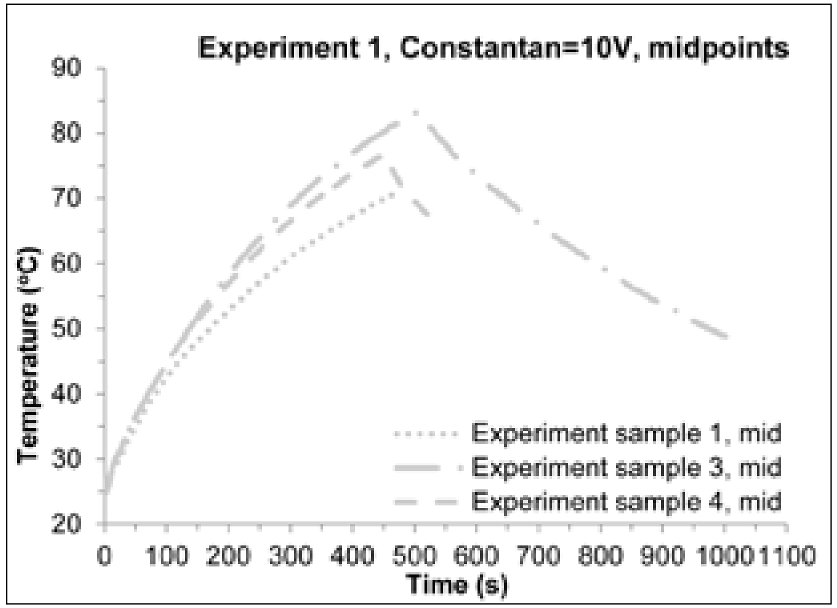

Figure 8.11 Temperature versus time for an activation value of 10V, middle data points.

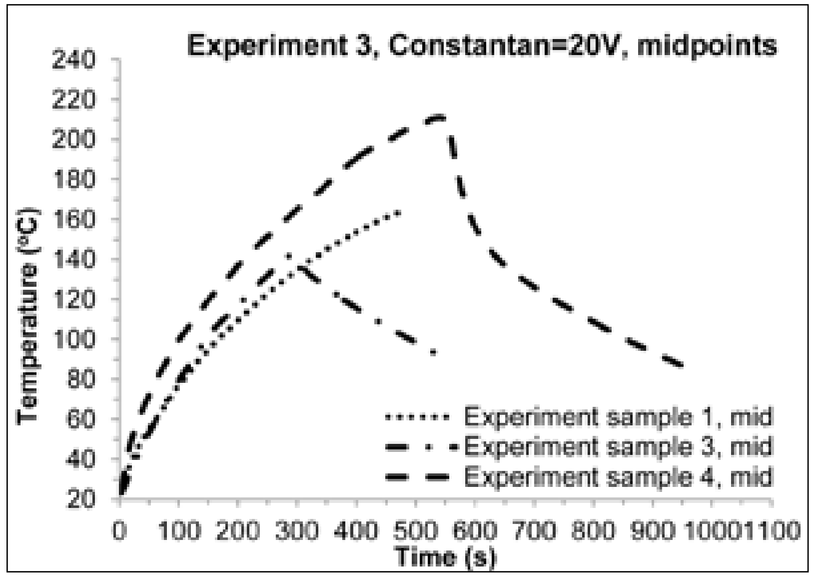

Figure 8.12 Temperature versus time for an activation value of 20V, middle data points.

In Table 8.6, an overview is given of the required heating time to reach a SMP temperature of 75˚C. The experimental results of the three samples are presented together with the analytical estimation. The required time to heat the SMP body to 75°C is determined analytically by the use of Equation 8.1. When comparing the heating time of the experimental data and the analytical estimation, some differences are found. In general, the results indicate that longer heating times are required during the experiments compared to the analytical estimation. However, the heating times of sample 4 during experiments 2 and 3 are very close to the analytical estimation.

Table 8.6 Required time to heat the SMP surface to 75ºC for experiment 1 to 3. The experimental results of the three samples are shown together with the analytical estimation.

Experiment	Estimation	Sample 1	Sample 3	Sample 4
1	199 s	-	372 s	418 s
2	87 s	168 s	157 s	111 s
3	49 s	96 s	89 s	54 s

8.4.2.2 Activation of the SMA Strips

In contrast to the validation experiments with the heating wires, the experiments with the SMA strips are limited to one sample. In the previous experiments a clear indication of the large temperature differences between the samples is noted. Therefore, the results of only one sample will be analysed subsequently for the validation of the thermal performance. Sample 3 will be used for further analysis. The purpose of these experiments is the validation of the numerical model.

Some thermographs of the heating cycle of the SMA strips are shown in Figure 8.13a to h. Sample 3 is activated with a current of 15 Ampere and a potential of approximately 1.43 Volts. The low conductivity properties of the SMP are demonstrated by the temperature discrepancy of the SMP and SMA surface. Especially, at the location of the connection bolts (red colour) high temperatures are reached. The bolts have a temperature of 114.6°C after 120 seconds of activation. By a similar heating time of the SMA strips, the SMP surface temperature reached an average temperature of 40˚C. Even after 200 seconds the overall SMP surface temperature does not exceed 55˚C. Also note the energy dissipation near the electrical connections.

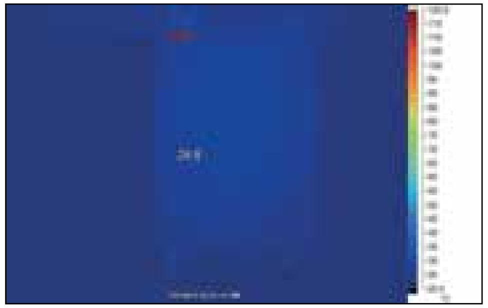

Figure 8.13 Thermograph SMA activation I=15A t=0s

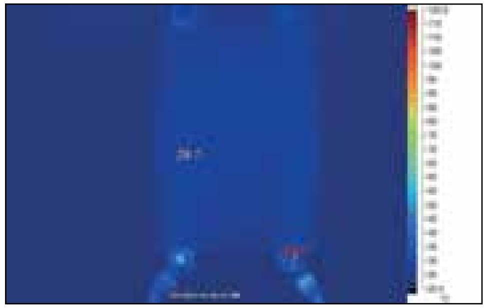

Figure 8.13b t=30s

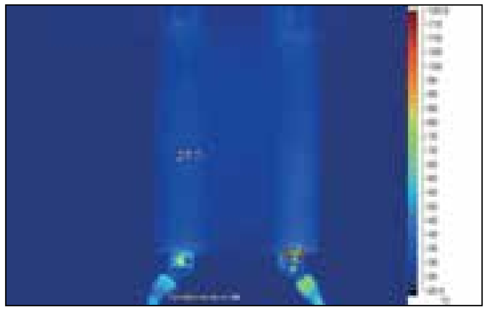

Figure 8.13c t=60s

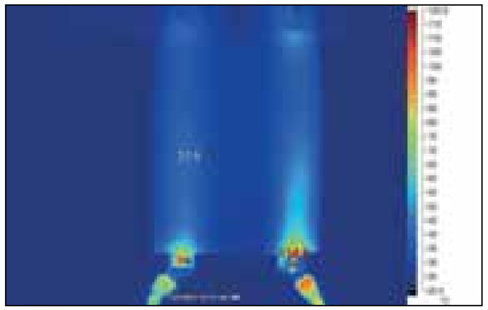

Figure 8.13d t= 120s

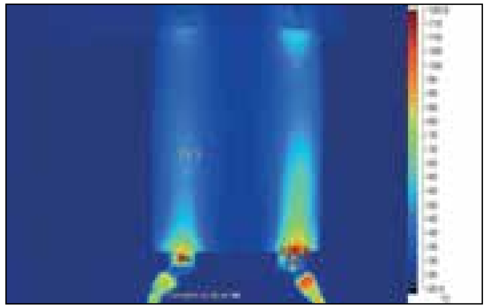

Figure 8.13e t= 180s

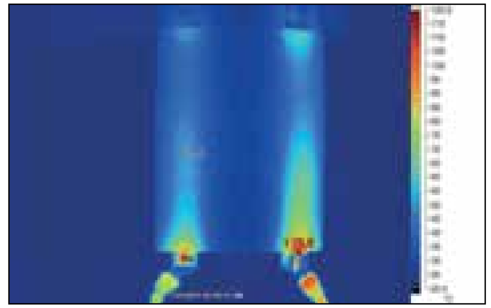

Figure 8.13f t=200s

The thermal performance is analysed with similar data points as used for the analysis of the heating wires. In Figure 8.14, the SMP surface temperatures of the three data points are shown.

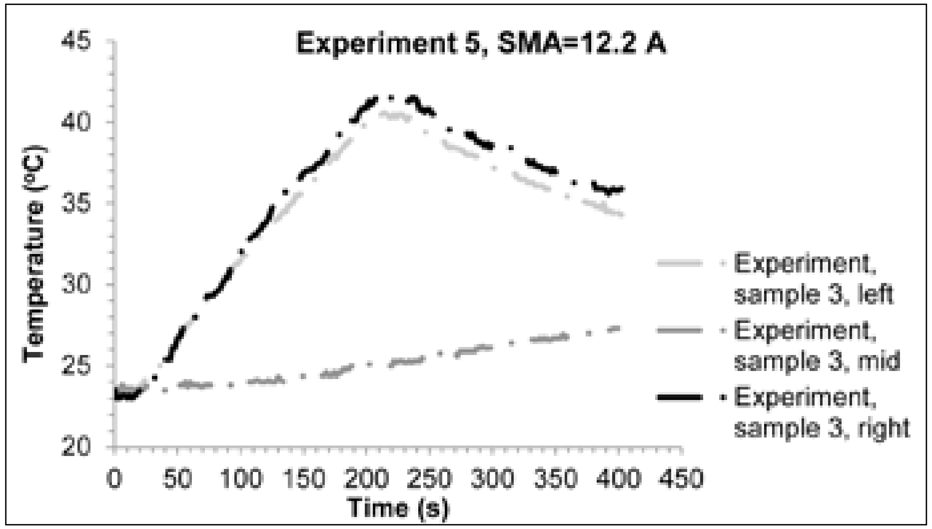

Figure 8.14 Temperature versus time for the activation of the SMAs strips with 12.2Ampere.

As the left and right data points are located above the SMA strips, a clear temperature rise can be found here. As is mentioned before, the SMP is a good insulator. Therefore, the temperature values of the midpoints remain stable. Only a slight temperature raise of 3.7˚C is found during the heating cycle.

In contrast to the left and right data points of the heating wires, the temperatures of the left and right points of the SMA strips are remarkably close. This could be due to the fact that the heat generating surface of the SMA is considered to be much larger than the small heating wires, which leads to a homogenous temperature region. Another difference between the heating wires and SMA strips data can be found in the heating time of the SMP surface. During heating with the heating wires, the SMP surface temperature shows a direct increase upon activation, whereas during the activation of the SMAs, the SMP surface temperature rises only after 20 seconds. The SMA strips are located at the centre of the SMP cross-section and the heating wires are located more at the surface of the SMP body. Temperature raises of the heating wires are therefore observed earlier at the SMP surface compared to the heating of the SMA strips. It takes some time for the heat to travel to the SMP surface. Likewise, the data curve of the heating wires is showing a steeper slope compared to the SMA strips.

For further comparison, the right data points of the experiments are used (see Figure 8.15). Clearly, the right and left data points are showing a more explicit thermal performance in relation to the midpoint. As both data points are practically similar, the selection of the right data point is rather arbitrary.

The data of all experiments of the SMA activation is shown in Figure 8.15. The SMP surface temperature has been analysed for the right data points by variable activation settings. In the low temperature region, the SMP surface temperatures of the different experiments are comparable. At the higher temperature region the difference in surface temperature rises according to the SMA temperature. The slopes of the curves are of similar magnitude and are in good relation with the activation settings. During experiment 4 and 6 only the heating of the sample is captured. Both the heating and cooling performance are analysed during experiment 5.

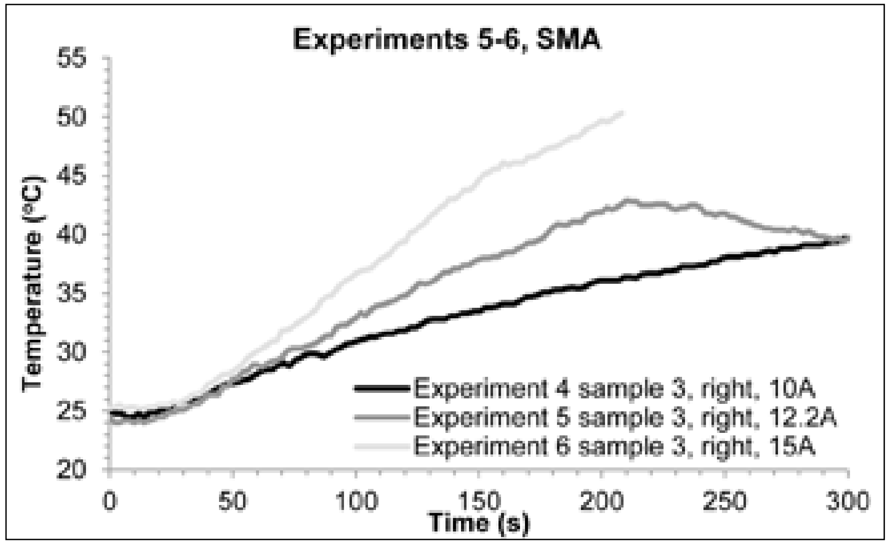

Figure 8.15 Experimental data of the activation of the SMA strips, temperature versus time, left points.

8.5 Thermoelectric Finite Element Analysis

The thermoelectric behaviour of the smart composite is simulated by the use of a finite element model, scripted with ANSYS[19] software, version 12.01. The SMP body is constructed out of SOLID 70 elements. SOLID 70 is a three dimensional thermal solid, which contains heat conduction capabilities (ANSYS help webpage). As the diameter of the constantan wires is considerably smaller in relation to the prototype, it is decided to use a LINK element for the integrated heating wires. The LINK element must enable both thermal and electrical conduction simulations, since the wires are used as resistive heating elements. LINK68 has both these characteristics. Comparable characteristics are required for the SMA strips, which are constructed using thermoelectric SHELL157 elements.

19. ANSYS is simulation software, used for complex calculations by the use of the finite element method.

The model is constructed with nodes on every mm. This is precise enough for the intended analysis. The SMA_1 and SMA_3 strips are electrically coupled in both the model and the prototype. Coupling of the SMA strips required only one variable power supply. The strips are coupled in series, which enables an equal distribution of electric current by variable resistance. When the strips are coupled in parallel a slight difference of resistance may lead to unequal heating of the strips. The ANSYS model is presented in Figure 8.16.

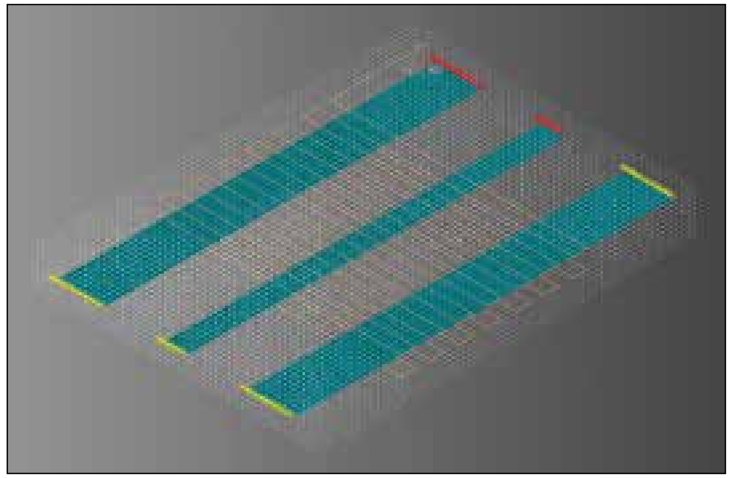

Figure 8.16 ANSYS model, with nodes representing the SMP body, SMA strips and heating wires

8.5.1 Boundary Conditions

The initial ambient temperature as well as the body temperature is set at 25°C. This is similar to the ambient temperature of the validation experiments.

All nodes located on the external surface of the prototype are loaded with convection, which is applied to the SOLID 70 elements. This means that natural convection with the environment is simulated. The heat transfer coefficients are not available in literature or given by the supplier. Therefore, the convection coefficient (h_{conv} in W/(m^2K)) (or film coefficient h_f) is estimated using the following equation (Thirumaleshwar 2006):

$$h_{conv} = Nu * k / l$$ **Equation 8.6**

Nu is the Nusselt number, k=thermal conductivity of air (W/m/K) and l the characteristic length (m). Literature on this subject is suggested for further elaboration on the thermal calculation, (Holman 1997; Baehr 2006; Thirumaleshwar 2006; Incropera 2007).

After the determination of the heat transfer coefficient, the convection energy (Q_{conv} in W) leaving the surface can be calculated (Holman 1997):

$$Q_{conv} = h_{conv} * \Delta T * A_{conv}$$ **Equation 8.7**

Where ΔT (°C) represents the surface temperature subtracted by the environmental temperature and the A_{conv} (m^2) denotes the area of the convection surface.

The previous two equations showed that the convection and radiation coefficient are temperature dependent, this is calculated and presented in Figure 8.9. Here, a variable surface temperature is shown by a constant environmental temperature of 25°C. This figure demonstrates that both values rise by increasing mean temperatures.

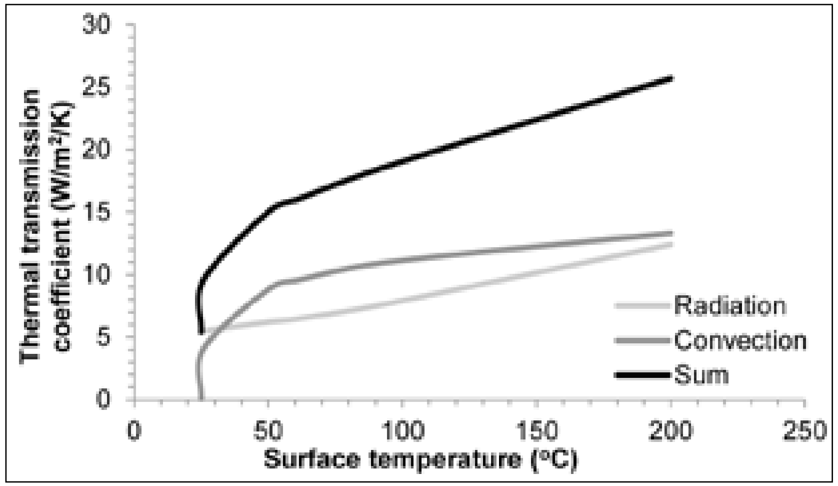

Figure 8.17 Thermal transmission coefficients by ambient temperature Ta=25oC

The temperature dependent convection coefficient is applied as a material property in the material model of the SOLID 70 element. Furthermore, convection is applied as a surface load on these elements. Hereby, a bulk temperature of 25°C is specified. ANSYS will evaluate the convection coefficient by calculating the average between the bulk and the surface temperature constantly.

In order to identify radiation load, SURF 152 elements are created as an overlay on the external surface nodes. The SURF152 element is a three dimensional component, on which a thermal surface effect can be applied. In this case radiation is applied as a surface effect. The SURF152 element is linked to an additional external node and has a set environmental temperature of 25°C.

8.5.2 Material Properties

The temperature dependent material properties used in the ANSYS simulations are shown in Figure 8.18. This figure is derived from the material properties in Table 8.1.

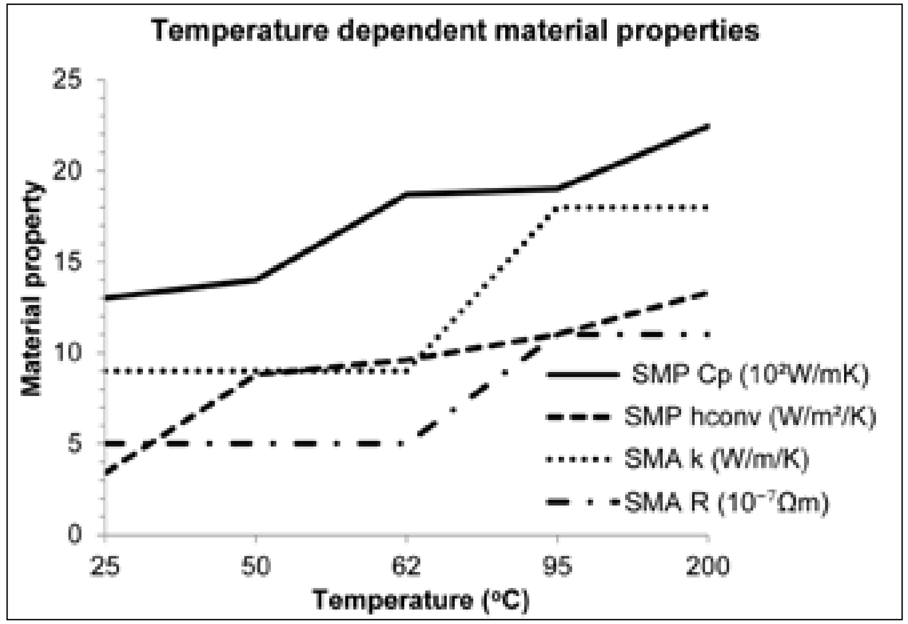

Figure 8.18 Temperature dependent material properties used in ANSYS. The switching points correspond with the transition temperatures of the specific materials.

8.5.3 Results and Comparison with Experiments

In the following paragraph, the data of the finite element simulations is analysed using similar activation settings as the executed experiments. An image of the numerical simulation of the heating wires activation is presented in Figure 8.19. The heating wires are activated with 15 V. The colour gradient represents the temperature distribution in the SC. In Figure 8.20, a representation of the numerical simulation of the SMA_{1+3} strips activation is presented. The SMA_{1+3} strips are activated with 10 A during this simulation. Note that the area between the two strips remains below a temperature of 35°C, while the SMA_{1+3} strips have a local temperature of 70°C.

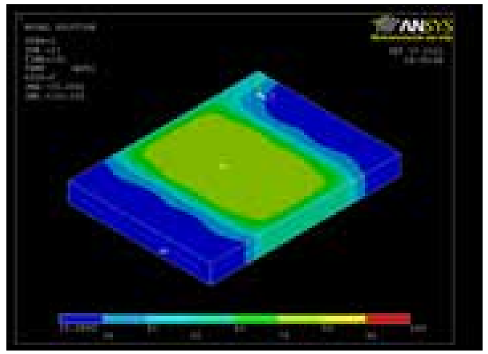

Figure 8.19 Numerical temperature model of the SC. The heating wires are activated with 15 Volt.

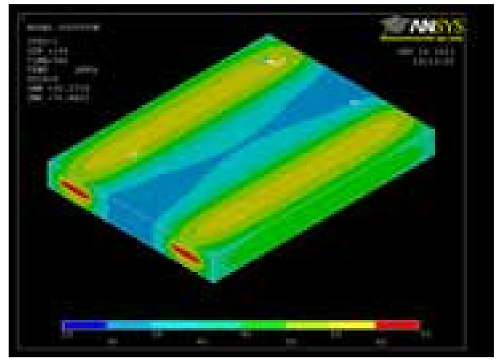

Figure 8.20 Numerical temperature model of the SC during the activation of SMA_{1+3} with 10 Ampere and a heating time of 942 seconds. The activation of the SMA_{1+3} strips does not influence the SMA_2 temperature, but only the SMP surface temperature right above the activated SMA strips.

8.5.3.1 Activation of the Heating Wires

In Figure 8.21, the results of the finite element simulation and the corresponding experimental data are shown for the activation of the heating wires with 10 Volt. The middle points are used for this analysis.

The results of Figure 8.21 indicate that the curve of the simulation follows the experimental data curve of sample 1. Although the cooling phase of sample 1 is not analysed, it can be concluded that the cooling curve shows comparable cooling behaviour in relation to the experimental data curve of sample 3. Both cooling curves are of similar order of magnitude.

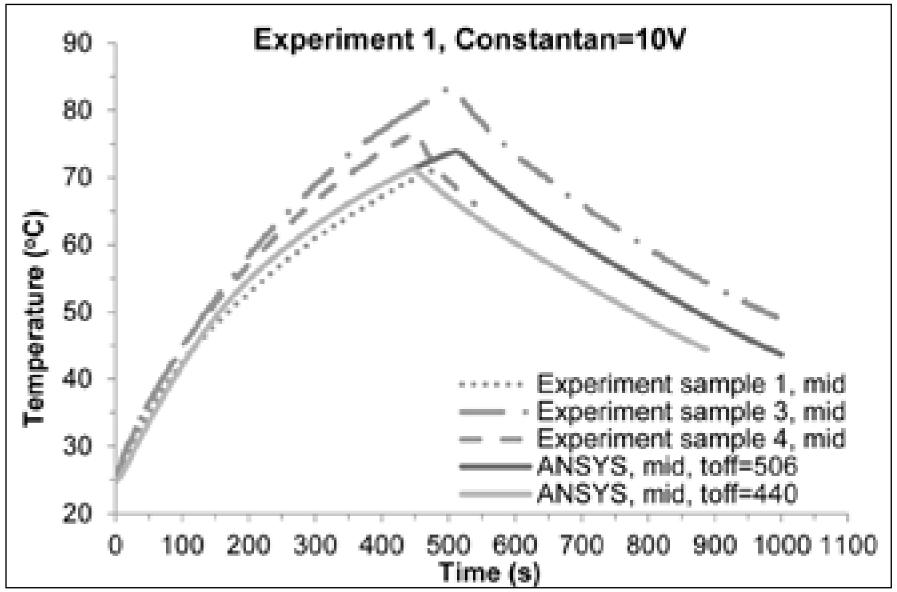

Figure 8.21 Numerical and experimental data of the SMP surface temperature for experiment 1, temperature versus time. Solid lines indicate the numerical simulations.

In Table 8.7, the peak temperatures of experiment 1 at a time of 450 seconds are shown. The peak temperatures of sample 3 and 4 are respectively 8.8 and 3.9˚C higher in relation to the simulation value. In general, it can be stated that a good agreement is achieved between the experimental and simulation data of experiment 1.

Table 8.7 Peak temperature after 450 seconds at U=10V for midpoint

10V	t in s	T in ˚C
Numerical data	450	71.4
Experiment Sample 1	450	69.8
Experiment Sample 3	450	80.2
Experiment Sample 4	450	75.3

In Figure 8.22, the data output of experiment 2 and the finite element simulation is given for all midpoints. As the activation times of the different samples vary, the ANSYS simulations have been executed with an activation time of 454 seconds and 420 seconds. The simulation data matches the curve of sample 1 precisely. Note that the temperature difference between the numerical data and the experimental data of sample 3 and 4 rises with increasing temperature. Differences of 15.6˚C and 8.1˚C are found between the numerical data and sample 3 and 4 respectively around 400 seconds of activation.

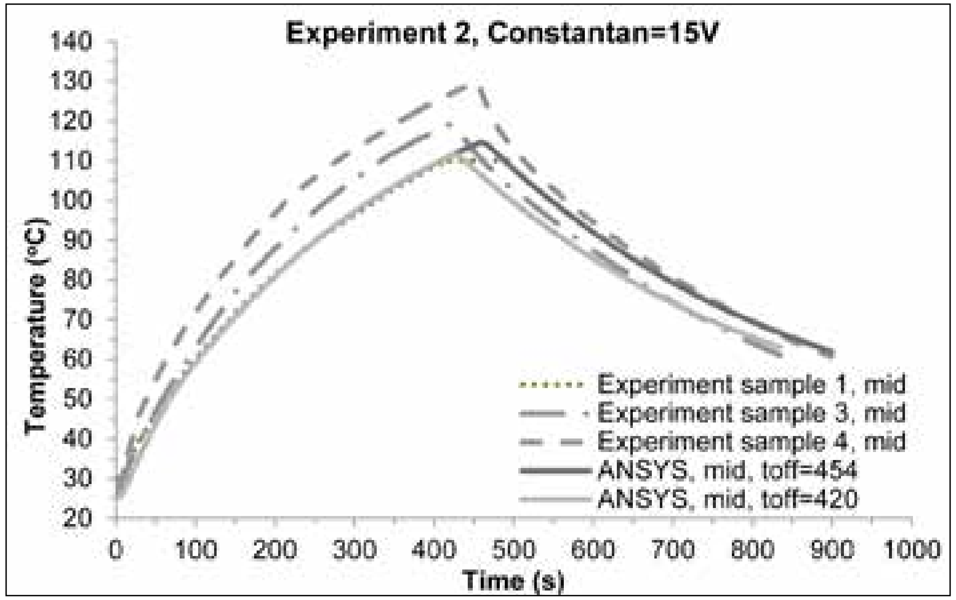

Figure 8.22 Numerical and experimental data of the SMP surface temperature for experiment 2, temperature versus time. Solid lines indicate the numerical simulations.

In Figure 8.23, the findings of experiment 3 and the related simulation values are plotted against time. The findings indicate that a close similarity is found between the numerical data and the experimental results of sample 1 and 3. Subsequently, a considerable dissimilarity is detected with sample 4; a temperature difference of 24˚C is found at the higher temperature region above 120˚C. It is not clear what the exact cause of this deviation is. A possible explanation is that this is caused by a manufacturing deviation. This idea is supported by the fact that the surface temperature of sample 4 is higher during all experiments (Figure 8.21 to Figure 8.23). During the cooling stage, the surface temperature drops considerably to a value close to the simulation data.

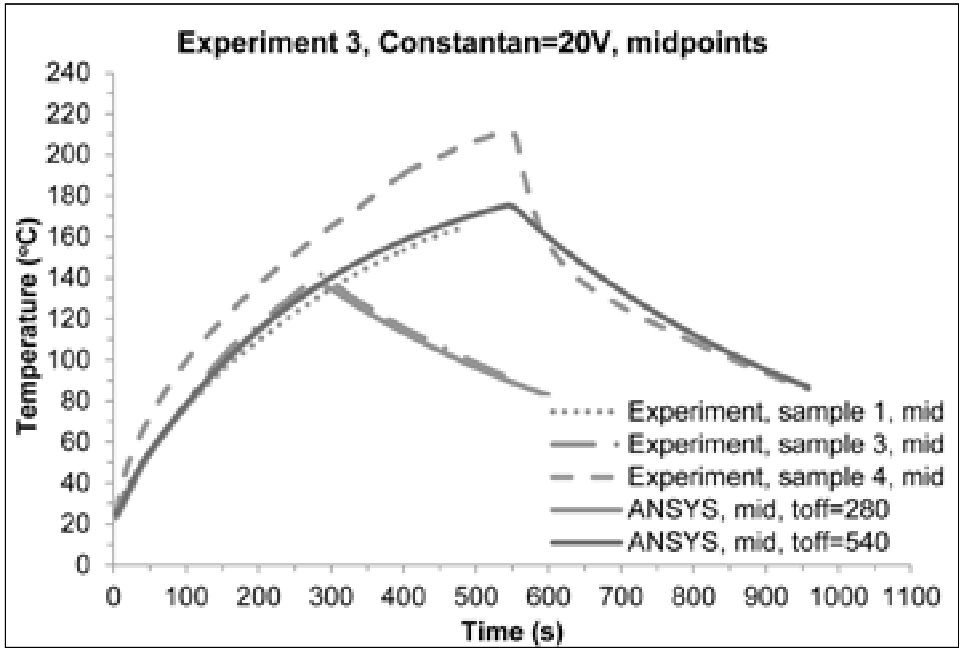

Figure 8.23 Numerical and experimental data of the SMP surface temperature for experiment 3, temperature versus time. Solid lines indicate the numerical simulations.

8.5.3.2 Activation of the SMA Strips

The data of the activation of the SMA_{1+3} strips with 10 A is presented in Figure 8.24. The thermal performance of three data points is analysed. The figure shows that the temperature difference increases at higher temperatures. At a time of 800 seconds, the difference in temperature between the numerical data and the experimental data is 8.8˚C.

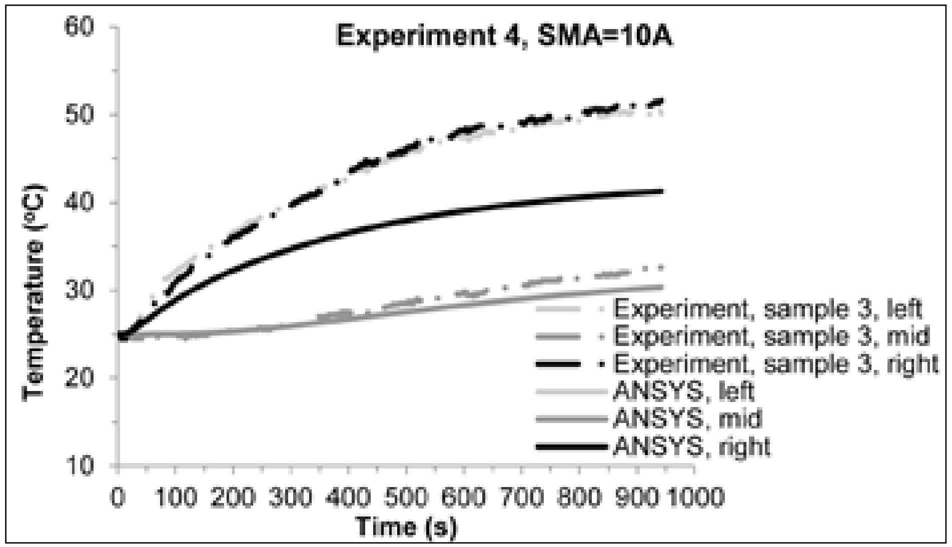

Figure 8.24 Numerical and experimental data of the SMP surface temperature for experiment 4, temperature versus time. The SMA strips are activated with 10 A. Solid lines indicate the numerical simulations.

In Figure 8.25, the experimental data and the numerical data is shown for the activation of the SMA strips with 12.2 Ampere. At the peak (210 seconds), a difference of about 5.6˚C is found between the experimental data and numerical data. The activation of the SMA strips hardly influenced the middle point data, for this reason relatively little divergence is observed between the experimental and the numerical data at this location.

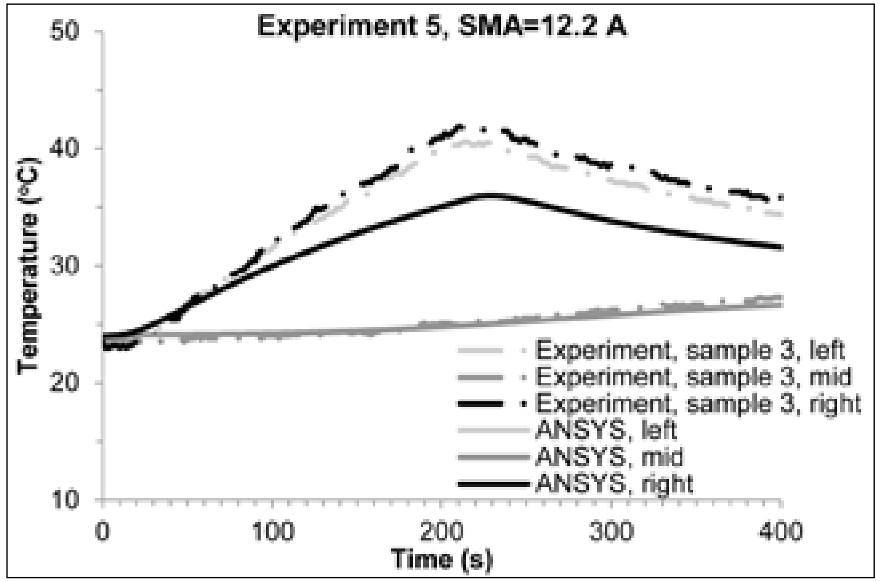

Figure 8.25 Numerical and experimental data of the SMP surface temperature for experiment 5, temperature versus time. The SMA strips are activated with 12A. Solid lines indicate the numerical simulations.

In Figure 8.26, the data of experiment 6 together with the numerical data for the activation of the SMA strips with 15 Ampere is shown. In comparison to the previously discussed results of the SMA strips, a discrepancy is found that increased at higher temperatures. At t=200 s the difference between the experimental and numerical data is approximately 8˚C.

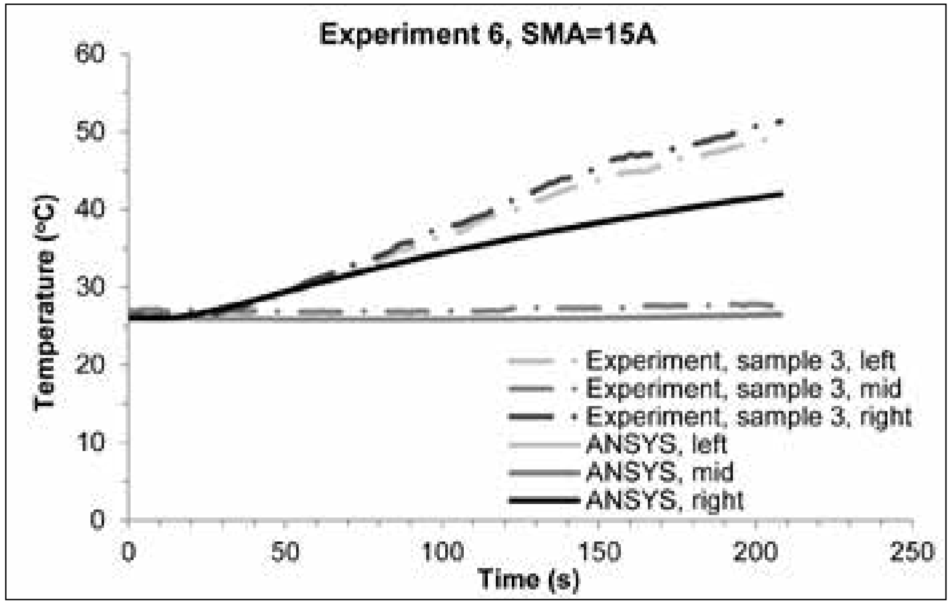

Figure 8.26 Numerical and experimental data of the SMP surface temperature for experiment 6, temperature versus time. The SMA strips are activated with 15A. Solid lines indicate the numerical simulations.

8.5.3.3 Activation of Both the Heating Wires and SMA Strips

The heating wires are activated with 15 Volt and 0.94 Ampere for 156 seconds and after 120 seconds the SMA strips are activated with 12.1 Ampere for 245 seconds. In Figure 8.27, the SMP surface temperature is presented for both the numerical and the experimental data. Based on the results of experiment 2, it could be expected that during the first heating step, the numerical temperature data would be lower compared to the experimental data. Likewise, this effect can also be found in Figure 8.27. In general, the temperature differences are considerably smaller compared to the individual activated components.

An interesting event occurred during the activation of the SMA strips. In relation to the SMA experiments, it was expected that the numerical model would show a lower surface temperature. Instead, a higher temperature is found of approximately 4˚C after 300 seconds of activation of the SMA strips. This difference is related to the concurrent activation of the heating wires.

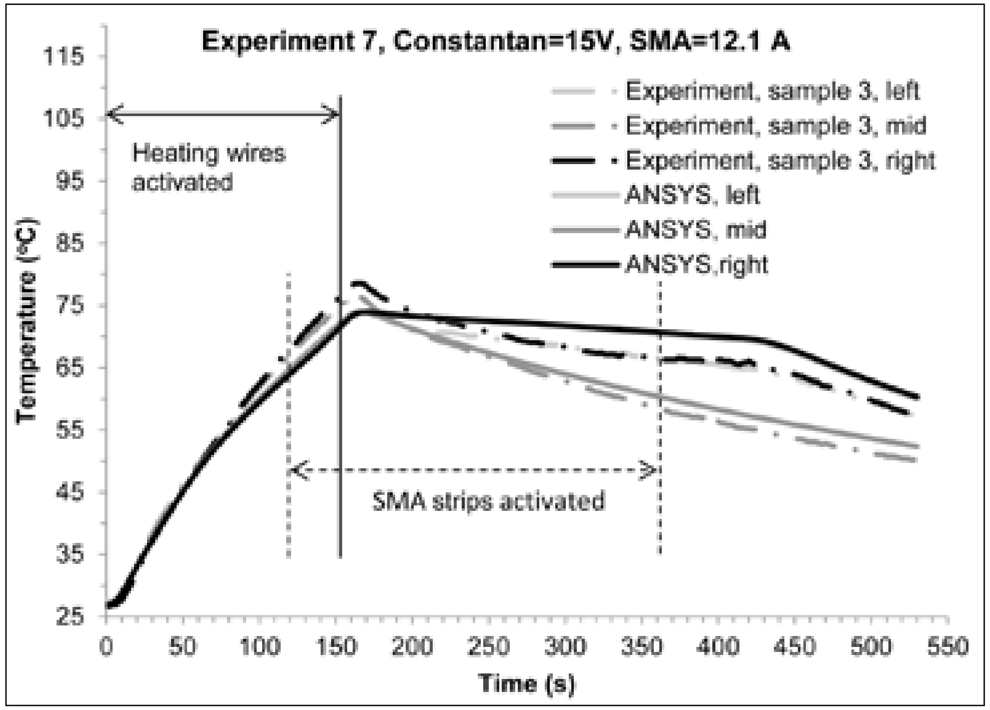

Figure 8.27 Numerical and experimental data of the SMP surface temperature for experiment 7, temperature versus time. Solid lines indicate the numerical simulations.

8.6 Discussion

8.6.1 Uncertainties in Experiments and Simulations

8.6.1.1 Material Properties

Naturally, the material properties are an important aspect for the simulations. As discussed before, the used material properties are obtained from material suppliers or associated material models. Differences between the provided material specifications and the actual applied materials can be expected. Although the overall results indicate that the differences are well within an acceptable range, it is important to determine the temperature dependent material properties in further research. The precise determination of the material properties is, however, beyond the scope of this research

8.6.1.2 Sample Dimensions

The differences between the data of the various samples as well as between the numerical model and the samples can be explained by the fact that the prototypes are manufactured by hand. As a result of the manual milling process, the location of the wires varied slightly in depth, which resulted in a difference in surface temperature. The same holds true for the positioning of the SMA strips in the SMP. Due to the manufacturing by hand it is not possible to produce identical prototypes.

Optimization of the manufacturing process will enhance the performance of the smart composite and will lead to a closer resemblance with the numerical model.

Temperature differences in the entire heating area of the samples can be explained by the design of the heating system. As described in chapter 6, the heating wires are positioned undulated as a parallel array of wires in the indicated heating area. This leads to temperature differences on the material surface (see Figure 8.7). The undulated pattern is clearly visible during the activation of the heating wires.

8.6.1.3 Thermal Aspects

In Figure 8.28, the SMP surface temperature with a constant heat transfer coefficient of 5 W/m^2/K is shown together with the temperature curve of a temperature dependent coefficient. As is discussed earlier, the heat transfer coefficient increases with increasing surface temperature. The amount of emitted energy to its surrounding increases accordingly. This results in a lower surface temperature in relation to a surface temperature experiencing a constant low heat transfer coefficient. This effect is illustrated in Figure 8.28. The figure confirms that the temperature dependency of the heat transfer coefficient cannot be neglected.

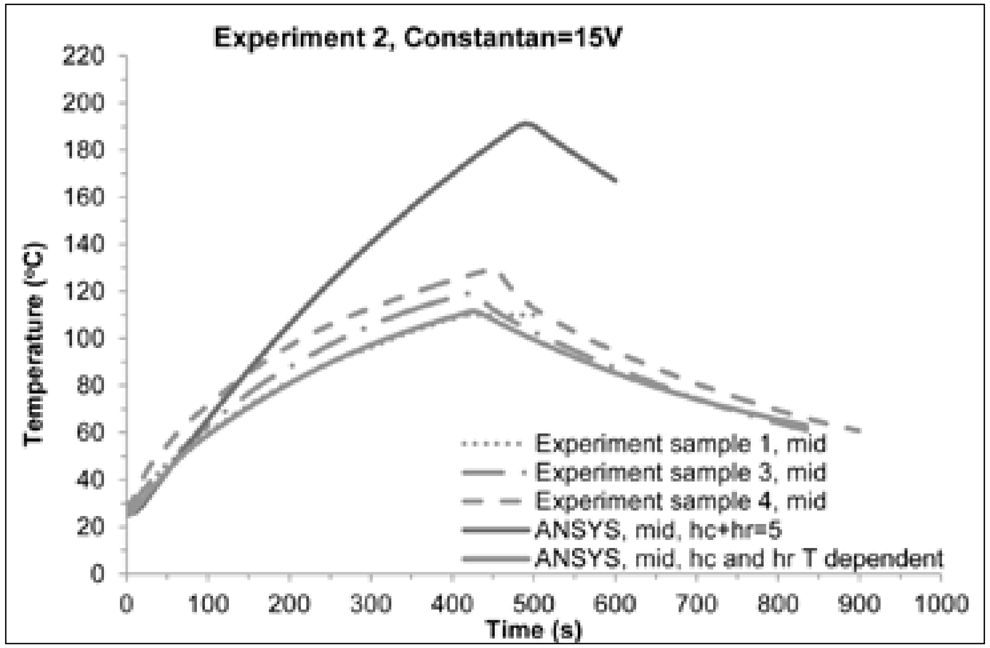

Figure 8.28 Simulation data of temperature dependent transmission coefficient and constant transmission coefficient compared with validation experiments. Solid lines indicate the numerical simulations.

8.6.1.4 Thermoelectric Experiments

When observing the SMP surface temperature during the activation of both the heating wires and the SMA strips, the temperature increased almost directly upon activation of the heating wires. During the activation of the SMA strips, an average time of 25 seconds is required before an increase of temperature is found. This can be explained by the fact that the SMA strips are located at the centre of the SMP body. The heating wires are located more at the surface. Due to the low conduction

properties of the SMP, an increase of temperature of the heating wires is experienced earlier compared to an increase of temperature of the SMA strips. The slow heating of the SMP body by the SMA strips is favourable, as the antagonist shaped SMA strip should not be heated during the same heating cycle.

The data points are situated at similar locations for the distinctive samples. It is however possible that in some situations, the data points are located exactly on top of a heating wire. It is possible that by other experiments the data points are located next to heating wire and sometimes in between two wires. Due to the low thermal conductivity values of the SMP, the temperatures can therefore differ substantially. However, it should be mentioned that the experimental data of sample 1 is always found in the lowest region of the surface temperature compared to the results of the other samples. This is more likely due to manufacturing dissimilarities. The heating wires can be located deeper in the SMA body compared to the other samples.

8.6.2 Validation of the Finite Element Model

A good correspondence between the validation experiments and the finite element analysis is achieved. The presented data proved that the finite element model can be used as a tool for the thermal performance prediction of the Smart Composite. The numerical data showed a remarkable resemblance with the experimental data of sample 1. The deviations between the numerical data and the experimental data of sample 3 are of acceptable order. Last, some considerable differences are found between the numerical data and the experimental data of sample 4.

In Table 8.8, the component properties and activation settings for the different experiments are shown. The length of the heating wires varies slightly due to manual manufacturing. This difference is negligible when analysing the activation settings of the heating wires. The activation settings for experiment 1-3 give agreeable results when comparing the samples with the numerical and analytic values.

The experimental data delivers a higher SMP surface temperature and higher power generation during the activation of the SMA strips when compared to the numerical data. The activation values of the SMA strips differ considerably between the experimental data and the numerical data (see Table 8.8 test 4-6, highlighted). This can be attributed to the differences in length of the SMA strips used in the experiments and the numerical model. In order to enable activation, SMA strips with larger lengths in relation to the numerical model are used for the validation experiments. The numerical model is constructed with SMA strips that had similar lengths as the SMP body. Due to the increase in resistance caused by a larger length, the SMA strips in the sample generated a higher temperature at a constant electric current. When calculating the activation settings analytically with this length, the results are more comparable (Table 8.8, analytic SMA I=0.3). The generated power by 10 amperes measured 8.6 Watt for the experimental values and 6.6 Watt for the calculated values. This difference is substantially smaller compared to the numerical power generation by the SMA strips (2.7 Watt). This power difference explains the higher SMP surface temperature during the validation of the numerical data.

For further use of the numerical model, the SMA dimensions should be adapted to the prototype dimensions. Additionally, the activation method of the SC should be optimized. The current heating method demands extra SMA material to enable the activation. Due to the high material costs, it is preferred to find another solution for the SMA activation. Follow-up study of the optimization of the activation method is recommended.

Table 8.8 Voltage, current and resistance acquired during the experiments and simulations and calculated analytically. Additionally, the related dimensions of the components are given.

	Sample 1	Sample 3	Sample 4	ANSYS	Analytic SMA I=0.16	Analytic SMA I=0.3	
Constantan	$2.5\cdot10^{-04}$	$2.5\cdot10^{-04}$	$2.5\cdot10^{-04}$	$2.5\cdot10^{-04}$	$2.5\cdot10^{-04}$	$2.5\cdot10^{-04}$	m
Diameter	$4.9\cdot10^{-08}$	$4.9\cdot10^{-08}$	$4.9\cdot10^{-08}$	$4.9\cdot10^{-08}$	$4.9\cdot10^{-08}$	$4.9\cdot10^{-08}$	m2
Area Length	1.51	1.54	1.54	1.64	1.64	1.64	m
Specific resistivity	$4.9\cdot10^{-7}$	$4.9\cdot10^{-7}$	4.9·10-^{7}	$4.9\cdot10^{-7}$	$4.9\cdot10^{-7}$	$4.9\cdot10^{-7}$	Ω*m
Resistance	15.07	15.37	15.37	16.32	16.32	16.32	Ω
SMA							
Length	0.30	0.30	0.30	0.16	0.16	0.30	m
Width	0.01	0.01	0.01	0.01	0.01	0.01	m
Thickness	$5\cdot10^{-4}$	$5\cdot10^{-4}$	$5\cdot10^{-4}$	$5\cdot10^{-4}$	$5\cdot10^{-4}$	$5\cdot10^{-4}$	m
Specific resistivity martensite	$5\cdot10^{-7}$	$5\cdot10^{-7}$	$5\cdot10^{-7}$	$5\cdot10^{-7}$	$5\cdot10^{-7}$	$5\cdot10^{-7}$	Ω*m
Resistance martensite	$3\cdot10^{-2}$	$3\cdot10^{-2}$	$3\cdot10^{-2}$	$1.6\cdot10^{-2}$	$1.6\cdot10^{-2}$	$3\cdot10^{-2}$	Ω
Specific resistivity austenite	$1.1\cdot10^{-6}$	$1.1\cdot10^{-6}$	$1.1\cdot10^{-6}$	$1.1\cdot10^{-6}$	$1.1\cdot10^{-6}$	$1.1\cdot10^{-6}$	Ω*m
Resistance austenite	$6.6\cdot10^{-2}$	$6.6\cdot10^{-2}$	$6.6\cdot10^{-2}$	$3.5\cdot10^{-2}$	$3.5\cdot10^{-2}$	$6.6\cdot10^{-2}$	Ω
Experiment 1							
U	10.1	10	10	10	10		V
I	0.62	0.62	0.62	0.62	0.61		A
R	16.29	16.13	16.13	16.23	16.32		Ω
P	6.26	6.20	6.20	6.16	6.13		W
Experiment 2							
U	15	14.9	15	15	15		V
I	0.93	0.94	0.94	0.92	0.92		A
R	16.13	15.85	15.96	16.35	16.32		Ω
P	13.95	14.01	14.1	13.76	13.79		W
Experiment 3							
U	19.5	20	20	20	20		V
I	1.22	1.24	1.26	1.223	1.23		A
R	15.98	16.13	15.87	16.35	16.32		Ω
P	23.79	24.8	25.2	24.46	24.51		W
Experiment 4							
U martensite				0.16	0.16	0.30	V
U austenite		0.86		0.27	0.35	0.66	V
I		10		10	10	10	A
R martensite				0.02	0.02	0.03	Ω
R austenite		$8.6\cdot10^{-2}$		0.03	0.04	0.07	Ω
Specific resistivity austenite		$1.4\cdot10^{-6}$		$1.1\cdot10^{-6}$	$1.1\cdot10^{-6}$	$1.1\cdot10^{-6}$	
P martensite				1.62	1.60	3	W
P austenite		8.6		2.67	3.52	6.60	W
Experiment 5							
U martensite				0.20	0.20	0.40	V
U austenite		0.86		0.28	0.43	0.87	V
I		12.2		12.2	12.2	13.2	A
R martensite				$2\cdot10^{-2}$	$2\cdot10^{-2}$	$3\cdot10^{-2}$	Ω
R austenite		$7\cdot10^{-2}$		$2\cdot10^{-2}$	$4\cdot10^{-2}$	$7\cdot10^{-2}$	Ω
Specific R		$1.2\cdot10^{-6}$		$1.1\cdot10^{-6}$	$1.1\cdot10^{-6}$	$1.1\cdot10^{-6}$	
P martensite				2.43	2.38	5.23	W
P austenite		10.49		3.36	5.24	11.50	W
Experiment 6							
U martensite				0.25	0.24	0.48	V
U austenite		1.43		0.41	0.53	1.06	V
I		15		15	15	16	A
R martensite				$2\cdot10^{-2}$	$2\cdot10^{-2}$	$3\cdot10^{-2}$	Ω
R austenite		0.1		$3\cdot10^{-2}$	$4\cdot10^{-2}$	$7\cdot10^{-2}$	Ω
Specific R		$1.6\cdot10^{-6}$		$1.1\cdot10^{-6}$	$1.1\cdot10^{-6}$	$1.1\cdot10^{-6}$	
P martensite				3.79	3.60	7.68	W
P austenite		21.45		6.19	7.92	16.90	W

8.7 Conclusions

A finite element model has been developed with the use of ANSYS software for the determination of the thermoelectric activation of the SC. The numerical model has been validated by heating experiments. For comparison purposes, these experiments have been executed with different prototypes. During these experiments the activation of the heating wires and the SMA strips are tested separately.

Due to the large differences between the samples, the numerical and experimental data showed a good resemblance for some samples, but gave large temperature differences with another sample. For experiments 1 to 3, the data of the simulation and sample 1 is practically similar (Figure 8.21 to Figure 8.22). Especially sample 4 gave deviating results when compared to the numerical data. Due to the fact that the differences are similar during all experiments it can be concluded that these could indeed be attributed to manufacturing deviations between the samples. In general, it can be concluded that the ANSYS model can reliably reproduce the heating experiments and that the model is properly validated.

The following aspects indicate that the finite element model can be used as a simulation tool for the thermal performance of the smart composite.

- Small temperature differences during the activation of the heating wires (experiment 1-3) in the low temperature area. Temperature differences increase by higher temperature. Since the SMP body temperature will not exceed a temperature of 92˚C, this is acceptable.
- Temperature differences during the activation of the SMA strips (experiment 4-6) can be explained by the activation method and the dimension differences of the SMA strips. The temperature differences are acceptable, based on the given arguments.
- During the concurrent heating of the heating wires and SMA strips (experiment 7), very small temperature differences are found. This experiment shows that the numerical model can be very well used for thermoelectric analysis.

8.8 Estimation of Heating Settings for the Smart Composite

Now that the finite element model has been validated and its accuracy is considered to be in good correspondence with the thermal performance of the samples, the numerical model can be used for further analysis. The simulation model will be used here to determine the heating power and switching times. The most optimal heating settings will be determined for both the SMP and the SMA strips.

First, the numerical data from experiment 7 is analysed (Figure 8.31). Not only the SMP surface temperature is analysed here, but also the SMA surface temperature and the temperature located at the edge of the SMP body is included in this figure (Figure 8.29). The SMP corner-point will determine whether the entire SMP body temperature would reach the desired temperature. The SMA_1 and SMA_2 surface temperatures will verify whether the SMA surface temperature remains below A_s.

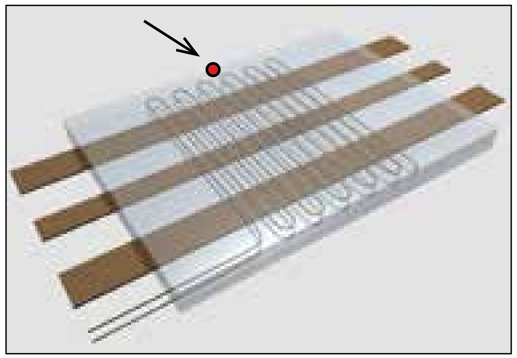

Figure 8.29 Corner point used for SMP surface temperature analysis.

Figure 8.31 shows that the SMP surface temperature right above the heating wires reaches the minimum transition temperature of 58˚C after 92 seconds. The SMP surface temperature did not exceed 75˚C during the entire heating time of 154 seconds. It should be noted that locally, inside the composite body, a higher temperature is found at SMA_2 (Figure 8.30). This can be explained by the location of the SMA_2 strip; at the centre of the SMP body, surrounded by heating wires. Since the SMP body is experiencing convection and radiation loss to its surrounding, the surface temperature will be considerably lower compared to the “insulated” SMA strips. During the activation period of the heating wires, the SMA_2 strip reached a maximum temperature of 80˚C. Thus the SMA_2 strip is not activated during the entire experiment. Note that the SMA_2 surface temperature dropped immediately after deactivation of the wires.

As the entire SMP body should reach a minimum temperature of 58˚C for a full transformation into the rubbery state, the temperature at the corner-point is analysed here. The overall temperature of the SMP corner-point remained below 55˚C (see Figure 8.31). This indicates that the load settings of the heating wires did not meet the heating criteria.

The curve of the SMA_1 surface temperature clearly shows the activation cycle of the simulation. The SMA_{1+3} strips are activated after 120 seconds and reached their maximum temperature of 90.6˚C after 83 seconds of activation. This temperature is still below the austenite transition temperature of 106°C. The results indicate that the activation of the heating wires and the SMA strips have not met the required heating criteria yet. The heating wires should be activated longer or with a higher power in order to reach a full SMP body temperature of 58°C. A similar adjustment of the SMA heating settings is required; a higher current is demanded in order to acquire a transition temperature of 106°C. It should be kept in mind that the SMA_2 surface temperature should remain below 92°C for all occasions. The optimized heating settings will be determined in the following paragraphs. First, the heating conditions for the heating wires are discussed. Second, heating conditions for the SMA strips are analysed.

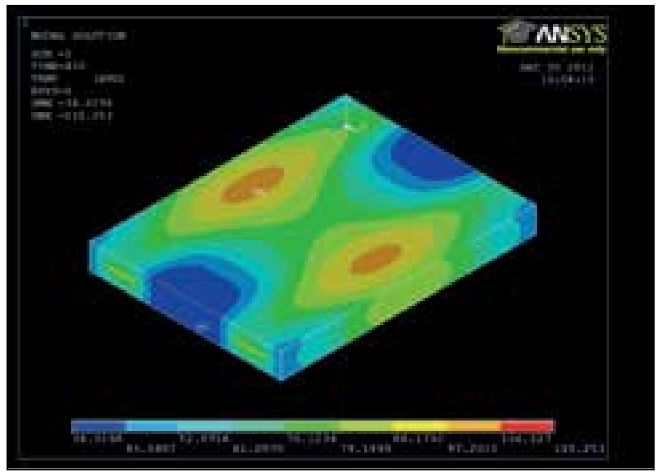

Figure 8.30 Results finite element analysis. It can be clearly seen that the local temperature at the SMA surface is considerable higher compared to the SMP surface temperature.

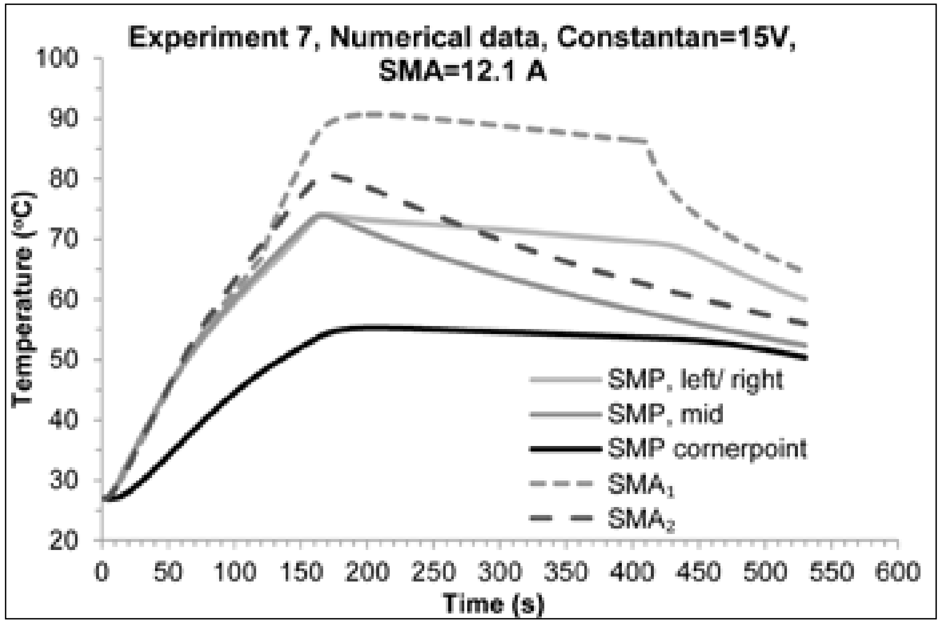

Figure 8.31 Temperature and related heating time of the numerical results for the SMP, SMA_1 and SMA_2 surface temperature. The wires are activated with 15 V for 154 seconds. The SMA_{1+3} strips are activated with 12.1 A after 120 seconds and switched off at t=408 seconds.

8.8.1 Determination of Activation Time and Power Settings for Heating Wires

The activation settings for the heating wires are analysed by variable power settings by the use of the finite element model. In Figure 8.32, the SMA_1 and SMA_2 surface temperatures are presented together with the SMP surface temperatures for the heating settings of experiment 1 to 3. As could be expected, the SMA_2 surface temperature is the highest for all three experiments, followed by the SMA_1 surface temperature. With the heating settings of experiment 1 with 10V, the SMA surface temperature did not exceed the A_s of 92°C. However, with the heating settings of experiment 3 of 20V, the SMA strips did exceed the A_f almost 30 seconds after the SMP reached 58°C.

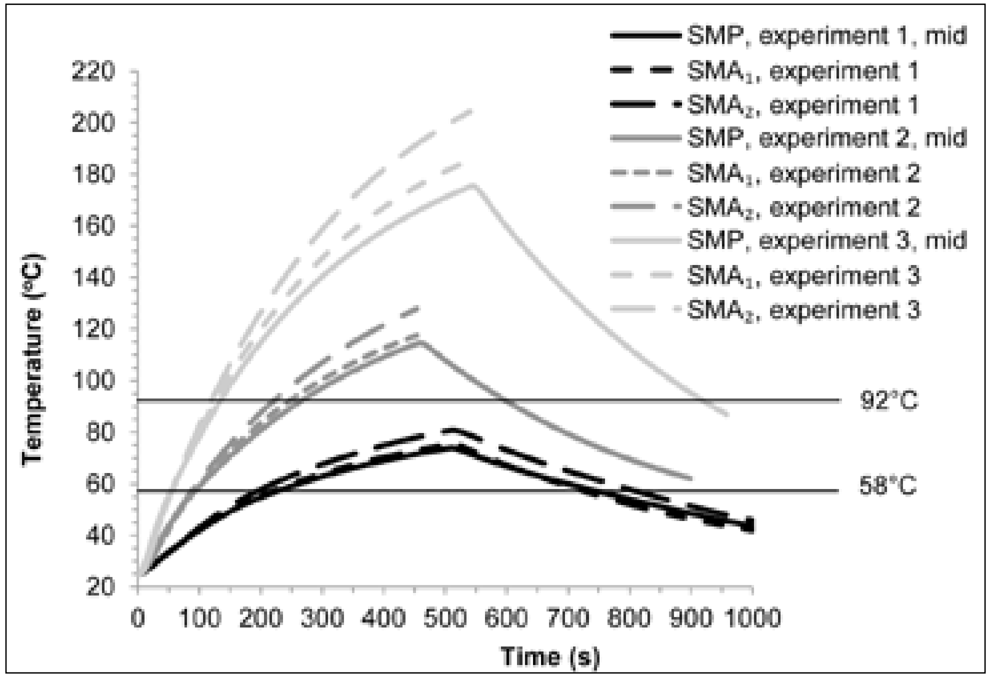

Figure 8.32 SMP, SMA_1 and SMA_2 surface temperatures of the numerical simulations of the heating wires with the settings of 10 Volt (experiment 1), 15 Volt (experiment 2) and 20 Volt (experiment 3).

The data of all experiments (Figure 8.32) is used to analyse the heating time at which the SMP corner-point reached a minimum temperature of 58°C and the SMA_2 body a temperature of 92°C. The relation between the applied electrical power and the time of activation is given in Figure 8.33. Expectedly, higher surface temperatures should be found on SMA_2 than on SMA_{1+3}. The SMA_2 strips are deeper embedded in the SMP body and less convection and radiation is possible. Therefore, the surface temperature of the SMA_2 strip is used in this analysis. The lower limit is determined by the activation criteria of the SMP. All the data below this line indicate that the SMP body temperature is too low in order to initiate the deformation. The upper limit is determined by the activation criteria of the SMA strips. During the heating of the SMP, the temperature of all SMA strips should be kept below the austenite start temperature (A_s) of 92°C. When the SMA temperature will rise above this line, the transformation and related deformation of the SMA will start. This uncontrolled operation should be prevented. Note that for high power inputs the operation window for the possible heating times is rather narrow.

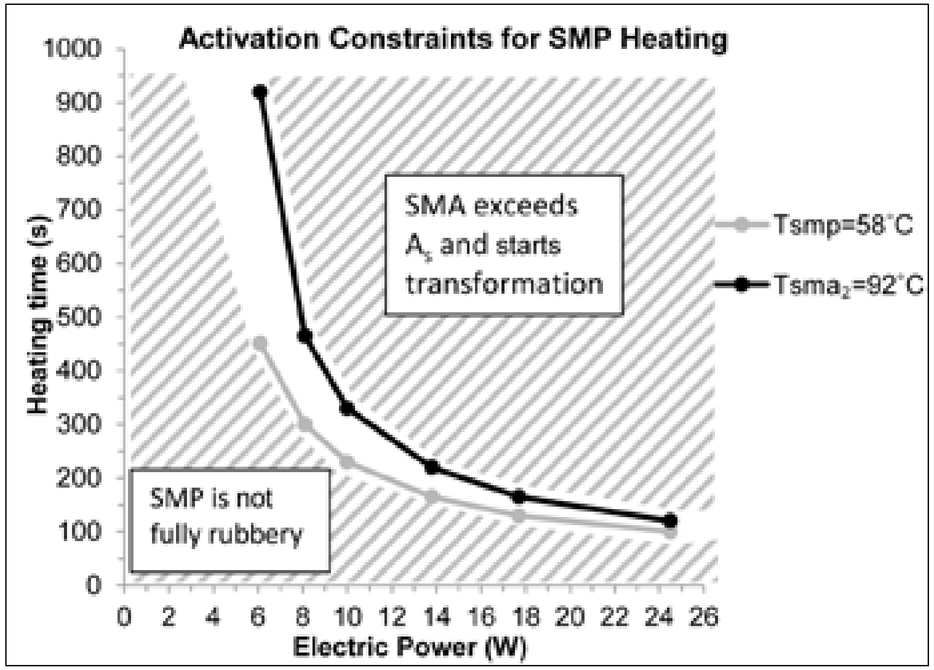

Figure 8.33 Activation window for the heating of the SMP. The shaded parts indicate that the activation settings do not meet the heating criteria.

8.8.2 Determine Activation Time and Power Settings SMA_{1+3}

Following, the power input for the activation of both the SMA_1 and SMA_3 strips will be determined. First, the SMA surface temperatures are analysed with the activation settings used in experiments 4 to 6. Second, the activation settings are adjusted in order to meet the required transformation temperature A_f (106°C).

In Figure 8.34, the numerical data of the activation settings used in experiments 4 to 6 is presented. The results indicate that the SMA_2 surface temperature is identical to the SMP midpoint surface temperature. This can be explained by the low conduction properties of the SMP body. The activation of strips SMA_{1+3} did not influence the SMA_2 temperature at all. This behaviour is illustrated in Figure 8.20. The increasing SMP surface temperature right above the activated SMA strips is clearly visible.

The SMA_1 surface temperature did not even reach the transformation start temperature of 92°C (A_s) with the applied currents and heating times. Either the activation power should be increased or the time of activation.

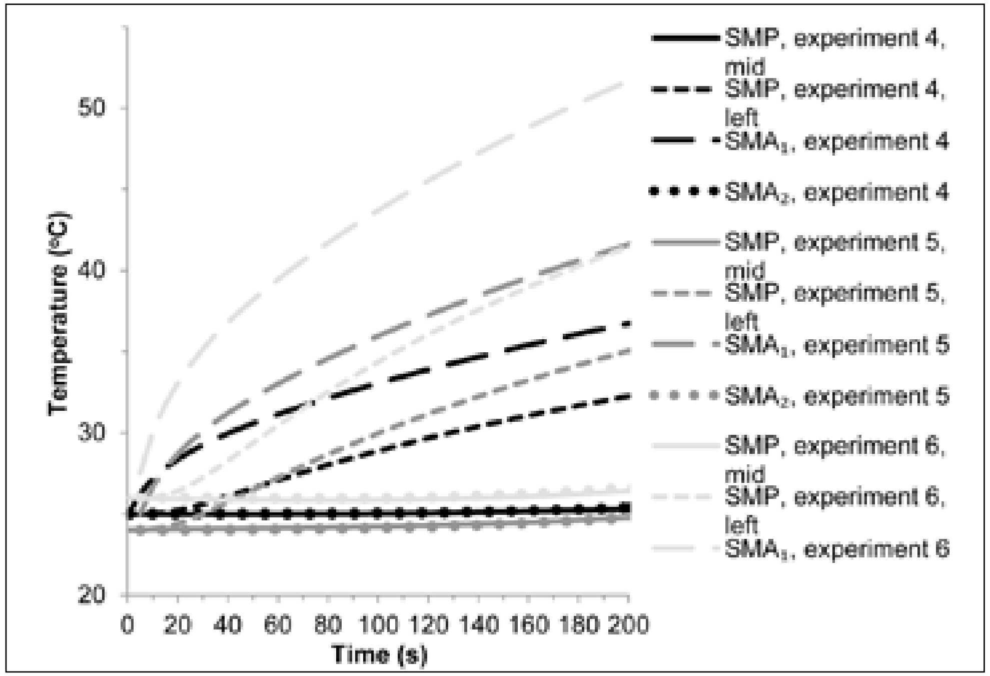

Figure 8.34 SMP mid, SMP left, SMA_1 and SMA_2 surface temperatures of the simulations of the SMA_{1+3} strips with the settings of 10 Ampere (experiment 4), 12.2 Ampere (experiment 5) and 15 Ampere (experiment 6). Note that the data of SMP mid and SMA_2 are similar. The SMA_1 strip do not meet the A_s temperature after heating for 200 seconds.

Additional simulations are performed in order to determine the required activation settings for the SMA_{1+3} strips. Since the SMA strips will always be activated after the SMP body reaches a minimum temperature of 58°C, the initial condition of the SC is set at this temperature. The activation with 10 Ampere is excluded from this analysis, as the SMA strips did not meet the A_s after a heating time of 1000 seconds (Figure 8.24).

In Figure 8.35, the SMA surface temperatures and related heating times are given for the different electric currents. The activation with 12.2 Ampere is not sufficient for initiating the transformation of the two SMA strips. When applying an electric current of 15 Ampere, the SMA strips will start the transformation after 245 seconds. However, after 400 seconds a temperature of 103°C has been reached, this will not enable a full transformation. Longer heating times are required when using this electric current.

The A_f has been reached after 87 seconds during the activation of the SMA strips with 20 Ampere. The A_s has been reached after 57 seconds. It is to be expected that faster transformation times are found by increasing electric current. When applying a current of 25 Ampere, the A_s has been reached after 27 seconds and the A_f after approximately 40 seconds. With this heating setting, the temperature increases rather fast. Long heating times should be restricted to prevent (over)heating above 150°C.

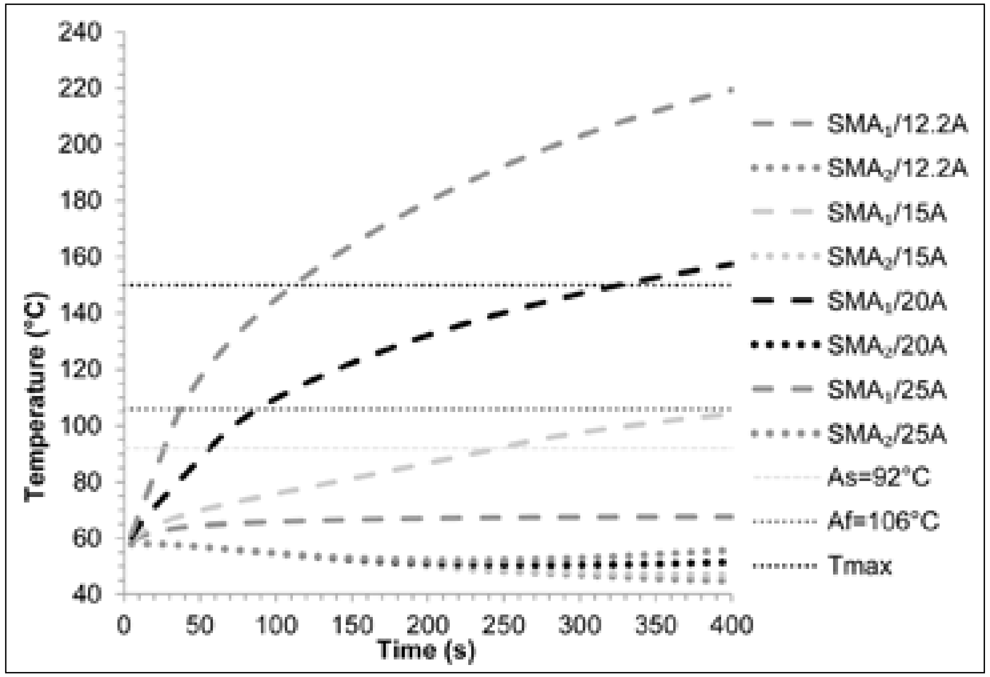

Figure 8.35 The SMA temperature and heating time is given for different electric currents. It should be mentioned that the activation with 12.2 Ampere did not meet the transformation temperature. The SMA_2 temperatures are not influenced by the high SMA_1 temperatures and show a slow cooling and a slight concurrent heating after approximately 250 seconds.

In Figure 8.36, the activation window for SMA_{1+3} is shown. The power settings with the related heating times are given for an A_f of 106°C and a T_{max} of 150°C. When the SMA_1 temperature remains below the A_f a full transformation cannot be realized. The upper limit is determined by the maximum SMA_{1+3} body temperature. When the temperature rises above this line, degradation of the SMA performance will occur. With higher power inputs faster heating times are found. This will shorten the activation of the SMA_{1+3} considerably. Consequently, this means that the T_{max} will be reached shortly after the A_f. The heating window will become quite narrow at high power inputs. Likewise, very large heating windows will be found at lower power inputs.

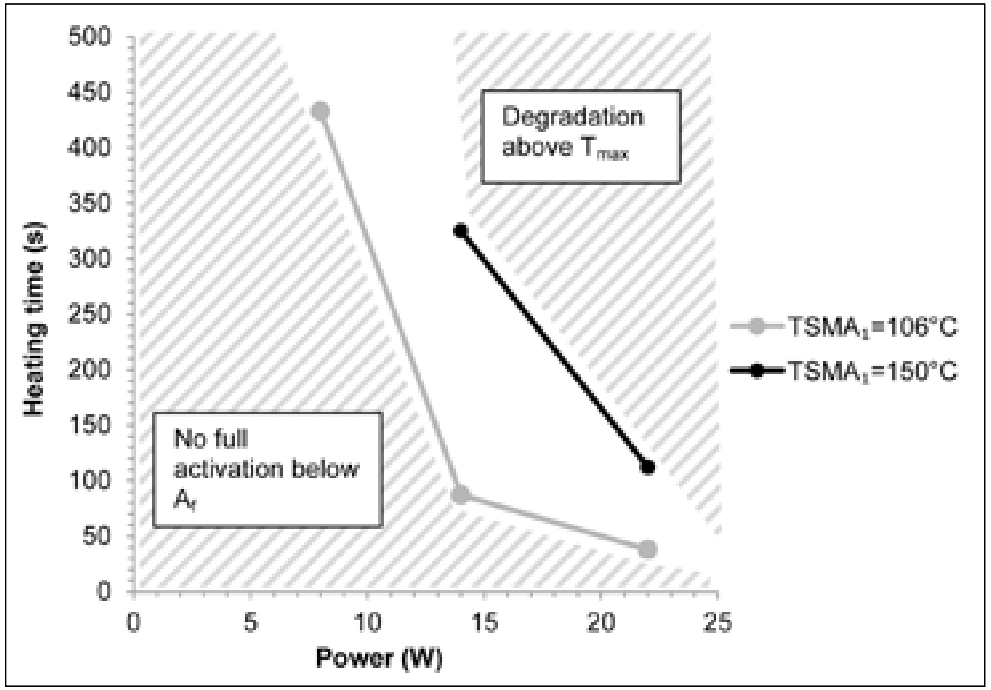

Figure 8.36 Activation window for the heating of SMA_{1+3}. The shaded parts indicate that the activation settings do not meet the heating criteria.

8.9 Conclusions

The optimal heating settings are determined by the use of the numerical model. Especially during the heating of the SMP body, the SMA temperatures are relevant. By increasing power inputs, the operation field of activation settings becomes rather narrow. Power inputs between 10 to 16 Watts give the most satisfying heating times. With the current wire length this power is related to an electric potential of 13 to 16 Volts and an electric current of 0.8 to 1 Ampere. The wires can be heated respectively 100 to 55 seconds before the SMA_2 reaches the A_s.

An electric current higher than 15 Ampere is required for the activation of the SMA_{1+3} wires in order to reach the A_f within 400 seconds of activation. The influence of the activation of the SMA_{1+3} strips on the SMA_2 surface temperature was almost unnoticeable. A very small temperature rise is found after 200 second of activation. Therefore, the heating time is not restricted by the SMA_2 temperature. However, it should be prevented that the SMA_{1+3} surface temperatures will exceed the maximum temperature of 150°C. Power inputs between 14 and 22 Watt delivered acceptable heating times. Electric currents between 20 to 25 Ampere and potentials of 0.7 to 0.88 Volts are related to these power inputs.

The cooling times are not included in this analysis. However, based on the cooling curves of the simulation data, the cooling time could be estimated. The SMP will be turned off before the SMP body temperature will reach a temperature of 92°C or when the SMA strips meet the A_f. Based on the cooling curves of the finite element model, a cooling rate of approximately 0.1 °C per second is estimated in the temperature region of 92-58°C. The cooling rate is related to the thermal transfer coefficient, which is temperature dependent. High surface temperatures will lead to higher cooling rates at a stationary ambient temperature. After deactivation of the SMP, the T_{smp} decreases from 92°C to T_{smp}<58°C in approximately 340 seconds. During this cooling time the material will regain the glassy properties and the deformation is fixated.

8.10 References

ANSYS help (webpage) Retrieved 2012 from www.ANSYS.com.

Baehr, H. D., Stephan, Karl (2006). Heat and mass transfer, Springer.

Conrad Electronic (webpage) Retrieved 2011 from www.conrad.nl.

Corner Stone Research Group Industries (webpage) Retrieved 2008-07-09 from www.crg-industries.com.

Holman, J. P. (1997). Heat transfer. New York, McGraw-Hill.

Incropera, F., Dewitt, D. (2007). Introduction to heat transfer, Wiley

Leng, J., Lan, X., et al. (2011). “Shape-memory polymers and their composites: Stimulus methods and applications.” Progress in Materials Science **56**(7): 1077-1135.

Memory Metalle GmbH (webpage) Retrieved 2008-04-16 from www.memory-metalle.com.

Moore, E. R. (1989). Styrene Polymers, John Wiley & Sons, Inc.

Thirumaleshwar, M. (2006). Fundamentals of Heat and Mass Transfer. New Delhi, Dorling Kindersley.

TiNi Alloy Company (webpage) Retrieved 2012 from www.tinialloy.com.

Verkerk, G., Broens, J. B., et al. (1992). Binas, Wolters-Noordhoff bv.

CHAPTER 9

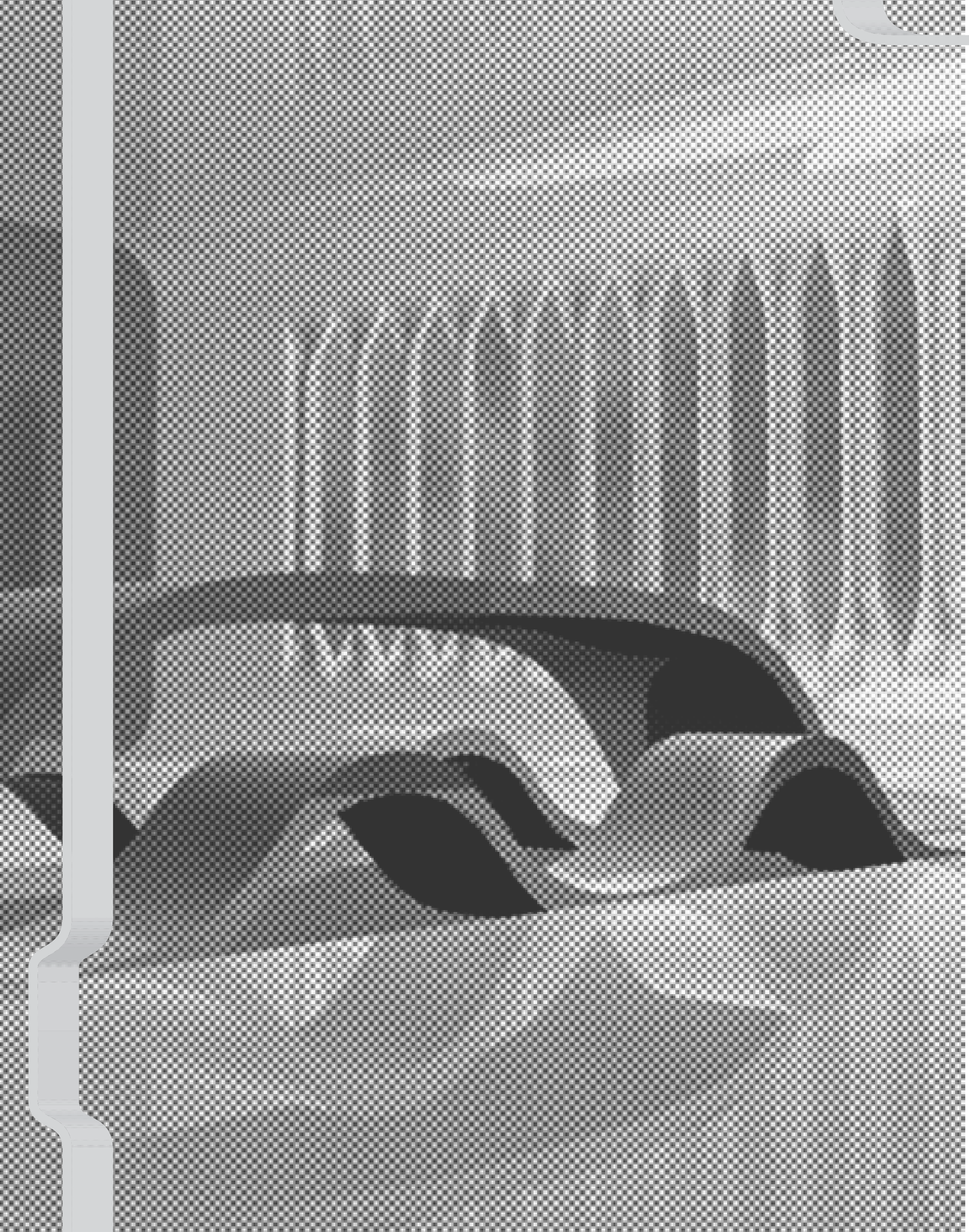

DISCUSSION AND CONCLUSION

9.1 Introduction

The architectural paradigm has shifted considerably over the last 20 years. It is highly influenced by new innovative digital design methods, material innovation, socio-cultural aspects, user interaction and sustainability challenges. The adaptive building concept is regarded to contribute extensively to the optimization of the building performance such as, for example, climate control and spatial use. The multi-functional use of buildings will lead to an optimized use of the current building stock. Additionally, it would enable the personification of buildings and spaces.

This research shows that it is possible to translate dynamic parameters into tangible expressive environments with the use of smart material systems, rather than complex mechanical structures. Knowledge transfer between different fields of science played an important role during this process. By implementing knowledge from other specializations into the field of architecture, new building solutions can become reality. This research is an exploration at the intersection of architecture and smart material technology. The integration of smart material systems in architecture will lead to novel ideas and performances in architecture. The concept was physicalized with the fabrication of a functional prototype; the adaptive building component (ABC).

The research included the conceptual, technological and user challenges faced when realizing adaptive architecture with smart material technology. With the realization of a real-time performing prototype the presented adaptive building concept is taken one step further away from a concept and one step closer to reality.

9.2 Adaptive Architecture and Smart Material Systems

Adaptive architecture was categorized into the following different levels of sophistication:

1. Flexible
2. Active
3. Dynamic
4. Interactive
5. Intelligent
6. Smart

This division was based on technological and performative advancements. These increase in terms of complexity from top to bottom.

An inventory of the current adaptive building stock indicated that performance is mainly realized from the flexible to dynamic level, while some profound examples were given on the interactive level. With the current available technologies it is possible to realize interactive and intelligent architecture. The performance level is hereby mostly dependent on the degree of sophistication of the control system. This system provides the processing of the input and output parameters. For the realization of smart architecture, profound developments are required in terms of system and material technology.

Smart material systems in the building system are currently realizing structural, climate, energy and architectural performances. These materials are unobtrusively integrated in existing building components. The intrinsic performative characteristics of the smart material systems enable small and scale lightweight applications. This is a great advantage compared to mechanical systems. Due to the extensive miniaturization of material systems, sensors, actuators and control mechanisms will become part of the micro-system of the material. Inherently, systems, such as (O) LEDs and photovoltaics and others, were also included in this material group.

No practical examples have been found of the implementation of smart material systems for shape-morphing building components. However, this performance has been envisioned by mechanical solutions, which have led to large and complex construction sizes and the generation of considerably high noise levels. Therefore, this research has been focussing on the realization of an adaptive building component (ABC) with the use of smart material systems. In particular the conceptual and technological challenges which are required to realize such a component have been studied in this research.

9.3 Design

The presented design scenarios illustrated advanced building performances on different levels of the building system. These design prospects were not only found on the studied scale of the prototype, but also promised application possibilities on larger scales. The surface tessellation will be more likely to elaborate on at this stage of the research, compared to the larger scale design scenarios.

Further development on the smart composite is required to push this technology to an application level. Naturally, the smart composite prototype cannot be transferred directly into the proposed design variations. However, it does provide an understanding of its performative behaviour.

This research aimed to map new design territories in architecture making use of smart material technologies. However, this does not mean that the application of the smart composite is restricted to this design field. Research on the implementation of smart material technology has been executed in the field of aerospace, wind turbine and automotive. Especially, immediate shape adaptation for aerodynamic optimization was studied extensively. The application of the smart composite could result in interesting applications in these fields. However, it is recognized that also here the thermo-responsive character of the smart composite might restrict the application area. The hereto related relatively slow responsive times prevent immediate fast performances. When looking at mechanical systems, the large construction sizes and weights are demanding for better solutions. Smart material system show potential for this improvement, although, extensive development is required before commercial application is possible.

9.4 User Receptiveness

The user receptiveness on the subject of adaptive environment was studied by different methods. Firstly, an internet inquiry was executed. The participant had to rate a variable amount of adaptive scenarios. The considerable high score indicated that the participant reacted positive on the proposed scenarios. The scenarios were diverse and covered different adaptive aspects of the building systems. It can be concluded that the purpose of the study was understood by the participant.

Secondly, interviews were performed with middle aged adults (40 to 60 years old) and students. During this study, the participants had to propose their own vision on an apartment configuration, based on different activities. Hereby, the participant was given a total freedom on the room configuration, shape and settings. As immediate adaptation of a building is still very conceptual, a mind-set was presented before the interview was taken. The mind-set explained that the participant should not be restricted by technical possibilities; all ideas were possible. The proposed changes were fully based on the creativity and vision of the participant. Some very interesting proposals came forward from the interview, but most proposed settings were based on realistic technological solutions. In the student group everybody proposed a change of floor and walls, whereas the middle aged group scored very low at this point. The middle aged group was more restricted to current technologies. They mainly focused on electronic advancements, such as wireless products. Thereby, less spatial solutions and out of the box solutions were given compared to the student group.

Last, an inquiry with the use of a (scaled) prototype gained interesting information on the spatial preferences of the participant. A user study has tested the concept of an adaptive floor plan and an adaptive window configuration. Also here, the configurations were based on daily activities. For the configuration of the floor plan this functional parameter was recognized as an influential aspect of the spatial use. However, the location, shape and transparency of windows are evidently more influenced by the time of the day and the amount of sunshine than to activity. The participants adjusted the window settings according to the proposed activities in some sense, but they indicated that other parameters have much more influence on these building attributes than the ones that were given.

The studies have delivered a good basis on the subject of user receptiveness on adaptive environments. Only the adaptive performance was subject of interest. The control and the level of adaptivity were beyond the scope of research.

Technological advancements are opening up possibilities for the performance of buildings. Knowledge about the receptiveness of the user can be used for the optimization of the building performance. In product development, user studies are a common tool for product optimization and testing. Particularly, in the building industry, user studies can prevent malfunctioning and define and optimize the building performance before the building is built.

9.5 Prototyping

The presented concept of the shape morphing performance of adaptive building systems was proved to be realistic by the fabrication of a small prototype. The deformation of the prototype was based on intrinsic material properties instead of the more traditional mechanically operated deformations. Multiple challenges have been successfully solved in order to develop a functional prototype.

9.5.1 Performance

The smart composite (SC) prototype featured a reversible shape deformation from a flat configuration into a 90° angle. The deformation was obtained without continuous restrain or active control. The smart composite was fabricated of Shape Memory Alloys (SMAs) embedded in a Shape Memory Polymer (SMP) matrix. The SMAs were performing as an actuator, enabling the deformation, while the SMP facilitated the fixation of this deformation. This way, the presented prototype has successfully been translated from the conceptual shape morphing performance into a physical ABC.

The deformation performance of all individual components was analysed by torsion testing. It was argued that by superposition of the delivered forces of the individual components, the performance of the composite could be observed. This aspect was validated by performance experiments of the SC prototype. The performance curves of the individual components and SC prototype were not fully identical, but were of a similar order of magnitude and showed a comparable bending angle. The deviations could be explained by the way the individual components were applied in the composite, which were related to the research set-up.

The low frequency of the SC performance does not lead to profound problems for the proposed applications. However, the application possibilities would be enlarged when the response time is increased. Especially, on the subject of shape optimization of façade tessellation for wind loads or ventilation purposes this will lead to a considerable gain. The thermoelectric activation of both components has a large influence on the activation time. Optimization can only be realized by the use of alternative activation methods, such as light and magnetism.

9.5.2 Fatigue

The high material fatigue of the SMA actuators is currently a restriction for wide architectural application. Although the fatigue factors are known (Loughlan, et al. 2002) they cannot be fully overcome. The smart composite must be able to accommodate a minimum performance lifetime in order to enable a realistic application. This performance is primarily dependent on the application method. The scenario of aerodynamic façade optimization will expect more alterations compared to the scenario of interior arrangement. Naturally, this will relate to a shorter lifetime, due to the thermal load and constrained recovery.

Based on the current available technologies, SMAs are the most suitable smart material actuators for the proposed application. This actuator delivers large stresses and large deformations, has relatively small dimensions and requires low energy activation. Other actuators cannot deliver such good performance, require considerably high actuation energy and generally have large dimensions. By determining a good balance between actuators' dimensions and performance, the large fatigue should be overcome.

9.5.3 Activation

The studied SC is based on thermo-responsive smart material systems. These materials are commercially available and very well developed. The reversible deformation is established by active control. This clearly indicates that energy is required for the activation of the SC, which results in an increase of the building energy consumption. Additionally, the environmental temperature will increase due to the thermal activation. By outdoor application this energy will be released to the environment and will not lead to a considerable increase of the outdoor temperature. For indoor applications, however, it is not desirable that the activation of the SC will lead to a substantial increase of the room temperature. This thermal increase should be monitored and kept within acceptable borders. Additionally, the loss of energy is an important disadvantage of current activation methods. However, the whole lifecycle and performance of the SC should be considered. When the SC will be applied as an adaptive daylight system, considerable energy gains in terms of cooling and heating will be found.

In chapter 6, different methods of activation for both SMP and SMA have been discussed. However, these materials are not developed on a commercial level. Further improvement of these materials will broaden the application field considerably. Especially, the elimination of the dependency of external power would be advantageous. Further study on other activation methods is recommended. However, in order to achieve an active control of the adaptive building component external energy application is inevitable. Thermo-responsive SMPs and SMAs are commercially available and extensively studied.

The performance of the SC can be optimized by accurate thermoelectric control and will increase the performance on a long term application and reduce the fatigue factor. By proper thermal activation, malfunctioning is severely reduced. The thermoelectric behaviour of the smart composite was simulated by the Finite Element Method (FEM). The numerical model was validated by thermal imaging experiments. The optimum activation settings of both the SMA and the SMP were determined with this model. This model can serve as a control tool for various design applications of the SC. Validation experiments demonstrated a good agreement between the simulation data and the experimental data. This model can be effortlessly adjusted to different scales of application.

The SMP is heated by integrated resistive wiring. These wires are embedded in the SMP matrix at the bending location. Optimization of the resistive heating method can increase the performance in terms of response time and heat loss. When more wires are integrated in the SMP matrix instead of the applied two layers, a lower activation stimulus is required in order to meet similar SMP body temperatures. Other conductive elements, such as carbon black, which are discussed in chapter 6, can improve the heating of the SMP. However, it should be noted that an increase of the conductive elements in the SMP body will affect the SMP performance in terms of stiffness and recovery behaviour. For the demonstration of the SC performance, the heating wires did meet the desired heating performance.

Ambient cooling is realized by the dissipation of thermal energy by ambient radiation and convection. This is not only a considerably slow process, but also a waste of energy. The performance of the SC can be optimized by the integration of a forced cooling system. The SMA strips are inserted in the rectangular canals of the SMP matrix. These canals could also be used for forced cooling by air or liquid material (Hulskamp 2011). By cooling the SC, the controllability is increased as well as the temperature impact on the environment. The gained heat in the cooling medium could be saved by regenerative heat recovery systems. Further development of this cooling system is recommended in order to optimize the response time and control the thermal loss.

9.5.4 Materialization and Fabrication

After the material analysis the utilized smart material systems came forward as the most appropriate materials for the desired performance. The intended reversible deformation is neatly met.

The production techniques are limited by the experimental character of the prototype. The laboratory settings add to this limitation, as these are not optimized for the fabrication of SC. However, for prototype purposes the SC meet the performance intent. The manual fabrication of the SC is very laborious; the post-processing of the SMP and the integration of the heating wires require optimization for further large scale application. Obviously, optimization of the manufacturing and assemblage method will be required for commercial large scale applications.

9.6 Final Remarks

The smart composite prototype has demonstrated the application of smart materials systems for immediate shape morphing behaviour. The faced conceptual and technological challenges have been addressed in order to obtain a shape-morphing building component. The performance of the fabricated prototype represented a significant technological advancement in terms of shape deformation and fixation.

As little is known of the application of the smart materials and the realization of adaptive building components, it was required to exceed the regular paths of architectural design. Only on this way it was possible to realize a real-time performing prototype. Interdisciplinary design was a crucial factor for the implementation of smart technologies in the built environment.

The design of the SC was optimized based on experimental data, reflecting the research driven design methodology. The experiments were executed in order to gain insight into the desired performance of the components. The executed torsion and thermal experiments were completely based on the required performance, determined by the presented design scenarios. This reflects the design driven research methodology.

Due to the intrinsic character of the smart material performance, the material could easily be embedded in the existing building structure. The integration of smart material systems will enhance the development of multifunctional building components. Rethinking the obsolete performance of a static building is required when buildings become fully adaptive. By designing adaptive environments, the designer has to consider an adaptive scenario of how the building will perform and how the users are related to this performance. The aspect *time* plays an increasingly role in the design process.

It is recognized that this thesis encompasses a wide and versatile study on the subject of adaptive architecture and smart material systems. Smart material systems show promising performance for architectural application, as is shown with the fabrication of the SC prototype. This study provides insight on the implementation of shape morphing components in the building system and hopes to stimulate other research on this subject.

9.7 Recommendations

An explorative study has been performed on user receptiveness for immediate adaptive environments. This study has been executed with a small participant group. Although this is not uncommon for explorative studies, consensus will be created by larger groups. Hereby, a close collaboration with specialists is required.

Optimization of the smart composite prototype is required for practical application. Aspects, such as fatigue, scaling, activation, costs, control, energy input and performance are important and require more detailed investigation, should the SC be brought on the market.

The executed experiments gave a good insight on the SC performance. These experiments can be used for the realization of a numerical material model. Further material studies should bring a clear view on the relation between the performance and the material dimensions. A numerical model can serve as a design tool for further product development. This design tool can be used for the validation of the presented design scenarios, the optimization of the SC performance as well as the analysis of the scaling capacities of the SC. By simulating the performance of the SC for different scales and applications, the location of the actuators can be optimized. The development of this model will require extensive research and collaboration with material specialists.

SMPs are known to be rather brittle, the strength and stiffness are considered low for structural purposes. In order to optimize the structural performance of the SC, fibre reinforcement shows great improvements on mechanical properties (Liang, et al. 1997; Gall, et al. 2000; Abrahamson, et al. 2003; Leng, et al. 2011). Reinforcement of the SMP will increase the elasticity modulus in rubbery phase, which decreases the induced strain. Consequently, the deformation stress will increase as the material will become much stiffer. Further research on the implementation of fibres is advisable; a good balance between the embedded fibres and required strain should be determined. Additionally, the weave and location of the fibres is expected to have an influence on the SC performance. Collaboration with material specialists and control engineers is crucial for further development of the SC.

9.8 References

Abrahamson, E. R., Lake, M. S., et al. (2003). "Shape Memory Mechanics of an Elastic Memory Composite Resin." Journal of Intelligent Material Systems and Structures **14**(10): 623-632.

Gall, K., Mikulas, M., et al. (2000). "Carbon Fiber Reinforced Shape Memory Polymer Composites." Journal of Intelligent Material Systems and Structures **11**(11): 877-886.

Hulskamp, A. W. (2011). The smart rotor concept on wind turbines actuator Dissertation, Delft University of Technology.

Leng, J., Lan, X., et al. (2011). "Shape-memory polymers and their composites: Stimulus methods and applications." Progress in Materials Science **56**(7): 1077-1135.

Liang, C., Rogers, C. A., et al. (1997). "Investigation of Shape Memory Polymers and Their Hybrid Composites." Journal of Intelligent Material Systems and Structures **8**(4): 380-386.

Loughlan, J., Thompson, S. P., et al. (2002). "Buckling control using embedded shape memory actuators and the utilisation of smart technology in future aerospace platforms." Composite Structures **58**(3): 319-347.

appendix 1 chapter 2

Overview analysed projects

Rietveld-Schröder huis, Gerrit Rietveld, 1924

This house is built in the timeline of “de Stijl”. This house contains an “open floor plan”, which indicates that no structural and fitted elements provide a division of space. By use of sliding elements, the open space can be reconfigured in smaller areas, when required. The sliding of the walls has to be executed manually, which defines a flexible architecture.

Figure 0.1 Rietveld-Schröder house interior picture with sliding walls

Tugendhat house, Mies van der Rohe, 1956

House with open floor plan, where draperies on a ceiling track are used for space division. This reconfiguration of the space is executed manually, and is therefore categorized as flexible architecture.

Figure 0.2 Tugendhat house. Photo courtesy Andrei Kandl

Aluminium house, Floyd D'Angelo, 1962

The house is executed with a mechanical revolving system, facilitating a 130 degree rotation. Based on reverse heliotrope behaviour of the building, the windows will turn away from the sun. The sun direction was detected with a photovoltaic cell, enabling the rotation of the building (Aluminum house webpage). The sun was actively detected and controlled the house position; therefore this is categorized as dynamic architecture.

Figure 0.3 Aluminium house. Image courtesy unknown.

Fukuoka apartment building, Steven Holl, 1992

The apartments are made with free floor plans. By manually reconfiguring the hinged walls, extra rooms can be created. The walls can be reconfigured to enlarge the living room during day time or to enlarge the bedroom during night time. This system is considered flexible architecture.

Figure 0.4 Fukuoka apartment building.

Delfts Blauw, De Architecten Cie, 1998

The sun shading system is constructed of a sliding system. Within the sliding principle, different settings are possible. The shutters can be relocated along the rails by a motorized control system. The angle of the louvers can be adjusted manually. This is considered active architecture.

Figure 0.5 Delfts blauw, Delft, De Architecten Cie., 1998

Cyclebowl, Atelier Brückner, 2000

This temporary pavilion was built for the Hannover Messe. The façade of this pavilion was constructed out of ETFE film. By pneumatic activation, the transparency of the skin could be adjusted. Additionally, inflatable tubes were integrated in the roof system for active daylight control. By inflating them, the tubes were performing as a sun shading system (Ritter, et al. 2007). Slatted openings at the roof were controlled by a dynamic system for natural ventilation purposes. The louvers are opened or closed depending on the measured carbon dioxide level, humidity and temperature (Jeska 2008).

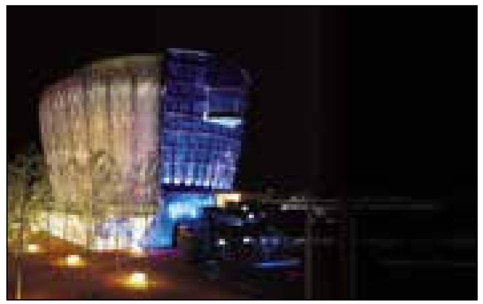

Figure 0.6 Cyclebowl façade. Image courtesy Atelier Brückner.

Figure 0.7 Cyclebowl roof system with integrated active daylight system. Image courtesy Atelier Brückner.

Naked house, Shigeru Ban, 2000
This house is constructed with an open floor plan. The bedrooms are closed element which can be moved through the open space, creating new configurations. This flexible architecture enables a continuous adjustment of the space configuration.

Figure 0.8 Naked house, Image courtesy Architectureweek.com

Rotorhouse, Lugi Colani, 2000
The house is executed with a rotating area, in which the kitchen, bathroom and bedroom are located. By the use of a remote control, the preferred room can be selected. This automated control is considered active architecture.

Figure 0.9 Rotorhouse, exterior

Figure 0.10 Rotorhouse, Interior.

Suite Vollard, Bruno de Franco and Sergio Silka, 2001
Suite Vollard is an 11-story building of which every floor can rotate individually 360 degrees in both directions. One rotation will take approximately an hour. Speed of rotation is variable to a maximum of a determined comfortable speed. The rotation is activated by the user via a control panel with integrated voice recognition. This performance is considered active architecture.

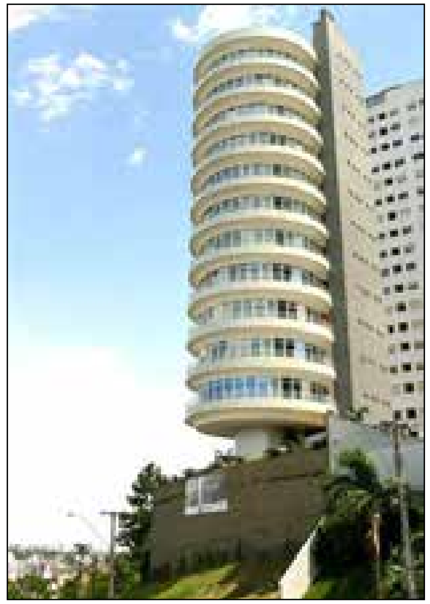

Figure 0.11 Suite Vollard. Image courtesy unknown.

Chanel Ginza, Peter Marino Associated, 2004
This building façade is designed to perform as a lighting and marketing tool. Next to this, a sufficient daylight system is integrated in the building façade. The façade was constructed out of a three layered system. Motorized roller shades are used for daylight control, activated by a sensor system. The electro chromic window system changes the transparent window surface into a dark screen, which enables optimized visualizations. A LED system provides marketing and lighting possibilities during night time. Only black and white projects are possible. This dynamic architecture is one of the many media oriented façades in the Ginza area in Tokyo.

Figure 0.12 Figure 6 Chanel Ginza. Image courtesy Kenzo

Galleria Department store, UNstudio, 2004
The façade system features different light settings due to changing colour patterns, which vary over time. Moving visualization on the building surface is enabled by integrated LEDs in the façade system. By the use of diffuse glass panels, pixelating visualisations are possible. The dynamic aspect here can be found in the fact that the lights can not only be turned on or off, but also different colour arrangements can be made. A different colour program can be designed by the owner of the building. This enables a constantly changing façade representation in terms of colour and pattern. The colour pattern is controlled by a pre-set colour program. These programs can be adjusted manually, depending on the required image representation. This façade is considered dynamic.

Figure 0.13 Galleria Department store, Seoul, UNStudio, 2003. Image courtesy UNStudio

Allianz Arena, Herzog & De Meuron, 2005
The building is constructed out of ETFE cushions, of which the pressure is automatically adjusted to maintain the stiffness. The colour of every cushion can be adapted to set preferences in the colours white, red or blue. This building is considered dynamic.

Figure 0.14 Allianz Arena. Image courtesy Joachim Schneider

Shanghai Qizhong Centre, Environmental Design Institute, 2005
The retractable roof can be opened and closed for climate protection purposes. Every component is moving over a rail system. This motorized system is controlled manually. The magnolia-like roof system takes approximately 8 minutes for opening and closing. This manual control is considered active.

Figure 0.15 Shanghai Qizhong Centre

Figure 0.16 Shanghai Qizhong Centre.

Enteractive, Electroland, 2006

A LED system is integrated in the façade of the Metloft apartment building. This projection system is controlled by the visitor's behaviour. A control panel is located at the entrance of the apartment building and is a reflection of the facade pattern. The visitor can move over the control panel, activating a reaction based on light patterns and sound. This reaction can in turn provoke a reaction by the visitor initiating a different light performance. This interactive system can be controlled by multiple visitors simultanuously.

Figure 0.17 Enteractive, Electroland. Image courtesy Electroland.

Sliding house, dRMM, 2009

The exterior skin is made of a mobile element, which can slide over a rail system. This mobile element can provide shelter for the adjacent glass house, or the open space between the two buildings. The sliding is enabled by electric motors, of which the batteries are charged by solar panels. The sliding house is considered active architecture.

Figure 0.18 Sliding house. Image courtesy dRMM.

Chabot College, tBP Architects, 2009

Windows can change their transparency according to amount of sun radiation. The window can be fully transparent or translucent to prevent heating and glare. The system is automated controlled by the use of sensors. This dynamic system can be overruled by the users, and changed manually.

Figure 0.19 Chabot College. Image courtesy Eric Sahin.

POLA, Hoberman Associates, 2009

Adaptive shading system can be controlled manually. Windows can open and close automatically by a temperature sensoring system. By implementing a LED system, the facade is used as a light show during night-time.

Figure 0.20 POLA Ginza building. Image courtesy Mamoru Ishguro

References

Aluminum house (webpage) Retrieved 2012 from www.preservationnation.org.

Jeska, S. (2008). Transparent plastics design and technology. Basel, Birkhäuser.

Ritter, A. and Müller, A. (2007). Smart Materials in Architecture, Interior Architecture and Design. Boston, Birkhäuser.

Appendix 2 Chapter 5

Questionnaire Internet Inquiry

Algemene vragen

- **Wat is uw leeftijd?**

jaar

- **Wat is uw geslacht?**

❍ Man
❍ Vrouw

- **Heeft u een partner?**

❍ ja
❍ nee

- **Uit hoeveel personen bestaat uw huishouden?**(inclusief uzelf)

personen

- **Wat is uw woonsituatie?**

❍ Appartement
❍ Rijtjeshuis
❍ Twee onder een kap
❍ Vrijstaand huis
❍ Studentenhuis
❍ Anders

- **Wat is uw hoogst behaalde opleiding?**

❍ Basis onderwijs
❍ lbo
❍ vmbo/mavo
❍ havo
❍ vwo
❍ MBO
❍ HBO
❍ WO
❍ Anders

- **Wat is uw inkomen per jaar?**

❍ geen inkomen, ben student
❍ ben werkeloos
❍ minder dan 20.000 euro
❍ 20.000 tot 50.000 euro
❍ meer dan 50.000 euro

- **Bent u in het bezit van een auto?**

❍ ja
❍ nee

- **Wat voor vervolgopleiding heeft u gedaan/doet u?**

- **Wat is uw beroep?(als u nog niet werk hoeft u niks in te vullen)**

- **Waar is uw woning?**

❍ Centrum
❍ Buitenwijk
❍ Dorp
❍ Platteland
❍ Anders

- **Geef de mate aan van hoe creatief uzelf bent.**

niet creatief ❍ ❍ ❍ ❍ ❍ ❍ ❍ ❍ ❍ ❍ Heel erg creatief

- **Wat is uw schoenmaat?**

Wilt u voordat u met de volgende vragen begint, het hier onderstaande stukje tekst lezen om u in te leven voor de volgende vragen.

U leeft in het jaar 2030 en u woont in een eenpersoonsappartement. De ruimte is niet al te groot waar u eet, slaapt, woont, studeert en u ontvangt er af en toe visite. Stelt u voor dat u net als een tovenaar uw appartement kan veranderen zoals u het wilt hebben. Alles is mogelijk alles kan. U kunt bijvoorbeeld uw muren van uw kamer verschuiven, uw kamer vergroten, de kleur van uw muur veranderen, de badkamer wegtoveren en een bed te voor schijn halen. Uw ramen draaien mee met de richting van de zon en uw voorgevel ziet er elke dag anders uit. Stelt u voor dat uw huis van een zeer flexibel materiaal is en dat u alles kan vervormen zoals u dat wilt.

Wij doen onderzoek naar wat men aanpasbaar wil hebben in een woning. Daarnaast onderzoeken wij de mate in hoe ver men aanpasbaarheden accepteert en hoe men hier tegenover staan. Er volgen een aantal voorbeelden van aanpasbaarheden. Hoe staat u tegenover deze aanpasbaarheden?

- **U kunt uw balkon in- en uitschuiven.**

heel erg negatief ❍ ❍ ❍ ❍ ❍ Heel erg positief

- **Uw ramen kunnen met de zon meebewegen.**

heel erg negatief ❍ ❍ ❍ ❍ ❍ Heel erg positief

- **U kunt meerdere in- en uitgangen creëren in uw kamers.**

heel erg negatief ❍ ❍ ❍ ❍ ❍ Heel erg positief

- **U kunt met een druk op de knop de hardheid van uw vloerbedekking veranderen (bijvoorbeeld van zachte vloerbedekking naar hard laminaat).**

heel erg negatief ❍ ❍ ❍ ❍ ❍ Heel erg positief

- **U kunt uw dak open en dicht doen.**

heel erg negatief ❍ ❍ ❍ ❍ ❍ Heel erg positief

- **U kunt met een druk op de knop de kleur van de muren veranderen.**

heel erg negatief ❍ ❍ ❍ ❍ ❍ Heel erg positief

- **U kunt uw schilderijen in ramen veranderen.**

heel erg negatief ❍ ❍ ❍ ❍ ❍ Heel erg positief

- **U kunt uw meubels uit de vloer laten komen en er weer in laten verdwijnen.**

heel erg negatief ❍ ❍ ❍ ❍ ❍ Heel erg positief

- **U kunt de buitenkant van uw huis van een kubusachtige vorm naar elke denkbare vorm omtoveren.**

heel erg negatief ❍ ❍ ❍ ❍ ❍ Heel erg positief

- **U kunt uw huis van buiten licht laten geven.**

voorbeelden

heel erg negatief ❍ ❍ ❍ ❍ ❍ Heel erg positief

- **U kunt een deel van uw interieur laten verdwijnen als er bijvoorbeeld bezoek is.**

heel erg negatief ❍ ❍ ❍ ❍ ❍ Heel erg positief

- **U kunt uw huis verplaatsen.**

heel erg negatief ❍ ❍ ❍ ❍ ❍ Heel erg positief

- **U kunt uw huis laten zweven.**

heel erg negatief ❍ ❍ ❍ ❍ ❍ Heel erg positief

- **U kunt uw huis aan de buitenkant met een gordijn afsluiten van zonlicht.**

heel erg negatief ❍ ❍ ❍ ❍ ❍ Heel erg positief

- **U kunt meer/minder kamers creëren door muren te verplaatsen**

heel erg negatief ❍ ❍ ❍ ❍ ❍ Heel erg positief

- **U kunt uw woningruimte vergroten/verkleinen door de buitenmuren te verplaatsen.**

heel erg negatief ❍ ❍ ❍ ❍ ❍ Heel erg positief

- **U kunt uw huis onzichtbaar maken.**

heel erg negatief ❍ ❍ ❍ ❍ ❍ Heel erg positief

- **U kunt uw kamers verrijden.**

voorbeeld: *NAKED HOUSE - Saitama, Japan*

heel erg negatief ❍ ❍ ❍ ❍ ❍ Heel erg positief

- **Uw wanden bewegen tijdens een film.**

heel erg negatief ❍ ❍ ❍ ❍ ❍ Heel erg positief

- **U kunt uw elektrische apparaten overal neerzetten, want u bent niet gebonden aan de plaats van stopcontacten.**

heel erg negatief ❍ ❍ ❍ ❍ ❍ Heel erg positief

- **U kunt op uw vloer gaan slapen. Elke plek in uw vloer kan in een matras veranderen.**

heel erg negatief ❍ ❍ ❍ ❍ ❍ Heel erg positief

- **U kunt uw muren zacht maken.**

heel erg negatief ❍ ❍ ❍ ❍ ❍ Heel erg positief

- **U kunt overal openingen maken in uw wanden om naar buiten te gaan.**

heel erg negatief ❍ ❍ ❍ ❍ ❍ Heel erg positief

- **U kunt van uw trap een glijbaan maken en dit weer omkeren.**

heel erg negatief ❍ ❍ ❍ ❍ ❍ Heel erg positief

- **U kunt een ruimte van functie laten veranderen, bijvoorbeeld van badkamer naar keuken.**

voorbeeld: *Rotor house van Luigi Colani*
Functie van de kamer veranderen door het rond te draaien.

heel erg negatief ❍ ❍ ❍ ❍ ❍ Heel erg positief

- **U kunt de sfeer in huis aanpassen, doordat de meubels van materiaal en kleur kunnen veranderen.**

heel erg negatief ❍ ❍ ❍ ❍ ❍ Heel erg positief

- **Uw ramen kunt u wel of niet transparant maken.**

heel erg negatief ❍ ❍ ❍ ❍ ❍ Heel erg positief

Open vragen

- **Wat ziet u als nadelen van een aanpasbaar/veranderbaar huis?**

- **Wat ziet u als voordelen van een aanpasbaar/veranderbaar huis?**

- **Als u nog opmerkingen of vragen heeft over deze vragenlijst kunt u deze hier invullen.**

- **Als u op de hoogte gehouden wilt worden over de resultaten van dit onderzoek, vul dan uw e-mail adres in.**

Appendix 3 Chapter 5

Adaptive floor plan settings

Floor plans and furniture arrangements for the specific activities

Legenda:

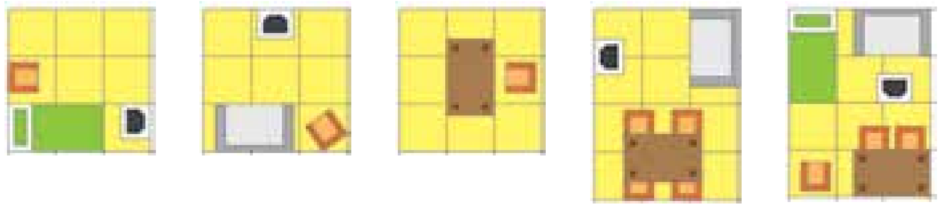

Subject A Sleeping | Subject A Relaxing | Subject A Studying | Subject A Dining | Subject A General

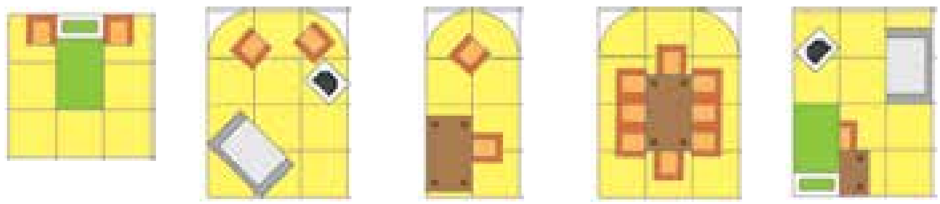

Subject B Sleeping | Subject B Relaxing | Subject B Studying | Subject B Dining | Subject B General

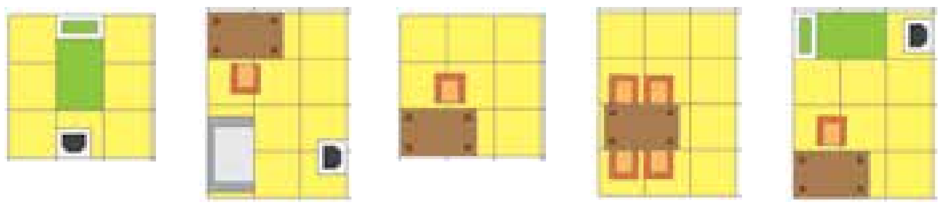

Subject C Sleeping | Subject C Relaxing | Subject C Studying | Subject C Dining | Subject C General

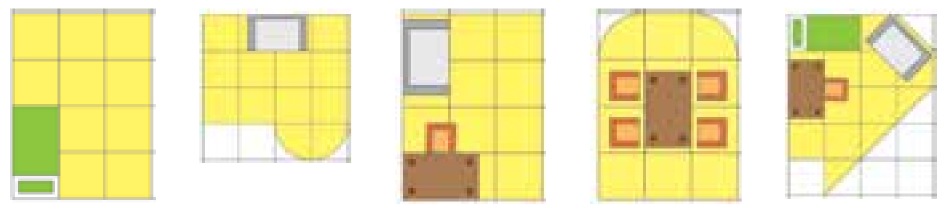

Subject D Sleeping | Subject D Relaxing | Subject D Studying | Subject D Dining | Subject D General

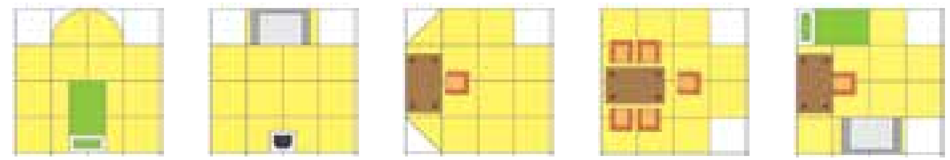

Subject E Sleeping | Subject E Relaxing | Subject E Studying | Subject E Dining | Subject E General

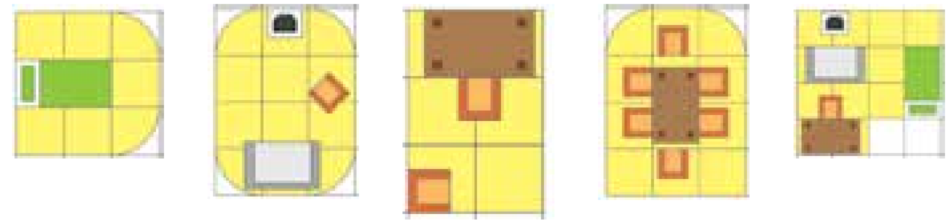

Subject F Sleeping | Subject F Relaxing | Subject F Studying | Subject F Dining | Subject F General

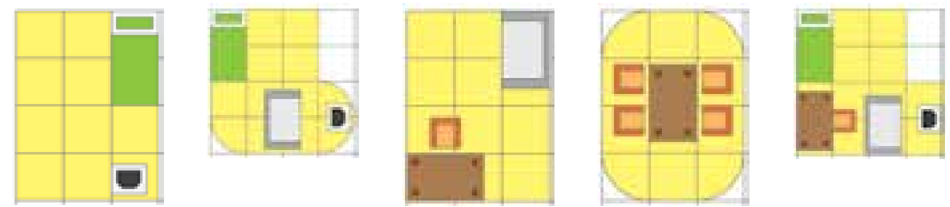

Subject G Sleeping | Subject G Relaxing | Subject G Studying | Subject G Dining | Subject G General

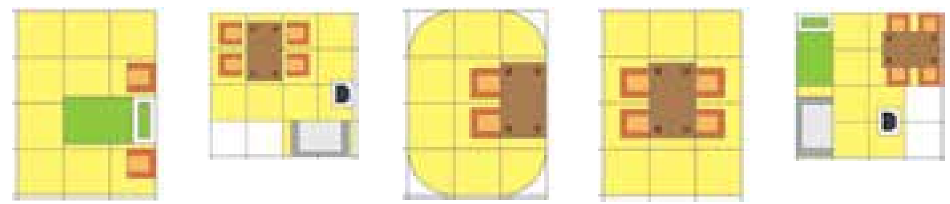

Subject H Sleeping | Subject H Relaxing | Subject H Studying | Subject H Dining | Subject H General

Appendix 4 Chapter 8

Finite element model in ANSYS

```
Fini
/clear
WIDTH= 60e-3 !x
THICKNESS = 8e-3
LENGTH= 80e-3 !z
STEP=10
fini
/prep7

! Element types
et,1,70 !SMP
et,2,68 !Constantan
et,3,157 !SMA
!create SURF 152 for radiation
et,5,152
keyopt,5,5,1
keyopt,5,9,1

! Material Properties
! SMP
mptemp,1,25,50,62,95,200
mp,dens,1,1050
mp,kxx ,1,.17
mpdata,c
,1,1,1300,1400,1870,1900,2243
mpdata,hf,1,1,3.4,8.8,9.6,11,13.3
!Constantan
mp,dens,2,8900
mp,kxx ,2,22
mp,c   ,2,410
mp,rsvx,2,.49e-6
!SMA
mp,dens,3,6450
mp,c   ,3,322
mpdata,kxx,3,1,9,9,9,18,18
mpdata,rsvx-
,3,1,5e-7,5e-7,5e-7,11e-7,11e-7
!surf 152
mp,emis,5,0.9

! Real constants
r,1,
r,2,.49e-7
r,3,.50e-3
!surf 152
r,5,1,5.67e-8
toffst,273.15

! Solid modelling
block,0,WIDTH,0,THICK-
NESS,0,LENGTH
! Cut X-direction
wprot,,,90
wpoff,,,3e-3
vsbw,all
wpoff,,,2e-3
vsbw,all
wpoff,,,10e-3
vsbw,all
wpoff,,,12.5e-3
vsbw,all
wpoff,,,5e-3
vsbw,all
wpoff,,,12.5e-3
vsbw,all
wpoff,,,10e-3
vsbw,all
wpoff,,,2e-3
vsbw,all
wpcsys,-1,0
! Cut Y-direction
wprot,,-90
wpoff,,,2e-3
vsbw,all
wpoff,,,2e-3
vsbw,all
wpoff,,,2e-3
vsbw,all
wpcsys,-1,0
! Cut Z-direction
wprot
wpoff,,,20.5e-3
vsbw,all
wpoff,,,3e-3
vsbw,all
wpoff,,,3e-3
vsbw,all
wpoff,,,3e-3
vsbw,all
wpoff,,,3e-3
vsbw,all
wpoff,,,3e-3
vsbw,all
wpoff,,,3e-3
vsbw,all
wpoff,,,3e-3
vsbw,all
wpoff,,,3e-3
vsbw,all
wpoff,,,3e-3
vsbw,all
wpoff,,,3e-3
vsbw,all
wpoff,,,3e-3
vsbw,all
wpoff,,,3e-3
vsbw,all
wpcsys,-1,0
! Mesh solids
type,1
mat,1
real,1
esize,1e-3
vmesh,all

! Mesh links
!Constantan
type,2
mat,2
real,2
lsel,s,loc,y,2e-3
lsel,a,loc,y,6e-3
lsel,u,loc,x,0,2e-3
lsel,u,loc,x,5e-3
lsel,u,loc,x,15e-3
lsel,u,loc,x,27.5e-3
lsel,u,loc,x,32.5e-3
lsel,u,loc,x,45e-3
lsel,u,loc,x,55e-3
lsel,u,loc,x,58e-3,60e-3
lsel,u,loc,z,0
lsel,u,loc,z,80e-3
lsel,u,,,24
lsel,u,,,242
lsel,u,,,385
lsel,u,,,451
lsel,u,,,581
lsel,u,,,772
lsel,u,,,843
lsel,u,,,984
lsel,u,,,1042
lsel,u,,,1098
lsel,u,,,1312
lsel,u,,,1366
lsel,u,,,1550
lsel,u,,,1582
lsel,u,,,1852
lsel,u,,,2122
lsel,u,,,162
lsel,u,,,285
lsel,u,,,510
lsel,u,,,547
lsel,u,,,782
lsel,u,,,811
lsel,u,,,1052
lsel,u,,,1116
lsel,u,,,1322
lsel,u,,,1384
lsel,u,,,1489
lsel,u,,,1592
lsel,u,,,1688
lsel,u,,,1820
lsel,u,,,1862
lsel,u,,,2132
lsel,a,,,2032
lsel,a,,,2063
cm,Li_1,line
lmesh,all

! Mesh shells
type,3
mat,3
real,3
asel,s,loc,y,4e-3
asel,r,loc,x,5e-3,1.5e-2
cm,SMA_1,area
amesh,all
asel,s,loc,y,4e-3
asel,r,loc,x,2.75e-2,3.25e-2
cm,SMA_2,area
```

```
amesh,all
asel,s,loc,y,4e-3
asel,r,loc,x,4.5e-2,5.5e-2
cm,SMA_3,area
amesh,all
allsel

! Electric earth link and shell ends - z=0
! first constantan, element type 2
esel,s,type,,2
nsle
nsel,r,loc,z,0
nsel,r,loc,y,0.2e-2
d,all,volt,0
!Then on SMA_1 and 2
cmsel,s,SMA_1
cmsel,a,SMA_2
nsla,s,1
nsel,r,loc,z,0
d,all,volt,0
allsel

! Link ends node parameter - for con-
stantan on z=0 and y=6e-3, node gets
parameter for easier selection
cmsel,s,Li_1
nsll,s,1
nsel,r,loc,z,0
nsel,r,loc,y,6e-3
*get,Li_1_prime,node,,num,max
allsel

! Coupled sets for shell ends + node
parameter -for SMA_2 on z=80e-3 for
SMA_3 on z=0
cmsel,s,SMA_2
nsla,s,1
nsel,r,loc,z,80e-3
cp,1,volt,all
*get,SMA_2_prime,cp,1,term,1,node
allsel
cmsel,s,SMA_3
nsla,s,1
nsel,r,loc,z,0
cp,2,volt,all
*get,SMA_3_prime,cp,2,term,1,node
allsel
! couple sets for end points on SMA_1
and SMA_3 on z=80e-3
cmsel,s,SMA_1
cmsel,a,SMA_3
nsla,s,1
nsel,r,loc,z,80e-3
cp,next,volt,all
allsel

!create esurf
!first node
!location node
n,next,0.5*WIDTH,10*THICK-
NESS,0.5*LENGTH
*get,radnode,node,,num,max
d,radnode,temp,25esel,s,type,,1
nsel,s,ext
type,5
real,5
mat,5
esurf,radnode
finish

! Convection boundary condition on
edges solid
/prep7
esel,s,type,,1
nsel,s,ext
sf,all,conv,-1,25
Allsel
fini

!!!!!!START LOADING
allsel
/solu
! Solution settings
antype,trans
deltim,5
outres,all,all
kbc,1
tunif,25
!!!!!!!!!!!!!!!!!!!!!!!!!!!!!!!
! Loading wires experiment 1-3
! 1st loadstep
d,Li_1_prime,volt,10
! Loading SMA
d,SMA_2_prime,volt,0
d,SMA_3_prime,volt,0
time,400
Save
solve
!2nd loadstep cooling wires
/solu
! Delete loads previous loadstep
ddele,Li_1_prime,volt
! Loading wires
d,Li_1_prime,volt,0
time,800
save
solve

!!!!!!!!!!!!!!!!!!!!!!!!!!!!!!!
!Loading SMA experiment 4-6
!1st loadstep
f,SMA_3_prime,amps,10
time,200
save
solve

!2nd loadstep cooling SMA
/solu
! delete force op SMA
fdele,SMA_3_prime,amps
!loading SMA
d,SMA_3_prime,volt,0
time,402
save
solve
,1,1,1300,1400,1870,1900,2243
mpdata,hf,1,1,3.4,8.8,9.6,11,13.3
!Constantan
mp,dens,2,8900
mp,kxx ,2,22
mp,c   ,2,410
mp,rsvx,2,.49e-6
!SMA
mp,dens,3,6450
mp,c   ,3,322
mpdata,kxx,3,1,9,9,9,18,18
mpdata,rsvx-
,3,1,5e-7,5e-7,5e-7,11e-7,11e-7
!surf 152
mp,emis,5,0.9

! Real constants
r,1,
r,2,.49e-7
r,3,.50e-3
!surf 152
r,5,1,5.67e-8
toffst,273.15

! Solid modelling
block,0,WIDTH,0,THICKNESS,0,LENG
TH
! Cut X-direction
wprot,,,90
wpoff,,,3e-3
vsbw,all
wpoff,,,2e-3
vsbw,all
wpoff,,,10e-3
vsbw,all
wpoff,,,12.5e-3
vsbw,all
wpoff,,,5e-3
vsbw,all
wpoff,,,12.5e-3
vsbw,all
wpoff,,,10e-3
vsbw,all
wpoff,,,2e-3
vsbw,all
wpcsys,-1,0
! Cut Y-direction
wprot,,-90
wpoff,,,2e-3
vsbw,all
wpoff,,,2e-3
vsbw,all
wpoff,,,2e-3
vsbw,all
wpcsys,-1,0
! Cut Z-direction
wprot
wpoff,,,20.5e-3
vsbw,all
wpoff,,,3e-3
vsbw,all
wpoff,,,3e-3
vsbw,all
wpoff,,,3e-3
vsbw,all
wpoff,,,3e-3
vsbw,all
```

```
wpoff,,,3e-3
vsbw,all
wpoff,,,3e-3
vsbw,all
wpoff,,,3e-3
vsbw,all
wpoff,,,3e-3
vsbw,all
wpoff,,,3e-3
vsbw,all
wpoff,,,3e-3
vsbw,all
wpoff,,,3e-3
vsbw,all
wpoff,,,3e-3
vsbw,all
wpoff,,,3e-3
vsbw,all
wpcsys,-1,0
! Mesh solids
type,1
mat,1
real,1
esize,1e-3
vmesh,all

! Mesh links
!Constantan
type,2
mat,2
real,2
lsel,s,loc,y,2e-3
lsel,a,loc,y,6e-3
lsel,u,loc,x,0,2e-3
lsel,u,loc,x,5e-3
lsel,u,loc,x,15e-3
lsel,u,loc,x,27.5e-3
lsel,u,loc,x,32.5e-3
lsel,u,loc,x,45e-3
lsel,u,loc,x,55e-3
lsel,u,loc,x,58e-3,60e-3
lsel,u,loc,z,0
lsel,u,loc,z,80e-3
lsel,u,,,24
lsel,u,,,242
lsel,u,,,385
lsel,u,,,451
lsel,u,,,581
lsel,u,,,772
lsel,u,,,843
lsel,u,,,984
lsel,u,,,1042
lsel,u,,,1098
lsel,u,,,1312
lsel,u,,,1366
lsel,u,,,1550
lsel,u,,,1582
lsel,u,,,1852
lsel,u,,,2122
lsel,u,,,162
lsel,u,,,285
lsel,u,,,510
lsel,u,,,547
lsel,u,,,782
lsel,u,,,811
lsel,u,,,1052
lsel,u,,,1116
lsel,u,,,1322
lsel,u,,,1384
lsel,u,,,1489
lsel,u,,,1592
lsel,u,,,1688
lsel,u,,,1820
lsel,u,,,1862
lsel,u,,,2132
lsel,a,,,2032
lsel,a,,,2063
cm,Li_1,line
lmesh,all

! Mesh shells
type,3
mat,3
real,3
asel,s,loc,y,4e-3
asel,r,loc,x,5e-3,1.5e-2
cm,SMA_1,area
amesh,all
asel,s,loc,y,4e-3
asel,r,loc,x,2.75e-2,3.25e-2
cm,SMA_2,area
amesh,all
asel,s,loc,y,4e-3
asel,r,loc,x,4.5e-2,5.5e-2
cm,SMA_3,area
amesh,all
```



```
allsel

! Electric earth link and shell ends - z=0
! first constantan, element type 2
esel,s,type,,2
nsle
nsel,r,loc,z,0
nsel,r,loc,y,0.2e-2
d,all,volt,0
!Then on SMA_1 and 2
cmsel,s,SMA_1
cmsel,a,SMA_2
nsla,s,1
nsel,r,loc,z,0
d,all,volt,0
allsel

! Link ends node parameter - for con-
stantan on z=0 and y=6e-3, node gets
parameter for easier selection
cmsel,s,Li_1
nsll,s,1
nsel,r,loc,z,0
nsel,r,loc,y,6e-3
*get,Li_1_prime,node,,num,max
allsel

! Coupled sets for shell ends + node
parameter -for SMA_2 on z=80e-3 for
SMA_3 on z=0
cmsel,s,SMA_2
nsla,s,1
nsel,r,loc,z,80e-3
cp,1,volt,all
*get,SMA_2_prime,cp,1,term,1,node
allsel
cmsel,s,SMA_3
nsla,s,1
nsel,r,loc,z,0
cp,2,volt,all
*get,SMA_3_prime,cp,2,term,1,node
allsel
! couple sets for end points on SMA_1
and SMA_3 on z=80e-3
cmsel,s,SMA_1
cmsel,a,SMA_3
nsla,s,1
nsel,r,loc,z,80e-3
cp,next,volt,all
allsel

!create esurf
!first node
!location node
n,next,0.5*WIDTH,10*THICK-
NESS,0.5*LENGTH
*get,radnode,node,,num,max
d,radnode,temp,25esel,s,type,,1
nsel,s,ext
type,5
real,5
mat,5
esurf,radnode
finish

! Convection boundary condition on
edges solid
/prep7
esel,s,type,,1
nsel,s,ext
sf,all,conv,-1,25
Allsel
fini

!!!!!!START LOADING
allsel
/solu
! Solution settings
antype,trans
deltim,5
outres,all,all
kbc,1
tunif,25
!!!!!!!!!!!!!!!!!!!!!!!!!!!!!!
! Loading wires experiment 1-3
! 1st loadstep
d,Li_1_prime,volt,10
! Loading SMA
d,SMA_2_prime,volt,0
d,SMA_3_prime,volt,0
time,400
Save
solve
!2nd loadstep cooling wires
/solu
! Delete loads previous loadstep
```

```
ddele,Li_1_prime,volt
! Loading wires
d,Li_1_prime,volt,0
time,800
save
solve

!!!!!!!!!!!!!!!!!!!!!!!!!!!!!!!!
!Loading SMA experiment 4-6
!1st loadstep
f,SMA_3_prime,amps,10
time,200
save
solve

!2nd loadstep cooling SMA
/solu
! delete force op SMA
fdele,SMA_3_prime,amps
!loading SMA
d,SMA_3_prime,volt,0
time,402
save
solve
```

SUMMARY

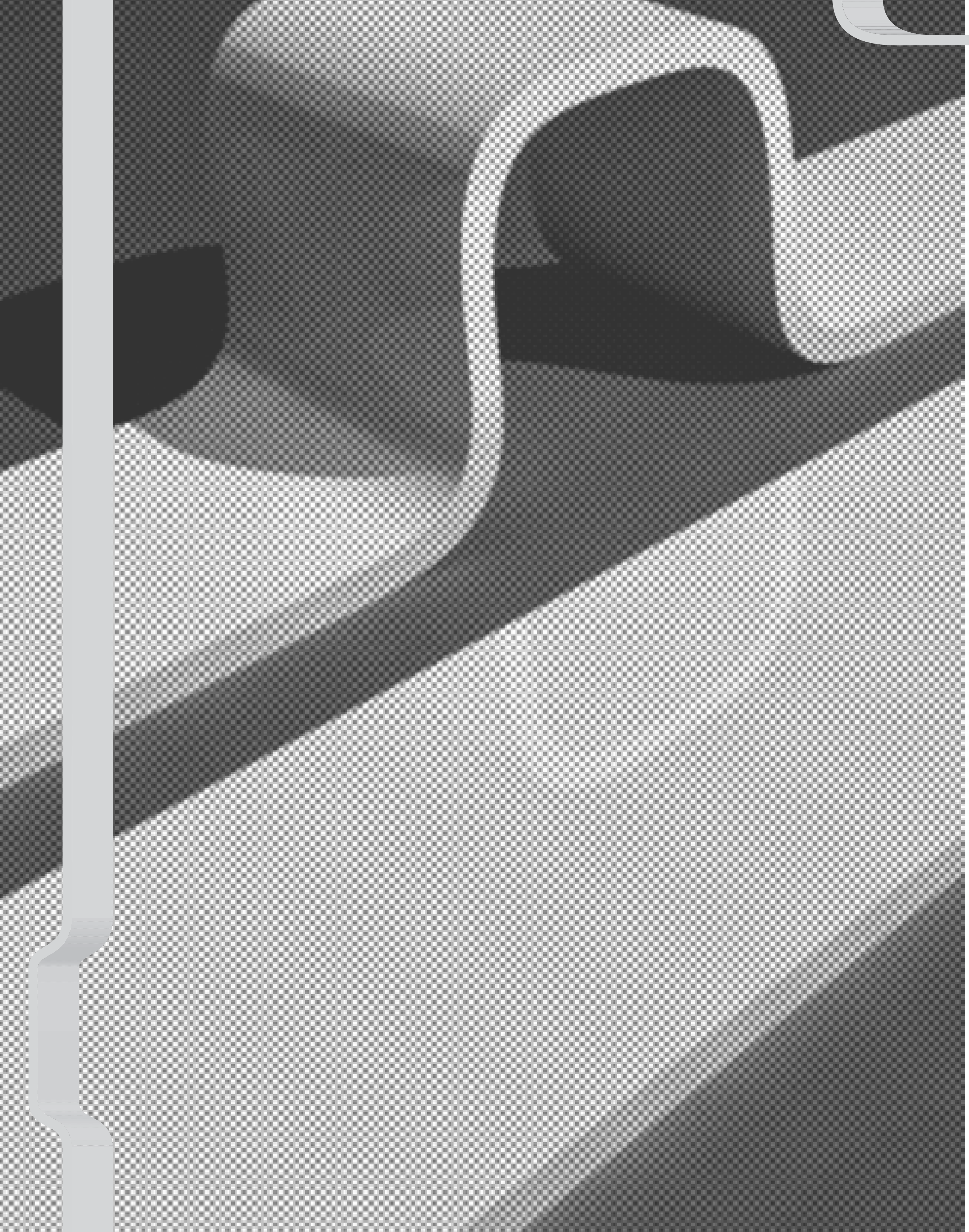

SMART MATERIALS FOR THE REALIZATION OF AN ADAPTIVE BUILDING COMPONENT

Over the last 150 years more technological advancements have been made compared to any other time in history. Additionally, the pace of innovation has increased enormously. Technological innovations such as internet, electronic devices and mobility have an important influence on the socio-cultural developments of society. However, when considering the built environment there is clearly a discrepancy between our living environment and perception and our present way of living. Technological advances should become more embedded in architecture.

Digital architectural design has emerged from building visualization and representation into geometrical design models. These models simulate performative digital environments that are constantly adjusting to dynamic parameters. Finally, these models are translated into real-time buildings by the use of computer numerical controlled fabrication. These realized buildings are losing the performative character of the digital models. The next step should be found in the realization of performative buildings that can inherently adapt according to desired dynamic parameters. The immediate adaptive building performance will relate to time and movement. Architecture should become more adaptive in order to remain relevant.

This research focusses on the realization of adaptive architecture with the use of advanced material technology. Current material research has shown significant advances with the development of “smart” materials. Smart materials are “capable of automatically and inherently sensing or detecting changes in their environment and responding to those changes with some kind of actuation or action” (Ansari, et al. 1997). These materials have intrinsic characteristics that enable the detection of an external stimulus and initiate an appropriate action, by adapting the material properties (Srinivasan, et al. 2001). Smart materials have both sensory and actuation characteristics. By introducing smart materials in the building system immediate adaptive environments can be realized.

The purpose of this research is to study the application and performance of smart materials for the realization of a shape morphing adaptive building component (ABC). The ABC should be able to realize a reversible hinge-like deformation. This means that a flat strip of materials should be able to bend into a 90° angle. The deformation should be fixated without constant energy input and recover into the initial flat configuration when desired.

This research has started with an overview of the current state of adaptive architecture. Additionally, the application of smart material systems in architecture has been analysed. Design scenarios illustrate the application field of the ABC in the building system. An example is given of a small scale ABC that can be applied as façade tessellation for ventilation or daylight control. Another presented concept is the aerodynamic envelope optimization for high-rise buildings. Additionally, the shape morphing principle can be envisioned on large scale building applications. Building components such as adaptive space divisions or furniture elements will contribute to an optimization of the multifunctional use of space.

When the building system can sense, process and act, a new functional relationship is established between the building and its users. Immediate adaptive environments will change the user perspective on the built environment. Adaptive architecture will lead to a whole new paradigm of the building design and use. By an internet inquiry and interviews, an insight is created into the participant's receptiveness on immediate adaptive environments. In general, the participants reacted positively on the presented adaptive scenarios, such as adaptive furniture, adaptive windows, adaptive interior walls and adaptive interior colour.

The user study is finalized with an interview whereby physical models represented the adaptive concept of specific building components. With the use of (scaled) prototypes, the determined adaptive architectural performances were tested on the participant's receptiveness. The concept of an adaptive floor plan and adaptive window settings were tested for different activities. The results indicated that the participants changed the floor plan according to almost every proposed activity.

The window configuration of a single-room apartment could be adjusted with the adaption of the location, shape and transparency. The adaptation of the shape of the window is not considered relevant for the participants (76% of the participants did not change the shape of the windows even once). However, the location and transparency is changed considerably frequent (76% adjusted this setting once or more). Additionally, a window is removed or added rather frequently (70% of the participants changed this setting once or more). It should be noted that the participants mentioned during the interview that the proposed settings were difficult to visualize with the current available technologies. However, the participants addressed that the adaptive building concept is interesting and useful, which is also indicated by the large amount of changes.

After the study on the user receptiveness, the realization of a shape morphing building component is analysed. Shape adaptation in architecture is an interesting field of research in terms of functionality and realization. The performance is demonstrated by the fabrication of a full working prototype. After a smart material analysis, a composite system of shape memory alloys (SMAs) embedded in a shape memory polymer (SMP) matrix is presented that met the design requirements. The performance of this smart composite (SC) is analysed thoroughly.

Both the SMA and the SMP are thermo-responsive materials and are activated by resistive heating. By increasing the SMP body temperature, the material transformed into rubbery phase and can then easily be deformed by external forces. When cooling under the transformation temperature, the deformation will be fixated. The SMAs are integrated in the SMP matrix in order to perform as actuators and enable the deformation and recovery of the SC. Antagonist shaped SMA actuators are used for the deformation and subsequent recovery. As the SMP has memory properties and enables recovery after deformation, more actuators were required for the deformation of the SC than for the recovery. Both materials will be controlled by resistive heating. This will enable an accurate and active activation of both materials. As the SMP is not conductive, constantan heating wires were integrated into the SMP matrix in order to enable local heating of the SMP.

The SC principle is tested by the fabrication of a small scale prototype (Figure 1). First, the material characteristics of all individual components were analysed by experimentation. The required forces for the deformation of the SMP matrix and the delivered forces by the SMA strips were studied by torsion experiments. All experiments were executed with uniform external heating, in order to ensure a uniform heating. By superimposing the results of the individual components, the performance of the ABC could be determined. Based on the acquired data it became clear that the deformation angle could only reach 100° (the inner angle of the ABC is calculated here). This result is validated by torsion experiments with a full working SC prototype.

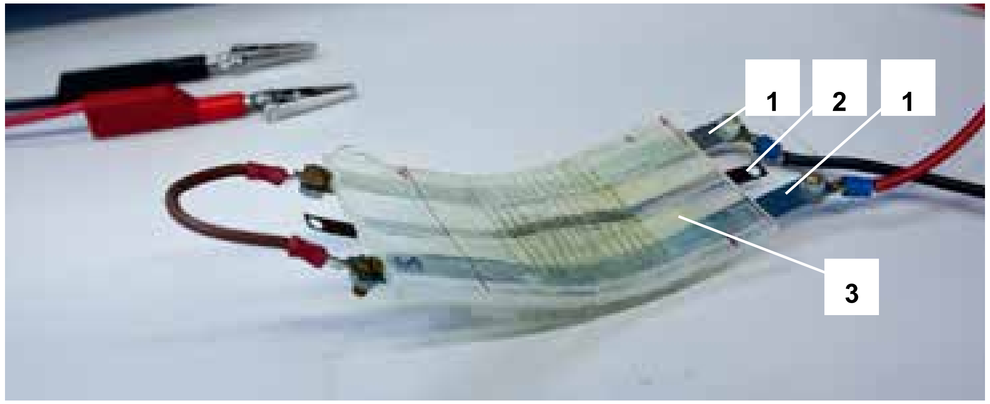

Figure 1 Smart Composite; 1: Shape Memory Alloy actuators, take care of the deformation of the SC. 2: Shape Memory Alloy actuator facilitates the recovery of the SC. 3: Shape Memory Polymer matrix with embedded heating wires.

The fabrication method and prototyping of the SC is analysed thoroughly and adjusted in order to optimize the SC performance. The integration of both the heating wires and the SMAs in the SMP matrix required special investigation. As the SMP is cured by a temperature which is close related to the SMA activation temperature, the SMA strips were embedded in the SMP matrix after curing. The SMP is constructed out of two elements, which were connected by super glue after the integration of the SMA strips. Super glue is tested as most profound adhesive during the conducted tensile experiments.

An approximate deformation of 90° is obtained during torsion experiments with the SC prototype. However, it should be noted that the SMA actuators did show a considerable fatigue upon cycling. After 4 cycles merely, the deformation only reached an angle of 100°. Therefore, oversizing of the actuators is required in order to avoid fatigue.

In general, it could be stated that the desired performance of the SC is realistic with the current materials. The performance of the SC prototype has shown a reversible shape deformation with the use of smart material systems. The significant technical advantage of this system is obtained by the fixation of the deformation without constant energy input. However, optimization in terms of cycling, performance and manufacturing is required in order to realize large–scale application in building systems.

Accurate control of the individual smart materials systems is an important aspect in optimization of the SC performance. The thermoelectric activation of both the

SMA and SMP were simulated by finite element modelling. The simulation software *ANSYS* is used here in order to create the model. This numerical model is validated by thermal experimentation with the use of a thermal imager. The validation experiments indicated that the finite element model is in good agreement with the physical material performance. Both the thermal activation of the SMAs as the integrated heating wires gave near identical thermal outputs. The finite element analysis is used for the determination of the most profound operating settings of both the SMAs as the heating wires. The numerical model can be adjusted to different dimensions and can determine the accurate thermal control of the smart composite.

This research can be considered a first step into the new paradigm of architecture, whereby shape-morphing environments are realized by the use of smart material technology. The promising results of the fabrication and performance of the SC, show a realistic future for shape morphing building components based on intrinsic material characteristics. With the fabrication of the SC, the translation from virtual into real-time adaptive building components has been envisioned. Disadvantages of mechanical shape morphing systems, such as large construction sizes, complex structures and noise generation could be overcome by integrating smart material technology.

References

Ansari, F., Maji, A., et al. (1997). Intelligent civil engineering materials and structures a collection of state-of-the-art papers in the applications of emerging technologies to civil structures and materials. New York, ASCE.

Srinivasan, A. V. and Mcfarland, D. M. (2001). Smart structures analysis and design. Cambridge, UK, Cambridge University Press.

SAMENVATTING

SLIMME MATERIALEN VOOR HET REALISEREN VAN EEN ADAPTIEF GEBOUWCOMPONENT

De laatste 150 jaar hebben veel meer technologische ontwikkelingen plaatsgevonden vergeleken met alle voorliggende decennia. Deze ontwikkelingen volgen elkaar in een hoog tempo op. Technologische innovaties op gebied van internet, elektronische producten en mobiliteit drukken een enorme stempel op de socio-culturele ontwikkelingen van de maatschappij. Wanneer hierbij wordt gekeken naar de invloed op de gebouwde omgeving, dan is er een duidelijk verschil zichtbaar tussen onze huidige manier van leven en wereld perceptie en onze leefomgeving. Het is duidelijk dat technologische ontwikkelingen een belangrijkere rol moeten gaan spelen in architectuur.

Digitale technieken in de architectuur werden voornamelijk toegepast voor het visualiseren van ontwerpen. Daarna hebben deze technieken zich ontwikkeld tot de ontwikkeling van geometrische ontwerpmodellen. Deze modellen simuleren performatieve digitale omgevingen die zich continu kunnen aanpassen aan dynamische parameters. Deze modellen kunnen worden vertaald naar real-time gebouwen met het gebruik van computer gestuurde numerieke constructiemethoden. De volgende stap zou gevonden moeten worden in het realiseren van performatieve gebouwen waarbij de omgeving zich continue zou kunnen aanpassen aan de hand van dynamische parameters. Het gedrag van deze continue adaptieve gebouwen is gerelateerd aan tijd en beweging. Architectuur moet zich meer ontwikkelen op het gebied van adaptatie, zodat het meer in relatie blijft staan met de huidige ontwikkelingen en de gebruiker.

Dit onderzoek concentreert zich op het toepassen van geavanceerd materiaaltechnologie voor de realisatie van adaptieve architectuur. De ontwikkeling van *slimme* materiaaltechnologie speelt een belangrijke rol in het huidige materiaal onderzoek. Slimme materialen beschikken over de eigenschap dat ze automatisch veranderingen kunnen waarnemen in hun omgeving en hierop kunnen reageren met een bepaalde actie of activatie (Ansari, et al. 1997). Dit ‘gedrag’ is gebaseerd op intrinsieke materiaaleigenschappen, waarbij een externe stimulus wordt gedetecteerd en er een reactie tot stand komt waarbij de materiaaleigenschappen worden aangepast (Srinivasan, et al. 2001). Slimme materialen hebben dus sensorische- en activeringseigenschappen. Door slimme materialen toe te passen in het gebouwsysteem kunnen continue adaptieve gebouwen gerealiseerd worden.

In dit onderzoek worden de mogelijkheden bekeken van het toepassen van slimme materialen voor het realiseren van vorm veranderbare adaptieve gebouwcomponenten (ABC). Het idee is dat het ABC een omkeerbaar scharnier-achtige vervorming moet kunnen realiseren. Dit betekent dat een platte strook materiaal een verbuiging in een hoek van 90° zou moeten kunnen halen. Deze vervorming moet gefixeerd kunnen worden zonder de continue toevoeging van een energiebron. Vervolgens moet het ABC zich kunnen herstellen in de oorspronkelijke configuratie. Dit gedrag zal volledig gebaseerd moeten zijn op de intrinsieke eigenschappen van materialen, zonder de toevoeging van externe actuatoren of mechanismes.

De huidige stand van zaken op het gebied van adaptieve architectuur is geanalyseerd

in dit onderzoek. Daarnaast is een overzicht gegeven van de toepassing van slimme materiaalsystemen in de architectuur. Met gebruik van ontwerp scenario's wordt er een beeld geschept van de toepassing mogelijkheden van de ABC in de architectuur. Op een kleine schaal kan het ABC worden toegepast als geveltesselatie voor de controle van ventilatie en daglicht. Daarnaast wordt er een scenario gepresenteerd voor de aerodynamische optimalisatie van de buitenschil bij een hoge windbelasting op de gevel. Ook zou het principe van de ABC op een grotere schaal toegepast kunnen worden. Gebouwcomponenten zoals adaptieve ruimteverdelingselementen of meubels kunnen bijdragen aan het optimaliseren van de multifunctionaliteit van een gebouw.

Er ontstaat een nieuwe functionele relatie tussen het gebouw en de gebruikers wanneer een gebouw kan voelen, verwerken en reageren. Door de realisatie van continu adaptieve gebouwen verandert de perceptie van de gebruiker op de gebouwde omgeving behoorlijk. Adaptieve architectuur leidt tot een nieuw paradigma van het architectonische ontwerpen en het gebouwgebruik. Daarom is het receptieve vermogen van de gebruikers op adaptieve gebouwen onderzocht met behulp van een internet enquête en interviews. Hier kwam uit dat de deelnemers over het algemeen positief reageerden op de voorgelegde adaptieve scenario's. Een voorbeeld van deze scenario's zijn adaptieve meubels, adaptieve ramen, adaptieve binnenwanden en adaptieve interieurkleuren.

Het gebruikersonderzoek werd afgesloten met interviews waarbij gebruik werd gemaakt van fysieke modellen om de adaptieve architectonische werking te verbeelden. De gebruikers ontvankelijkheid voor een adaptieve plattegrond en ramen werd getest aan de hand van verschillende activiteiten. De uitkomsten laten zien dat de deelnemers de plattegrond veranderden aan de hand van bijna elke activiteit.

De raamconfiguratie van een één-kamer appartement kon door de deelnemers worden aangepast door middel van het veranderen van de locatie, de transparantie en de vorm. Tijdens het onderzoek bleek dat de vorm van het raam niet werd aangepast (76% van de deelnemers veranderde de vorm niet). Daarentegen werd de locatie en de transparantie van de ramen frequent veranderd. Ook werden ramen regelmatig verwijderd en toegevoegd (70% van de deelnemers veranderde deze setting). Een belangrijke beperking in dit onderzoek is dat de deelnemers zich de technische realisatie van de voorgelegde scenario's moeilijk konden voorstellen met het gebruik van de huidige technologieën

Na het gebruikersonderzoek is de realisatie van de vorm veranderbare gebouwcomponent geanalyseerd. De werking is gedemonstreerd aan de hand van een volledig werkend prototype. Eerst zijn slimme materialen met vorm veranderbaar vermogen geanalyseerd. Hieruit blijkt dat een composiet van geheugenlegering (SMA) geïntegreerd in een geheugenpolymeer (SMP) matrix het vereiste gedrag zou moeten kunnen vertonen. De werking van dit slimme composiet (SC) is uitgebreid bestudeerd.

De SMA en de SMP worden beide aangestuurd door middel van warmte, i.e. zijn thermo-responsief. De SMP zal rubberachtig gedrag vertonen, wanneer de temperatuur verhoogd wordt boven een bepaald transitietemperatuur. In deze fase kan de SMP gemakkelijk vervormd worden. De vervorming wordt gefixeerd door middel van afkoeling beneden de transitietemperatuur. De SMA functioneert als een actuator en zal de vervorming realiseren. Antagonist SMA actuatoren worden toegepast om de deformatie en het opvolgende herstel naar de oorspronkelijke vlakke configuratie te verwezenlijken. Omdat de SMP ook over geheugencapaciteiten beschikt, vervormt deze uit zichzelf terug naar de oorspronkelijke vlakke vorm. Daardoor zijn er meer actuatoren nodig voor de vervorming van het SC dan voor het herstel. De aansturing van beide materialen gebeurt door middel van weerstandsverwarming. Deze methode maakt het mogelijk om de materialen accuraat en actief the controleren. Omdat de SMP een slechte geleider is, zijn constantaan draden geïntegreerd in de SMP matrix zodat de SMP lokaal verwarmd kan worden

De werking van het bovenbeschreven principe is getest met een prototype (zie Afbeelding 1). Allereerst zijn de materiaaleigenschappen van alle individuele componenten geanalyseerd door middel van experimenten. De benodigde krachten voor de vervorming van de SMP matrix en de geleverde krachten van de SMA actuatoren zijn vastgesteld door middel van torsie experimenten. Alle experimenten zijn uitgevoerd met uniforme externe verwarming, zodat de temperatuur goed gecontroleerd kan worden. De uiteindelijke werking van de SC is vastgesteld door middel van superpositie van de resultaten van de individuele componenten. Het werd duidelijk aan de hand van deze resultaten dat de vervorming alleen een hoek van 100° kan bereiken (de binnenhoek van de vervorming werd hierbij gemeten). Deze resultaten zijn gevalideerd met de torsieresultaten van een goed functionerend prototype.

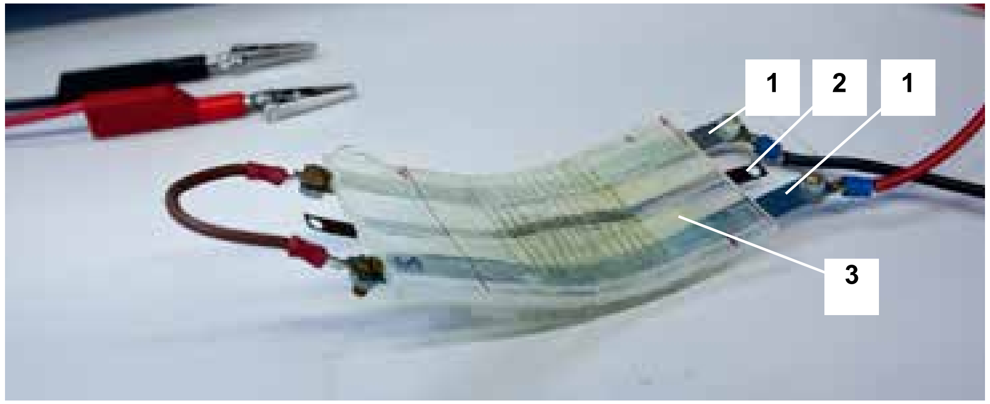

Afbeelding 1 Slim Composiet (SC). 1: geheugenlegering zorgen voor de vervorming van de SC. 2: geheugenlegering zorgt voor het herstel van de SC. 3: geheugenpolymeer matrix met geïntegreerde verwarmingsdraden.

De vervaardigingsmethode en uitvoering van de SC is aangepast zodat de werking geoptimaliseerd kon worden. De integratie van de verwarmingsdraden en de SMA strippen vergde extra aandacht. Omdat de SMP uithardt bij een hoge temperatuur die dicht bij de activatie temperatuur ligt van de SMA, is het niet mogelijk om de SMAs in het SMP mee te gieten. Daarom is besloten om de SMP uit twee delen te fabriceren. Deze delen zijn na het integreren van de SMA strippen met elkaar verbonden met secondelijm. Secondelijm gaf de beste resultaten tijdens de uitgevoerde trektesten.

Tijdens de torsie experimenten met de SC prototype is een vervorming van 90°

behaald. Daarbij moet de kanttekening geplaats worden dat er een behoorlijke materiaalmoeheid optrad tijdens het herhalen van de vervorming. Al na 4 vervormingen was er alleen een vervorming mogelijk tot 100°. Het is daarom belangrijk om de actuatoren te over-dimensioneren, zodat een vervorming van 90° haalbaar blijft.

Over het algemeen kan geconcludeerd worden dat de voorgestelde vervorming realistisch is met de gekozen materialen. Het SC prototype heeft een omkeerbare vervorming laten zien met het gebruik van slimme materiaaltechnologie. Een belangrijk technisch voordeel is de fixatie van de vervorming zonder de continue energietoevoer. Toch is optimalisatie op het gebied van materiaal moeheid, functie en fabricage nodig voor het gebruik van slimme materialen op architectonische schaal.

Het accuraat activeren van de verschillende componenten speelt een belangrijke rol in de optimalisatie van de SC. De thermo-elektrische activatie van de SMA en de SMP is gesimuleerd met het gebruik van een eindige-elementen-model. Hierbij is gebruik gemaakt van het softwarepakket *ANSYS*. Het numerieke model is gevalideerd aan de hand van uitgevoerde experimenten, waarbij de warmtedistributie is vast gelegd met een warmtebeeldcamera. Uit de resultaten van de experimenten bleek dat het eindige-elementen-model goed overeenkwam met het fysieke model. Bijna identieke temperatuur curves werden gevonden voor zowel de thermische activatie van de SMA strippen als de verwarmingsdraden. Hierna is het model gebruikt voor het vaststellen van de optimale aansturingsinstellingen. Het numerieke model kan worden aangepast voor verschillende dimensies en kan hierbij vrij accuraat de thermische aansturing van het SC bepalen.

Dit onderzoek kan worden gezien als een eerste stap van een nieuw paradigma in de architectuur, waarbij vorm veranderbare gebouwen worden gerealiseerd met het gebruik van slimme materiaaltechnologie. De veelbelovende resultaten laten zien dat het in de toekomst realistisch is om vorm veranderbare gebouwcomponenten te fabriceren waarbij het gedrag van de materialen gebaseerd is op intrinsieke materiaaleigenschappen. Door het vervaardigen van een werkend prototype heeft er een vertaling plaatsgevonden van de virtuele wereld naar real-time functionerende adaptieve gebouwcomponenten. Dit brengt verschillende voordelen met zich mee ten opzichte van mechanische vorm veranderbare system, waarbij zaken zoals grote afmetingen, complexe structuren en geluidoverlast opgelost worden.

References

Ansari, F., Maji, A., et al. (1997). Intelligent civil engineering materials and structures a collection of state-of-the-art papers in the applications of emerging technologies to civil structures and materials. New York, ASCE.

Srinivasan, A. V. and Mcfarland, D. M. (2001). Smart structures analysis and design. Cambridge, UK, Cambridge University Press.

ACKNOWLEDGEMENTS

First, I would like to thank the Delft Centre for Materials for the sponsoring of the materials and the printing of the dissertation. Without the Young Wild Idea award I would not have been able to perform this research. Sometimes, it's good to take a walk on the wild side and you definitely encourage this with your award.

I owe my gratitude to the Delft University of Technology for giving me the opportunity to perform this research. Prof. Mick Eekhout and Prof. Wim Poelman you have the (disputable) honor to convince me to start this project ;) Thank you for sharing your knowledge, enthusiasm, interest, support and your faith in my capabilities. Liek Voorbij, you were the supervisor every PhD candidate should wish for. Thank you for your encouragement, endless discussions, support and clear vision. I owe many thanks to Prof. Patrick Teuffel for the supervision and support during the last few years.

During my PhD research I made journey through the University of Delft. Performing material research without a material lab and facilities urged me to be creative in finding solutions with the tools available. I have found my way through the different labs and fields of knowledge. I learned so much along the way, and as knowledge doesn't stand on its own, there were many people who were so generous to share their knowledge and ideas with me. It was a sometimes difficult (and often rainy) journey but the wisdom and enthusiasm I received, is priceless. It is almost impossible to name everybody, but I should thank some people in particular.

Special thanks to Ben Norder from DelftChemTech of the Faculty of Applied Sciences, for introducing me into the material science, endless hospitality and support. Thank you Prof. Steven Picken for the lab use. Thank you ever so much Sebastiaan Lindstedt, Fred Bosch and Prof. Adriaan Beukers from the Faculty of Aerospace Engineering for the use of the utilities of the composite lab and support during the manufacturing of the polymer samples.

The last years I have spent at the lab of Precision and Micro Engineering lab of the Faculty of Mechanical, Maritime and Materials Engineering (3ME). Thank you very much for your advice and expertise, especially for helping me out after the fire at the Faculty of Architecture; Kaspar Jansen, Harry Jansen, Patrick van Holst, Rob Luttjeboer and Jos van Driel. Kaspar, thank you very much for everything! Your enthusiasm and interest made me work harder and urge for my goals. With your critical comments and interesting discussions you triggered me to continue my research and actually finalize it. Thank you so much for adopting me in your lab and for becoming my co-promoter.

Kees and Louis from the Staalwerkplaats, how could I ever thank you for your endless help, valuable solutions and all the good times? I learned to mill my own molds and everything is possible with you two. With your help I conquered it all: steel, aluminum, Tefal, polymer and I even glass for the manufacturing of my molds. All my fingers are still there, what a blessing!

I owe many thanks to Ton Mol (DEMO), Hans Weerheim (Aerospace), Hans Drop

(3ME workshop) and Ton Riemslag (3ME) for the use of the tools, machines and practical tips.

Special thanks to Rien van de Ruijtenbeek from 3ME and Wybe Wagenaar from Infinite for all the help with ANSYS. Your patience and clear explanations contributed to a validated model. I would like to thank Arend Harteveld from the section Ergonomics of the Faculty of Industrial design.

I owe my gratitude to the bachelor 6 students of the Faculty of Industrial Design and 3ME for their contribution to this research project and for their enthusiastic input.

I would like to thank all my colleagues of the Building Technology department, Hyperbody Research Group and Media Studies. Thank you for the interesting conversations and for sharing your knowledge and experiences, you created a valuable working environment. I should thank my colleagues from room 7.17, and in particular Sannie, Gillian, Daan, Shohre, Marlous, Peter and Karel for introducing me to the world of science. Special thanks to Thaleia, Lidia and Barbara for your support, friendship, critical discussions and sharing laughs and tears. Your encouragement and positivity made me focus on my goals and forget the side issues. I should mention Walter, soup master and unforgettable colleague and Jaap and Rutger; your work spirit and persistence are inspirational. Special thanks to Fred Veer and Martin TenPierik for sharing your valuable knowledge at crucial moments. Andrew and Gerrie thank you for transferring goniometric complexity into simplicity! Thank you ICT, especially Kaweh and Errol, for all your help in stressful moments.

My gratitude goes to the OdC members, it were/are difficult times and your work is important. I learned a lot from you all. I should thank the committee members of Material Design for sharing their broad interest in materials, development and application; the meetings are so valuable I enjoy being part of the team.

I really should thank Punch ladies 1; you were there to play that beautiful and addictive game with me. Thank you so much for all the fun and laughs! You are all champions! I would like to thank my friends, for their interest and faith in me and especially for all the good times.

I owe my thanks to the two paranimphs, who took the stand with me. I can't believe you accepted this offer, thanks so much for your support and courage. Alex, thank you for all the proof reading, suggestions and interesting discussions. Jans, I cannot even count all the cappuccino's you made for me, thank you for being a listening ear and for all the fun. I really could not have done this without you two.

The biggest gratitude goes to my wonderful parents, who always believed in me and convinced me that I should face my challenges. There is always a bridge to cross the ravine and otherwise we should build the bridge ourselves. You taught me to be independent and strong in my own capabilities and beyond. The famous saying: "Nobody is going to do it for you, so you have to do it yourself" learnt me from a young age that being a girl is no restriction for "building my own bridge" by hand. Without your love and persistence I couldn't have done this. Your interest and support in what I do is admirable.

Thank you Pien and Nicola, it is good to be shouldered in between you two. You prevented me from falling down. Your support, discussions and fun helped me so much, my sisters you mean the world to me. Thanks so much for standing by my side, unconditionally. You two make me who I am. Nicolette special thanx for all the editing and Anna for all the reading. Yuri, thank you for helping out with the many ICT problems! All those viruses and crashes, I survived them all. Jochem, it was good to have some relaxing conversations with the other stress ball in the family, especially when there are some good cocktails involved.

Thank you Giel and Francis, Carola and Rene for your interest and concerns. I am finally finished!

Last, but not least I want to thank my lovâh. Owen, I owe you so much. I couldn't have done this without you. Sorry for all the craziness, it (I) was sometimes a rollercoaster. Thank you for always standing by my side, I didn't fall out! I still can't believe we are here.

I appreciate that I got this great opportunity to develop myself and perform research. I consider myself lucky and I hope that one day everybody at any place in the world will be able to realize their dreams. I owe a lot to everybody who fought for equal education and development. I will always cherish the important values; freedom and equality.

Charlotte

2013

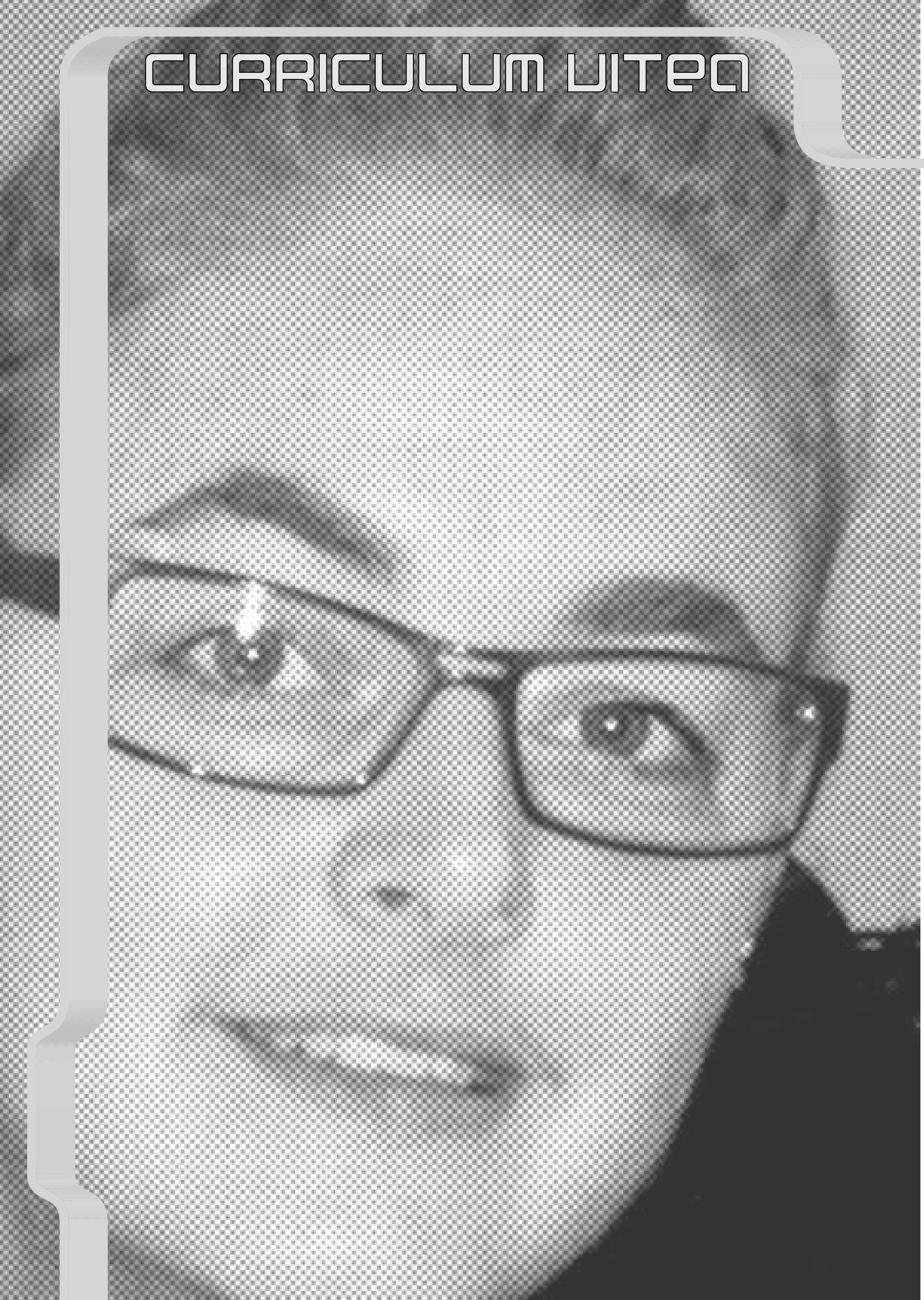

CURRICULUM VITEA

Charlotte Lelieveld was born on October 5th, 1979 in Zoetermeer, The Netherlands. She graduated Athenaeum high school in 1998 and started, after a period of travelling and working, with a study of Architecture at the Delft University of Technology in 2000.

In 2003, she studied as an exchange student at the Massachusetts Institute of Technology, USA. In 2005, she attended the fashion department of the Gerrit Rietveld Academy in Amsterdam, The Netherlands.

She received a Master of Science degree in Architecture with honours from the Delft University of Technology in the Netherlands in 2005. She graduated at the Hyperbody Research Group chaired by Professor Kas Oosterhuis. During her graduation her interest in the application of advanced materials in architecture developed, with a special focus of smart material systems.

In 2006 she started as a researcher at the chair of Product Development, department of Building Technology, Delft University of Technology (TUD). Here, she worked at a material library for students. Additionally, she organized several material events, such as symposia, an excursion, a workshop and several discussion nights (www.materialdesign.nl). The design, application, fabrication and development of materials were issue of interest. The designer was not only focus of attention during these events, but also the collaboration with the manufacturer and developers were important issues.

She conducted her Ph.D. research at the department of Architectural Engineering + Technology, TUD. Her main interest lies in the implementation of smart material technology into the building system for the realization of adaptive architecture. Her research focused on the design, manufacturing, testing and optimization of an adaptive building component, where she finds herself on the crossing of different knowledge fields. Her work has been granted by the Young Wild Idea Award of the Delft Centre of Materials. Her work has been published in magazines and international conference proceedings. She has given several lectures nationally and internationally.

She has tutored Bachelor and Master students at the faculty of Industrial Design Engineering, the faculty of Mechanical, Maritime and Materials Engineering and the faculty of Architecture, TUD.

Charlotte plays basketball and likes to travel to deserted places. She enjoys cooking and good food. She has a special interest in old-timer cars, which she also tries to repair with varying success.

PUBLICATIONS

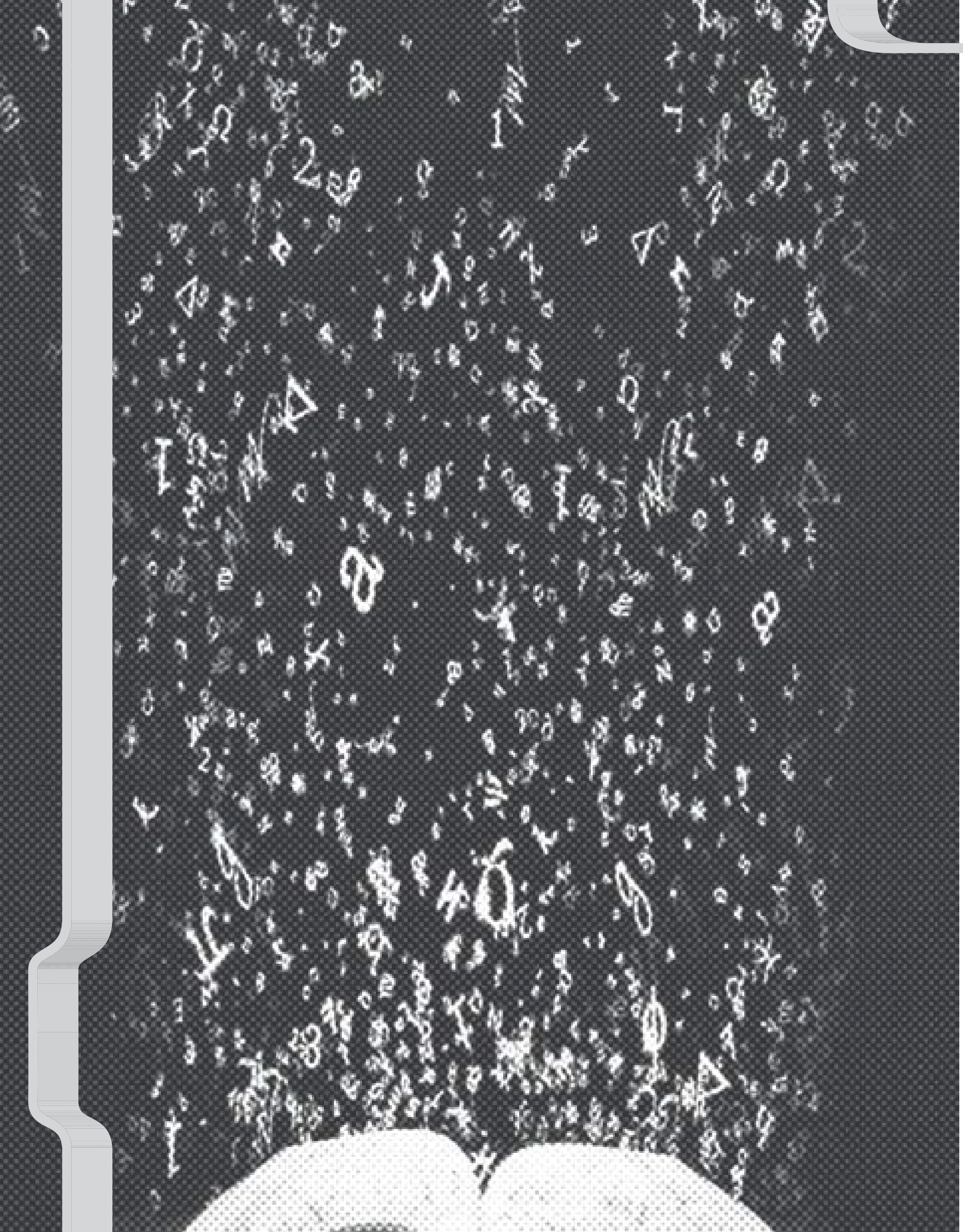

(Refereed) Journals

Lelieveld, C. M. J. L. and A. I. M. Voorbij (2008) Dynamic Material Application for Architectural Purposes. Advances in Science and Technology 56, 595-600.

Hellinga, H. I. and C. M. J. L. Lelieveld (2011). “Intelligente daglichtsystemen: De toepassingsmogelijkheden van ‘Smart Materials’ “ Bouwfysica 2: 17-21.

Lelieveld, C. M. J. L. (2011). Slimme Materialsystemen voor Dynamische Architectonische Toepassingen. Stedebouw & Architectuur innovatiecatalogus. Amsterdam, The Netherlands, Weka Uitgeverij: 10-13.

Book chapter

Lelieveld, C. M. J. L. (2007). MaterialZ: Early Specialist Involvement. The Architecture Annual 2006-2007. H. Bekkering, A. d. Doeschate, D. Hauptmannet al. Rotterdam, The Netherlands, 010 Publishers: 36-39.

International refereed conferences

Lelieveld, C. M. J. L. and A. I. M. Voorbij (2007). The Application of Dynamic Materials in Adaptable Architecture. ManuBuild, The Transformation of the Industry– Open Building Manufacturing. M. Sharp. Rotterdam, The Netherlands, CIRIA, Classic House.

Lelieveld, C. M. J. L., A. I. M. Voorbij, et al. (2007). Adaptable Architecture. Building Stock Activation. Tokyo, Japan, TAIHEI Printing Co., Ltd. .

Poelman, W. and C. M. J. L. Lelieveld (2007). From Nano to Macro; Application of Dynamic Materials in Architecture. Shell and Spatial Structures: Structural Architecture -Towards the future looking to the past. Venice, Italy.

Lelieveld, C. M. J. L. and A. I. M. Voorbij (2009). Adaptable Architecture with the Application of Dynamic Materials. Lifecycle Design of Buildings, Systems and Materials. E. Durmisevic. Enschede, The Netherlands.

Lelieveld, C. M. J. L. and P. Teuffel (2010). Smart Composite for Architectural Applications. International Association for Shell and Spatial Structures (IASS). L. Y. Qilin Zhang, Yuyin Hu. Shanghai, China, China Architecture & Building Press.

Lignarolo, L., C. M. J. L. Lelieveld, et al. (2011). Shape Morphing Wind-Responsive Facade Systems Realized With Smart Materials. Adaptive Architecture. F. Stacey and M. Stacey. Londen, UK.

IMAGE COURTESY CHAPTERS

Table of content- New Babylon by Constant Nieuwenhuys
List of terms, symbols and abbreviations- Cassie Langmann Portfolio webpage.
Chapter 1- Commercial Office Tower, Dubai by Contemporary Architecture Practice.
Chapter 2- Allianz Arena, Herzog & De Meuron by Joachim Schneider.
Chapter 3- Magneto rheological fluid: Morpho Towers by Sachiko Kodama.
Chapter 6- NiTi Micrograph by Choi J. et.al (2003). “Calcium phosphate coating of nickel–titanium shape-memory alloys” Biomaterials 24 (21).
Appendices- Cyclebowl by Atelier Brückner.
Publications- Wallpaper Million.

"Cat: Where are you going?
Alice: Which way should I go?
Cat: That depends on where you are going.
Alice: I don't know.
Cat: Then it doesn't matter which way you go."
— *Lewis Carroll, Alice in Wonderland*

TU Delft
Delft University of Technology

ISBN: 978-94-6186-114-6